Investigating the Role of Phosphorylation and Ubiquitylation Dependent Regulation of Hippo Signalling

Alexander Fulford

A thesis submitted for the degree of

Doctor of Philosophy (PhD)

PhD Supervisor: Paulo Ribeiro

Centre for Tumour Biology, Barts Cancer Institute,

Barts and The London School of Medicine and Dentistry,

Queen Mary University of London.

July 2017

Statement of Originality

I, Alexander Fulford, confirm that the research included within this thesis is my own work and that where it has been carried out in collaboration with, or supported by others, that this is duly acknowledged below and my contribution indicated. Previously published material is also acknowledged below.

I attest that I have exercised reasonable care to ensure that the work is original, and does not to the best of my knowledge break any UK law, infringe any third party's copyright or other Intellectual Property Right, or contain any confidential material.

I accept that the College has the right to use plagiarism detection software to check the electronic version of the thesis.

I confirm that this thesis has not been previously submitted for the award of a degree by this or any other university.

The copyright of this thesis rests with the author and no quotation from it or information derived from it may be published without the prior written consent of the author.

Signature: 

Date: July 2017

Abstract

The Hippo Pathway is a highly conserved regulator of tissue growth and size determination, limiting the activity of the transcriptional co-activator Yorkie (Yki), which promotes proliferation and inhibits apoptosis. Hippo signalling integrates and transduces cell polarity and cell-cell adhesion inputs thereby responding to the state of tissue architecture. The transmembrane apical polarity protein Crumbs (Crb) controls the activity of Yki by regulating Expanded (Ex), a protein that promotes Hippo signalling through kinase-dependent and -independent mechanisms to robustly inhibit Yki activity. Crb plays a dual role in the regulation of Ex by controlling its apical localisation, facilitating Yki inhibition, and by promoting Ex degradation, thus activating Yki. Crb regulates the stability of Ex by stimulating a phosphorylation-dependent ubiquitylation and proteasomal degradation. Characterisation of the precise mechanisms by which Crb regulates Ex has been the focus of this thesis.

Based on candidates identified by mass spectrometry and from literature, the Casein Kinase 1 (CK1) family of kinases, and the deubiquitylating enzyme (DUB) Usp2 have both been identified as novel regulators of Ex stability. CK1s promote Ex phosphorylation and degradation, acting as Ex inhibitors, while Usp2 promotes Ex function by promoting its stabilisation. Furthermore, in a screen to identify DUBs that regulate *Drosophila* adult wing size, CG10889 has been established as a novel regulator of growth that interacts with members of the Hippo pathway.

Acknowledgements

What makes a successful PhD student? The answer to this question remains as elusive to me as ever, even after nearly four years. However, what I do know is that it takes determination and support, for which thankfully, I have both in an academic and social capacity. A PhD is by no means a one man show.

Therefore, it is in due course that I thank my patient director. I owe so much to the man I hoodwinked into hiring me, Paulo. Having never even noticed the humble fruit fly on my perpetually black bananas as an undergraduate, he gave me the opportunity to discover the delights of this wonderful model organism. I'm sure my naivety was perhaps a draw as I was unaware I'd have the pleasure of making fly food so regularly over the subsequent years (if there was a 'Bake off- crème de la crème for fly food, I'm sure our lab would be in amongst the best). Your teaching has been truly invaluable and I appreciate everything you have done to help me along the way. I hope I have also played my part, as your first professional baby (a title Liliana will not be able to wrestle from me) in setting up your lab. What I am sure about, is that you'll be delighted to see the back of the seminal soundtrack to my time in the lab, Test Match Special. I am also extremely grateful to Nic and Maxine, who have been instrumental in my development as a 'scientist'. I am particularly thankful to Maxine, for sharing in the trials and tribulations of our time on this project.

Now, to the supporting cast who have crept the boards with me along the way. First and foremost, I must thank my lab mates Cecilia and Nina who have both made my time in our box room always enjoyable. In particular, I must thank Nina who has been so generous with her time. I wish you all the luck you truly deserve. Thank you to Katherine for your continual encouragement during the many times when I have felt my confidence lacking.

Onto the chorus and the Barts Brewing Quartet who provided me with many enjoyable evenings. In particular I need to thank Ed, not least for our weekly tagging sessions, and Ketan, who has been such a good friend throughout. To Arran, Caz and Emma for too few coffee breaks, and to Lily for introducing me to most of my closest friends at Barts (of which you are undoubtedly one). I also want to thank everyone who has been part of Friday football, and thanks to Bianca for being co-responsible for IT blocking Sporcle.

Thank you to the members of the audience; my friends outside of science and most importantly, my brothers, Hugo and Louis and parents, Nick and Clare. Their support and love cannot be overstated and I will be eternally indebted. Front and centre of the auditorium is Daniella, for the light in your eyes.

I must also thank the Executive Producers for financial support, CRUK and the Springboard Award (AMD/Wellcome Trust), without which I would never have been able to indulge myself.

Table of Contents

List of Figures

List of Tables

Abbreviations

Ack	Activated Cdc42 Kinase
AIP4	Atrophin-1 Interacting Protein 4
AJ	Adherens Junction
AMOT	Angiomotin
AMP	Adenosine Monophosphate
AMPK	AMP-Activated Protein Kinase
Ap	Apterous
AP-2	adaptor protein-2
aPKC	Atypical Protein Kinase C
App	Approximated
Arm	Armadillo
Arr	Arrow
ATP	Adenosine Triphosphate
attB	attachment-B site
attP	attachment-P
AU	Absorbance Units
Baz	Bazooka
β–Gal	β–Galactosidase
β_H-Spectrin	β_{Heavy}-Spectrin
BMP	Bone Morphogenetic Protein
bp	base pairs
BSA	Bovine Serum Albumin
β-TrCP	β-transducin repeats-containing protein
Cact	Cactus
Cas	CRISPR associated
Ci	Cubitus interruptus
CK1	Casein Kinase 1
Crb	Crumbs
Crb^{FL}	Crb Full-Length
Crb^{i} or Crb^{ICD}	Crb intracellular-domain
$Crb^{i\Delta F}$	Crb^{i} FERM-Binding Motif mutant
CRISPR	Clustered Regularly Interspaced Palindromic Repeats
CRL4	Cullin4A-RING E3 Ligase
CTGF	Connective Tissue Growth Factor
CTP	Cytidine Triphosphate
Cul1	Cullin 1
CycE	Cyclin-E
D	Dachs
DCAF1	DDB1- and CUL4-Associated Factor 1
Dco	Discs overgrown
Diap1	Drosophila Inhibitor of Apoptosis-1
Dl	Delta
Dlg	Discs Large
Dlish	Dachs Ligand with SH3s
Dlp	Dally-Like protein
DNA	Deoxyribonucleic Acid
Dnt	Doughnut on 2
Dpp	Decapentaplegic

Ds	Dachsous
dsRNA	double-stranded RNA
DUB	Deubiquitylating Enzyme
E. coli	Escherichia coli
ECD	extracellular domain
ECM	extracellular matrix
Ed	Echinoid
EGFR	Epidermal Growth Factor Receptor
Egr	Eiger
En	Engrailed
Ena	Enabled
Eph	Eph Receptor Tyrosine Kinase
ErbB4	Erb-B2 Receptor Tyrosine Kinase 4
ESCRT	Endosomal Sorting Complexes Required for Transport
Ex	Expanded
ex::GFP^{ki}	ex::GFP^{knockin}
Ex^{FL}	Ex Full-length
ex^{S453A}	full-length, S453A mutant Ex
ex^{WT}	full-length, wildtype Ex
F-Actin	Filamentous-Actin
FBM	FERM-Binding Motif
FBS	Foetal Bovine Serum
FBXL	F-box and Leucine-Rich Repeat Containing
FBXO	F-box Other
FBXW	F-Box and WD40 Repeat Domain Containing
FERM	4.1 Ezrin Radixin Moesin
Fj	Four-jointed
FLP	Flippase Recombinase
FRET	Forster Resonance Energy Transfer
FRMD6	FERM Domain Containing 6
FRT	Flippase Recombination Target
Ft	Fat
Ft^{ICD}	Ft intracellular-domain
Fz	Frizzled
G1 phase	Gap1-phase
GckIII	Germinal Center Kinase III
GFP	Green Fluorescent Protein
Gish	Gilgamesh
Gli	Glioma Associated Oncogenes
GPCR	G-Protein Coupled Receptor
Gprk2	G protein-coupled receptor kinase 2
Gsk3β	Glycogen Synthase Kinase-3β
GTP	Guanosine Triphosphate
h	hours
HECT	Homologous to E6AP Carboxy Terminus
Herc4	HECT and RLD Domain Containing E3
Hh	Hedgehog
Hpo	Hippo
Hppy	Happyhour
HRE	Hippo-Response Element
hs	heat-shock promoter

Hth	Homothorax
IKK	IκB Kinase
IL-1β	Interleukin 1β
IP	Immunoprecipitation
IOC	Interommatidial Cells
iso	Isoform
IκBα	Nuclear Factor of κ–Light Polypeptide Gene Enhancer in B-Cell
JAMM	JAB1/MPN/MOV34
JNK	c-Jun N-Terminal Kinase
jub	Ajuba LIM Protein
KD	Kinase dead
kDa	kilo Daltons
Kib	Kibra
LATS	Large Tumour Suppressor
LB	Lysogeny Broth
Lft	Lowfat
Lgl	Lethal (2) Giant Larvae
LIM domain	Lin11, Isl-1, Mec3 Domain
LKB1	Liver Kinase B1
LPA	Lysophosphatidic acid
LPS	Lipopolysaccharide
LRP	Low-Density Lipoprotein Receptor-Related Protein
Mad	Mothers Against Dpp
MAP4K	Mitogen-Activated Protein Kinase Kinase Kinase Kinase
MARCM	Mosaic Analysis with a Repressible Marker
Mats	Mob as tumour suppressor
MCP1	Monocyte Chemotactic Protein 1
MCPIP	Monocyte Chemotactic Protein-Induced Protein
Mer	Merlin
MINDY	Motif Interacting with Ubi-Containing Novel DUB Family
mins	minutes
MJD	Machado-Josephin Domain
Mnb	Minibrain
MOB1	Mps-One Binder 1
Moe	Moesin
Mop	Myopic
mRNA	messengerRNA
MS	mass spectrometry
Msn	Misshapen
MST	Mammalian Sterile-20-like Kinase
Myc	Myc proto-oncogene protein
N	Notch
NDR	Nuclear Dbf-2-Related
NDS	Normal Donkey Serum
Nedd8	Neural Precursor Cell-Expressed Developmentally
NEMO	NF-κB Essential Modulator
Neu	Neuralised
NF2	Neurofibromatosis Type-2
NF-kB	Nuclear Factor κ-Light-Chain-Enhancer of Activated B Cell
NLK	Nemo-Like Kinase
Nub	Nubbin

nt	Nucleotide
OTU	Ovarian Tumour Protease
PAGE	Polyacrylamide gel electrophoresis
Par	Partitioning-defective
Patj	Protein Associated to Tight Junctions
Pax3	Paired Box 3
PBM	PDZ-Binding Motif
PBS	Phosphate Buffered Saline
PCNA	Proliferating Cell Nuclear Antigen
PCP	planar cell polarity
PCR	Polymerase Chain Reaction
Per	Period
PKA	Protein Kinase A
PolyUbi	Poly Ubiquitin
PPARγ	Peroxisome Proliferator-Activated Receptor γ
PPi	Pyrophosphate
Ptc	Patched
Put	Punt
Pvr	PDGF and VEGF-Receptor Related Receptor Tyrosine Kinase
Ras	Ras Oncogene at 85D
Rassf	Ras Associated Family
RBR	RING-In-Between-RING
RHO	Ras Homolog
RING	Really Interesting New Gene
Riq	Riquiqui
RISC	RNA-induced silencing complex
RNA	Ribonucleic acid
RNAi / IR	Interference RNA
rpm	revolutions per minute
Rpn	Regulatory Particle of Non-ATPase
Rpt	Regulatory Particle of AAA-ATPase
RT	Room temperature
RUNX	Runt-Related Transcription Factor
s	seconds
S phase	Synthesis- phase
S1P	sphingosine-1-phosphate
SARAH	Sav-RASSF-Hpo
Sav	Salvador
Sax	Saxophone
SBD	Slmb Binding Domain
SCF	S phase kinase-associated protein 1 (skp1) - cullin 1 (cul1) - F-
Schip1	Schwannomin/Mer-interacting protein
Scrib	Scribbled
Sd	Scalloped
SD	Standard Deviation
Sdt	Stardust
Sgg	Shaggy
sgRNA	single guide RNA
Sik	Salt-Inducible Kinase
SJ	Septate Junction
Skp1	S phase kinase-associated protein 1

slmb	supernumerary limbs
Smo	Smoothened
socs36E	suppressor of cytokine signalling at 36E
Spi	Spitz
Stan	Starry Night
STAT	Janus Kinase (JAK)/Signal Transducer and Activator of
STRIPAK	Stratin Interacting Phosphatase and Kinase
SUMO	Small-Ubiquitin-Related Modifier
TAE	Tris-Acetate-EDTA
tAIF	Apoptosis Inducing Factor
TANK	TRAF Family Member-Associated NF-κB Activator
TAZ	Transcriptional Co-Activator with PDZ-Binding Motif
TBST	Tris buffered saline with 0.1% Tween
TBX5	T-Box Transcription Factor 5
TEAD	TEA Domain
TGF	Tissue Growth Factor
Tgi	Tondu-Domain-Containing Growth Inhibitor
Tim	Timeless
Tkv	Thickveins
TM	Trans-membrane
TNF	Tumour Necrosis Factor
TRAF	TNF Receptor Associated Factor
Tsh	Teashirt
TTF-1	Thyroid Transcription Factor 1
UAS	Upstream Activating Sequence
UBA	Ubiquitin Associated Domain
Ub or Ubi	Ubiquitin
UBL	Ubiquitin-Like Proteins
U-box	UFD2 homology
UCH	Ubiquitin C-Terminal Hydrolase
Upd	Unpaired
UPS	Ubiquitin Proteasome System
USP	Ubiquitin-Specific Proteases
UTP	Uridine Triphosphate
Vam	Vamana
Vestigial-like 4	VGL4
Vg	Vestigial
Vn	Vein
Vps26B	Vacuolar Protein Sorting 26B
Vps35	Vacuolar Protein Sorting 35
Wg	Wingless
Wts	Warts
YAP	Yes-Associated Protein
Yki	Yorkie
Zyx	Zyxin

Chapter 1 - Introduction

1.1. The Use of *Drosophila* melanogaster as a Model to Study Tissue Growth

The use of model organisms is vitally important for our understanding of basic biology and human disease. Use of model organisms relies on the premise that most fundamental biological processes are vital to all life, and as such have remained relatively unchanged throughout evolution from simple to complex organisms. Furthermore, due to the relative simplicity of the model organisms used, these fundamental processes are potentially easier to elucidate (Hariharan and Haber 2003). However, no individual model is perfect, and thus our understanding of biology and disease is most efficiently enhanced if studies in human cell lines and tissues, are augmented with the models at our disposal, namely *Saccharomyces cerevisiae* (yeast), *Caenorhabditis elegans* (worm), *Danio rerio* (zebra fish), *Mus musculus* (mouse) and last but not least, *Drosophila melanogaster* (fruit fly) (Hunter, 2008).

Drosophila melanogaster has remained one of the primary animal models since the early twentieth century, when T. H. Morgan, along with notable students A. H. Sturtevant, C. B. Bridges, and H. J. Muller defined the theory of chromosomal heritability, which led to Morgan being awarded the Nobel Prize in Physiology or Medicine in 1933 (Morgan, 1910). This power house of early genetics went on to define how genes are arranged in a linear order (Sturtevant, 1913), that genes are contained within the chromosome (Bridges, 1916), and that ionising radiation causes genetic damage, which resulted in H. J. Muller receiving the Nobel Prize in Physiology or Medicine in 1946 (Muller, 1928; Rubin and Lewis, 2000).

Since the early days of *Drosophila* research, a vast array of transgenic and mutant stocks, and genetic tools have become available making the fruit fly one

of the most genetically tractable model organisms. These techniques include the development of transgenic organisms (Rubin and Spradling, 1982; Spradling and Rubin, 1982), clonal/mosaic mutation analysis (Lee and Luo, 1999; Xu and Rubin, 1993), a tissue-specific bipartite expression system (Brand and Perrimon, 1993), genome-wide Interference RNA (RNAi) libraries (Dietzl et al., 2007; Perrimon et al., 2010), and more recently, the development of the Clustered Regularly Interspaced Palindromic Repeats (CRISPR)/CRISPR associated (Cas) technology (Port et al., 2014).

The *Drosophila* genome contains approximately half the number of genes compared to humans. The haploid genome consists of four chromosomes: one sex chromosome (chromosome 1), and three autosomes (chromosomes 2-4). The sequencing of the *Drosophila* genome in the year 2000 (Adams et al., 2000) confirmed the benefits of the fly as a model, as at least 70% of genes known to be involved in human pathologies are conserved in flies (Reiter et al., 2001). It is this evolutionary conservation, associated with low chromosome number, rapid life cycle, high fecundity and ease of maintenance, that make the fly an ideal model organism for the study of fundamental biology and disease.

Drosophila undergo dramatic morphological changes during their lifetime. Initially, rapid development occurs in the embryo, which after 24 hours hatches into the first instar larva. Larvae grow rapidly, moulting twice to form the third instar larva. During larval growth, all adult structures, whether ultimately located internally or externally, develop precursor counterparts within the protective larval cuticle. Once mature, the third instar larva will crawl from the food to pupate, forming a protective pupal case. Within the hard pupal case, the pupa undergoes metamorphosis, and most larval tissue disintegrates, dramatically reorganising the body plan from that of a larva, to the adult fly. The pupa will eventually eclose and emerge from the pupal case, after which the exoskeleton hardens, and the wings expand, and after only a short time, the animal is ready to mate and restart the cycle (Beira and Paro, 2016; Jennings, 2011).

The larval imaginal discs are of particular note, and form the precursors to many of the external adult appendages, including the eyes, wings, legs and halteres. These imaginal discs are derived from clusters of cells within the embryo that invaginate from the epidermal sheet, and become sac-like structures of single columnar epithelial tissue (Bate and Arias, 1991). The larger discs, the wing, leg and eye, proliferate exponentially from 20-50 cells to a final size of 20,000-50,000 cells (Bryant and Simpson, 1984; Garcia-Bellido, 1975; Hufnagel et al., 2007). The development of these structures is remarkably autonomous, as demonstrated through transplantation experiments, where immature larval imaginal discs grow to approximately the correct size and shape, when inserted into an adult abdomen (Bryant and Levinson, 1985). Due to this rapid and autonomous growth phase, the ease of dissection and imaging, and the genetic tools available for tissue specific manipulation, the imaginal discs are an excellent model to study the regulation of tissue growth, and as such will be used extensively in this thesis.

Indeed, much of what is known about growth and organ size control has involved the study of these *Drosophila* imaginal discs. In terms of growth, it seems likely that the basal state for unicellular organisms is one of constant proliferation, which is almost entirely dependent on nutritional supply (Edgar, 2006). With the evolution of more complex multi-cellular organisms, a degree of altruistic behaviour at the level of the individual cell was acquired. This allowed the construction of highly intricate body plans, which are homeostatically maintained throughout the life of that organism. In terms of tissue growth, at the cellular level this altruistic behaviour requires cooperation between cell growth and proliferation, as well as cell death, demanding complex interactions between many cells (Edgar, 2006). How the intrinsic property of cell growth is coordinated across an entire organ is a complex procedure involving only a handful of dynamic, integrated and plastic signalling pathways. These pathways integrate both through a ‘top-down’ mechanism of regulating growth, that is, an organising signalling centre to coordinate growth across the whole tissue, and ‘bottom-up’ mechanisms, in which local interactions of cells sense the intrinsic properties of

the tissue ultimately regulating proliferation. A balance between these two appears to occur, culminating in the precise regulation of final organ size (Hariharan, 2015).

One of the key signalling pathways involved in the regulation of cell growth is the conserved Hippo Pathway, which will be discussed in detail in 'The Tumour Suppressor Hippo Pathway'.

1.2. **The Ubiquitin System**

1.2.1. The Machinery of Ubiquitylation

The dynamic relationship between protein synthesis and degradation is key to most cellular processes. Prior to the discovery of the lysosome and the ubiquitin-proteasome-system (UPS) it was believed that proteins were stable components of the cell, and dietary uptake compensated for the natural breakdown of proteins over time (Ciechanover, 2012). In the 1950s, the lysosome was discovered and was considered *the* mechanism for protein degradation (De Duve et al., 1953). However, subsequent studies challenged this paradigm, including the observation that protein half-lives vary; that, in certain contexts, lysosomal inhibitors did not affect degradation of intracellular proteins and that proteolysis was an Adenosine Triphosphate (ATP)-dependent process (Ciechanover, 2012). This led to the initial discovery of the UPS (Ciechanover et al., 1978), which suggested that lysosome-independent protein degradation required two complementary features, a protease component (subsequently identified as the proteasome) and a heat–stable protein (later identified as ubiquitin) (Ciechanover, 2012). This discovery resulted in Ciechanover, Hershko and Rose being awarded the Nobel Prize for Chemistry in 2004.

Ubiquitin (Ubi) is a small, highly stable protein of 76 amino acids (8.5 kilo Daltons (kDa)) that is conserved throughout eukaryotic organisms, with only three minor changes from yeast to humans (Komander and Rape, 2012). Ubi contains a C-

terminal glycine residue that mediates its covalent linkage, typically to the side chain of lysine residues present in protein substrates. Importantly, Ubi itself can be subjected to post-translational Ubi conjugation, through several exposed lysine residues, and the N-terminal methionine. This facilitates the formation of polyubiquitin (polyUbi) chains, which are vital to the function of Ubi as a post-translational modification.

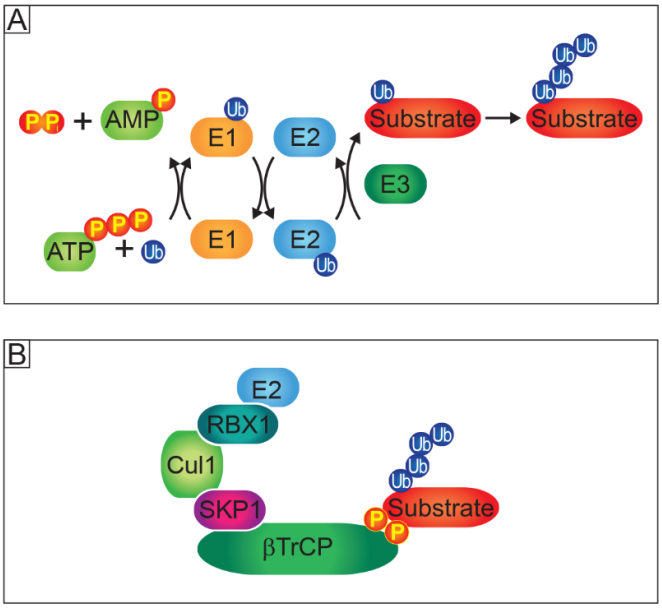

Figure 1-1 The Ubiquitylation system

Schematic representations of the ubiquitin conjugation pathway (A) and a generic SCF- β-*TrCP* complex (B). See text for details.

Ubi conjugation to substrates is a three-step process. Firstly, Ubi activating enzymes (E1s) activate the C-terminal glycine of Ubi in a two-step reaction. Initial formation of a Ubi-adenylate intermediate facilitates formation of a high energy thio-ester bond between the C-terminus of Ubi, and a cysteine of the E1 enzyme, which requires the breakdown of one ATP molecule into Adenosine

Monophosphate (AMP) and Pyrophosphate (PPi) (Pickart and Eddins, 2004). Activated Ubi, bound to the E1 is then transferred to a cysteine residue on the Ubi conjugating enzyme (E2). The Ubi ligases (E3s) provide the final link in the ubiquitylation machinery by promoting the transfer of Ubi from the E2 to a lysine or the N-terminal methionine residue of the substrate, forming an isopeptide bond (Figure 1-1A) (Komander and Rape, 2012; Pickart and Eddins, 2004). Humans contain only two E1s, approximately 30 E2s, but hundreds of E3s, most of which can modify multiple substrates, this stratification in the distribution of the Ubi conjugating enzymes allows ubiquitylation of a vast number of substrates with a high degree of specificity (Pickart and Eddins, 2004; Skaar et al., 2013). At least 80% of proteins are targeted by ubiquitin highlighting the diversity of substrates recognised, and the importance of the ubiquitylation system (Yen et al., 2008).

As alluded to, an important feature of the UPS is that within Ubi, at least seven lysine residues, and the N-terminus can be targeted for ubiquitylation: M1, K6, K11, K27, K29, K33, K48 and K63. The specific residue targeted, the subsequent Ubi chain length and the branching of these polyUbi chains are all important determinants of the fate of the protein substrate. The array of varied Ubi chain types helps explain the large number of biological outputs of ubiquitylation beyond proteasomal degradation, which include the regulation of lysosomal degradation, protein-protein interactions, protein activity and protein localisation (Komander and Rape, 2012).

1.2.2. E3 Ligases

The E3 ligases are a large and varied collection of genes, which can be grouped into four families: Homologous to E6AP Carboxy Terminus (HECT), Really Interesting New Gene (RING), UFD2 homology (U-box) and RING-In-Between-RING (RBR) proteins, which employ different mechanisms to recognise and ubiquitylate their substrates. Unlike other E3s, HECTs accept the activated Ubi from the E2 and form an intermediate thioester bond between Ubi and a catalytic cysteine residue. Large conformational changes are required to transfer the Ubi

from the E2 to the HECT E3, which is facilitated by a flexible hinge between the C-terminal HECT domain and the N-terminal E2 interaction region (Metzger et al., 2012; Pickart and Eddins, 2004). Determination of chain topologies is not well understood, although it appears to involve specific interactions between the HECT protein, the E2 and Ubi itself (Komander and Rape, 2012). RING and U-box E3s assist the direct transfer of activated Ubi from E2s to the substrate, bridging the E2 to the substrate lysine (Pickart and Eddins, 2004). U-box E3s coordinate the transfer of activated Ubi with hydrogen-bonds and salt-bridges, whereas RING E3s use zinc ions coordinated by zinc finger domains (Metzger et al., 2012; Pickart and Eddins, 2004). RBR E3s are hybrids of RING and HECTs, using a RING domain to recruit the E2 enzyme, which transfers activated Ubi to a cysteine in the RING-like domain forming a thioester intermediate (Komander and Rape, 2012). RING proteins can be monomers, dimers or multi-subunit complexes (Komander and Rape, 2012; Metzger et al., 2012). Interestingly, the polyUbi chain topology created by the RING or U-box proteins is specified by the E2 enzymes, and not the E3s. If the E3 can bind multiple E2s, this E3 will be able to catalyse the construction of multiple Ubi chain topologies. If the E3 binds to one specific E2, then it is likely that only one Ubi chain type can be created (Komander and Rape, 2012; Ye and Rape, 2009).

1.2.3. F-box E3 Ligases

The cullin-RING-ligase family complexes form a large group of the modular RING E3 ligases, the S phase kinase-associated protein 1 (Skp1) - Cullin 1 (Cul1) - F-box (SCF) complexes being the best characterised, and most important to this study (Petroski and Deshaies, 2005; Skaar et al., 2013). SCF complexes contain the catalytically inert Cul1 scaffold, which bridges the RING protein Rbx1 with Skp1, which in turn binds to an F-box subunit, which confers substrate specificity (Figure 1-1B) (Skaar et al., 2013). F-box proteins can be subdivided into three classes, the F-Box and WD40 Repeat Domain Containing (FBXW), the F-box and Leucine-Rich Repeat Containing (FBXL) and the remaining F-box Other (FBXO) class (Skaar et al., 2013). Each class of F-box proteins contain C-terminal

protein-protein interaction motifs that are important for substrate recognition (Fuchs et al., 2004). In the canonical model, F-box proteins recognise their substrates through recruitment to a phosphorylated degradation motif or phosphodegron (Skaar et al., 2013). Phosphodegrons can be substrates for multiple kinases, or require priming phosphorylation, which creates a hierarchical sequence of phosphorylation events, leading to F-box recruitment. Importantly, these phosphodegrons are also subject to the action of phosphatases, which inhibits the function of the SCF complex and subsequent target ubiquitylation (Skaar et al., 2013). Variations on this phosphodegron include the substitution of the S/T residue with a phosphomimetic amino acid, such as aspartate or glutamate (Skaar et al., 2013). The delicate and precise regulation of substrate status allows for very accurate regulation of F-box binding, and therefore ubiquitylation, providing the cell with excellent control of protein dynamics. In addition to the canonical phosphodegron sequences, many other degrons exist, for example, unmodified degrons, cofactor-dependent degrons, restricted access degrons (which require conformational change of the substrate to expose the degron sequence) and inducible, non-covalent degrons to name a few (Skaar et al., 2013).

An F-box protein of particular relevance to this study is *Drosophila supernumerary limbs (slmb)*, the orthologue of the mammalian β-*transducin repeats-containing protein* (β-*TrCP*). Slmb/β-TrCP is a FBXW family protein, containing an N-terminal F-box motif, and seven C-terminal WD40 repeats, interacting with phosphorylated substrates conforming to a canonical $DpSGX_{(1-2)}pS$ phosphodegron motif, although the space between the G and the C-terminal pS may extend further than two amino acids in some instances (Fuchs et al., 2004; Skaar et al., 2013). Upon substrate phosphorylation and recognition by Slmb/β-TrCP, the SCF complex targets substrates for ubiquitylation and degradation via the proteasome (Fuchs et al., 2004). Slmb/β-TrCP is involved in a large number of vital cellular processes, including NF-kB (Nuclear Factor κ-Light-Chain-Enhancer of Activated B Cell), Wnt and Hedgehog (Hh) signalling and the cell cycle among others (Frescas and Pagano, 2008; Fuchs et al., 2004). In

Drosophila, *slmb* directly regulates the stability of Armadillo (Arm), Cubitus interruptus (Ci) (Jiang and Struhl, 1998), Period (Per) (Grima et al., 2002; Ko et al., 2002), Polo-like-kinase-4 (Klebba et al., 2013) and Oskar (Morais-de-Sa et al., 2013) highlighting the range of functions *slmb* is involved in. Moreover, *slmb* has recently been identified as a regulator of the Hippo pathway component Expanded (Ex) interacting with both N-terminal and C-terminal phosphodegrons (Ribeiro et al., 2014; Zhang et al., 2015a), and the regulation of this interaction will be the main focus of this study. It is important to note that Slmb recognises phosphorylated substrates, as is normal for F-box proteins, and this aspect will be discussed in more depth in 'Results 3 – The Role of Casein Kinase 1 Family Kinases in the Regulation of Expanded'.

1.2.4. Deubiquitylating Enzymes

Like many protein post-translational modifications, ubiquitylation is a reversible process. Deubiquitylating Enzymes (DUBs) act analogously to phosphatases, their function being divided into three categories: generation of free Ubi molecules from polyUbi precursor genes, often co-translationally; removal of Ubi from post-translationally modified proteins, thereby reversing the Ubi-chain signal; and editing of Ubi chain length and/or type to alter the Ubi-chain signal (Komander et al., 2009; Reyes-Turcu et al., 2009).

There are approximately one hundred DUBs in the human genome, although not all are predicted to be catalytically active, and can be broken down into seven families. Five DUB families are composed of papain-like cysteine proteases: the Ubiquitin C-Terminal Hydrolases (UCHs), Ubiquitin-Specific Proteases (USPs), Ovarian Tumour Proteases (OTUs), the Machado-Josephin Domain (MJD) and the recently discovered Motif Interacting with Ubi-Containing Novel DUB Family (MINDY) (Abdul Rehman et al., 2016; Kristariyanto et al., 2017) DUBs. The sixth family, the JAB1/MPN/MOV34 metalloenzymes (JAMMs) are dependent on zinc ions to coordinate their enzymatic activity (Komander et al., 2009; Reyes-Turcu et al., 2009). The Monocyte Chemotactic Protein-Induced Proteins (MCPIPs)

DUBs remain a controversial group without definitive DUB activity (Fraile et al., 2012). Most of these DUBs rely on two or three crucial amino acid residues constituting a catalytic diad or triad motif (Komander et al., 2009).

Ubi chain cleavage can occur in various ways, some DUBs having exo-deubiquitylating activity, removing Ubi from the end of a chain, some have endo-deubiquitylating activity, cleaving an isopeptide bond from within a Ubi chain. Other DUBs selectively remove mono-Ubi directly from the substrate rather than from within the Ubi chain. DUBs can also be highly specific to certain Ubi chain topologies, others being unspecific in their chain selection, rather, specificity is conferred by substrate interactions (Komander et al., 2009; Reyes-Turcu et al., 2009).

DUBs must be very tightly regulated in order to limit their protease capacity to a specific set of substrates. In order to prevent non-specific protease activity, the DUB catalytic site is often not easily accessible to the substrate, with *in vitro* enzymatic capacity of DUBs being very low, suggesting high levels of regulation in order to confer full activity and specificity (Komander et al., 2009). Ubi binding is often an important step in exposing the DUB active site, the interaction between DUB and Ubi covering 20-40% of the surface of Ubi, driving rearrangements necessary for access to the active site. These interactions are far in excess of a conventional Ubi-Ubi binding interaction domain, which would normally cover only 10% of the Ubi surface (Komander et al., 2009; Reyes-Turcu et al., 2009). The nature of the isopeptide Ubi-Ubi bond also prevents spurious DUB activity, the conventional peptide bond having a much lower degree of rotational freedom when compared to the isopeptide bonds commonly targeted by DUBs (Komander et al., 2009).

The activity of DUBs is also regulated by the intrinsic structure of DUBs, which contain multiple variations in the N- and C-terminal regions to the catalytic domain. These are involved in Ubi binding and protein-protein interactions, which are key to enzymatic activation and also the recognition of specific substrates

and chain topologies (Komander et al., 2009; Reyes-Turcu et al., 2009). These domain interactions help determine DUB specificity by localising the proteins to the correct cellular compartment, and by enabling interactions with adaptors or scaffold proteins, which can bridge the DUB with the correct substrate. Certain DUBs can also be highly transcriptionally regulated, only being expressed within a very specific temporal window limiting excessive activity. Moreover, as with most proteins, DUBs are post-translationally modified by phosphorylation and ubiquitylation, and these can either activate or inhibit DUB activity or substrate recognition, adding a further level of regulation to prevent incorrect action of these enzymes (Komander et al., 2009; Reyes-Turcu et al., 2009). The importance of these layers of regulation is highlighted by the fact that DUBs often work in multi-protein complexes, for example, within the proteasome, or within the Endosomal Sorting Complexes Required for Transport (ESCRT) complex during endocytosis, where adaptor/scaffold binding provides the DUBs with relevant substrates. Moreover, DUBs can be directly coupled to E3 ligases, which can often auto-ubiquitylate themselves, therefore helping to sustain E3 activity. These E3 can also regulate their cognate DUB, suggesting trans-regulation between the E3 and DUB is highly controlled, with precise regulation of ubiquitin signalling being commonplace. This interaction between DUB and E3 ligase is also important for Ub chain topology editing, thus changing the fate of the substrate protein (Komander et al., 2009; Reyes-Turcu et al., 2009).

1.2.5. The Proteasome

A diverse range of outcomes exist for ubiquitylated proteins, depending on the polyUbi chain length and branching. Tied up with the initial identification of ubiquitin as a post-translational modification is the proteasome, and ubiquitin-mediated proteasomal degradation (Ciechanover, 2012). Key to this process is polyubiquitylation, particular through polyUbi chains consisting of K48 linkages, although K11, K29 and K63 have been reported to be proteasome-targeting (Komander and Rape, 2012). The reason for certain Ubi linkages targeting

substrates to the proteasome and not others remains unclear (Komander and Rape, 2012).

The proteasome is a large, cylindrical, multi-protein complex responsible for the hydrolysis and degradation of a vast array of proteins in an ATP-dependent manner (Ciechanover, 2012; Tanaka, 2009). Structurally, the proteasome consists of a core 20S unit, consisting of two cylinders of 4 rings stacked on top of each other, each ring made from seven individual subunits (Adams, 2003; Tanaka, 2009). The two inner rings (β-rings) are the catalytic core of the proteasome each containing three active threonine protease units: a trypsin-like, a chymotrypsin-like and a post-glutamyl peptide hydrolase, which cleave peptides at the C-terminus of basic, hydrophobic and acid amino acids respectively (Adams, 2003; Tanaka, 2009). This degrades the protein chains entering the proteasome into small polypeptide chains, which are degraded into individual amino acids upon entering the cytosol. The outer rings (α-rings) of the 20S core bind the 19S regulatory subunit and facilitate the passage of denatured proteins through the 20S β-rings. In isolation, this 20S subunit of the proteasome is catalytically latent, and is only active upon interaction with one or two 19S units, forming either the 26S or 30S proteasome (Adams, 2003; Tanaka, 2009). The 19S regulatory particles contain two distinct subunits, the Regulatory Particle of AAA-ATPase (Rpt) subunits, and Regulatory Particle of Non-ATPase (Rpn) subunits. Upon binding to the 20S core, the Rpt AAA-ATPase of the 19S unit helps capture client proteins, and drive the substrate unfolding into the 20S unit, consuming ATP in the process. The Rpns serve to deubiquitylate captured polyUbi substrates (Adams, 2003; Tanaka, 2009).

1.2.6. Functions of Ubiquitylation

Regulation of protein turnover by ubiquitylation and proteasomal degradation has wide reaching consequences for cellular dynamics. Rather than simply removing proteins from the cell, the active protein turnover performed by the UPS is crucial in the regulation of many cellular functions. For example, proteasomal turnover

of proteins helps to fine tune signalling pathways either resulting in their activation or inhibition, illustrated by ubiquitylation and activation of the NF-κB pathway, via phosphorylation-mediated ubiquitylation and degradation of the NF-κB inhibitor IκBα (Nuclear Factor of κ–Light Polypeptide Gene Enhancer in B-Cell Inhibitor-α) (Komander and Rape, 2012). Alternatively, degradation of substrates can inhibit signalling, as is the case in Wnt signalling, where β-Catenin, an adhesion protein that is also involved in modulation of transcription in the nucleus, is constitutively degraded in the absence of signalling by a destruction complex that includes β-TrCP (Aberle et al., 1997; Jiang and Struhl, 1998). An interesting example can be seen in Hh signalling, where the main effector Gli (Glioma Associated Oncogenes) the mammalian orthologue of Ci, is partially degraded by the proteasome, thereby transforming this transcriptional activator into a transcriptional repressor (Jiang and Struhl, 1998; Price, 2006).

However, ubiquitylation does not simply target proteins for proteasomal degradation. Ubiquitylation can also help degrade proteins through the lysosome, regulate the endocytic pathway, as well as modulating protein-protein interactions, protein activity and localisation (Chen and Sun, 2009; Komander and Rape, 2012; Mukhopadhyay and Riezman, 2007). In the case of the endocytic pathway and lysosomal degradation, mono-ubiquitylation or K63 chain formation of plasma membrane proteins can drive internalisation and endocytosis (Komander and Rape, 2012; Mukhopadhyay and Riezman, 2007). The Epidermal Growth Factor Receptor (EGFR) is a prime example of this, as ubiquitylation of its cytoplasmic domain can drive entry of EGFR into endocytic vesicles, which modulates downstream signalling (Mukhopadhyay and Riezman, 2007). Experimental evidence also suggests that Ubi-mediated endocytosis enables EGFR-mediated signalling within the endosome, or drives lysosomal degradation (Komander and Rape, 2012; Mukhopadhyay and Riezman, 2007).

Ubiquitylation can also influence protein-protein interactions through various ubiquitin binding domains, for example in the regulation of Deoxyribonucleic Acid (DNA) replication and damage response (Chen and Sun, 2009; Komander and

Rape, 2012). The Proliferating Cell Nuclear Antigen (PCNA) helps orchestrate normal DNA replication, the response to DNA damage and DNA replication surveillance (Mailand et al., 2013). Upon DNA damage during replication, monoUbi PCNA promotes interaction with the lesion bypass Y-family polymerase resulting in trans-lesion DNA synthesis. However, generation of polyUbi PCNA chains promotes DNA template switching and error free replication (Mailand et al., 2013). Ubiquitylation can also negatively regulate protein interactions, either with other proteins, as in the case of the Smad4:Smad2 interaction, or with important signalling co-factors, as in the case of Met4 (Komander and Rape, 2012). Moreover, M1 ubiquitylation of NF-κB Essential Modulator (NEMO) can even drive the allosteric activation of IκB Kinase (IKK), suggesting ubiquitylation can directly influence activation of proteins (Komander and Rape, 2012). Ubiquitylation can also affect protein localisation, beyond the endocytic internalisation discussed above, as in the case of p53, where ubiquitylation controls nuclear localisation (Komander and Rape, 2012).

Just as E3 ligases are analogous to kinases as post-translational modifiers, DUBs are analogous to phosphatases, with most of the E3 ligases being antagonised on some level by DUBs. Therefore, just as E3s can regulate protein turnover, signalling and protein localisation to affect many biological processes, so too can DUBs, whether it be in reversing the Ubi-chain signal by removing a poly-Ub chain, perpetuating E3 ligase activity by reversing auto-ubiquitylation, or helping to change Ubi signals by allowing Ubi-chain editing (Komander et al., 2009; Reyes-Turcu et al., 2009). The importance of ubiquitylation is evident with multiple components of the ubiquitylation machinery, including DUBs and E3s, being mutated or altered in many diseases, including cancer and neurodegenerative diseases (Popovic et al., 2014). It is curious to note that whilst there are many hundreds of E3s, there are only approximately one hundred DUBs. This is perhaps reflective of the capacity of DUBs to recognise and enzymatically cleave Ubi-chains independently of the substrate, unlike E3 ligases, which predominantly require substrate recognition (Isono and Nagel, 2014).

1.2.7. Ubiquitin-Like Proteins

In addition Ubiquitin-Like Proteins (UBLs) are members of the Ubi family, which encompasses nearly 20 proteins. The UBLs regulate a distinct set of biological processes from canonical Ubi conjugation, and are involved in nuclear transport, translation, autophagy and antiviral signalling (van der Veen and Ploegh, 2012). Small-Ubiquitin-Related Modifier (SUMO), and Neural Precursor Cell-Expressed Developmentally Downregulated 8 (Nedd8) are two of the best characterised classes of UBLs, Nedd8 sharing the highest homology to Ubi, and are subject to substrate conjugation by specific ligases and deconjugation by proteases (van der Veen and Ploegh, 2012). In this thesis, several UBL proteases were assessed for their potential regulation of tissue size in the *Drosophila* wing.

1.2.8. Concluding Remarks

Ubiquitylation is involved in an enormous array of biological functions, including the regulation of signalling pathways. In this study, the mechanism of ubiquitylation and deubiquitylation of the *Drosophila* tumour suppressor Expanded, a component of the Hippo pathway, known to be regulated by the E3 ligase Slmb, will be discussed (Ribeiro et al., 2014; Zhang et al., 2015a). In addition, the ability of DUBs to regulate tissue growth through an RNAi screen in *Drosophila* adult wings was assessed.

1.3. The Tumour Suppressor Hippo Pathway

In multicellular organisms, the regulation of growth requires an exquisite balance between cell proliferation and cell death, and the temporal and spatial regulation of these processes is vital for development and maintenance of adult homeostasis. The mechanisms involved in limiting excess proliferation and growth long remained a mystery. However, the development of a technique to generate genetic mosaics in *Drosophila* led to the rapid discovery of many genes involved in these growth regulatory pathways (see 2.3.6 – ‘The FLP/FRT

System') (Xu and Rubin, 1993). Genetic screens using this technique allowed the identification of genes that, when mutated, caused excessive proliferation and tumourigenic phenotypes, but that in the context of the whole animal, would otherwise be lethal.

Many of the genes identified were later recognised as being members of a highly conserved tumour suppressive pathway, coined the 'Hippo pathway', due to the fact that mosaic mutant animals displayed overgrown and folded cuticle, thereby resembling the creased hide of the hippopotamus (Udan et al., 2003). The importance of this pathway in development is highlighted firstly, by the ancient nature of pathway orthologues, which predate the evolution of multicellular metazoa (Sebe-Pedros et al., 2012), and secondly, by their highly conserved nature throughout most animal species, including vertebrates (Bossuyt et al., 2014; Meng et al., 2016).

1.3.1. The Core Hippo Pathway Kinase Cassette

Large-scale genetic screens aimed at identifying tumour suppressor genes initially led to the discovery of the Nuclear Dbf-2-Related (NDR) kinase *warts (wts)* (Justice et al., 1995; Xu et al., 1995), whose name derives from the fact that mutant *wts* clones create 'wart'-like growths of proliferative cells. Later screens isolated three additional genes, *salvador (sav)* (Kango-Singh et al., 2002; Tapon et al., 2002), *hippo* (*hpo)* (Harvey et al., 2003; Jia et al., 2003; Pantalacci et al., 2003; Udan et al., 2003; Wu et al., 2003) and *mob as tumour suppressor (mats)* (Lai et al., 2005) whose clonal phenotypes are remarkably similar to *wts*. Mutant cells are able to proliferate faster than wild-type cells, with increased cell growth and cell cycle progression. Moreover, in the eye, mutations in these genes cause a dramatic increase in the number of interommatidial cells (IOCs). During development, the IOCs are produced in excess, and then removed by a wave of apoptosis to create the highly ordered retina (Cagan and Ready, 1989; Edgar, 2006; Miller and Cagan, 1998). As mutations in *hpo*, *sav*, *wts* or *mats* all prevent IOC elimination, part of the normal function of these genes is to promote

apoptosis within the eye. Accordingly, mutant cells for any of these genes cause an autonomous transcriptional upregulation of the *cyclin-E (cycE)* and *drosophila inhibitor of apoptosis-1 (diap1)* genes, which promote cell cycle progression and apoptosis resistance, respectively (Harvey et al., 2003; Pantalacci et al., 2003; Tapon et al., 2002; Udan et al., 2003; Wu et al., 2003). Genetic epistasis experiments place *wts* downstream of *hpo*, putatively identifying a hierarchical kinase cascade, involved in limiting tissue growth (Harvey et al., 2003; Jia et al., 2003; Udan et al., 2003; Wu et al., 2003).

Hpo, Sav, Mats and Wts form the core Hippo pathway cassette whereby the two serine/threonine (S/T) kinases Hpo and Wts are sequentially phosphorylated and activated. The elucidation of the molecular mechanisms involved in the activation of the core kinase cassette has been greatly aided by biochemical and structural analyses performed on the highly homologous mammalian orthologues *Mammalian Sterile-20-like Kinase 1/2* (*MST1/2*; *hpo* orthologues), and *Large Tumour Suppressor* (*LATS1/2*; *wts* orthologues), along with the adaptor proteins *SAV1* (*sav* mammalian orthologue) and the mammalian *mats* orthologue Mps-one Binder 1 *(MOB1)*. The high level of homology is such that, overgrowth in a *hpo* mutant eye can be recovered by *MST2* overexpression (Wu et al., 2003). The first step in the kinase cascade is the activation of Hpo (by MST1/2 heterodimerisation in mammals), either through phosphorylation at T195 within the activation loop by the Sterile-20-like Tao-1 (Boggiano et al., 2011; Poon et al., 2011), or by autophosphorylation (Glantschnig et al., 2002; Lee and Yonehara, 2002; Ni et al., 2015; Pantalacci et al., 2003; Udan et al., 2003). Activated Hpo then interacts with, and phosphorylates Sav, Mats and Wts (Callus et al., 2006; Chan et al., 2005; Hirabayashi et al., 2008; Ni et al., 2015; Praskova et al., 2008; Wei et al., 2007; Wu et al., 2003), where Sav acts as a scaffold bridging Hpo and Wts (Wu et al., 2003), while Mats acts as a Wts activating co-factor primarily at the cell membrane (Hergovich et al., 2006; Ho et al., 2010; Lai et al., 2005). Full kinase activity of Wts occurs upon Hpo-mediated phosphorylation of the hydrophobic motif at T1077A (Yu et al., 2010), and activation loop autophosphorylation (Staley and Irvine, 2012; Wei et al., 2007).

These studies proposed that Hpo/MST phosphorylation is essential for Mats/MOB allosteric modulation of Wts/LATS (Ni et al., 2015).

Despite these data revealing the activation mechanism of this core kinase cassette, a recent study suggested Hpo phosphorylation is not necessary for the allosteric modulation of Wts. In *Drosophila*, the use of a 'Wts-FRET (Forster Resonance Energy Transfer) sensor' proposed that Wts conformation is modulated by Mats independently from Hpo, with Mats binding driving Wts into an open conformation, which allows Wts to be then phosphorylated by Hpo to confer full Wts activity (Vrabioiu and Struhl, 2015). The mechanisms proposed in these biochemical and *in vivo* studies can be unified if Mats is considered to allosterically modulate Wts both before and after Hpo-mediated phosphorylation of Wts and Mats to fully activate Wts (Manning and Harvey, 2015).

Neither Vrabioiu *et al.*, or Ni *et al.* address how Sav interacts with Wts/LATS at the direct structural level, and this remains an open question. Sav contains two WW domains, responsible for the interaction with Wts, the WW domain being a protein-protein interaction motif containing two highly conserved tryptophan residues, which specifically interacts with the proline-rich PPxY motifs, and define many of the Hippo pathway interactions (Salah and Aqeilan, 2011; Tapon et al., 2002). Sav also contains a C-terminal SARAH (Sav-RASSF-Hpo) domain responsible for Hpo binding (Callus et al., 2006; Harvey et al., 2003; Jia et al., 2003; Lee et al., 2008; Pantalacci et al., 2003; Scheel and Hofmann, 2003; Wu et al., 2003). Sav is also inherently unstable, and is stabilised through interactions with Hpo (Pantalacci et al., 2003), which prevents Sav ubiquitylation by the E3 ligase Herc4 (HECT and RLD Domain Containing E3) and subsequent proteasomal degradation (Aerne et al., 2015).

Data obtained in mouse embryonic fibroblasts suggests induction of LATS activation loop phosphorylation at high cell density is independent of MST (Zhou et al., 2009). This led to the discovery of two new S/T kinases, and the expansion of the Hippo kinase cassette to include *Drosophila* Happyhour (Hppy) and

Misshapen (Msn), mammalian MAP4K1/2/3/5 and MAP4K4/6/7 respectively, all part of the MAP4K family (Mitogen-Activated Protein Kinase Kinase Kinase Kinase) (Li et al., 2014a; Li et al., 2015; Meng et al., 2015; Zheng et al., 2015). These kinases directly phosphorylate and activate Wts/LATS in a partially redundant manner (Meng et al., 2015; Zheng et al., 2015). The specific context for when Wts/LATS is regulated by Hpo, Hppy or Msn remains to be thoroughly investigated, but it may be tissue, temporally or input specific.

1.3.2. Yorkie – A Warts Substrate

Early studies of the Hippo pathway focused on identifying tumour suppressors, but how these genes directly inhibited tissue growth remained elusive. In order to identify substrates of Wts that controlled growth, a yeast-two-hybrid screen using the N-terminal portion of Wts as bait, led to the identification of the WW domain-containing protein Yorkie (Yki), the orthologue of the mammalian Yes-Associated Protein (YAP), as the downstream effector of the Hippo pathway (Huang et al., 2005). Overexpression of *yki* is able to phenocopy *hpo* or *wts* loss of function mutations, recapitulating tissue overgrowth and apoptosis through upregulating *cycE* and *diap1* respectively (Huang et al., 2005). Moreover, *yki* mutation results in tissue undergrowth, even when *wts* is also mutated, placing *yki* downstream of *hpo, sav* and *wts* (Huang et al., 2005).

Initial experiments showed that Yki was indeed a Wts substrate (Huang et al., 2005), which is primarily phosphorylated at S168, a serine residue conserved in YAP (S127) (Dong et al., 2007; Oh and Irvine, 2008). Wts phosphorylates Yki at three sites (S111, S168, S250), whereas LATS phosphorylates YAP at five sites (S61, S109, S127, S164 and S381) (Hao et al., 2008; Oh and Irvine, 2009; Zhao et al., 2007), and while all of these conform to the Wts/LATS HXRXXS consensus sequence, the S168/S127 site appears to be the most important site for growth regulation (Dong et al., 2007; Oh and Irvine, 2008, 2009; Zhao et al., 2007). Overexpression of a non-phosphorylatable Yki^{S111A}, Yki^{S168A} and Yki^{S250A} transgenes in *Drosophila* causes overgrowth phenotypes compared to wildtype

Yki overexpression, with the Yki^{S168} being the most important for growth (Dong et al., 2007; Oh and Irvine, 2008). Interestingly, unlike in *Drosophila* where mutations disrupting the Yki^{S168} phosphorylation site are homozygous lethal (Zhao et al., 2007), a mutation in the mouse YAP^{S112}, equivalent to human YAP^{S127} does not affect normal development and only results in tissue overgrowth when subjected to stress (Chen et al., 2015). Therefore in mammals, it appears the existence of the additional LATS phosphorylation sites facilitates robust and compensatory inhibition of YAP (Chen et al., 2015). Moreover, this helps explain the increased severity of phenotypes when expressing a YAP^{S5A} construct, containing S>A point mutations in all the LATS sites (Zhao et al., 2007).

The region surrounding the S168 Wts phosphorylation site in Yki conforms to the 14-3-3 family protein binding site consensus sequence RXXpSXP, and thus, Wts phosphorylation induces interaction between Yki and 14-3-3, which serves to sequester Yki in the cytosol (Oh and Irvine, 2008, 2009). This mechanism of regulating Yki localisation is conserved in mammals, LATS phosphorylating YAP controlling the interaction with the 14-3-3 protein (Zhao et al., 2007). Interestingly, in addition to LATS, Akt can also phosphorylate YAP at S127, thus controlling its localisation (Basu et al., 2003). Prior to the delineation of the Hippo pathway, YAP was identified as a transcriptional co-activator (Yagi et al., 1999). Therefore, exclusion from the nucleus is a potent mechanism to inhibit the function of Yki/YAP in the regulation of transcription. Wts-mediated phosphorylation of Yki may also have a role in promoting its nuclear export, as well as its retention in the cytosol, although this is much less well documented (Ren et al., 2010b). The additional Wts sites S111 and S250 do not appear to induce 14-3-3 interaction, but instead seem to limit Yki nuclear localisation and to regulate Yki function independently of 14-3-3, perhaps by influencing the ability of Wts to phosphorylate S168 (Oh and Irvine, 2009; Ren et al., 2010b). An additional orthologue of *yki* was later identified in mammals, *TAZ* (*Transcriptional Co-Activator with PDZ-Binding Motif*), which shares 50% homology with *YAP* (Lei et al., 2008). TAZ was previously described as a 14-3-3-binding partner and its function is modulated by a similar mechanism as YAP (Kanai et al., 2000). Like

YAP, TAZ also regulates growth and it is phosphorylated by LATS at S89, which similarly promotes TAZ cytoplasmic sequestration (Kanai et al., 2000; Lei et al., 2008).

In mammals, LATS can also regulate YAP stability in a way not conserved in *Drosophila*. As well as promoting exclusion from the nucleus, LATS-mediated phosphorylation of YAP at S381 primes it for additional phosphorylation by Casein Kinase 1 (CK1) δ/ε resulting in recognition by the F-box protein β-TrCP and culminating in proteasomal degradation of YAP (Zhao et al., 2010). This additional mechanism of YAP regulation is at least in part, responsible for the viability of mice with a YAP^{S112} mutation at the endogenous locus (Chen et al., 2015). In *Drosophila*, Yki stability can also be modulated, but this is achieved via a distinct mechanism that involves lysosomal rather than proteasomal degradation, regulated by the α–arrestin Leash (Kwon et al., 2013), and Myopic (Mop) a His-Domain Protein Tyrosine Phosphatase (Gilbert et al., 2011).

More recently, evidence is growing to suggest there are additional Yki/YAP kinases other than Wts/LATS. The mammalian orthologue of Nemo, Nemo-Like Kinase (NLK), directly phosphorylates YAP at S128, the neighbouring site to the canonical LATS S127 site. This phosphorylation appears to disrupt 14-3-3 binding, thereby promoting nuclear accumulation and activation of YAP, a mechanism which appears to be conserved in *Drosophila,* knockdown of *nemo* regulating the Yki transcriptional target Diap1 (Hong et al., 2017; Moon et al., 2017). Phosphorylation at YAP^{S128} directly antagonises Wts/LATS, although the functional relevance of this phosphorylation remains to be thoroughly explored (Hong et al., 2017; Moon et al., 2017). The NDR kinase family, of which Wts/LATS are members, also contains NDR1/2 in mammals. NDR1/2 have been shown to phosphorylate YAP at S127 restricting its activity in the intestine (Zhang et al., 2015b), and can even act downstream of MST, expanding the repertoire of the core signalling cassette (Tang et al., 2015).

1.3.3. Yorkie – A Transcriptional Co-Activator

Yki contains no DNA binding sequence and, therefore, is unable to promote gene transcription in isolation. However, fusion of Yki to the DNA binding domain of the Gal4 transcription factor is sufficient to drive *Upstream Activating Sequence (UAS)-luciferase* expression, which can be inhibited by *hpo* or *wts* overexpression (Huang et al., 2005). Confirmation of *yki* as a bona fide transcriptional co-activator came when the TEA Domain (TEAD) family transcription factor Scalloped (Sd) and the mammalian TEAD1-4 were identified as direct Yki/YAP binding partners (Goulev et al., 2008; Wu et al., 2008; Zhang et al., 2008; Zhao et al., 2008). Mutations or RNAi-mediated depletion of *sd* abolish the tissue overgrowth caused by *yki* overexpression or by Hippo pathway inactivation, placing *sd* downstream of the Hippo kinase cassette and *yki* (Goulev et al., 2008; Wu et al., 2008; Zhang et al., 2008). Overexpression of both *sd* and *yki* also enhances overgrowth of *yki* overexpressing clones, resulting in increased expression of *cycE* and *diap1* (Wu et al., 2008; Zhang et al., 2008). The direct interaction of Yki and Sd led to the characterisation of a minimal Hippo-Response Element (HRE), based on the *diap1* gene locus (Wu et al., 2008; Zhang et al., 2008). Interestingly, Sd also interacts with the co-transcriptional activator Vestigial (Vg), which is specifically expressed in the wing pouch and is responsible for determining wing identity (Halder et al., 1998; Simmonds et al., 1998). Sd interacts with Yki and Vg in a mutually exclusive manner, each co-activator regulating a distinct set of genes (Halder and Carroll, 2001; Wu et al., 2008).

Surprisingly, *sd* overexpression causes tissue undergrowth rather than the excess overgrowth as a result of *yki,sd* co-overexpression (Wu et al., 2008; Zhang et al., 2008). This apparent discrepancy was resolved by the discovery that the default function of *sd* is as a transcriptional repressor, and the *yki* binding alleviates this repression converting *sd* into an activating transcription factor (Koontz et al., 2013). Repression of *sd* target genes in the absence of nuclear Yki is mediated by Tondu-Domain-Containing Growth Inhibitor (Tgi), a Sd-binding

co-factor required for default repression, whose function is conserved in mammals by Vestigial-like 4 (VGL4) (Koontz et al., 2013). In addition to Sd, additional Yki-binding transcription factors have been identified, which include Homothorax (Hth) and Teashirt (Tsh) in the developing eye (Peng et al., 2009), and Mothers Against Dpp (Mad) (Oh and Irvine, 2011). In mammals, YAP/TAZ associate with a plethora of transcription factors in addition to TEAD1-4 including YAP binding partners SMAD1/2/3 (Alarcon et al., 2009; Varelas et al., 2008; Varelas et al., 2010), Runt-Related Transcription Factor (RUNX) (Yagi et al., 1999), Erb-B2 Receptor Tyrosine Kinase 4 (ErbB4) (Komuro et al., 2003), p73 (Strano et al., 2001) and TAZ binding partners RUNX, Peroxisome Proliferator-Activated Receptor γ (PPARγ) (Hong et al., 2005), Paired Box 3 (Pax3) (Murakami et al., 2006), T-Box Transcription Factor 5 (TBX5) (Murakami et al., 2005) and Thyroid Transcription Factor 1 (TTF-1) (Park et al., 2004) increasing the scope of Hippo signalling.

Tissue growth, as a result of Hpo signalling inhibition, or the activation of Yki switches on a transcriptional programme that can be split into three categories. Firstly, *yki* regulates tissue size through genes that control the cell cycle, cell growth (that is, cell mass) and apoptosis. Yki promotes cell cycle progression through the regulation of *cycE* (Harvey et al., 2003; Pantalacci et al., 2003; Tapon et al., 2002; Udan et al., 2003; Wu et al., 2003), a member of the cyclin family that drives the cell cycle from the Gap1 phase (G1) into the Synthesis phase (S phase) (Knoblich et al., 1994), and *E2F transcription factor 1 (E2F1)* (Goulev et al., 2008), which also promotes *cycE* expression (Neufeld et al., 1998). Yki also regulates cell proliferation through the micro-Ribonucleic Acid (RNA) *bantam*, (Brennecke et al., 2003; Nolo et al., 2006; Thompson and Cohen, 2006), and cell growth through *myc proto-oncogene protein* (*myc)* (Neto-Silva et al., 2010; Ziosi et al., 2010). Diap1 inhibits apoptosis-inducing caspases (Wang et al., 1999) and is transcriptionally regulated by Yki, thus providing a means to prevent apoptosis (Harvey et al., 2003; Pantalacci et al., 2003; Tapon et al., 2002; Udan et al., 2003; Wu et al., 2003). The coordinated, and cell autonomous expression of these genes by *yki* results in increased proliferation rates, cell growth and resistance to

apoptotic signals which, together, all contribute to the ability of *yki* to control tissue growth.

Secondly, the Hippo pathway and many other signalling pathways are highly integrated (Hansen et al., 2015; McNeill and Woodgett, 2010). To this end, the *yki* transcriptionally regulates genes crucial to several pathways, including ligands for the EGFR pathway *vein (vn)* and *spitz (spi)* (Ren et al., 2010a), Notch pathway *serrate* (Cho et al., 2006), Wnt pathway *wingless (wg)* (Cho et al., 2006; Cho and Irvine, 2004), Hh and Decapentaplegic (Dpp) pathways *dally* and *dally-like (dlp)* (Baena-Lopez et al., 2008) and Janus Kinase (JAK)/Signal Transducer and Activator of Transcription (STAT) pathway *unpaired (upd) 1-3* and *suppressor of cytokine signalling at 36E (socs36E)* (Karpowicz et al., 2010; Ren et al., 2010a; Shaw et al., 2010).

Lastly, genes involved in upstream activation of Hpo signalling also form a large portion of the *yki*-dependent transcriptional programme, including *expanded* and *merlin* (Hamaratoglu et al., 2006)*, kibra* (Genevet et al., 2010), and *four-jointed* (Cho et al., 2006; Willecke et al., 2006). Expression of these genes results in negative feedback of the Hippo pathway by inhibiting excessive *yki* activity and tissue overgrowth. Interestingly, high activity of *myc*, whilst promoting growth, can also inhibit *yki* through transcriptional and post-transcriptional mechanisms, further compounding the negative feedback mechanisms employed by Hippo signalling to tightly regulate *yki* activity (Neto-Silva et al., 2010).

1.3.4. Upstream Regulation of the Hippo Pathway

The focus of Hippo signalling is upon the core kinase Wts, and the ultimate Hippo effector Yki. A vast amount of work has gone into understanding what physiological and cellular signals impact upon these key proteins, leading to the identification of a wide array of upstream mediators of the pathway. Unlike with typical signalling cascades, the Hippo pathway is not regulated by a defined set of ligand-receptor interactions, but it is rather modulated by a diverse set of

upstream constituents. The following section will discuss these many and varied upstream members of the Hippo pathway, and how they ultimately regulate Wts and Yki.

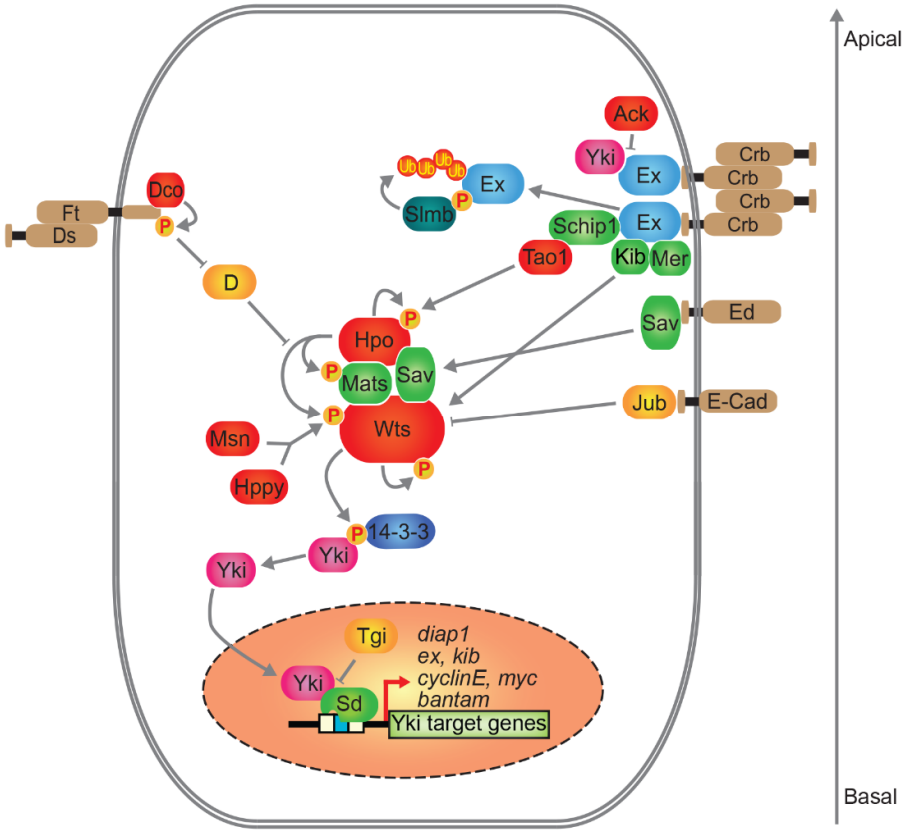

Figure 1-2 The *Drosophila* Hippo tumour suppressor pathway

Schematic representation of the Hippo pathway in *Drosophila* with particular focus on the role of Ex. See text for details.

1.3.5. Regulation by the Kibra, Expanded, Merlin Complex

Prior to the delineation of the Hippo kinase cascade, early genetic studies in *Drosophila* identified several tumour suppressor genes that would later find a place within the Hippo pathway. Two of these genes were *expanded* (*ex*) (Boedigheimer and Laughon, 1993; Boedigheimer et al., 1997), and *merlin* (*mer*),

the orthologue of the bona fide tumour suppressor gene *Neurofibromatosis Type-2* (*NF2*) encoding mammalian MER (LaJeunesse et al., 1998). Null mutations in *ex* are lethal (Blaumueller and Mlodzik, 2000), whereas hypomorphic mutations cause hyperplastic overgrowth of discs by affecting the rate of cell proliferation, rather than increasing the growth period (Boedigheimer and Laughon, 1993). Like *ex,* null mutations in *mer* are lethal, whereas hypomorphic mutations also cause overproliferation.

Ex and Mer both contain a highly conserved N-terminal FERM (4.1 Ezrin Radixin Moesin) domain (Boedigheimer et al., 1997; LaJeunesse et al., 1998) and co-localise at the apical surface of wing imaginal discs, directly interacting *in vitro* (McCartney et al., 2000) (for the domain architecture of Ex see Figure 1-3A). The structural and phenotypic similarity between *mer* and *ex* led to the discovery that these genes act partially redundantly in the regulation of tissue growth. *mer*, *ex* double mutants display dramatically enhanced tissue overgrowth compared to single mutants (McCartney et al., 2000), but despite their partial redundancy, *mer* and *ex* perform distinct functions. For example, in the developing eye, the main function of *ex* appears to be in the regulation of cell cycle exit, whereas *mer* serves to inhibit apoptosis (Pellock et al., 2007). Moreover, *ex* appears to inhibit Wg function as eyes that are entirely mutant for *ex* are paradoxically smaller than wild-type eyes despite overgrowth of the eye disc, which is attributed to ectopic Wg activity, a phenotype that is not observed in *mer* mutant eyes (Pellock et al., 2007). Tissue overgrowth of *mer;ex* double mutants is as a result of regulation of cell cycle and apoptosis, and *cycE* and *diap1* transcription is upregulated in the mutant tissue, reminiscent of previously identified Hippo pathway mutants (Hamaratoglu et al., 2006). This discovery prompted researchers to perform epistasis experiments involving core Hippo pathway members, which placed *mer* and *ex* genetically upstream of *hpo* and *wts*, as *hpo* overexpression phenotypes were not suppressed by loss of function of *mer;ex*. Moreover, *mer* and *ex* were found to stimulate Wts phosphorylation, resulting in Yki inhibition (Hamaratoglu et al., 2006).

Interestingly, recent data has suggested that Mer can also directly recruit Wts to the plasma membrane to activate Hippo signalling, which may be independent of Hpo kinase activity (Yin et al., 2013). These findings placed *ex* and *mer* as the first identified regulators of Hippo signalling. Moreover, in addition to acting at the plasma membrane, mammalian activated MER functions within the nucleus interacting with the E3 ligase Cullin4A-RING E3 Ligase (CRL4)-DDB1- and CUL4-Associated Factor 1 (DCAF1) ($CRL4^{DCAF1}$) (Li et al., 2014b). This interaction supresses the ability of $CRL4^{DCAF1}$ to ubiquitylate and inhibit LATS, this enabling the phosphorylation and inhibition of YAP (Li et al., 2014b).

In addition to the role of Ex and Mer regulating the Hippo kinase cassette, these proteins may affect growth through endocytosis, negatively regulating the membrane abundance of multiple signalling pathways receptors (Maitra et al., 2006). However as apical hypertrophy is a general outcome of increasing Yki activity (Genevet et al., 2009; Hamaratoglu et al., 2009), this could explain the increased abundance of apical receptors, and therefore the apparent effect of *ex/mer* on endocytosis seems likely to be a consequence of Yki regulation, rather than through a direct influence on endocytosis. In fact, apical hypertrophy was one of the first reported *wts* mutant phenotypes (Justice et al., 1995).

Despite the established role of Ex in regulating the Hippo kinase cassette activity, the direct mechanism has not been thoroughly characterised. A recent paper identified *schwannomin/Mer-interacting protein (schip1)*, as a novel component of the Hippo pathway, which interacts with Ex and Tao-1. The formation of this complex stimulates Tao-1 kinase activity, thus promoting signalling through the Hippo kinase cassette (Chung et al., 2016). This provides a mechanistic link between Ex and the core kinase cassette, although the authors speculate that Schip1 may also regulate Mer in certain contexts, such as the eye, where Mer functions independently of Hpo by directly interacting with Wts (Chung et al., 2016; Yin et al., 2013) (Figure 1-2).

The linear genetic epistasis of *ex* and the Hippo kinase cassette had to be re-evaluated once it was discovered that Ex can physically interact with Yki via the proline-rich PPxY motifs in the C-terminus of Ex, and the WW domain of Yki (Badouel et al., 2009; Oh et al., 2009). The interaction with Ex physically tethers Yki to the apical membrane, inhibiting its translocation into the nucleus. Therefore, *ex* has Hippo-dependent and -independent means of regulating Yki, and can act up- and downstream of Wts. The interaction between Ex and Yki is thought to be subject of regulation by Activated Cdc42 Kinase (Ack), a non-receptor tyrosine kinase. Ack phosphorylation of Ex at multiple tyrosine residues disrupts the interaction between Ex and Yki, thus Ack serves to enhance Yki activity (Hu et al., 2016). However, as *ack* mutants do not display overt growth phenotypes (Hu et al., 2016), the physiological relevance of this mechanism remains unclear.

Unlike many members of the Hippo pathway which have clear orthologues in mammals, the conservation of *ex* is unclear. There is no gene of high homology to the entirety of *ex*, rather it has been proposed that the function of *ex* has been split in mammals between FERM Domain Containing 6 (FRMD6) and Angiomotin (AMOT) (Genevet and Tapon, 2011). *FRMD6,* shares sequence homology with *ex*, primarily throughout the FERM domain and has been proposed as an N-terminal orthologue of *ex* as overexpression of FRMD6 in mammalian cells inhibits YAP activity by luciferase reporter assay (Zhao et al., 2007). Moreover, FRMD6 activates the Hippo pathway kinases, increasing phosphorylation of YAP (Angus et al., 2012; Moleirinho et al., 2013). However, the role of this gene in Hippo signalling is disputed, as another report suggests *FRMD6* possesses tumour suppressive functions independent of the Hippo pathway perhaps through regulation of receptor tyrosine kinases (Visser-Grieve et al., 2012; Xu et al., 2016), and overexpression of FRMD6 is not able to recover tissue overgrowth in *ex* mutant *Drosophila* eye discs (Angus et al., 2012).

Interestingly the unrelated *AMOT* genes are functionally analogous to the C-terminus of *ex*, despite encoding proteins that contain different domains (Bossuyt

et al., 2014). In evolutionary terms, *AMOT*–like genes can be found in all bilaterian phyla, except the dipteran lineage, which includes *Drosophila*. Therefore, it seems *Drosophila* lost *AMOT* genes, gaining the *ex* gene developing, at least in part, the same function as *AMOT* in the interaction and inhibition *yki/YAP* (Bossuyt et al., 2014).

Crucially, both Ex and AMOT contain PPxY motifs, both proteins being able to physically interact with Yki or YAP/TAZ respectively (Badouel et al., 2009; Paramasivam et al., 2011; Varelas et al., 2010; Wang et al., 2011; Yi et al., 2011; Zhao et al., 2011). The precise role of the *AMOTs* in the regulation of Hippo signalling and YAP has been difficult to determine. Initial reports suggested the physical interaction between AMOT and YAP inhibits the translocation of YAP to the nucleus (Chan et al., 2011; Oka et al., 2012; Varelas et al., 2010; Zhao et al., 2011), one report suggesting AMOT phosphorylation by LATS aids Atrophin-1 Interacting Protein 4 (AIP4) dependent degradation of YAP (Adler et al., 2013). However, conflicting studies have suggested AMOT promotes YAP function (Lv et al., 2015; Yi et al., 2013). Recently, these contradicting findings appear to be partially resolved and depend on the context of AMOT interaction with YAP. Interaction with the Crumbs (Crb) complex appears to result in AMOT-dependent inhibition of YAP (Varelas et al., 2010). In one recent report, AMOTL1 acts downstream of Fat4 in the heart to sequester YAP away from the nucleus. However, when Fat4 is lost, AMOT:YAP is relocated into the nucleus to drive a YAP-dependent transcriptional programme (Ragni et al., 2017). Therefore, the interaction partners of AMOT can help dictate its function. Post-translational status of AMOT also appears to significantly contribute to its activity in regulating YAP, phosphorylation of AMOT by LATS (Adler et al., 2013; Chan et al., 2013; Dai et al., 2013; Hirate et al., 2013), or AMP-Activated Protein Kinase (AMPK) (DeRan et al., 2014) promotes AMOT-mediated inhibition of YAP. Interestingly, AMOT and MER interact in mammals, as they do Ex and Mer *in Drosophila* (Das et al., 2015; McCartney et al., 2000; Moleirinho et al., 2017; Yi et al., 2011) suggesting functional conservation of signalling beyond interaction of AMOT with YAP.

Kibra (*kib*), named due to the high expression levels of *KIBRA* in mammalian kidney and brain (Kremerskothen et al., 2003), was identified as an upstream member of the Hippo pathway in *Drosophila* through the observation that overexpression in the developing eye results in a decrease in the adult organ size (Baumgartner et al., 2010; Tseng and Hariharan, 2002), and through two independent genetic screens (Genevet et al., 2010; Yu et al., 2010). Mutations in *kib* cause mild overgrowth phenotypes and cell autonomous increase in Hippo pathway target genes. Moreover, RNAi-mediated knockdown of *kib* in S2 cells causes a decrease in Hpo^{T195} and Yki^{S168} phosphorylation, consistent with the role of Kib as a member of the Hippo pathway (Baumgartner et al., 2010; Genevet et al., 2010; Yu et al., 2010). Kib contains two WW domains, which facilitates interaction with the PPxY motifs of Ex (Genevet et al., 2010). Interestingly, one of the WW domains of Kib only has a single tryptophan residue, similar to Sav. The atypical WW domain of Sav allows it to homodimerise (Ohnishi et al., 2007). As both Sav and Kib contain a similar atypical WW domain, it was discovered they can also heterodimerise (Yu et al., 2010). These interactions allows Kib to form a complex with Ex, Mer, Sav and Hpo at cellular junctions that potently regulates Wts activity, and thus tissue size through the Hippo kinase cascade (Baumgartner et al., 2010; Genevet et al., 2010; Yu et al., 2010) (Figure 1-2).

The functional relevance of the Kib/Ex/Mer complex has recently come under scrutiny, a recent report suggesting Mer/Kib act in parallel to Ex in a complex at the apical medial cortex distinct from the junctions, medial Mer/Kib stimulating Sav, Hpo and Wts interactions and thus Hippo signalling (Su et al., 2017). Indeed, contrary to the current paradigm, in which Crb promotes Hippo signalling solely through regulating Ex (Chen et al., 2010; Grzeschik et al., 2010; Ling et al., 2010; Ribeiro et al., 2014; Robinson et al., 2010), Crb appears to actively inhibit Kib at the apical junctions. However, the physiological relevance of medial Mer/Kib remains to be determined.

1.3.6. Regulation by Cell-Cell Contact, Tension and the Cytoskeleton

Hippo signalling and Yki activity is also regulated by many other important stimuli other than the Kib, Ex and Mer complex. Cell-cell contacts, mechanical tension and the cytoskeleton are major inputs into the Hippo pathway. Early evidence, predating the 'discovery' of the Hippo pathway suggested that the Mer orthologue MER was involved in regulating contact inhibition in mammalian cells (Morrison et al., 2001). Indeed, Hippo signalling was found to regulate contact inhibition outright on analysis of YAP localisation in sparse or densely cultured cells. At high density, YAP is excluded from the nucleus, whereas in sparsely seeded cells, YAP is strongly localised within the nucleus, nuclear exclusion upon high density being dependent on Hippo pathway activity (Schlegelmilch et al., 2011; Zhao et al., 2007).

Moreover, as FERM domain proteins such as Ex and Mer are associated linking the plasma membrane with the cortical cytoskeleton (Bretscher et al., 2002), the actin cytoskeleton was discovered to play a major role in Hippo signalling. In *Drosophila,* induction of Filamentous (F)-actin formation, through loss of actin capping proteins or activation of formins, promotes *yki* dependent tissue overgrowth (Fernandez et al., 2011; Sansores-Garcia et al., 2011). Zyxin (Zyx), a Lin11, Isl-1, Mec3 (LIM) domain containing protein, interacts with Enabled (Ena) to promote F-actin and Yki-mediated growth, which antagonises the genetic interaction between Ex and Capping Protein (CP) (Fernandez et al., 2011; Gaspar et al., 2015). Furthermore, cytoskeletal tension in *Drosophila* regulates wing growth through modulation of Wts and therefore Yki activity (Rauskolb et al., 2014). As seen in *Drosophila*, proteins that regulate F-actin polymerisation also regulate YAP/TAZ activity in mammals, and therefore Hippo signalling is able to respond to differences in cellular tension (Aragona et al., 2013). The response of YAP/TAZ to tension is also modulated by the extracellular matrix (ECM) rigidity and cell shape through the action of the Ras Homolog (RHO) GTPase and actomyosin, with cells compressed into small areas inactivating YAP/TAZ (Dupont et al., 2011). Indeed, loss of cell interaction with the ECM activates LATS

to inhibit YAP, which is required for anoikis, apoptosis induced by loss of ECM contact (Zhao et al., 2012). It remains controversial as to whether F-actin- and tension-mediated activation of YAP/TAZ requires the LATS kinases, as initial studies suggested YAP/TAZ activation was independent of the core Hippo kinases (Dupont et al., 2011). However, an increasing body of work suggests F-actin-mediated regulation of YAP/TAZ does require LATS1/2 kinases and AMOT (Adler et al., 2013; Dai et al., 2013; Hirate et al., 2013; Wada et al., 2011). Additionally, one study has suggested that the activation of YAP upon tension requires c-Jun N-Terminal Kinase (JNK) signalling to inhibit LATS activity (Codelia et al., 2014).

In addition to the actin cytoskeleton, the spectrin network has recently been identified as a Hippo regulator. Disruption of Spectrin proteins leads to activation of Yki, resulting in tissue overgrowth (Deng et al., 2015; Fletcher et al., 2015; Wong et al., 2015). However, the precise mechanism by which Spectrins regulate Hippo signalling remains to be clarified, one study suggesting apical β_{Heavy} (β_H)-Spectrin binds to Ex to regulate Yki activity (Fletcher et al., 2015), whereas another study suggests the Spectrins modulate cortical actomyosin through non muscle myosin II to regulate Yki activity (Deng et al., 2015).

1.3.7. Regulation by Extracellular Ligands

Although Hippo signalling is not predominantly regulated by a traditional ligand-receptor structure, Hippo signalling can be regulated by ligands that stimulate G-Protein Coupled Receptor (GPCR) signalling. In mammals, the discovery that cells treated with foetal bovine serum causes dephosphorylation of YAP led to the discovery that the molecules lysophosphatidic acid (LPA) and sphingosine-1-phosphate (S1P), through interaction with their GPCRs, stimulate YAP/TAZ activity by inhibiting Hippo signalling (Yu et al., 2012). The LPA and S1P GPCRs, when coupled to the $G\alpha_{12/13}$ subunit, activate the GTPase RHO, which triggers LATS inhibition, and YAP/TAZ activation (Yu et al., 2012). As with the actin cytoskeleton and tension, whether RHO affects YAP activity through the

modulation of LATS function remains controversial. For instance, it has also been reported S1P and LPA stimulate YAP independently of the core kinase cascade (Miller et al., 2012). Further studies identified several additional factors that regulate Hippo signalling through GPCRs, suggesting that a broad range of extracellular signals can regulate the Hippo pathway (Gong et al., 2015; Mo et al., 2012; Zhou et al., 2015). Interestingly, activation of the $G\alpha_S$ GPCR subunit by adrenaline or glucagon inhibits YAP/TAZ activity through stimulation of the LATS kinases (Yu et al., 2013; Yu et al., 2012). The adrenaline or glucagon the $G\alpha_S$ GPCR subunits generate cAMP as a second messenger molecule to stimulate Protein Kinase A (PKA) activity. Increased PKA activity stimulates LATS dependent phosphorylation of YAP by inhibiting RHO activity, this mechanism being conserved in *Drosophila* wing imaginal discs (Yu et al., 2013; Yu et al., 2012).

1.3.8. Regulation by Metabolism

Metabolic perturbations and nutrient levels have also recently been shown to influence Hippo signalling. The mevalonate pathway is a regulator of YAP/TAZ activity (Sorrentino et al., 2014; Wang et al., 2014), which is involved in the synthesis of isoprenoid precursors, including cholesterol, steroid hormones and haem cofactor, as well as the production of prenylation intermediates, and is therefore involved in a wide range of biological functions (Santinon et al., 2016). It has been suggested that the mevalonate pathway regulates Hippo signalling and YAP/TAZ activity through the modulation of RHO prenylation, which regulates its localisation and activity. Interestingly, this mechanism of YAP/TAZ regulation, although dependent on YAP phosphorylation, seems to be independent of LATS, which suggests that additional YAP/TAZ kinases may exist (Santinon et al., 2016; Sorrentino et al., 2014; Wang et al., 2014).

AMPK is crucial for regulating energy homeostasis, and therefore the metabolic state of the cell. Several studies have linked AMPK to Hippo signalling, and to the negative regulation of Yki-YAP/TAZ activity. Building on the discovery that

serum deprivation induces YAP exclusion from the nucleus (Miller et al., 2012; Yu et al., 2012), screening of small molecule compounds in this context led to the identification of AMPK as an inhibitor of YAP (DeRan et al., 2014). This initial study concluded that AMPK inhibits YAP through activating phosphorylation of AMOT, thus inhibiting YAP (DeRan et al., 2014). However, subsequent studies have suggested that AMPK directly phosphorylates YAP, potentially independently of LATS. However, the site of phosphorylation remains controversial, as both studies found YAP S94 as an AMPK target, which is noteworthy as this residue is vital for the YAP:TEAD interaction (Mo et al., 2015; Wang et al., 2015b). Moreover, the regulation of Hippo signalling by AMPK appears to be conserved in *Drosophila*, as AMPK represses Yki activity in the central brain/ventral nerve cord downstream of Liver Kinase B1 (LKB1) (Gailite et al., 2015).

The *Drosophila* Salt-Inducible Kinases 2 and 3 (Sik2/3) respond to nutrient levels promoting metabolism of lipids and glycogen (Choi et al., 2011) and are regulated by insulin signalling (Wang et al., 2008). Sik2/3 also promotes Yki activity by phosphorylation and inhibition of Sav, leading to increased expression of Yki target genes (Wehr et al., 2013). Furthermore, *Drosophila* fed a high sucrose diet in combination with oncogenic Ras Oncogene at 85D (Ras)/Src develop highly metastatic tumours, which remain sensitive to insulin signalling unlike *Drosophila* fed on a high sucrose diet only, which develop insulin insensitivity (Hirabayashi et al., 2013). Interestingly, the ability of these highly tumourigenic *Drosophila* to retain insulin sensitivity, which is essential for their aggressiveness, depends on Sik2/3 activity driving increased Yki activity and therefore Wg expression, which confers evasion of insulin resistance (Hirabayashi and Cagan, 2015). In addition, insulin also activates Yki through Akt mediated inhibition of Hpo (Strassburger et al., 2012).

1.3.9. The Hippo Pathway and Cell Polarity

Since the early characterisation of the Hippo pathway, links have been made to the organisation of epithelial tissues and their polarity. Epithelia are fundamental in the formation of distinct morphologies and the regulation of physiology. Epithelial cells are divided into discrete regions to facilitate their function called the apical domain and the basolateral domain, which are separated by junctional complexes. These junctional complexes are vital in establishing a semipermeable barrier, which allows epithelia to spatially control and coordinate their intracellular content (Tepass et al., 2001). The key junctional complexes in apicobasal polarity include the adherens junctions (AJs) and the septate junctions (SJs).

AJs form during embryogenesis through the fusion of spot AJs eventually forming a belt segregating the apical and basolateral membrane (Tepass and Hartenstein, 1994; Tepass et al., 2001). These junctions are characterised by E-cadherin and catenin localisation (Tepass et al., 2001). Key to the maintenance and stability of AJs are two apical protein complexes, the Par (Partitioning-defective) complex composed of Bazooka (Baz, also known as Par3), Par6 and Atypical Protein Kinase C (aPKC) and the more apical Crumbs (Crb) complex containing Crb, Stardust (Sdt) and Protein Associated to Tight Junctions (Patj) (Flores-Benitez and Knust, 2016; Harris and Peifer, 2004; Harris and Peifer, 2007; Muller and Wieschaus, 1996; Tepass, 1996, 2012; Wodarz et al., 2000).

Septate junctions form basally to the AJs, and are functionally analogous to tight junctions in vertebrates. As well as providing diffusible barriers between the apical and basal compartments within the cell, the AJs and septate unctions form strong adhesive cell-cell contacts, effectively creating a two-dimensional sheet of epithelia (Tepass et al., 2001). The Scribbled (Scrib) complex is key to the more basolateral region of the cell within the region of the septate junctions, containing Scrib, Discs Large (Dlg) and Lethal (2) Giant Larvae (Lgl). The Crb, Par and Scrib complexes antagonise each other to create and maintain distinct cellular regions within individual cells (Flores-Benitez and Knust, 2016; Tepass, 2012).

In addition to apicobasal polarity, planar cell polarity (PCP), the polarity within the plane of the tissue, is driven by two sets of genes, the Fat (Ft)/Dachsous (Ds) system, and the Frizzled (Fz)/Starry Night (Stan) system (Lawrence and Casal, 2013). Unlike with apicobasal polarity, where many components regulate Hippo signalling, only the Ft/Ds PCP system has been directly linked to growth via the Hippo pathway thus far.

1.3.10. The Fat-Dachsous Pathway – A Link Between Planar Cell Polarity and Growth

Like *ex*, *ft* was discovered as a tumour suppressor gene long before the identification of a conserved Hippo pathway, with the original *ft* mutants having been isolated in the early twentieth century (Mohr, 1923). Imaginal discs mutant for *ft* display enormous tissue overgrowth, as well as defects in bristle polarity (Bryant et al., 1988; Mahoney et al., 1991). Subsequent studies confirming the polarity defects caused by mutations in *ft* also identified several other genes which affect polarity, including *ds*, *four-jointed* (*fj*) (Adler et al., 1998; Casal et al., 2002; Rawls et al., 2002; Strutt and Strutt, 2002; Yang et al., 2002; Zeidler et al., 1999, 2000), and *dachs (d)* (Mao et al., 2006). These genes were found to interact in a common pathway regulating PCP.

The *ft* and *ds* genes encode large transmembrane proteins that are part of the cadherin family. Ft contains a large extracellular region with EGF-like and Laminin AG-domain-like repeats (Mahoney et al., 1991), whereas Ds contains tandemly repeated extracellular cadherin domains (Clark et al., 1995). The gene *fj* encodes a Golgi-resident kinase which can phosphorylate the extracellular domains of both Ds and Ft during their maturation (Brittle et al., 2010; Ishikawa et al., 2008; Simon et al., 2010). Interestingly, unlike *ft* which is uniformly expressed, *ds* and *fj* are expressed in opposing gradients in developing tissues (Clark et al., 1995; Yang et al., 2002; Zeidler et al., 1999), which is instructive in forming correct PCP orientation by providing directional information to the cells (Ambegaonkar et al., 2012; Bosveld et al., 2012; Brittle et al., 2012). Ft and Ds form heterodimers (Cho

and Irvine, 2004; Ma et al., 2003; Mao et al., 2006; Matakatsu and Blair, 2004; Strutt and Strutt, 2002), and their affinity is modulated by Fj-mediated phosphorylation, with phosphorylation of Ft increasing its affinity to Ds, whereas phosphorylation of Ds decreases its affinity for Ft (Brittle et al., 2010; Ishikawa et al., 2008; Simon et al., 2010). These interactions manifest in the asymmetrical localisation of Ft and Ds on opposing edges of a cell (Brittle et al., 2012), this polarised organisation of Ft/Ds heterodimers being defined by the *ds*/*fj* expression gradients, as well as the action of *fj* in regulating their affinity, the overall result creating a gradient of Ft activity throughout the tissue.

The effect of *ft* on growth has been difficult to dissect, with initial studies suggesting *ft* and *d* regulated growth through *wg* (Cho and Irvine, 2004; Rodriguez, 2004). However, upon early delineation of the Hippo pathway, it became apparent that *ft* mutant tissue displays many of the hallmarks of Hippo pathway mutants, such as transcriptional regulation of the Hippo pathway target genes *cycE* and *diap1*, and dependence on *yki* for overgrowth (Bennett and Harvey, 2006; Cho et al., 2006; Silva et al., 2006; Willecke et al., 2006). These early studies linking Ft to the Hippo pathway placed *ft* upstream of *ex* as loss of *ft* results in a decrease in *ex* apical localisation, and regulates Ex stability, and overgrowth induced by *ft* mutation in the eye could be rescued by expression of Ex (Bennett and Harvey, 2006; Silva et al., 2006; Willecke et al., 2006). Furthermore, it appeared that *ft,ex* double mutants displayed similar phenotypes to *ft* or *ex* alone, and were not additive suggesting that *ft* acted upstream of *ex* to regulate Hippo signalling (Bennett and Harvey, 2006; Cho et al., 2006; Silva et al., 2006; Willecke et al., 2006). However, later observations reported that *ft,ex* double mutants phenotypes are in fact additive, and that imaginal discs are larger than either *ft* or *ex* mutants alone, suggesting that *ex* and *ft* act in parallel (Feng and Irvine, 2007; Oh and Irvine, 2008), growth phenotypes being mediated by Wts and Yki as overexpression of Wts is able to recover lethality of null *ft* or *ex* mutants (Feng and Irvine, 2007; Oh and Irvine, 2008).

The apically-localised unconventional myosin D was identified as a member of Ft-Ds signalling, which acts downstream of Ft to regulate growth (Mao et al., 2006). Apical localisation of D is antagonised by Ft (Mao et al., 2006). Overexpression of *ft* inhibits the localisation or stability of D, whereas *ft* mutant clones show elevated D levels (Mao et al., 2006). Epistasis experiments suggested the influence of *ft* on growth depended entirely on *d*, therefore placing *d* downstream of *ft* (Cho et al., 2006; Feng and Irvine, 2007). When uninhibited by Ft, D promotes Yki activity to stimulate growth (Cho et al., 2006; Feng and Irvine, 2007; Mao et al., 2006).

As with PCP, the key proteins Ds and Fj are also involved in regulating growth, the interactions between these genes playing a key part in this regulation (Clark et al., 1995; Villano and Katz, 1995). However, the regulation of growth by Ft does not entirely depend on Ds, as *ft* mutants have more severe growth defects, and these mutants can be rescued by a form of Ft which cannot bind Ds, therefore Ft has functions in growth independent of Ds (Matakatsu and Blair, 2006). Additional Fat pathway interacting proteins exist to modulate growth through Hippo signalling. The CK1 family member *discs overgrown* (*dco*) also regulates tissue growth, at least in part through Fat-Hippo signalling by phosphorylating the cytoplasmic domain of Ft (Cho et al., 2006; Feng and Irvine, 2009; Sopko et al., 2009). Normal levels of Ft and Ds require the gene *lowfat* (*lft*) (Mao et al., 2009), while stability and localisation of D is regulated by the E3 ligase FbxL7, which may also affect Ft and Ds (Bosch et al., 2014; Rodrigues-Campos and Thompson, 2014). Recently, CG10933 named Dachs Ligand with SH3s (Dlish) by Zhang *et al.,* or Vamana (Vam) by Misra *et al.* was intricately involved in regulating Fat pathway activity (Misra and Irvine, 2016; Zhang et al., 2016). These studies identified that Dlish/Vam promotes localisation of D to the subapical region, which is essential for its inhibition of Wts (Misra and Irvine, 2016; Zhang et al., 2016). The localisation of D is depend on the palmitoylation of Dlish/Vam by the palmitoylatransferase Approximated (App), which had previously been shown to regulate both PCP and growth (Matakatsu and Blair, 2008; Zhang et al., 2016). Ft also interacts and inhibits App activity reducing D membrane

localisation and thus providing a mechanism for Ft-dependent inhibition of growth (Zhang et al., 2016). Furthermore, App negatively regulates Ft through direct palmitoylation antagonising the function of Dco, and simultaneously stimulates D function by driving its subapical localisation through palmitoylation of Dlish/Vam (Matakatsu et al., 2017; Zhang et al., 2016). Most of the components discovered to regulate growth in the Fat pathway appear to act downstream of Ft, however the WD40 protein Riquiqui (Riq) and the kinase Minibrain (Mnb) act downstream of Ds. Riq acts as a scaffold for Mnb, which phosphorylates and inactivates Wts to inhibit Hippo signalling (Degoutin et al., 2013).

While it is clear that the components listed above regulate Fat and Hippo signalling, how they act mechanistically remains somewhat unclear. A recent study, which analysed the conformational status of Wts suggested that, unlike many proteins, which regulate the kinase activity of the Hippo pathway and Wts, Ft/Ds regulate Wts conformation (Vrabioiu and Struhl, 2015). Ft/Ds activity promotes a closed and inactive conformation of Wts. This effect of Ft/Ds seems to be entirely dependent on the function of D, and directly antagonises the effect of Mats, which promotes the allosteric transition of Wts to an open, active confirmation (Vrabioiu and Struhl, 2015).

However, the mechanisms that convert the cellular distribution of these PCP proteins into orientation of polarisation are not well defined, moreover, how this regulates coordinated growth also remain mysterious (Matis and Axelrod, 2013). Interestingly, it has been reported that Fat signalling is regulated by morphogen gradients (Lawrence and Struhl, 1996; Rogulja et al., 2008). The morphogen Dpp is able to define the polar localisation of D within cells, which is important in the regulation of Fat and Hippo signalling (Rogulja et al., 2008). Intriguingly, a contemporary report suggested that differences in concentration of Ft/Ds between cell boundaries regulates Fat and Hippo signalling, defining a cell-communication based mechanism of growth regulation (Willecke et al., 2008), which is consistent with the potential of Fat signalling to respond to positional signals defined by morphogen gradients. In an alternative model, Fat signalling

promotes incorporation of cells into the wing pouch, thus driving imaginal disc growth (Zecca and Struhl, 2010). This process is dependent on the steepness of the Ds/Fj expression gradient, which is at its maximum at the edge of the pouch, and Hippo signalling. This model is dependent on another morphogen Wg, and thus multiple morphogenetic signals may feed into the Fat and Hippo pathways to help define the overall tissue size (Zecca and Struhl, 2010). However, the morphogenetic control of Fat and Hippo signalling remains controversial, as Ds/Fj expression gradients, and D polarised localisation are maintained when Dpp is expressed uniformly throughout the disc, suggesting Dpp and Fat work in parallel to regulate growth, rather than sequentially (Schwank et al., 2011).

1.3.11. Basolateral Polarity, Junctions and Hippo Signalling

Mutations in Hippo pathway genes cause 'hyperplastic' tumours, that is, tumours which extensively proliferate, at a faster rate than wildtype cells, but that retain normal morphology and ultimately differentiate into adult tissues (Bilder, 2004). The original class of *Drosophila* tumour suppressors form 'neoplastic' tumours, where the overproliferative tumours lose all morphological characteristics and are incapable of terminal differentiation (Bilder, 2004). Interestingly, in most cases, these tumours do not proliferate at a faster rate than wildtype cells, but rather do not stop growing (Hariharan and Bilder, 2006). Three junctional proteins Lgl (Bridges and Brehme, 1944; Gateff and Schneiderman, 1974), Dlg (Stewart et al., 1972) and Scrib (Bilder et al., 2000) were all defined as neoplastic tumour suppressors (Hariharan and Bilder, 2006). These genes are required for embryonic development, however large maternal contribution facilitates development until late larval stages. By this point, proliferative tissues such as imaginal discs and the nervous system are dramatically disrupted, and animals do not pupate (Bilder, 2004; Hariharan and Bilder, 2006). *lgl*, *dlg* and *scrib* genetically interact and are important in the establishment and maintenance of apicobasal polarity. Dlg and Scrib are localised primarily to the septate junctions on the basolateral membrane, whereas Lgl localisation depends on its

phosphorylation status, being excluded from the apical region by aPKC-mediated phosphorylation (Bilder, 2004; Hariharan and Bilder, 2006; Humbert et al., 2008).

One method these basolateral genes use to regulate growth is through Hippo signalling, although *lgl* and *scrib* appear to have distinct mechanisms of regulation. In the case of *lgl*, there appear to be tissue-specific means of regulating *yki*. In the eye epithelium, overgrowth associated with *lgl* knockdown is highly sensitive to levels of Yki.

Partial RNAi-mediated knockdown of *lgl* not strong enough to disrupt apicobasal polarity is associated with increased aPKC activity. This disrupts Hpo localisation, increasing Yki-mediated transcription, although the mechanism by which Hpo is mislocalised remains unclear (Grzeschik et al., 2010). Therefore, Lgl promotes Hippo pathway activity by preventing Hpo mislocalisation. However, in the wing, where *lgl* knockdown was strong enough to cause loss of polarity, activation of Yki requires JNK signalling. Moreover, in this context, aPKC indirectly activates Yki in a seemingly JNK-dependent manner (Richardson and Portela, 2017; Sun and Irvine, 2011).

In addition, *lgl* loss or aPKC activation causes the mislocalisation of the *Drosophila* Ras Associated Family (Rassf) tumour suppressor away from the cell junctions (Grzeschik et al., 2010). Rassf antagonises Hippo signalling by perturbing the interactions between Hpo and Sav (Polesello et al., 2006), and by recruiting the Stratin Interacting Phosphatase and Kinase (STRIPAK) phosphatase complex, to promote Hpo dephosphorylation, inactivation and Yki-mediated transcription (Ribeiro et al., 2010). Therefore, it was originally postulated that mislocalisation of Rassf and Hpo may facilitate the Rassf-mediated disruption of the interaction between Hpo and Sav and, thus, lead to Hippo pathway inactivation (Grzeschik et al., 2010). However, a subsequent study revealed that the STRIPAK complex is also mislocalised in *lgl* mutant tissue, and suggested that the activity of Rassf and the STRIPAK complex in this context was not functionally significant to Yki activation (Parsons et al., 2014).

Therefore, Yki-mediated tissue overgrowth induced by *lgl* disruption is dependent on the mislocalisation of Hpo, which is dependent on aPKC activation.

In the case of *scrib* mutation, the regulation of the Hippo pathway is more complex. As with *lgl* mutations, strong RNAi-mediated knockdown of *scrib*, sufficient to disrupt apicobasal polarity, results in Yki-associated tissue overgrowth in the eye imaginal disc (Doggett et al., 2011). Moreover, when an entire tissue is mutant for *scrib*, Yki is activated resulting in tissue overgrowth (Chen et al., 2012). However, unlike the situation of *lgl* mutation, this requires aPKC but not JNK signalling (Doggett et al., 2011). However, when *scrib* mutant clones face competition from surrounding wildtype cells, which normally cause the mutant clones to be eliminated due to increased cell death mediated by JNK signalling (Brumby and Richardson, 2003). This elevated JNK signalling also inhibits the *scrib* clone from overproliferating by inhibiting Yki, artificial increase of Yki within the *scrib* clones being sufficient to rescue the clones from elimination, resulting in neoplastic growth (Chen et al., 2012). Therefore, in this situation, JNK inhibits Yki activity.

Recently, the switch in function of JNK to promote or inhibit Yki signalling has been more thoroughly elucidated. During tissue homeostasis JNK appears to inhibit Yki, as overexpression of the Tumour Necrosis Factor (TNF) ligand *eiger (egr)*, which stimulates JNK signalling, inhibits tissue overgrowth induced by *yki* overexpression. Thus JNK acts in an anti-tumorigenic manner (Enomoto et al., 2015). This inhibition of *yki* occurs at the level of *wts,* as overexpression of *eiger* does not suppress tissue overgrowth induced by *wts* mutation, unlike with *hpo*, where *egr* overexpression inhibits clonal overgrowth cause by *hpo* mutation, although the precise mechanism of Wts activation is unclear (Enomoto et al., 2015).

The switch to promote JNK into pro-tumorigenic activator of Yki, seen with *scrib* and *lgl* mutation may be influenced by several mechanisms, one key route being the hyperactivation of Ras (Enomoto et al., 2015; Yamamoto et al., 2017). In the

presence of hyperactive Ras, mediated by an increase in EGFR signalling, JNK enhances Yki activity through an increase in F-actin levels, which inhibits Wts (Enomoto et al., 2015; Yamamoto et al., 2017). This process may also involve the gene *ajuba LIM protein* (*jub*), which localises to AJs. Jub is an inhibitor of Hippo signalling, interacting with Wts and Sav to inhibit the phosphorylation of Yki (Das Thakur et al., 2010; Enomoto et al., 2015; Sun et al., 2015). The inhibition of Hippo signalling by Jub is regulated by tension, as high tension exposes binding sites within α-Catenin at the AJs, promoting Jub binding and Wts inhibition (Rauskolb et al., 2014). Further study in *Drosophila* and mammals revealed that *jub* is activated by JNK to promote inhibition of *wts* and therefore activate *yki* (Sun and Irvine, 2013). The mechanisms by which the neoplastic tumour suppressors regulate growth remains a complex issue, with context dependent regulation of Hippo signalling through JNK and aPKC.

In addition to the described basolateral and junctional proteins that regulate the Hippo pathway, the adhesion protein Echinoid (Ed), which is a component of the AJs, stimulates Hippo signalling (Yue et al., 2012). Ed interacts with Sav promoting its stability thus enhancing Hippo signalling and Yki inhibition. Moreover, the localisation of Ed appears to be important in forming a Hippo signalling complex at the border between AJs and the apical membrane, antagonising the more basal Jub (Sun et al., 2015).

It is clear that polarity is a key regulator of Hippo signalling, with the basolateral membrane crucially modulating activity of Yki. The role of the apical domain, with a focus on the Crb complex will be thoroughly discussed below.

1.3.12. The Crumbs Complex

Crb was initially described as an apically localised protein responsible for the establishment and maintenance of cell polarity (Tepass et al., 1996; Tepass and Knust, 1993; Tepass et al., 1990; Wodarz et al., 1993). Mutant embryos for *crb* show multiple holes in the cuticle, which look like crumbs, hence the gene name

(Jurgens et al., 1984). Crb is expressed in almost all tissues, with the exception of the intestine (Tepass and Knust, 1990), and once polarity is established Crb is required for its maintenance in most epithelial tissues, with the exception of late embryonic epidermis, larval imaginal discs and early malpighian tubule development (Campbell et al., 2009; Pellikka et al., 2002; Tanentzapf and Tepass, 2003; Tepass, 2012). Crb forms a complex with Sdt (Bachmann et al., 2001; Hong et al., 2001), Veli (also known as Lin7) (Bachmann et al., 2008b; Bachmann et al., 2004) and Patj (formerly Discs Lost) (Bhat et al., 1999). Mutations in *sdt* are smiliar to that of *crb* and cause severe polarity defects in the embryo (Bachmann et al., 2001; Hong et al., 2001), whereas mutations in *veli* do not have obvious polarity defects (Bachmann et al., 2008a) and null mutations in *patj* do not display embroyic polarity defects, rather cause polarity defects in specific tissues, such as the follicular epithelia (Penalva and Mirouse, 2012; Zhou and Hong, 2012).

Structurally, Crb consists of a large extracellular sequence containing epidermal growth factor (EGF)-like repeats and Lamin AG-like domains, a single-pass transmembrane domain, and a relatively short intracellular domain consisting of only thirty seven amino acids (Bulgakova and Knust, 2009). This intracellular region contains two conserved protein binding domains, a FERM-Binding Motif (FBM) and a PDZ-Binding Motif (PBM), which are responsible for many of the known functions of Crb (Figure 1-3B) (Tepass, 2012). Overexpression of a *crb* construct containing the transmembrane and intracellular domains (Crb^{i}) is able to recover the lethality of *crb* mutant embryos, and cuticle patterning to the same extent as overexpression of full length Crb (Klebes and Knust, 2000; Wodarz et al., 1995). Rescue of the *crb* mutant relies on the function of both the FBM and the PBM motifs (Klebes and Knust, 2000). This small intracellular domain is responsible for a large number of binding interactions, including the Crb complex member Sdt, which acts as a scaffold for many interaction partners, and the other apical determinants aPKC and Par6 (Bachmann et al., 2001; Hong et al., 2001; Kempkens et al., 2006; Sotillos et al., 2004). The interaction with Par6 is crucial

in aiding the exclusion of Baz, a component of the AJs, from the apical region (Morais-de-Sa et al., 2010; Walther and Pichaud, 2010).

While most of the known functions of Crb have been ascribed to the small intracellular domain, the function of the extracellular domain has remained relatively elusive. However, several pieces of evidence now suggest that the extracellular domain of Crb is more important than originally thought, and is involved in the formation of homophilic interactions in *cis* and *trans* (Thompson et al., 2013). When analysing *Drosophila* morphogenesis, neither the extracellular or intracellular domains of Crb were sufficient to rescue overgrowth induced by *crb* mutation, only a *crb* construct containing both of these sequences was able to recover this phenotype, alluding to a role for the extracellular domain of Crb (Richardson and Pichaud, 2010). Moreover, if Crb^{i} is overexpressed in follicle cells, it is unable to localise apically, and rather localises in endosomes (Fletcher et al., 2012). Moreover, a Crb construct consisting of wildtype extracellular Crb, but where the intracellular domain has been replaced with Green Fluorescent Protein (GFP), is able to localise to the apical membrane only in the presence of wildtype Crb, but not in the context to *crb* mutations. These data suggest the extracellular domain of Crb is vital to the stabilisation of Crb at the apical surface, and forms Crb-Crb homophilic interactions in *cis* (Fletcher et al., 2012; Letizia et al., 2013).

Evidence for homophilic interactions in *trans* comes through analysis of Crb, and Crb complex members at *crb* mutant clone boundaries. Crb protein is lost in the cell membrane directly in contact with *crb* mutant clone tissue, but remains on the cell membrane when in contact with surrounding wildtype cells (Hafezi et al., 2012; Pellikka et al., 2002), which is also true for the Crb binding partners Ex and Patj (Chen et al., 2010). These data suggest that Crb interactions in *trans* are essential for its correct localisation. This conclusion is also supported by data obtained in zebrafish, where the *crb* orthologues *crb2a* and *crb2b* form *trans*-dimers to function as cell adhesion molecules (Zou et al., 2012).

In addition to its role in polarity, *crb* is also involved in regulation of tissue growth. This was originally described to be the result of Notch regulation, with Crb acting in a negative feedback loop to repress the γ–Secretase complex, which activates Notch signalling (Herranz et al., 2006), or through regulation of Notch (N) and/or Delta (Dl) endocytosis, thereby inhibiting the pathway (Richardson and Pichaud, 2010). More recently, endocytosis of Notch has been described to be inhibited by extracellular interaction between Notch and Crb, therefore limiting ligand-independent Notch activity (Nemetschke and Knust, 2016).

Crb also regulates growth through Hippo signalling by regulating Ex. The FBM of Crb is able to interact with the FERM domain of Ex, and is essential in regulating the apical localisation of Ex (Chen et al., 2010; Grzeschik et al., 2010; Ling et al., 2010; Robinson et al., 2010). The localisation of Ex appears to be important for stimulating Hippo signalling, as many members of the Hippo pathway are apically localised, forming a hub of signalling culminating in the inhibition of Yki (Genevet and Tapon, 2011; Sun et al., 2015). Indeed, the core Hippo kinases Hpo and Wts have been proposed to actively relocalise upon Hippo pathway stimulation, to Crb-positive regions within the wing disc epithelia, triggering Yki inhibition (Sun et al., 2015). In tissues mutant for *crb*, the Yki target genes *diap1*, *ex* and *cycE* are upregulated, coinciding with excess proliferation and overgrowth. Moreover, in *crb* mutant tissue, Ex is incorrectly localised away from the apical membrane, and is dispersed throughout the cytosol (Chen et al., 2010; Grzeschik et al., 2010; Ling et al., 2010; Robinson et al., 2010). These data are consistent with the model whereby Crb regulates the Hippo pathway by regulating the apical localisation of Ex, aiding the formation of an apically active Hippo signalling hub, inhibiting Yki through Wts-dependent and -independent means (Chen et al., 2010; Grzeschik et al., 2010; Ling et al., 2010; Robinson et al., 2010).

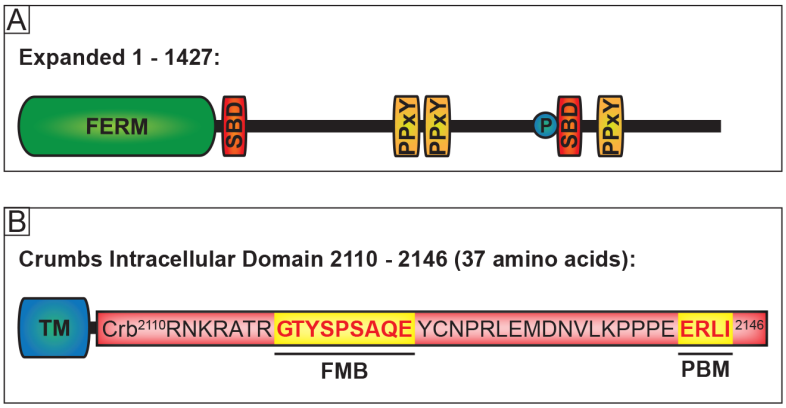

Figure 1-3 Ex and Crb protein architecture

Schematic representation of the domains and motifs within Ex (A) and Crb intracellular domain (B). Ex contains a FERM domain, two Slmb Binding Domains (SBD), three PPxY motifs and the circled P representing a Wts phosphorylation site at S1116 (Badouel et al., 2009; Ribeiro et al., 2014; Zhang et al., 2015a) (A). Architecture of Crb shows the transmembrane domain (TM) and the 37 intracellular amino acids, which includes the FERM Binding Motif (FBM) and the PDZ Binding Motif (PDM) both highlighted (Tepass, 2012) (B).

In addition to the regulation of Ex localisation to promote Hippo signalling, Crb also has a role in negatively regulating the Hippo pathway. Overexpression of Crb^{i} results in tissue overgrowth, and this effect is dependent on the FBM, but not on the PBM of Crb (Chen et al., 2010; Grzeschik et al., 2010; Ling et al., 2010; Robinson et al., 2010). This Crb^{i}-mediated overgrowth is also associated with an increase in Yki target gene expression, and is dependent on the Hippo pathway components *sav* and *yki*. This initially puzzling discovery, in direct contrast to *crb* mutant phenotypes, lead to the identification that Ex is highly sensitive to levels of Crb, with excess Crb promoting Ex degradation (Chen et al., 2010; Grzeschik et al., 2010; Ling et al., 2010; Robinson et al., 2010). Interestingly, Crb overexpression induces Ex phosphorylation through an undefined kinase (Ling et al., 2010). The Crb-mediated phosphorylation of Ex stimulates recognition of an N-terminal phosphodegron sequence by the E3 ligase Slmb, which ubiquitylates Ex resulting in its proteasomal degradation (Ribeiro et al., 2014). The

identification of the kinase responsible for the degradation of Ex, and the potential reversal of Ex ubiquitylation provide the main focus of this thesis (Figure 1-4). A recent study shows that *slmb* regulates *ex* in multiple ways, and that, as well as recognising an N-terminal phosphodegron sequence of Ex, Slmb also recognises a C-terminal degron sequence (Zhang et al., 2015a). This study proposes that the C-terminal Slmb degron of Ex is inhibited by Wts phosphorylation, which stabilises Ex. However, this Wts-dependent mechanism of Ex regulation appears to be independent of Crb-mediated Ex degradation and, in fact, seems to be superseded by it, as Wts overexpression is unable to rescue Crb-mediated Ex degradation (Zhang et al., 2015a).

Therefore, it seems that Crb activity acts as a rheostat for Hippo signalling. Crb is involved in Hippo pathway activation through the control of Ex localisation, but, it is simultaneously involved in switching off the pathway, through the regulation of Ex stability. This potentially acts as a highly precise mechanism for regulating tissue growth, although the physiological conditions whereby Crb stimulates Ex degradation remain to be determined.

The complexity of Crb-mediated regulation of Hippo pathway has been increased through a recent study analysing the localisation of Hippo pathway components. *Su et al.* suggest that, in addition to inhibiting the Hippo pathway through promoting Ex degradation, Crb can also block Hippo signalling by inhibiting Kib and Mer (Su et al., 2017). This study suggests that Kib and Mer activate the Hippo pathway at the medial cell cortex independently of Ex, rather than at the cell junctions as previously assumed, although the authors suggest this may be tissue or context dependent. At this medial cortex, Kib promotes formation of a Kib/Mer/Sav/Hpo/Wts complex promoting Hippo signalling (Su et al., 2017). Although evidence for the functionality of this complex is somewhat lacking, overexpression of Kib in the presence of RNAi-mediated depletion of *crb* results in wing undergrowth. This is in contrast to *crb* depletion alone, which causes wing overgrowth, and *kib* overexpression alone, which causes only a mild wing undergrowth. This suggests that Crb is able to repress the full functionality of Kib

with regards to Hippo signalling, however more work needs to be done to ascertain the importance of this medial cortex signalling platform (Su et al., 2017). The regulation of Ex localisation and stability by Crb, as well as the regulation of Kib activity, appears to provide a very intricate and subtle means for dynamic regulation of the Hippo pathway.

Interestingly, the most highly homologous *crb* orthologue in mammals *CRB3* (Karp et al., 2008) also regulates Hippo signalling. CRB3 is able to sense cellular density, and modulates YAP activity accordingly, through indirect interaction with AMOT (Varelas et al., 2010). The interaction of CRB3 with AMOT facilitates inhibition of YAP at cellular junctions through PPxY:WW domain interactions, siRNA mediated knockdown of *CRB3* resulting in activation of YAP/TAZ (Varelas et al., 2010). In this context, regulation of YAP/TAZ physically interact with SMAD2/3, CRB3-mediated inhibition of YAP/TAZ therefore also inhibiting SMAD2/3 nuclear translocation (Narimatsu et al., 2015; Varelas et al., 2010). CRB3 also has a role in promoting differentiation in airway epithelia, which is dependent on LATS1/2 phosphorylation and inhibition of YAP (Szymaniak et al., 2015). The most likely regulatory mechanism employed by *CRB3* to regulate Hippo signalling is through AMOT, which is functionally analogous to Ex.

The regulation of Hippo signalling by the apical polarity determinant Crb is becoming increasingly complex, both activating and repressing Yki-mediated transcription. The focus of this thesis will be the further characterisation of these intricate biochemical mechanisms.

1.3.13. The Physiological Relevance of Hippo Signalling

The initial discovery of Hippo signalling as a growth suppressive pathway led many of its mechanisms and components to be analysed in this context, as regulators of growth. In this capacity, it is increasingly apparent that the Hippo pathway is involved in cancer. Initial transgenic expression of YAP in the mouse liver resulted in tumourigenesis highlighting the potential for the Hippo pathway

to regulate cancer (Dong et al., 2007). Moreover, enrichment of nuclear YAP/TAZ is associated with a wide variety of human cancers in including lung, colorectal, liver, gastric, pancreatic and glioma (Harvey et al., 2013; Yu et al., 2015b; Zanconato et al., 2016). Intriguingly, despite a vast amount of evidence suggesting LATS1/2 are the major regulators of YAP activity, there are very few cancers that contain inactivating mutations in these genes, which is inconsistent with the idea that these kinases are the dominant regulators of YAP activity (Harvey et al., 2013; Zanconato et al., 2016). Indeed, LATS has even been shown to promote tumourigenesis by inhibiting the immune system from targeting tumour cells (Moroishi et al., 2016). It therefore seems likely that in cancer, Hippo pathway/LATS-independent mechanisms may contribute to the activity of YAP and thus tumourigenesis (Harvey et al., 2013; Zanconato et al., 2016).

It is becoming increasingly apparent that, as well as regulating growth during development, the Hippo pathway is also important in the regulation of differentiation, and in response to numerous stress signals. The upstream pathway members described, such as polarity, mechanical sensing and metabolic inputs all facilitate the response of Hippo signalling in normal physiology.

Hippo signalling regulates stem cell maintenance in numerous tissues, such as the intestine, liver, the nervous system and even human embryonic stem cells (Camargo et al., 2007; Cao et al., 2008; Imajo et al., 2015; Varelas et al., 2008; Yimlamai et al., 2014). In general terms, YAP/TAZ are expressed in progenitor/stem cell populations, and are important in regulating the proliferation and differentiation of these cells. In this context, the Hippo pathway appears to be important in inactivating YAP/TAZ in differentiated cells to maintain quiescence (Yu et al., 2015a; Zhou et al., 2009). The sensitivity of progenitor/stem cells to YAP activity is crucially important in response to injury, and highlights a key role of physiological Hippo signalling in promoting regeneration (Cai et al., 2010; Gregorieff et al., 2015; Taniguchi et al., 2015).

The role of Hippo signalling in regeneration is conserved from *Drosophila* to mammals. In the wing imaginal discs, Yki is hyperactivated upon injury, and is necessary for regeneration of the tissue (Grusche et al., 2011; Sun and Irvine, 2011), which is also true in the *Drosophila* intestine, where Yki regulates intestinal stem cell proliferation to replace dead or damaged cells (Karpowicz et al., 2010; Ren et al., 2010a; Shaw et al., 2010; Staley and Irvine, 2010). In mammalian cell culture, wounding drives YAP activation, which leads to the induction of a transcription programme stimulating expression of genes such as Connective Tissue Growth Factor (CTGF) that promote wound healing (Lee et al., 2014; Sisco et al., 2008; Zhao et al., 2007; Zhao et al., 2008).

In addition to responding to injury, Hippo signalling is important in responding to other situations of cellular stress. Studies of MST1/2 prior to the delineation of Hippo signalling showed these kinases are activated in response to toxic sodium arsenite or heat shock (Taylor et al., 1996). Some early studies also suggested MST1/2 were cleaved by caspases to promote apoptosis (Graves et al., 2001; Lee et al., 2001). Moreover, oxidative stress promotes MST activation, inducing apoptosis (Lehtinen et al., 2006) and stress induced by extra chromosomes stimulates LATS activity (Ganem et al., 2014). In *Drosophila*, the MST orthologue Hpo is activated by p53 in response to DNA damage (Colombani et al., 2006) highlighting the conservation of Hippo pathway responses to stress.

As previously discussed, the Hippo pathway responds to metabolic inputs, with low energy states stimulating Hippo signalling. This suggests that upon metabolic stress, Hippo signalling may be activated to limit proliferation and growth (DeRan et al., 2014; Mo et al., 2015; Wang et al., 2015b). In contrast to oxidative and metabolic stress, hypoxia appears to activate YAP/TAZ, stimulating the E3 ligase SIAH2 to degrade LATS, in a process that seems to involve the junctional protein Zyxin (Ma et al., 2015; Ma et al., 2016). It has also recently been reported that Hippo signalling in the *Drosophila* fat body is important for the response to infection by Gram-positive bacteria. In this instance, the Toll-pathway activates Hpo, thus inhibiting Yki. This limits the transcription of the Toll-response inhibitor

Cactus (Cact), thus promoting the Toll-pathway to produce antimicrobial peptides (Liu et al., 2016).

1.3.14. Aim – To Study the Relationship Between Crumbs and Expanded in the Regulation of Hippo Signalling

The Hippo pathway is a critical regulator of development, and is increasingly associated with tumourigenesis (Harvey et al., 2013; Yu et al., 2015b; Zanconato et al., 2016). However, many of the detailed interactions that define this complex signalling network remain undefined. This study aimed to address the precise mechanism by which the apical polarity determinant Crb acts as an upstream regulator of Hippo signalling to control the localisation and stability of Ex, a critical regulator of growth in *Drosophila*. This work has predominantly focused on the identification of a kinase (see 'Results 2 – Candidate Kinase Screen to Identify Regulators of Expanded Stability'), and to a lesser degree a DUB (see 'Results 4 – The Reversibility of Expanded Degradation') responsible for regulating Ex stability downstream of Crb (Figure 1-4). Furthermore, this study has attempted to define DUBs that control growth through interaction with *ex*, and could therefore act as novel members of the Hippo pathway (see 'Results 5 – A Screen to Identify Ubiquitylating Enzymes Involved in Regulating Tissue Growth').

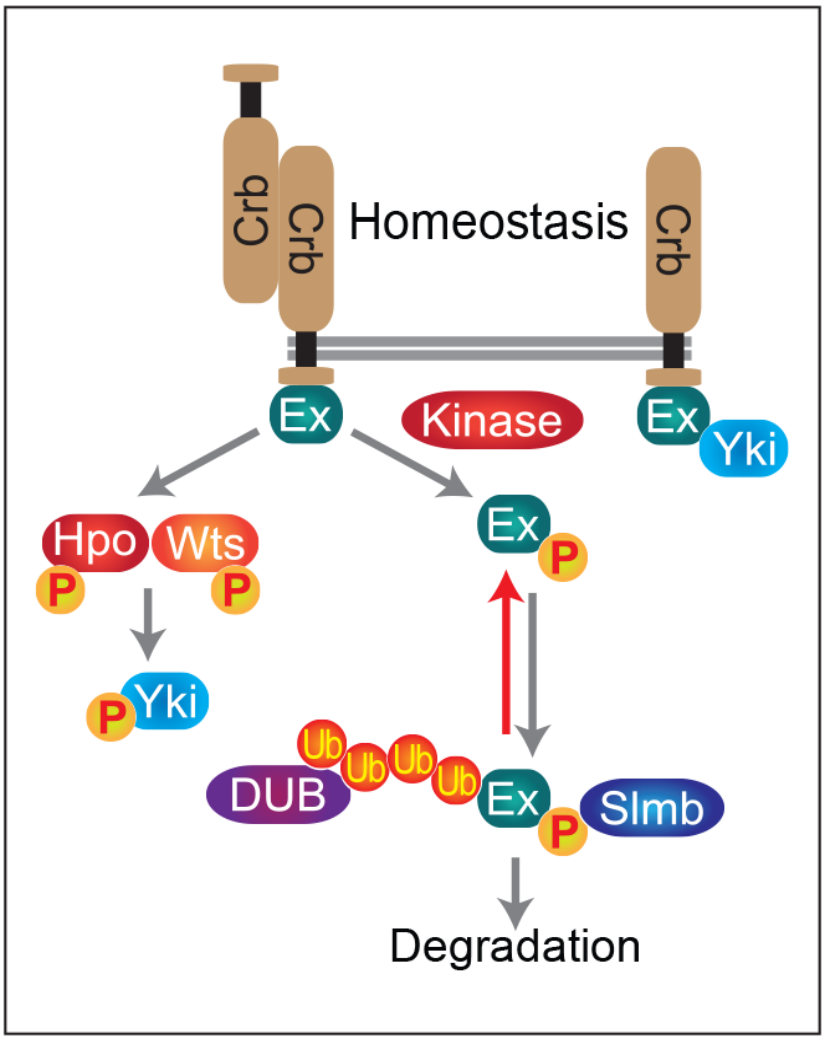

Figure 1-4 A model of Crb-mediated regulation of Ex

During homeostasis, Crb regulates Ex localisation at the apical membrane, but can also stimulate Ex phosphorylation and degradation. Crb-mediated phosphorylation occurs through an unidentified kinase, triggering recognition by the E3 ligase Slmb. Subsequent ubiquitylation should be reversible through catalysis by an unknown DUB.

Chapter 2 - Materials and Methods

2.1. Molecular Biology

2.1.1. Polymerase Chain Reaction

DNA fragments were amplified from plasmid DNA, genomic DNA or cDNA templates using oligonucleotide primers flanking the region of interest. Typically, Polymerase Chain Reaction (PCR) reactions were carried out in 20-50 µL reaction volumes and the Pwo Master-mix® (Roche) was used as DNA polymerase cocktail. PCR reactions were typically carried out as follows: (1) Initial denaturing - 95ºC for 2 minutes (mins); (2) Melting – 95ºC for 30 seconds (s); (3) Annealing –usually between 55-65ºC for 30 s, at a temperature typically 5ºC below the theoretical Tm of the primers used; (4) Extension - 72ºC for 1min/kb amplicon. PCR reactions were performed with 30 cycles of steps (2)-(4) and were kept at 4ºC for immediate use, or at -20ºC. See below for a list of the oligonucleotide primers used for PCR:

Table 2-1 List of PCR oligonucleotides

Primer name	Primer sequence
pENTR cloning primers – Primers contain BP recombinase recognition sequence: F: GGGGACAAGTTTGTACAAAAAAGCAGGCTCTACC R: GGGGACAAGTTTGTACAAAAAAGCAGGCTCTACC	
CG2577 F	GAACGACTGCGCTCCTCCCAA
CG2577 R	CGGCCAGAAGTTGCACTTCTCA
CG7094 F	GCAAAACAAGAAGCAACAAATGGG
CG7094 R	CTTTCGCTTGCTAATGCCTCCATC
CG9962 F	AACGACTACGAACTGGAAACCATG
CG9962 R	GACGACCTTTTTCACCACCACCC
CG12147 F	GCGGAACGGGAAAAGGGGCG
CG12147 R	AAGACAGGGCATCTGAGGGGA
Dnt F	ATGGAATCTGTGAATAAATGCGGTAAAAG
Dnt R	GACATAGCGCGTGATTTGTGAATAG
Sax F	GAGCTCTCCTCCGCCTCATC
Sax R	AACGCAGACCTCGTCGAAGTCCAGGC
Tkv F	GCGCCGAAATCCAGAAAGAAG
Tkv R	GACAATCTTAATGGGCACATCGATTAGAC

CAAX tagging primers	
CAAX R	GGGGACCACTTTGTACAAGAAAGCTGGGTCTCAGGACAGCA CACATTTCGAGCTCATGCAGCCAG
Ex F	ATGCGAGCATTTTGCACCGTCAGCGC
Ex$^{1\text{-}450\ CAAX}$ R	TTTCGAGCTCATGCAGCCAGGACCACTCTCATCGGGTGGGT TCAGTTTGTTGGAGCTGGTACTCGAGATAAC
Gish^{isoF} F	ATGCGAGCATTTTGCACCGTCAGCGC
Gish$^{isoF\ CAAX}$ R	TTTCGAGCTCATGCAGCCAGGACCACTCTCATCGGGTGGGT TCAGTTTTGTCTCCATTGTCTTCCCTGTCC
Sequencing primers	
Ac F	GAGCATTGCGGCTGATAAGG
BGH	GGCCTTAGAAGGCACAGTCGAG
M13 F	GTAAAACGACGGCCAGT
M13 R	GGAAACAGCTATGACCATGA
SV40	GGCATTCCACCACTGCTCCC

2.1.2. Agarose Gel Electrophoresis

DNA was analysed and/or purified by electrophoresis in 0.8-1% agarose gels in 40 mM Tris Acetate, 1 mM EDTA (TAE) solution (Sigma) containing 1% GelRed (Biotium) for 45 mins at 100 V. QIAquick Gel Extraction Kit™ (Qiagen) was used according to the manufacturer's protocol to extract and purify DNA from agarose gels. Gels were visualised using an Amersham Imager 600 (GE Healthcare) chemiluminescence imager.

2.1.3. dsRNA Synthesis and Purification

DNA templates for double stranded (ds)-RNA synthesis were generated by PCR using specific oligonucleotide primers with a 5' T7 RNA polymerase recognition sequence: TAATACGACTCACTATAGGG. Synthesis of dsRNA was performed using the Megascript T7 kit® (Ambion) according to the manufacturer's protocol. Briefly, reaction mixtures containing manufacturer defined volumes of PCR product as a DNA template, reaction buffer, ATP, CTP (Cytidine Triphosphate), GTP (Guanosine Triphosphate), UTP (Uridine Triphosphate), T7 enzyme and water were incubated at 37°C 12 hours (h). Reaction mixture was then treated with DNase I for 15 mins at 37°C to degrade unwanted DNA, and subjected to an

annealing step as follow: (1) 70°C for 10 mins (2) Ramp temperature down to 25°C at 2.5°C /s (3) hold at 25°C for 25 s (4) Maintain at 10°C for 5 mins (5) repeat steps (1)-(4). Precipitation and purification of dsRNA was performed using the $LiCl_2$ method (Barlow et al., 1963): After addition of 2x volume of RNase-free water, 0.1x volume of 5M $LiCl_2$ (Sigma) was added to the dsRNA product. Precipitation of the dsRNA was performed by adding 3x volume of 100% ethanol and incubating at -20°C for 20 minutes, before centrifugation at 13000 revolutions per minute (rpm) for 10 mins. After removal of the supernatant, 0.5 mL of 80% ethanol was added to the pellet and spun down at 13000 rpm for 5 mins. The dsRNA pellet was then air dried and dissolved in RNase-free water. See below for a list of the oligonucleotide primers used for dsRNA synthesis:

Table 2-2 List of dsRNA synthesis oligonucleotides

Primer name	Primer sequence
dsRNA synthesis primers – Primers contain T7 5' recombinase recognition sequence: TAATACGACTCACTATAGGG	
aPKC F	GCGTGCTTTCTGTGCCTACTG
aPKC R	GTTGATCACCTTCATGGCGTA
dnt F	GAGGACTTCGAGCTTTCAGAGACTA
dnt R	AGAACATCCTGAGTGTCGTTGTAG
eph F	GATTTTAAACTGGACCCACAAACAC
eph R	TAATGACATTCTCGAAACAATTTGA
gish F	TGGCCAAAGAATACATTGATTTAGA
gish R	GGCAGTGAACCCCTTAAGAAATAC
gprk2^{1} F	ACATCAATCACAAGAAGCTGGAC
gprk2^{1} R	AAAATACATAGAGCTCTCAAACTCCC
gprk2^{2} F	AGCGTTGGACGATAGATGTTCTAGT
gprk2^{2} R	GAACCTTCGGCAACTTAAACTTAG
hpo F	CTGTGTGGCAGACATATGGT
hpo R	CTCATCCACACCTTGCTCT
hppy F	GCGAAACGAATACAGAGCAA
hppy R	CACATGTACGCGATCTGGAC
lacZ F	TTGCCGGGAAGCTAGAGTAA
lacZ R	CCTTCCTGTTTTTGCTCAC
mnb^{5_1} F	GTCACTGGGCTGCATCTTG
mnb^{5_1} R	GATCCTGGCGGCTTGTACT
mnb^{11_1} F	CAAATTGGCTGCCAGCAT
mnb^{11_1} R	GAACCATCAGCACATTGCC
msn^{11_1} F	GATCGGGAAGTGCTAGTGGTAG
msn^{11_1} R	ATAAATGCTGTTCCTTTGGTACACT
msn^{13_1} F	TTACTAATCTCTTGCACAAATCTGCT
msn^{13_1} R	GATCTAGCAGCATTAAGCCATTCT

put F	TTTATACGAAAGAAGTCGTGTAAGATG
put R	AGGGCAAAACAAATTGTACGTTAT
pvr F	TTCTGTCCAATCGGTTCTCC
pvr R	CAACGATATCCGACAGGGAT
sax F	CACCATATTGCTACGACATGAAAAT
sax R	GTTCGAGGTGACCAGTATATTCTTT
slmb F	GCACAGGCCTTCACAACCACTATG
slmb R	TGCAGACCAGCTCGGATGATTT
tkv F	CGCTCCCTAACCTGCTACTG
tkv R	AAAACCACCGTTGTCTTCGG
wts F	CACAAAGTGGGACTGCC
wts R	GCAGGGTTTTCATCGCATAC

2.1.4. Gateway® Cloning

Plasmid constructs for cell transfection were generated using the Gateway® technology cloning system (Invitrogen). DNA coding sequences were amplified by PCR with oligonucleotide primers flanked by 5' BP Clonase® recombination recognition sequences. Amplified coding PCR product was incubated with BP Clonase® as per manufacturer's protocol to generate pENTR® (Invitrogen) plasmids. Entry clone plasmids were used in LR Clonase® reactions (Invitrogen) to move coding DNA into an expression vector (pDEST) containing a desired peptide tag for antibody recognition. The correct integration of coding DNA was initially confirmed by DNA restriction digest analysis (see below), followed by DNA sequencing. The insert sequence was confirmed by Sanger sequencing (Source Bioscience) using pENTR® specific primers (M13F and M13R), pDEST specific primers (ActF and SV40R) and gene specific primers. All pENTR and DEST vectors contain antibiotic resistance genes for selection. See below for a list of the expression plasmids used:

Table 2-3 List of expression plasmids

Plasmid name	Gene name
***Drosophila* actin5C-driven expression**	
pAHW aPKC	aPKC
pAHW aPKC^{CAAX}	aPKC – CAAX sequence
pAHW aPKCK^{293W}	aPKC – kinase dead
pAHW aPKC$^{293W\ CAAX}$	aPKC – CAAX sequence / kinase dead

pAFW CG10889	CG10889
pAHW CG10889	CG10889
pAFW CG10889^{C154A}	CG10889 – catalytic mutant
pAHW CG10889^{D138N}	CG10889 – catalytic mutant
pAFW CG10889^{Y413A}	CG10889 – PPxY mutant
pAHW CG10889 ^{Y413A}	CG10889 – PPxY mutant
pAHW CG2577	CG2577
pAHW CG7094	CG7094
pAHW CG9962	CG9962
pAHW CG12147	CG12147
pAHW CK1α	CK1α
pAHW CK1α^{K49R}	CK1α – kinase dead
pUAS Crb^{FL}	Crb – full length - inducible
pAMW Crb^{i}	Crb – intracellular domain
pAMW Crb$^{i\Delta FBM}$	Crb – intracellular domain / FBM mutant
pAHW D	D
pAHW Dco	Dco
pAHW Dco^{K38R}	Dco kinase dead
pAWV Dnt^{isoA}	Dnt
pAWF Ex	Ex – full length
pAWV Ex	Ex – full length
pAFW Ex$^{1-468\ CAAX}$	Ex$^{1-450}$ – CAAX sequence
pAWF Ex$^{1-468}$	Ex$^{1-468}$
pAWV Ex$^{1-468}$	Ex$^{1-468}$
pAFW Ex$^{1-468\ CAAX}$	Ex$^{1-468}$ – CAAX sequence
pAVW Ex$^{1-468\ CAAX}$	Ex$^{1-468}$ – CAAX sequence
pAHW Ft^{ICD}	Ft – intracellular domain
pAW Gal4	Gal4
pAWH GFP	GFP
pAWF GFP	GFP
pAWM GFP	GFP
pAWV GFP	GFP
pAWH Gish^{isoF}	Gish^{isoF}
pAWH Gish$^{isoF\ CAAX}$	Gish^{isoF} – CAAX sequence
pAWF Gish^{isoI}	Gish^{isoi}
pAWH Gish^{isoI}	Gish^{isoi}
pAWH Gish$^{isoI\ K91R}$	Gish^{isoi} – kinase dead
pAHW Hpo	Hpo
pAHW Mats	Mats
pAWF NTAN	NTAN
pAWV Sax^{isoB}	Sax^{isoB}
pAHW Sgg	Sgg
pAHW Sgg^{S9A}	Sgg – constitutively active
pAHW Sgg^{A81T}	Sgg – kinase dead
pAWF Slmb	Slmb
pAWV Tkv^{isoD}	Tkv^{isoD}
pAHW Ub	Ub
pAFW Usp2^{isoA}	Usp2^{isoA}
pAFW Usp2$^{isoA\ C540A}$	Usp2^{isoA} – catalytic mutant
pAFW Usp2^{isoC}	Usp2^{isoC}
pAFW Usp2$^{isoC\ C622A}$	Usp2^{isoC} –catalytic mutant
pAWF Wts	Wts
pAWH Wts	Wts
pAFW Yki	Yki
pAHW Yki	Yki
pAFW Yki$^{1-140}$	Yki$^{1-140}$
pAFW Yki$^{1-300}$	Yki$^{1-300}$

pAFW Yki$^{1-369}$	Yki$^{1-369}$
pAFW Yki$^{\Delta WW2}$	Yki^{WW2} – WW2 domain mutant
pAFW Yki $^{\Delta WW1+2}$	Yki^{WW1+2} – WW 1 and 2 domain mutant

2.1.5. DNA Restriction Enzyme Digestion

Correct integration of desired DNA into pENTR or pDEST vectors was first tested by DNA restriction enzyme digest reaction using defined restriction enzyme recognition sequences flanking the Gateway® integration sites. 5 µL reactions of 0.5 µL plasmid DNA, 1 µL appropriate restriction enzyme buffer, 0.3 µL Bovine Serum Albumin (BSA, Sigma) and 1 µL total restriction enzyme topped up with RNase-free water and incubated at 37ºC for 1 h. Double DNA digest contained 0.5 µL of each restriction enzyme. Agarose gel electrophoresis was performed on digested DNA to confirm correct DNA insertion.

2.1.6. Site-Directed Mutagenesis

Point mutations were generated using the QuikChange® Multi Site-Directed Mutagenesis Kit (Stratagene) according to the manufacturer's instructions. In brief, a reaction mixture containing manufacturer defined volumes of two complimentary oligonucleotides containing the relevant point mutation, plasmid DNA template and Pwo Master-mix® (Roche) were submitted to the following thermocycler programme: (1) Initial denaturing - 95ºC for 30 s (2) Melting – 95ºC for 30 s (3) Annealing – 55ºC for 1 min (4) Extension - 70ºC for 1min/kb of plasmid length. PCR reactions were performed with 16 cycles of steps (2)-(4) and held at 10ºC. Methylated DNA template was then digested through treatment of 1 µL of Dpn I at 37ºC for 1 h. Typically, mutagenesis was performed in existing pENTR® vectors. Mutagenesis was confirmed by Sanger sequencing.

2.1.7. Production of Transformation Competent Bacteria

Calcium competent bacteria capable of incorporating plasmid DNA were amplified from Top10 stock (Thermo Fisher). Top10 stock bacteria were plated on an antibiotic free Lysogeny Broth (LB)-agar plate and incubated overnight at 37°C. A single colony was selected and inoculated with 10 mL LB media and incubated overnight at 37°C. Next, 2 L of LB media was inoculated with 10 mL of the started culture and grown at 37°C until the absorbance at 600 nm was measured between 0.35 and 0.4 Absorbance Units (AU). Culture was chilled on ice for 30 mins and harvested by centrifugation at 3000 g for 15 mins at 4°C. Bacterial pellets were resuspended in 200 mL of 4°C $MgCl_2$ (100 mM Sigma) and harvested by centrifugation at 2000 g for 15 mins at 4°C. Pellet was resuspended in 400 mL of 4°C $CaCl_2$ (100 mM Sigma) and incubated at 4°C for 20 mins. Bacteria were harvested by centrifugation at 2000 g for 15 mins at 4°C and resuspended in 100 mL of 4°C $CaCl_2$ (85 mM), 15% glycerol. Bacteria were harvested by centrifugation at 1000 g for 15 mins at 4°C and resuspended in 4 mL of 4°C $CaCl_2$ (85 mM), 15% glycerol (Sigma). Bacteria were then aliquoted and snap frozen in liquid nitrogen and stored at -80°C.

2.1.8. Transformation of Competent Bacteria

Amplification of cloned plasmid DNA was performed through transformation of competent bacteria. 0.2-0.5 µL DNA was gently mixed with 5-20 µL competent bacteria on ice and incubated for 20 mins, followed by 45 s heat-shock at 42°C and 2 min incubation on ice. Transformed bacteria were then incubated with 400 µL of LB for 1 h at 37°C under shaking, and plated on LB-agar plates overnight at 37°C. Plasmids with antibiotic resistance genes were selected in LB-agar plates laced with the appropriate antibiotic.

2.1.9. Plasmid DNA Purification

Plasmid DNA from transformed bacterial colonies was purified using the QIAprep® miniprep (Qiagen) or NucleoBond® midiprep (Macherey-Nagel) kits according to the manufacturer's instructions.

2.1.10. Nucleic Acid Quantification

Nucleic acid concentration was quantified using a Nanodrop 1000 Spectrophotometer (Thermo Fisher). Quantification in ng/µL uses the Beer-Lambert equation based on absorbance at 260 nm and the defined extinction coefficients for nucleic acids. The purity of the sample was assessed by the ratio of sample absorbance at 260 nm and 280 nm. A ratio of approximately 1.8 or 2 was deemed pure for DNA or RNA respectively.

2.1.11. Preparation of Protein Lysates

Drosophila S2 cells were isolated by centrifugation at 1200 rpm for 3 mins and lysed in Triton X-100 lysis buffer (50 mM Tris pH 7.5, 150 mM NaCl, 1% Triton X-100, 10% glycerol and 1 mM EDTA, Sigma) supplemented with phosphatase inhibitor cocktails 2 and 3 (Sigma) and protease inhibitor cocktail (Roche) at 4ºC. Cell lysates were cleared by centrifugation at 13,000 rpm for 12 mins at 4ºC. Total protein concentration was determined by Bradford assay (Bio-Rad), whereby the absorption shift of Coomassie Brilliant Blue upon protein binding was visualised at 595 nm, and compared to a BSA protein standard. Lysates were next treated with 1:10 sample reducing buffer® (Invitrogen) and 1:4 LDS sample buffer® (Invitrogen) and either frozen at -20ºC or -80ºC (for short term or long term storage, respectively) or denatured at 95ºC for 5 mins for Western Blot analysis.

2.1.12. Protein Co-Immunoprecipitation

Agarose M2-FLAG beads (Sigma) were pre-washed with lysis buffer described in 'Preparation of Protein Lysates' and S2 cell lysates were incubated with 30 µL of M2-FLAG beads for 1-2 h at 4ºC on a rotating wheel, and recovered by centrifugation at 4000 rpm. Beads were then washed 3 times for 5 mins in lysis buffer and eluted by addition of 80 µL of 150 ng/µL 3xFLAG peptide for 40 mins at 4ºC on a rotating wheel. FLAG immunoprecipitates were recovered by centrifugation at 13000 rpm for 1min, and a mixture of 1:10 sample reducing

buffer® (Invitrogen) and 1:4 LDS sample buffer® (Invitrogen) was added to samples. Lysates were either frozen at -20ºC or -80ºC, or denatured at 95ºC for 5 mins for Western Blot analysis.

2.1.13. Ubiquitylation Assays

Ubiquitylation assays were performed on lysates previously transfected with HA-ubiquitin. Ubiquitylated proteins were isolated via HA-immunoprecipitation. Cells were harvested by centrifugation at 1200 rpm for 3 mins and washed with ice-cold Phosphate Buffered Saline (PBS). 10% of cell material was lysed as described in 'Preparation of Protein Lysates'. The remaining 90% was lysed in boiling 1% SDS-PBS for 5 mins at 100ºC, vortexed and incubated for a further 5 mins at 100ºC, and lysates were diluted fivefold with 0.5% BSA-1% Triton X-100 PBS. DNA was sheared by sonication and cell extracts were cleared by centrifugation at 13000 rpm for 10 mins at 4ºC. HA-agarose beads (Sigma) were pre-washed in PBS and incubated with samples diluted twofold with 0.5% BSA-1% Triton X-100 PBS using Bio-Spin Columns (Bio-Rad) overnight at 4ºC on a rotating wheel. Subsequently, columns were washed twice with 0.5% BSA-1% Triton X-100–PBS and twice with 1% Triton X-100–PBS. HA immunoprecipitates were eluted using 75 μL 0.2 M glycine pH 2.5 for 30 min at room temperature (RT) and the pH of the eluates was adjusted with 7 μL 1 M NH_4HCO_3 (Sigma). Samples were prepared for immunoblot analysis by addition of 1:10 sample reducing buffer® (Invitrogen) and 1:4 LDS sample buffer® (Invitrogen) and denaturing at 95ºC for 5 mins.

2.1.14. Immunoblotting

30-40 μg of total protein from cell lysates or 10-15 μL of immunoprecipitated sample was loaded into NuPAGE®Novex® 10% or 4-12% Bis-Tris gels (Invitrogen) and separated by electrophoresis as per manufacturer's recommendation. Typically, electrophoresis was performed at 4ºC for 20 mins at

100 V to concentrate the protein at the border between the stacking and resolving gel, and subsequently for 1 h at 195 V.

Proteins were transferred from gels onto Amersham Hybond-P® PVDF membranes (GE Healthcare). For the analysis of proteins whose size was less than 200 kDa, the transfer took place at 4°C for 100-120 mins at 100 V using transfer buffer (25 mM Tris, pH 8, 192 mM glycine and 20% methanol, Sigma). If proteins of interest were greater than 200 kDa, transfer took place at 4°C for 14-16 h at 18 V using transfer buffer (25 mM Tris, pH 8, 192 mM glycine and 10% methanol).

Membranes were then blocked for 30-60 mins in 5% milk in Tris buffered saline with 0.1% Tween (TBST) and subsequently incubated with primary antibody diluted in 5 mL 5% milk in TBST overnight, or for 1-2 h at RT. Membranes were then washed 3 times for 10 mins in 0.1%-TBST before incubation for 1h at RT with 5 mL horseradish peroxidase-conjugated secondary antibodies diluted in 5% milk in TBST. Membranes were developed by chemiluminescence using ECL PLUS® HRP substrate (Pierce). See below for a list of the antibodies used for immunoblot analysis:

Table 2-4 List of immunoblot antibodies

Primary Antibody	Species	Dilution	Source
aPKC^{sc-216}	Rabbit	1:5000	Santa-Cruz
Crb^{Cq4}	Mouse	1:1000	DSHB
FLAG^{M2}	Mouse	1:5000	Sigma
HA^{3F10}	Rat	1:2500	Roche
c-MYC^{9E10}	Mouse	1:2500	Santa-Cruz
αTub^{E7}	Mouse	1:5000	DSHB
V5^{Novex}	Mouse	1:5000	Invitrogen
Secondary Antibody	**Species**	**Dilution**	**Source**
Mouse^{HRP}	Sheep	1:5000	Amersham
Rabbit^{HRP}	Donkey	1:5000	Amersham
Rat^{HRP}	Goat	1:5000	Amersham

2.1.15. Quantification of Immunoblots

Densitometric quantification of immunoblots was performed on x-ray films scanned using an 'Epson Perfection V700' flatbed scanner using the 'Gel Analyzer' function within ImageJ software. For experiments involving dsRNA treatment of S2 cells, quantified Ex levels and Crb levels were normalised to the tubulin loading control. The ratio of these normalised values was then calculated to account for variablilty in Crb levels. These values were then normalised to the mean Ex level for the $Crb^{\Delta FBM}$ negative control, which was set to 1 to gain a relative level of Ex compared to this negative control. For experiments involving kinase overexpression, Ex levels normalised against the tubulin loading control were normalised directly against the mean Ex level from $Crb^{\Delta FBM}$ negative control, which was set to 1 to gain a relative level of Ex compared to this negative control.

2.2. Cell Culture

2.2.1. *Drosophila* S2 Cell Culture

The *Drosophila* Schneider S2 cell line used throughout this study is composed of semi-adherent cells derived from late stage (20-24 h) embryos and represents a macrophage-like lineage (Schneider, 1972). S2 cells were maintained in Schneider's medium® (Invitrogen) supplemented with 10% foetal bovine serum (FBS, Invitrogen) and 1% Penicillin/Streptomycin (Sigma). Cells were passaged in T75cm^2 flasks (Corning) every 2-3 days to a 1:10 dilution. Prior to splitting, cells were collected by centrifugation for 3 mins at 1200 rpm and washed with PBS or media to remove debris. Frozen cell stocks were stored in liquid nitrogen in a 7.5% DMSO, FBS or 10% DMSO, FBS solution.

2.2.2. Transient Transfection of S2 Cells

For plasmid DNA transfections, cells were seeded in 6-well plates 20 minutes prior to transfection at a concentration of 2.0 $x10^6$ cells/mL/well. Mini- or Midi-

prep purified plasmid DNA was diluted in 100 µL EC buffer with Effectene Enhancer® and Effectene Transfection Reagent® (Qiagen) as per the manufacturer's protocol, and added to plated cells in a dropwise manner. Typically, 3.2 µL of Effectene Enhancer® and 10 µL Effectene Transfection Reagent® were used. Unless otherwise stated, cells were harvested 48 h after transfection.

2.2.3. *Drosophila* S2 Cell dsRNA Treatment

For dsRNA treatment, cells were seeded in 6-well plates at 1.5 x10^6 cells/mL/well and left to adhere for 20 minutes. After removing media, cells were incubated with 1 mL/well serum-free media and treated with 20 µg dsRNA for 1 h, before addition of 2 mL/well of complete media. Subsequent DNA transfections occurred 24 h after dsRNA treatment. Cells were harvested between 48-72 h after initial dsRNA treatment.

2.3. Fly Genetics

2.3.1. Fly Husbandry

Drosophila stocks and crosses were maintained in vials containing fly food made in-house according to the following recipe:

For 3 L H_20: 240 g maize powder, 54 g yeast extract, 30 g soya powder, 240 g malt, 120 g molasses, 26 g agar, 18.6 mL propionic acid, 1.2 mL phosphoric acid and 36 mL of 10% Nipagin in 70% ethanol (Sigma).

All crosses were carried out at 25^{o}C unless specified.

2.3.2. Maintenance of Stable Stocks

Drosophila homozygous lethal genotypes were maintained using balancer chromosomes. Balancer chromosomes contain multiple, overlapping inversions to suppress meiotic recombination, as well as carrying dominant phenotypic markers and recessive lethal or recessive sterile mutations. This prevents homozygous lethal genotypes being segregated through meiotic recombination, or loss of desired genotype due to dominant deleterious effects, thus facilitating the maintenance of stable transgenic lines.

2.3.3. Enhancer Trap-Gene Expression Analysis

Enhancer traps are genetic constructs that allow for analysis of gene specific expression patterns. Enhancer trap constructs contain a reporter, typically the *lacZ* gene from *Escherichia coli (E. coli)* encoding the β–Galactosidase (β–Gal) protein, fused to the transposase promoter within a *P*-element. As *P*-element integration frequently occurs in close proximity to gene promoters (Spradling et al., 1995), the transposase promoter, and thus the reporter gene may come under the spatial and temporal control of specific genes (Bier et al., 1989) and can be used to study gene specific expression patterns.

Many defined enhancer traps have been generated, and the following were used in this study: *P{lacW}diap1^{j5C8} (diap1-lacZ)* (Spradling et al., 1999) and *P{lacW}ex^{697} (ex-lacZ)* (Boedigheimer and Laughon, 1993).

2.3.4. The UAS-Gal4 System – Spatiotemporal Control of Gene Expression

The Gal4 protein is a transcription factor responsible for the regulation of galactose metabolism genes in *Saccharomyces cerevisiae* by binding the upstream activation sequence (UAS) and stimulating transcription (Hashimoto et al., 1983). High level of conservation between eukaryotic transcription

machineries means the Gal4-UAS system can activate transcription in other species, such as *Drosophila*, and the development of this technique has transformed *Drosophila* genetics (Brand and Perrimon, 1993).

Many *Drosophila* enhancer traps have been generated using the Gal4 transcription factor as a reporter, which will therefore come under the specific control of genes close to the site of Gal4 *P*-element insertion. Experimental combination of these Gal4 enhancer traps with transgenes containing *UAS* sequences results in transgenic expression within the specific spatial and temporal Gal4 expression pattern (Brand and Perrimon, 1993). This technique is therefore used ubiquitously to drive expression of transgenes in known spatial and temporal patterns (Figure 2-1A).

The following Gal4 enhancer traps were used: *P{ap-Gal4.VNC} (apterous-Gal4, ap>)* (Rincon-Limas et al., 1999) to drive expression in the dorsal compartment of the wing, *P{en2.4-Agl4}e16E (engrailed-Gal4, en>)* (Brand and Perrimon, 1993) and *P{Gal4}hhGal4 (hedgehog-Gal4, hh>)* (Tanimoto et al., 2000) to drive expression in the posterior compartment of the wing, *P{GawB}Bx^{MS1096} (MS1096-Gal4, MS1096>)* to drive expression in the whole wing (Capdevila and Guerrero, 1994), *P{GawB}nubbin-Gal4, nub>)* to drive expression in the wing pouch (Azpiazu and Morata, 2000), and *P{GawB}ptc$^{559.1}$ (patched-Gal4, ptc>)* to drive expression along the wing anterior-posterior boundary (Brand and Perrimon, 1993).

See below for a list of the *UAS* overexpression lines used:

Table 2-5 List of *UAS* overexpression lines

UAS-line	Chromosome
CK1α^{HA}	III
Crb^{i}	III
D^{2D}	II
D^{V5}	II
Dco	III
Ds$^{(II)}$	II
Ds$^{(L14)}$	II

Ex	II
Ex^{S453A}	II
Ft^{HA}	II
GFP$^{::CD8}$	II
Gish^{isoB}	II
Gish$^{isoB\ Kinase\ Dead}$	II
Gish^{isoF}	III
Sgg^{isoB}	II
Sgg$^{isoB\ A81T}$	II
Usp2$^{(II)}$	II
Usp2$^{(III)}$	III

2.3.5. Interference RNA

Interference RNA (RNAi) guides the sequence specific degradation of messenger (m)-RNA to control gene expression. Specific RNAi sequences encode dsRNA which is processed by the enzyme Dicer creating a guide RNA strand, which is incorporated into the RNA-induced silencing complex (RISC), where sequence specificity of the RNA targets mRNA, commonly for degradation thus silencing the target gene (Wilson and Doudna, 2013). Several *Drosophila* stock centres and large laboratory consortia have systematically generated genome-wide RNAi transgene libraries under the control of *UAS* elements (Perrimon et al., 2010), which enable the rapid and efficient study of gene function.

See below for a list of the RNAi lines used, with the exception of RNAi lines used for the DUB modifier screen. See Table 7-1 for list of RNAi lines used in the DUB modifier screen.

Table 2-6 List of *UAS-RNAi* lines

Gene	RNAi line	Chromosome
CG2577	105471 KK	II
CG7094	108273 KK	II
CG9962	108721 KK	II
CG10889	10889R-3	II
CG12147	101875 KK	II
d	102550 KK	II
ds	-	II
eph	TRIP HMS01986	II

ft	-	II
gckIII	107158 KK	II
gckIII	TRIP HMS04487	II
gish	108680 KK	II
gprk2	TRIP HMS02330	II
hpo	104169 KK	II
lacZ	n/a	II
mnb	107066 KK	II
msn	101517 KK	II
patj	31620 GD	III
put	TRIP HMS01944	II
sax	TRIP HMS04520	II
sdt	23822 GD	III
sgg	101538 KK	II
tkv	TRIP HMS02185	II
usp2	14619R-1	III
usp2	14619R-3	III
usp2	104382 KK	II
wts	12072R-1	III

For RNAi lines used in *nub>DUB^{IR}* screen, see Table 7-1

2.3.6. The FLP/FRT System

Generation of genetic mosaics is a useful tool for phenotypic analysis of specific mutations. Tissue containing mutant clones can be achieved by generating mitotic recombination between homologous chromosomes using the Flippase Recombinase (FLP) isolated from yeast 2μ plasmid, which mediates highly efficient site-specific recombination between specific Flippase Recombination Target (FRT) DNA sequences (Golic and Lindquist, 1989; Senecoff et al., 1985). During mitosis, activity of the FLP recombinase can catalyse recombination between non-sister chromatids, which results in a high frequency of recombinant mitotic clones. If a heterozygous mutant gene is located within the chromosome arm that is recombined, homozygous mutant clones will be generated and can be phenotypically analysed. This technique will also generate homozygous wild-type tissue and heterozygous mutant/wild-type tissue. If the wild-type FRT chromatid contains a marker such as GFP, the mutant tissue will be marked by an absence of GFP (Figure 2-1B). Recombination is induced when *Drosophila*

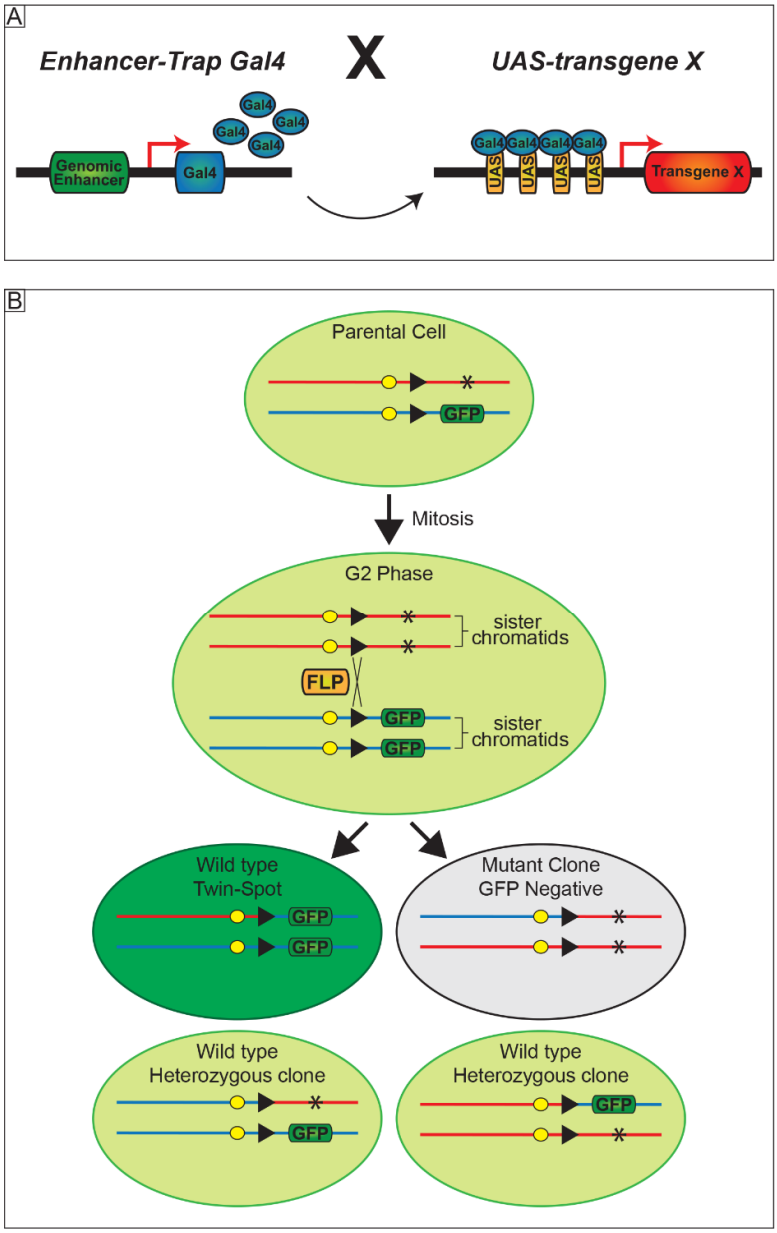

Figure 2-1 The Gal4-UAS and the FLP-FRT systems

Schematic representation of the Gal4-UAS system whereby the Gal4 transcription factor under the control of a genomic enhancer drives the expression of any gene downstream of the UAS sequence (A). See 'The UAS-Gal4 System – Spatiotemporal Control of Gene Expression' for details. Representation of the FLP-FRT system to induce negatively labelled homozygous mitotic clones, where GFP is used as a fluorescent marker (B). See 'The FLP/FRT System' for details.

stocks containing a FLP transgene driven, typically under the control of the heat-shock promoter (*hsFLP*) are combined with *P*-element transformed chromosomes containing FRT sites in close proximity to the centromeres. If *hsFLP* provides the FLP source, the heat-shock promoter drives expression of FLP at 37^{o}C, and one hour incubation during larval development is normally sufficient to efficiently induce recombination (Xu and Rubin, 1993).

2.3.7. Immunofluorescence Analysis

Drosophila wing imaginal discs from third instar larvae were dissected in PBS and fixed in 4% paraformaldehyde in PBS, 0.1% Triton X-100 for 25 mins at room temperature. Samples were washed in 0.1% Triton X-100, PBS, and blocked for 1 h at room temperature in 5% Normal Donkey Serum (NDS)-PBS, 0.1% Triton X-100. Primary antibody diluted in 5% NDS-PBS, 0.3% Triton X-100 were incubated overnight at 4^{o}C. After washing for 1 h in 0.1% Triton X-100, PBS, samples were incubated with secondary antibody diluted in 5% NDS NDS-PBS, 0.3% Triton X-100 for 1 h at room temperature and washed in 0.1% Triton X-100, PBS for 3 h, the penultimate wash step was supplemented with 1:1000 DAPI for DNA visualisation. Samples were mounted in Mowiol media (84 mL stock – 9.6 g Mowiol 4-88, 12 ml glycerol, 24 ml H_2O, 48 ml 0.2 M TrisHCL, pH 8.5, Sigma) on glass slides (VWR) sealed with cover slips (WVR) and stored at 4^{o}C for at least 24 h prior to imaging. See below for a list of the antibodies used for immunofluorescent analysis:

Table 2-7 List of immunofluorescence antibodies

Primary Antibody	**Species**	**Dilution**	**Source**
β-Galactosidase	Mouse	1:500	Promega
Ci^{2A1}	Rat	1:100	DSHB
Crb^{Cq4}	Mouse	1:10	DSHB
Crb^{ICD}	Rat	1:200	F. Pichaud
GFP^{ab13970}	Chicken	1:1000	Abcam
GFP$^{::FITC - ab6662}$	Goat	1:1000	Abcam
HA^{3F10}	Rat	1:100	Roche
c-MYC^{9E10}	Mouse	1:100	Santa-Cruz
V5^{Novex}	Mouse	1:250	Invitrogen
Secondary Antibody / Fluorophore	**Species**	**Dilution**	**Source**
Chicken^{ab150169} /Alexa 488	Goat	1:1000	Abcam

Mouse / Alexa 647	Donkey	1:1000	Jackson Immuno
Mouse / FITC	Donkey	1:500	Jackson Immuno
Mouse RRX	Donkey	1:250	Jackson Immuno
Rat^{ab175710} /Alexa 568	Goat	1:1000	Abcam
Rat / RRX	Donkey	1:500	Jackson Immuno

2.3.8. Confocal Microscopy

Images of imaginal wing discs were obtained using an LSM 510 or LSM 710 laser scanning confocal microscope (Zeiss) using a 40x oil immersion lens. Images were analysed using the LSM Image Browser (Zeiss), ImageJ and Photoshop software. Image colours, brightness and contrast were adjusted in Photoshop (Adobe).

2.3.9. Adult Wing Analysis

Adult *Drosophila* of the appropriate genotype were collected and stored in 70% ethanol prior to wing dissection. Adult wings were dissected in isopropanol and mounted in Euparal (Anglian Lepidopterist Supplies, UK) on glass slides (VWR) sealed with cover slips (VWR) and baked at 65^{o}C for 5 h.

Adult wing images were captured using a Panoramic 250 High Throughput Scanner, and wing area was quantified using the ImageJ software. For quantification of the posterior wing area / total wing area ratio, the posterior wing was measured to include the entire wing below the longitudinal vein 4.

Wing area data were transformed using Excel (Microsoft) and graphs were constructed using GraphPad Prism 5. Statistical analysis was performed in GraphPad Prism 5 using the Student's t-test, or by one-way ANOVA, with either the Dunnett's post hoc test or the Turkey's range post hoc test depending on the data. Analysis is defined within the specific figure legends.

Chapter 3 - Results 1 – Polarity Proteins as Regulators of Expanded Stability

3.1. **A Novel Tool to Study the Regulation of Expanded Protein Stability *In Vivo***

One of the technical difficulties in observing Ex protein levels *in vivo* is that depletion of Ex activates a Yki-dependent transcriptional programme, which in turn increases Ex protein levels as a result of Yki-mediated *ex* expression. This axis of Hpo signalling results in a negative feedback loop limiting excessive Yki activity (Figure 1-2). As a consequence of this feedback loop, assessing Ex protein levels using an Ex-specific antibody reflects not only post-translational, but also transcription-dependent regulation of Ex. Therefore, directly regulating Ex post-translational stability will affect *ex* transcription. To avoid this feedback loop, a transgenic *Drosophila* line was generated (Paulo Ribeiro – Barts Cancer Institute) containing a GFP-tagged Ex^{1-468} truncation under the control of the ubiquitin promoter (*ubi-ex$^{1-468}$::GFP)*. This N-terminal fragment of Ex includes the FERM domain, and has been previously identified as the minimal region of Ex required to be degraded in response to Crb (Ribeiro et al., 2014). The ubiquitin promoter drives the expression of the *ubi-ex$^{1-468}$::GFP* reporter constitutively in all tissues and, unlike endogenous *ex*, is refractory to Yki-mediated transcription. Thus, by analysing changes in GFP levels, changes in exogenous Ex levels can be directly assessed while avoiding the confounding effect of the Yki feedback loop. Unfortunately, a full length version of this reporter could not be recovered, possibly due to the pro-apoptotic and anti-proliferative functions of full length Ex, even when expressed at low levels under the *ubi* promoter. The function of the N-terminal fragment of Ex appears to be in regulating its correct localisation, which is dependent on the FERM domain of Ex, and the FBM of Crb, rather than explicitly regulating growth (Badouel et al., 2009). As correct localisation of Ex is vital to its regulation of the Hippo pathway (Chen et al., 2010; Grzeschik et al., 2010; Ling et al., 2010; Ribeiro et al., 2014; Robinson et al., 2010; Sun et al.,

2015), the study of the Ex^{1-468} N-terminal fragment is still valid as a tool for understanding of its overall function.

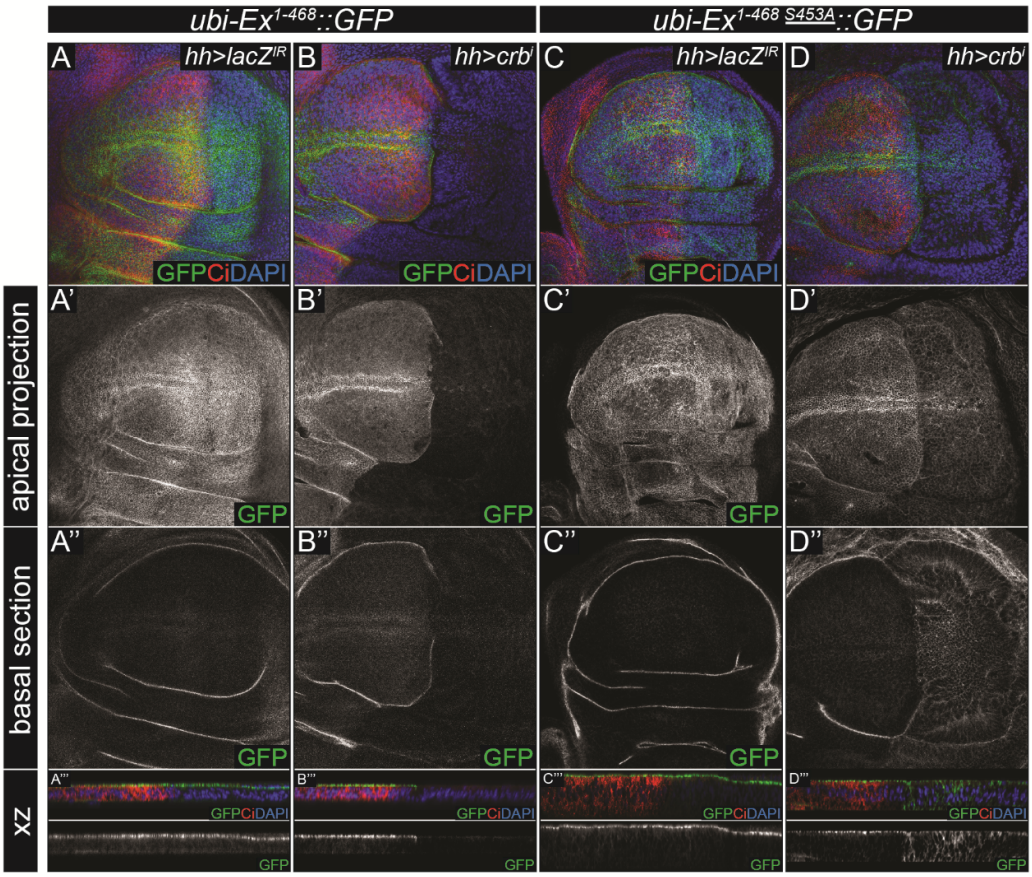

Figure 3-1 Validation of *ubi-ex$^{1-468}$::GFP* as a tool for analysing Ex protein levels *in vivo*

Third instar larvae wing imaginal discs expressing *ubi-ex$^{1-468}$::GFP* (A-B) and *ubi-ex$^{1-468\ S453A}$::GFP* (C-D) were dissected and processed for immunofluorescence analysis. Confocal micrographs of GFP staining (A, B, C, D - green in merged image) in maximum intensity projection of the apical domain (A, A', B, B', C, C', D, D'), a basal plane (A'', B'', C'', D'') and transverse xz sections (A''', B''', C''', D''') of wing imaginal discs. Nuclei are marked by DAPI staining (blue) and the posterior *hh>Gal4* expression domain marked by the absence of Ci staining (red). Overexpression of *hh>lacZ^{IR}* has no effect on *ubi-ex$^{1-468}$::GFP* levels (A-A''') or *ubi-ex$^{1-468\ S453A}$::GFP* (C-C'''). Expression of *hh>crb^{i}* causes loss of *ubi-ex$^{1-468}$::GFP* (B-B'''). Expression of *hh>crb^{i}* causes apical loss (D-D''') coupled with basal increase (D'', D''') of *ubi-ex$^{1-468\ S453A}$::GFP.*

To validate that the *ubi-ex$^{1-468}$::GFP* reporter behaved as expected and accurately reported modulation of Ex protein levels, wing imaginal discs were analysed for GFP, in combination with *hh-Gal4* to drive UAS-mediated overexpression in the posterior compartment (Tanimoto et al., 2000). Anti-Ci staining was used as a marker of the anterior compartment (Eaton and Kornberg, 1990; Orenic et al., 1990). While the *ubi-ex$^{1-468}$::GFP* is expressed universally throughout the wing disc, specific transgenes were expressed only in the posterior compartment. Therefore, in these experiments, the anterior compartment serves as an internal control, where the expression of the *ubi-ex$^{1-468}$::GFP* reporter should not be affected by transgene expression. This allows for accurate identification of genotypes that impact upon Ex levels in the posterior compared to the anterior compartment.

In control discs overexpressing *UAS-lacZ^{IR}*, the *ubi-ex$^{1-468}$::GFP* reporter was localised at the apical junctions of cells, similar to wildtype endogenous Ex (Figure 3-1A) (Boedigheimer et al., 1997; McCartney et al., 2000). When *ubi-ex$^{1-468}$::GFP* levels were analysed in a cross-section of a single plane of the wing disc, the GFP signal was predominantly localised to the apical membrane surface. This suggests that Ex$^{1-468}$::GFP localisation accurately reflects that of endogenous Ex. Overexpression of *crb$^{intracellular-domain}$* (*crb^{i}*) is known to stimulate Ex degradation (Chen et al., 2010; Grzeschik et al., 2010; Ling et al., 2010; Robinson et al., 2010) and was therefore used as a positive control to validate the *ubi-ex$^{1-468}$::GFP* reporter. This *crb^{i}* fragment contains the thirty seven amino acid intracellular tail of Crb, as well as the transmembrane region, but no extracellular domain (Figure 1-3B) (Ling et al., 2010). In the presence of *UAS-crb^{i}*, *ubi-ex$^{1-468}$::GFP* appears to be almost entirely lost from the apical surface of the tissue (Figure 3-1B), without a concurrent increase in basal levels of Ex. This suggests the *ubi-ex$^{1-468}$::GFP* reporter is responsive to Crb-mediated degradation similar to endogenous Ex.

An additional *ubi-ex$^{1-468}$::GFP* reporter line was also generated containing a S453A (*ubi-ex$^{1-468\ S453A}$::GFP*) point mutation. This serine residue closely

conforms to the canonical Slmb phosphodegron consensus ^{452}TSGIVS^{457} and, accordingly, the Ex^{S453A} point mutant is unable to bind to Slmb, and is refractory to Crb-mediated degradation in S2 cells (Ribeiro et al., 2014). Similar to the wildtype *ubi-ex$^{1-468}$::GFP* reporter and endogenous Ex, *ubi-ex$^{1-468\ S453A}$::GFP* was apically localised (Figure 3-1C) as seen through XY and XZ sections. However upon *crb^{i}* overexpression, apical *ubi-ex$^{1-468\ S453A}$::GFP* is predominantly lost, coupled with a dramatic increase in basal levels of the reporter (Figure 3-1D), which is not observed in the wildtype reporter (Figure 3-1A). This reflects the inability of *crb^{i}* to stimulate degradation of Ex with a mutation at S453. Crb is an apically localised polarity determinant, however overexpressed Crb^{i} has been reported to localise on all plasma membranes (Klebes and Knust, 2000). Consistent with this, in collaboration with Maxine Holder of the Francis Crick Institute staining for the intracellular domain of Crb (Crb^{ICD}) (Walther et al., 2016) revealed that wildtype Crb localises to the apical membrane, whereas in addition to being apically localised, *crb^{i}* is also localised throughout the basal membranes of the wing imaginal disc (collaborator data not shown). Therefore it is likely that the increase in basal *ubi-ex$^{1-468\ S453A}$::GFP* (Figure 3-1D) is the result of physical interaction between Ex and Crb, and thus as Crb is localised throughout the plasma membrane of the wing disc, so too is Ex. It would be interesting to assess the localisation of the *ubi-ex$^{1-468\ S453A}$::GFP* reporter on expression of full-length Crb, which only localises to the apical region of the wing disc due to the stabilising effect of homophilic cis- and trans-interactions (Fletcher et al., 2012; Thompson et al., 2013).

In order to further characterise these reporter lines, their ability to regulate tissue size was analysed, as the overexpression of Ex should result in reduced growth through inhibition of Yki. Adult wings from control flies expressing GFP under the control of *hh-Gal4* were dissected and their size was measured. The average size of wildtype wings was compared to adult wings from the *hh>GFP, ubi-ex$^{1-468}$::GFP* reporter lines. No statistical difference was observed in adult wing size between the controls or the reporter lines, suggesting either the ubiquitin promoter is too weak to drive sufficient Ex expression to inhibit Yki, or the Ex^{1-}

^{468} truncation itself is insufficient to significantly inhibit Yki, perhaps because the main growth inhibitory region of Ex is the C-terminus PPxY motif-containing portion, which is absent from Ex$^{1-468}$ (Figure 3-2).

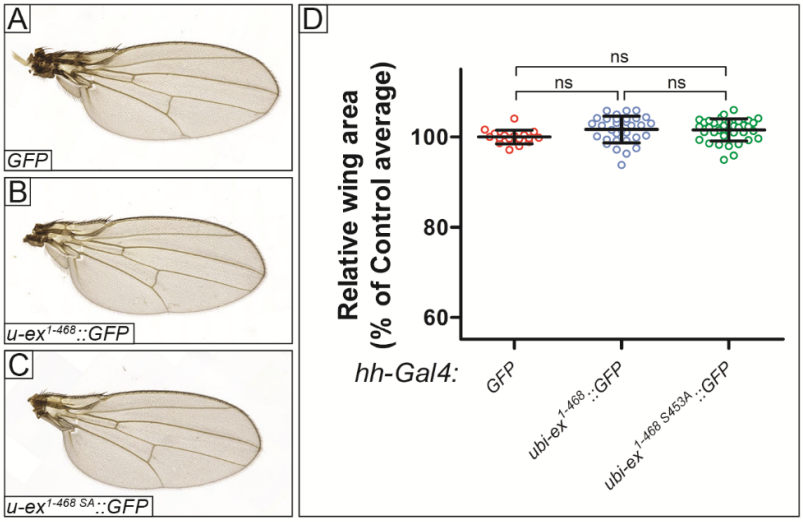

Figure 3-2 Expression of *ubi-ex::GFP* reporters does not alter adult wing size

Adult wings expressing *GFP* as a control (A), *GFP; ubi-ex$^{1-468}$::GFP* (B) or *GFP; ubi-ex$^{1-468\ S453A}$::GFP* (C) under the control of the *hh-Gal4* driver. Wing area was quantified using ImageJ and normalised to the average area of *GFP* expressing control wings (D). Individual data points are shown as well as average ± Standard Deviation (SD) for each genotype. Quantification shows no statistical difference in size between any of the groups analysed. Groups were compared by a one-way ANOVA with a Turkey's range post hoc test.

3.2. **Expanded Protein Turnover as a Contributing Factor to Tissue Growth**

The Ex^{S453A} residue is important for the stability of Ex and, unlike wildtype Ex $^{1-468}$, Ex$^{1-468\ S453A}$ is not efficiently degraded by Crb^{i} (Ribeiro et al., 2014). However, the contribution of this point mutation on growth control is unclear. Therefore, adult wings were analysed using full-length, wildtype Ex *(ex^{WT})* or full-length

mutant Ex^{S453A} (*ex^{S453A}*) *UAS*-overexpression constructs (see 2.3.4 for details). These were compared to *UAS-GFP* control wings, and *UAS-crb^{i}* wings, which increase adult tissue size through degradation of Ex and activation of Yki (Chen et al., 2010; Grzeschik et al., 2010; Ling et al., 2010; Robinson et al., 2010)

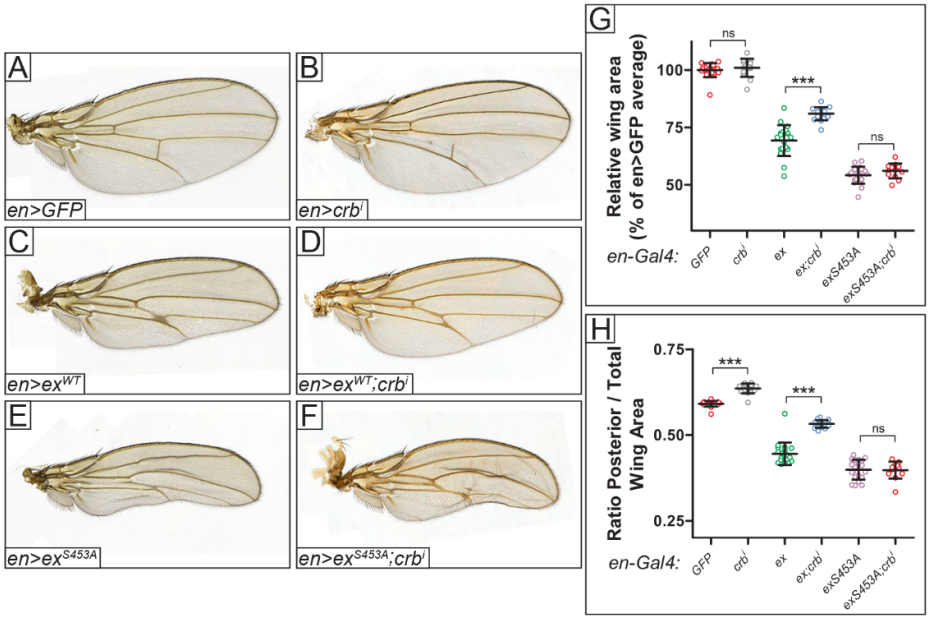

Figure 3-3 Ex^{S453A} regulates tissue growth in a Crb^{i} refractory manner

Adult wings from *Drosophila* raised at 18°C expressing *GFP* as a control (A), *crb^{i}* (B), *ex^{WT}* (C), *ex^{WT}, crb^{i}* (D), *ex^{S453A}* (E), or *ex^{S453A}, crb^{i}* (F) under the control of *en-Gal4*. Wing area was quantified using ImageJ and normalised to the average area of *GFP* expressing control wings (G). The ratio of the area of the posterior compartment of the wing and the total wing area was also calculated (H). Individual data points are shown as well as average ± SD for each genotype. Results show a statistical difference (*** = P < 0.0001) between all genotypes with the exception of the pairwise comparisons *en>GFP* and *en>crb^{i}* (G), and *en>ex^{WT}, crb^{i}* and *en>ex^{S453A}, crb^{i}* (G, H). Groups were compared by a one-way ANOVA with a Turkey's range post hoc test.

The *en-Gal4* driver was used to overexpress constructs only in the posterior compartment of the wing (Brand and Perrimon, 1993; Morata and Lawrence,

1975), and the ratio of posterior wing area to total wing area was used to analyse the ability of these transgenes to modulate tissue growth within this compartment.

Compared to the *en>GFP* control, wings expressing *en>crb^{i}* had an increased posterior to whole wing area ratio, with a defect in the posterior cross-vein (PCV) (Figure 3-3A-B, G-H). Surprisingly, the whole wing area of *en>crb^{i}* wings is not statistically larger than the *en>GFP* control wings, despite an increase in the posterior area, perhaps due to the number of wings analysed being too low, due to a compensatory decrease in the anterior compartment size, or because development occurred at 18^{o}C resulting in lower levels of Crb expression compared to development at 25^{o}C (Figure 3-3A-B, G-H). Wings overexpressing *en>ex^{WT}* were significantly undergrown, with a reduced posterior to whole wing ratio compared to control (Figure 3-3C, G-H) consistent with the known function of Ex in controlling Yki activity. Interestingly, there was a significant suppression of *en>ex^{WT}* undergrowth in wings overexpressing both *en>ex^{WT}* and en>*crb^{i}* (Figure 3-3D, G-H). This is presumably the result of Crb^{i}-mediated degradation of Ex resulting in a reduced ability of Ex protein to activate the Hpo pathway, and de-repress of Yki and tissue growth.

Wings overexpressing *en>ex^{S453A}* were undergrown compared to both *en>GFP* and *en>ex^{WT}* (Figure 3-3E, G-H). Moreover, unlike in the *en>ex^{WT}* case, *en>ex^{S453A};crb^{i}* wings were the same size as wings expressing *en>ex^{S453A}* alone (Figure 3-3F, G-H), reflected in the posterior to whole wing area ratios and relative wing area. Firstly, this shows that the Ex^{S453A} has a stronger effect on tissue growth than Ex^{WT}, and secondly, that overexpression of *crb^{i}* could not suppress the undergrowth caused by *en>ex^{S453A}* expression. These data are consistent with the model whereby a mutation at S453 in Ex results in the inability of Crb to stimulate Ex degradation, thus enhancing the effective function of Ex protein in inhibiting Yki. Moreover, despite overexpression of *crb^{i}* resulting in basal redistribution of *ubi-ex$^{1-468\ S453A}$::GFP* (Figure 3-1D), it appears enough Ex is available at the apical membrane to sufficiently stimulate Hippo signalling and inhibit growth. This is perhaps due to the fact that *crb^{i}* overexpression, whilst

localising throughout the plasma membrane, still exhibits strong localisation to the apical membrane (collaborator data not shown).

3.3. **The role of the Crumbs Complex in Regulating Expanded Stability**

Crb regulates cell polarity as part of a complex of proteins that localises at the apical surface of cells (Tepass, 2012). Whilst Crb is a known regulator of Ex localisation and stability (Chen et al., 2010; Grzeschik et al., 2010; Ling et al., 2010; Ribeiro et al., 2014; Robinson et al., 2010), little is known about the role of the other members of the Crb complex in the regulation of Ex localisation and stability. To this end, the role of *patj* and *sdt*, two key members of the apical Crb complex, were tested by RNAi-mediated depletion in the developing wing. Ex levels were assessed using the *ubi-ex$^{1-468}$::GFP* reporter, therefore analysing their involvement in Crb-mediated regulation of Ex protein stability.

Depletion of *patj* using the *hh>Gal4* posterior compartment driver resulted in no change in the *ubi-ex$^{1-468}$::GFP* reporter (Figure 3-4A). However, depletion of *sdt* resulted in loss of apical *ubi-ex$^{1-468}$::GFP* (Figure 3-4B) alluding to a potential role in regulating the stability or localisation of Ex. Sdt is a vital member of the Crb complex, and helps stabilise Crb protein at the apical membrane. Loss of *sdt* results in internalisation and mislocalisation of Crb (Hong et al., 2001; Tepass and Knust, 1993). Therefore, the localisation of Crb was analysed in the background of *sdt* depletion, resulting in the loss of Crb from the apical membrane (Figure 3-4C). As apical localisation of Ex is dependent on Crb, and Sdt controls Crb localisation (Chen et al., 2010; Grzeschik et al., 2010; Hong et al., 2001; Ling et al., 2010; Ribeiro et al., 2014; Robinson et al., 2010; Tepass and Knust, 1993), the loss of apical Ex upon RNAi-mediated depletion of *sdt,* is most likely the result of Crb depletion.

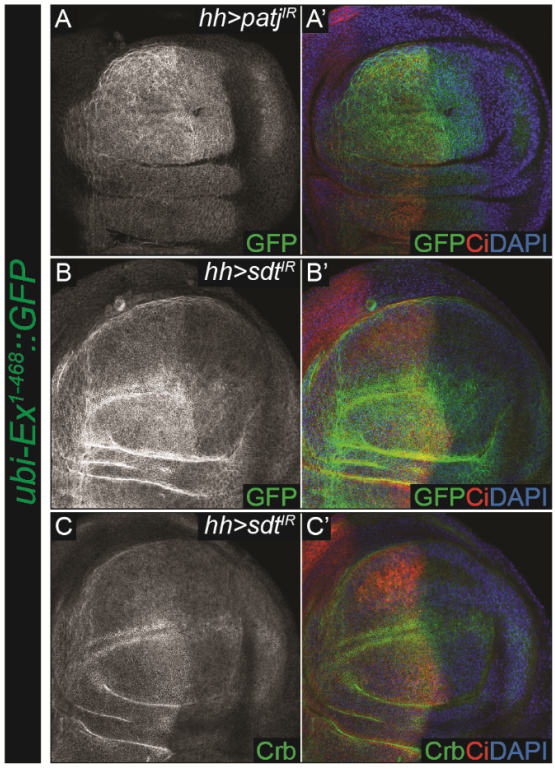

Figure 3-4 Regulation of Ex protein stability by the Crb complex members Sdt and Patj

Confocal micrographs of third instar larvae wing imaginal discs expressing *ubi-ex$^{1-468}$::GFP* (A-B' - green in merged images) or stained for Crb (C-C' – green in merged image). Single channel images show maximum intensity projection staining in the apical domain region. Nuclei are marked by DAPI staining (blue) and the posterior *hh-Gal4* expression domain is marked by the absence of Ci staining (red). Depletion of *patj* by expression of *patj^{IR}* under the control of *hh-Gal4* has no effect on *ubi-ex$^{1-468}$::GFP levels* (A), whereas *sdt^{IR}* causes loss of GFP (B). Crb apical staining is also lost in *hh>sdt^{IR}* tissue (C).

3.4. **The Role of Fat Signalling in the Regulation of Expanded Stability**

The link between Hpo signalling and PCP has been known for many years, with initial reports suggesting that Ex acted as a downstream effector of Ft in the regulation of tissue growth (Reddy and Irvine, 2008), and has been discussed

more generally in the introduction to this thesis (see 1.3.10). However, the precise involvement of Ex in Fat-Hippo signalling has yet to be sufficiently elucidated.

Initial results showed elevated *ex* mRNA in *ft* mutant tissue, however this mRNA increase did not correlate with an increase in Ex protein levels in eye and wing discs. This effect was in sharp contrast to *wts* mutant tissue, which showed a dramatic increase in Ex protein due to enhanced Yki activity (Bennett and Harvey, 2006). Mutant clones for *wts* also showed enhanced apical localisation of Ex, consistent with the increase in protein levels. However, in *ft* mutant clones, the apical localisation of Ex was reduced, despite no impact on Ex protein concentration (Bennett and Harvey, 2006; Silva et al., 2006; Willecke et al., 2006). This reduction but not complete loss in apical Ex protein in *ft* mutant tissue was later confirmed by immunofluorescence (Feng and Irvine, 2007), presumably due to residual Ex localised to the membrane by Crb. This suggested that Ft may be involved in regulating Ex translation, localisation and/or the stability of Ex (Bennett and Harvey, 2006; Silva et al., 2006; Willecke et al., 2006). Moreover, in *ds* overexpression or *fj* mutant clones, Ex levels are non-autonomously decreased at the clonal boundaries, a phenotype that is dependent on Fat, suggesting Ds may also act through Fat to regulate localisation and stability of Ex (Willecke et al., 2008).

D also appears to influence Ex localisation, as in *d*,*ft* double mutant clones, Ex localised normally to the apical surface of cells, unlike in *ft* tissue where apical Ex levels were partially reduced (Feng and Irvine, 2007). These data potentially allude to a role of Ft-D in the regulation of Ex stability. In *ft* mutant clones, apical D levels are increased and Ex levels are decreased, whereas in *d,ft* mutant clones, Ex apical localisation and levels appear normal (Feng and Irvine, 2007). This could suggest that D stimulates Ex degradation or loss from the apical membrane in *ft* mutant clones, and this degradation would not occur in the *ft,d* double mutant clones, hence Ex levels and localisation would be unaffected.

Overexpression of *d* or RNAi-mediated depletion of *crb* in the wing results in only mild overgrowth phenotypes. However, *d* overexpression in combination with RNAi-mediated *crb* depletion results in a dramatically enhanced overgrowth phenotype (Chen et al., 2010). This suggests that *crb* and *d* act in parallel to regulate growth through the Hpo pathway, presumably with D regulating Wts activity, and Crb regulating Ex localisation in this context (Chen et al., 2010). However, the possibility of D and Crb acting synergistically to regulate Ex localisation or stability has not been formally investigated.

Therefore, the interaction between the Fat pathway and Crb-dependent regulation of Ex protein stability was analysed**.** This was initially performed by assessing Ex stability in *Drosophila* S2 cells overexpressing Crb^{i} or a FERM-binding mutant of Crb, $Crb^{intra\Delta FBM}$ ($Crb^{i\Delta F}$), which does not induce Ex degradation, presumably due to its inability to interact with Ex (Ling et al., 2010). The stability of Ex was then assessed by overexpression of either the intracellular domain of Ft (Ft^{ICD}), which is sufficient to regulate growth via the Hippo pathway (Matakatsu and Blair, 2006; Pan et al., 2013) or D, in combination with Crb^{i}. As expected, Crb effectively degraded either the Ex^{1-468} truncation or $Ex^{Full\text{-}length}$ (Ex^{FL}) (Figure 3-5A-B lanes 1), with $Crb^{i\Delta F}$ unable to stimulate their degradation (Figure 3-5A-B lanes 2). Crb stimulates phosphorylation of Ex priming it for degradation. This phosphorylation means Ex cannot migrate as effectively during SDS-Polyacrylamide gel electrophoresis (PAGE) resulting in a band shift when compared to the un-phosphorylated state. It is possible to see this mobility retardation of Ex^{FL} as a result of Crb-induced phosphorylation, in addition to depletion (Figure 3-5B lanes 1, 4, 6) (Ling et al., 2010; Ribeiro et al., 2014). Overexpression of Ft^{ICD} did not appear to alter the stability of Ex compared with the $Crb^{i\Delta F}$ control, and did not affect the ability of Crb^{i} to degrade Ex (Figure 3-5A-B lanes 1-4). In contrast, D appeared to mildly stabilise Ex^{1-468} but not Ex^{FL}, although expression levels of D were very low so are perhaps not responsible for this effect, particularly as overexpressing D did not affect the ability of Crb^{i} to degrade Ex *in vivo* (Figure 3-5A-B lanes 1-2, 5-6, E).

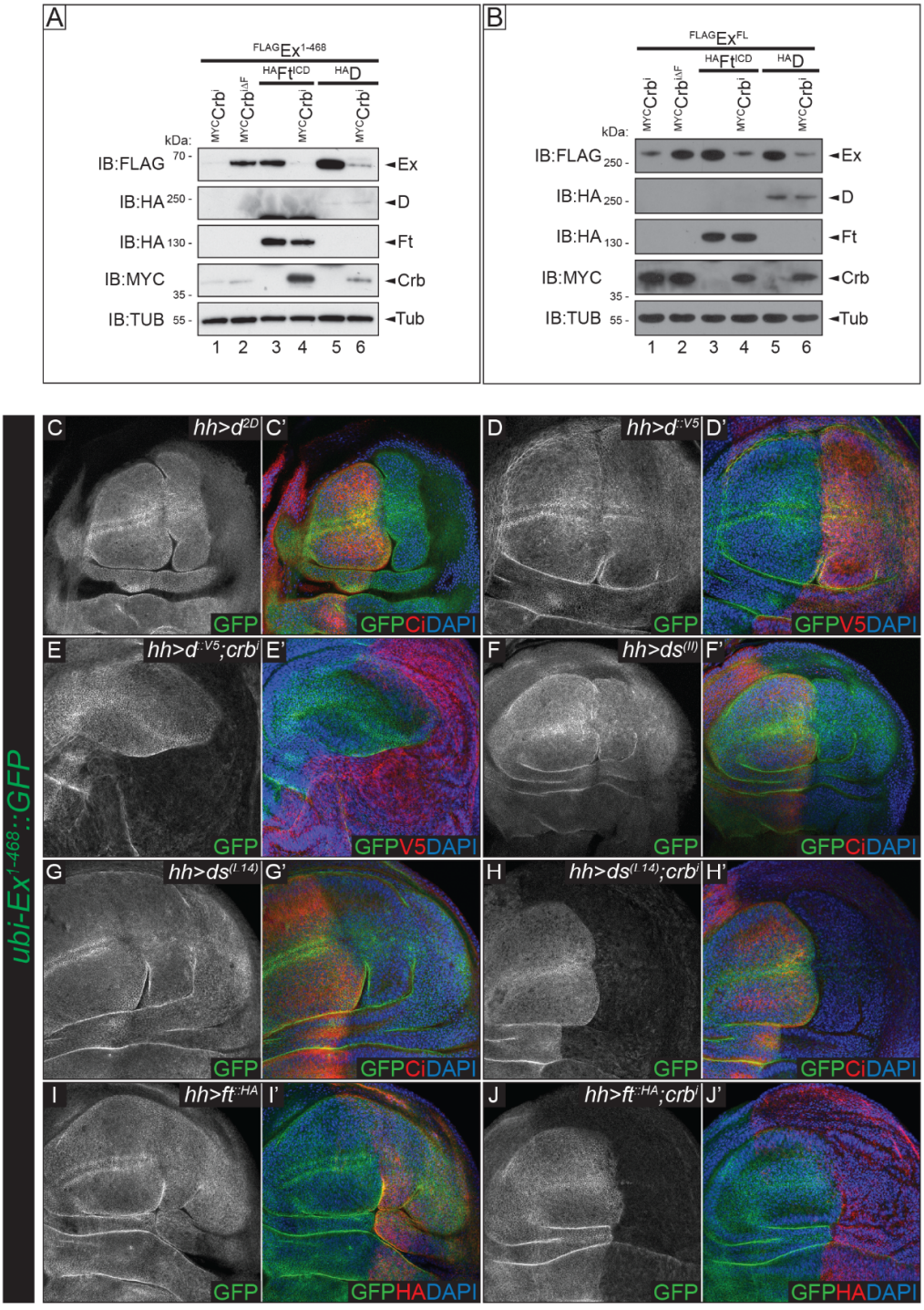

Figure 3-5 Fat pathway components have no effect on Ex stability
(Continued on next page)

(Continued from previous page) Immunoblot of S2 cell lysates expressing FLAG-tagged Ex^{1-468} (A) or Ex^{FL} (B). Expression of Myc-tagged Crb^{i} but not of $Crb^{i\Delta F}$ causes degradation of Ex^{1-468} (A – lanes 1, 2, 4, 6) and Ex^{FL} (B – lanes 1, 2, 4, 6). Compared to Crb^{i} or $Crb^{i\Delta F}$ controls, expression of HA-tagged Ft^{ICD} or D does not alter the stability of Ex^{1-468} (A - lanes 3-6) or Ex^{FL} (B - lanes 3-6). Lysates were probed with the indicated antibodies. Tubulin (Tub) was used as a loading control (A-B). Confocal micrographs of third instar larvae wing imaginal discs expressing *ubi-ex$^{1-468}$::GFP* (C-J'). Single channel images show GFP staining in maximum intensity projection of the apical domain. Nuclei are marked by DAPI staining (blue) and the posterior compartment where *hh-Gal4* is expressed is marked by the absence of Ci staining (red) (C', F', G', H'), the presence of V5 staining (D', E') or HA staining (I', J'). Overexpression of *d^{2D}* (C), *d$^{::V5}$* (D), *ds$^{(II)}$* (F), *ds$^{(L14)}$* (G) or *ft$^{::HA}$* (I) using *hh-Gal4* had no effect on *ubi-ex$^{1-468}$::GFP levels*. Co-expression of *crb^{i}* with *d$^{::V5}$* (E), *ds$^{(L14)}$* (H) or *ft$^{::HA}$* (J) failed to modify the phenotype seen with expression of *crb^{i}* alone with regards to the levels of *ubi-ex$^{1-468}$::GFP* (see Figure 3-1B).

The role of the Ft pathway was also interrogated *in vivo* using the constitutively expressed *ubi-ex$^{1-468}$::GFP* reporter with *hh-Gal4* to drive transgene overexpression. Consistent with previous work, overexpression of *d*, particularly *d$^{::V5}$* resulted in overgrown discs, presumably as a result of Wts inhibition (Figure 3-5C-D) (Cho et al., 2006; Mao et al., 2006). However, despite overgrowth, the discs showed no change in *ubi-ex$^{1-468}$::GFP* reporter levels compared to the anterior compartment internal control (Figure 3-5C-D). Moreover, when *d* and *crb^{i}* were co-expressed, *ubi-ex$^{1-468}$::GFP* was completely lost from the posterior compartment, suggesting that *d* does not influence Ex stability (Figure 3-5E). There also appeared to be an enhanced growth phenotype when both *d* and *crb^{i}* were co-expressed, compared to that of *d* or *crb^{i}* alone suggesting these proteins work in parallel to regulate growth, and that D does not regulate growth directly via Ex stability (Figure 3-5E). Furthermore, overexpression of the tumour suppressors *ds* or *ft* does not influence *ubi-ex$^{1-468}$::GFP* reporter levels (Figure 3-5F-G, I), and nor does overexpression of either of these proteins influence the ability of Crb to stimulate degradation of Ex as *ubi-ex$^{1-468}$::GFP* was still lost from cells when *ds* or *ft* were co-expressed with *crb^{i}* (Figure 3-5H, J).

Loss of function phenotypes of Fat pathway genes were also analysed. The kinase Mnb acts downstream of Ds, along with its adaptor protein Riq to phosphorylate and inhibit Wts, therefore activating Yki (Degoutin et al., 2013). This inhibition of Wts is independent of D-mediated Wts inhibition, which is downstream of Ft but not Ds (Degoutin et al., 2013). dsRNA-mediated depletion of *mnb* in S2 cells had no influence on the ability of Crb to regulate Ex stability or electrophoretic mobility (corresponding to phosphorylation) (Figure 3-6A). Other Fat pathway genes, such as *d, ds* and *ft* were not assessed in S2 cells because these polarity proteins are not sufficiently expressed in unpolarised S2 cells to warrant dsRNA treatment. In addition to cell data, RNAi-mediated depletion of *mnb in vivo* showed no change in *ubi-ex$^{1-468}$::GFP* reporter levels. When *crb^{i}* was co-expressed with *mnb^{IR}*, there was complete loss of *ubi-ex$^{1-468}$::GFP* suggesting that *mnb^{IR}* has no influence on Ex stability (Figure 3-6B-C). Depletion of *d* resulted in posterior compartment undergrowth consistent with published data suggesting D inhibits Wts (Figure 3-6D) (Mao et al., 2006). Interestingly, *ubi-ex$^{1-468}$::GFP* reporter levels were decreased in the posterior compartment, particularly at the posterior/anterior boundary edge suggesting D may stabilise Ex (Figure 3-6D), which is in complete contrast to our hypothesis proposing that D may destabilise Ex. However, as overexpression of D did not seem to influence *ubi-ex$^{1-468}$::GFP* reporter levels, these data are difficult to interpret. Moreover, as *d^{IR}* caused a decreased *ubi-ex$^{1-468}$::GFP* levels, co-expression with *crb^{i}* resulted in complete loss of *ubi-ex$^{1-468}$::GFP* in the posterior compartment similar to that of *crb^{i}* alone (Figure 3-6E).

RNAi-mediated depletion of *ds* or *ft* resulted in overgrowth of the posterior compartment, consistent with their well-known roles as tumour suppressors (Figure 3-6F, H) (Bryant et al., 1988; Clark et al., 1995), althought the overgrowth in the case of *ft* knockdown is very weak when compared to the *ft* mutant phenotypes, possible due to the inefficiency of the RNAi line. In Figure 3-6F it appears that the *ubi-ex$^{1-468}$::GFP* reporter levels are increased at the anterior-posterior boundary, however this is likely to be due to local tissue folding as the two compartments seem to be rejecting each other, concentrating membrane-

localised proteins such as Ex. However, *ubi-ex$^{1-468}$::GFP* levels away from the boundary interface appear to be consistent with the internal anterior control. Depletion of *ft* does also not appear to change the levels of *ubi-ex$^{1-468}$::GFP* (Figure 3-6H). The complete loss of *ubi-ex$^{1-468}$::GFP* observed upon *crb^{i}* overexpression is not altered by either *ds* or *ft* RNAi-mediated depletion (Figure 3-6G, I). However, combination of *crb^{i}* overexpression with either *ds^{IR}* or *ft^{IR}* led to an enhancement of the overgrowth phenotype (Figure 3-6G, I), similar to the situation seen with *crb^{i}* plus *d* overexpression. This suggests that tissue growth regulation downstream of Ft and Crb likely act in parallel. Moreover, these data do not support a role for the Ft pathway in the regulation of Ex levels.

3.5. **Concluding Remarks**

In this chapter, the use of a novel tool for the analysis of Ex stability *in vivo* has been established and validated. Importantly, as the newly generated Ex protein level reporter is under the control of the *ubiquitin* promoter, it facilitates the analysis of levels and localisation of Ex that are only influenced by post-translational mechanisms, and does not reflect the transcriptional control of endogenous *ex* by Yki, which has previously been a severe limitation in the analysis of Ex protein. However, it is important to state that the reporter lines generated are only a truncated version of Ex, encompassing amino acids 1-468 rather than the full 1427 amino acid protein. Whilst this is useful in the study of Crb-mediated Ex stability, as this N-terminal region is still sensitive to Crb-mediated degradation, there will be further post-translational regulation of Ex at the C-terminus which cannot be assessed using these truncated Ex reporters.

Moreover, the role of the previously identified Ex^{S453A} point mutation has been confirmed *in vivo* (Figure 3-3). The S453A mutation results in enhanced stability of Ex, making it refractory to the action of Crb (Ribeiro et al., 2014). This culminates in increased activity of Ex, which leads to a more severe tissue undergrowth phenotype when compared with the wildtype counterpart providing evidence to the functional relevance of Ex turnover by Slmb.

The ability of the Crb complex and Fat pathway to influence Ex stability has also been assessed, with the confirmation that Crb localisation by Sdt is vital to the localisation of Ex *in vivo* (Figure 3-4). This is interesting as there is limited data regarding the function of Sdt in regulating growth (Bachmann et al., 2001; Hong et al., 2001; Tepass and Knust, 1993). The only report suggesting that other members of the complex besides Crb can regulate growth, describes a genetic interaction between activated Ras^{V12} and loss of *sdt*, which results in extremely large tumours, with metastatic properties compared to Ras^{V12} or *sdt* mutations alone (Pagliarini and Xu, 2003). As Ex is a potent regulator of tissue growth, it is intriguing that loss of *sdt* causes a significant loss of apical Ex, presumably through regulating the stability of the Crb complex (Figure 3-4). It would be expected that, if Sdt regulates Crb complex stability (Bachmann et al., 2001; Hong et al., 2001), and apical levels of Ex, loss of *sdt* would result in overgrowth phenotypes similar to *crb* mutation. Whilst this was not formally investigated in this thesis, it would be an interesting area for follow-up.

Furthermore, previous evidence pointed to a potential role of the Ft pathway in the regulation of Ex stability (Staley and Irvine, 2012). However analysis of *ft, ds, d* and *mnb* provides limited evidence that the Fat pathway directly regulates Ex stability, with only knockdown of *d* causing a reduction in Ex reporter (Figure 3-6D). This result is still preliminary and needs further validation as, while *d* depletion causes a loss of *ubi-ex$^{1-468}$::GFP* staining, the converse is not true, and D overexpression does not cause enhanced Ex stability (Figure 3-5). More recently the genes App, Dlish/Vam and FbxL7 have been proposed to regulate levels, localisation and activities of D and Ft at the membrane (Bosch et al., 2014; Matakatsu et al., 2017; Misra and Irvine, 2016; Rodrigues-Campos and Thompson, 2014; Zhang et al., 2016). Perhaps analysis of these members of the Fat pathway may help in describing how Ft is able to regulate Ex localisation and stability (Bennett and Harvey, 2006; Silva et al., 2006).

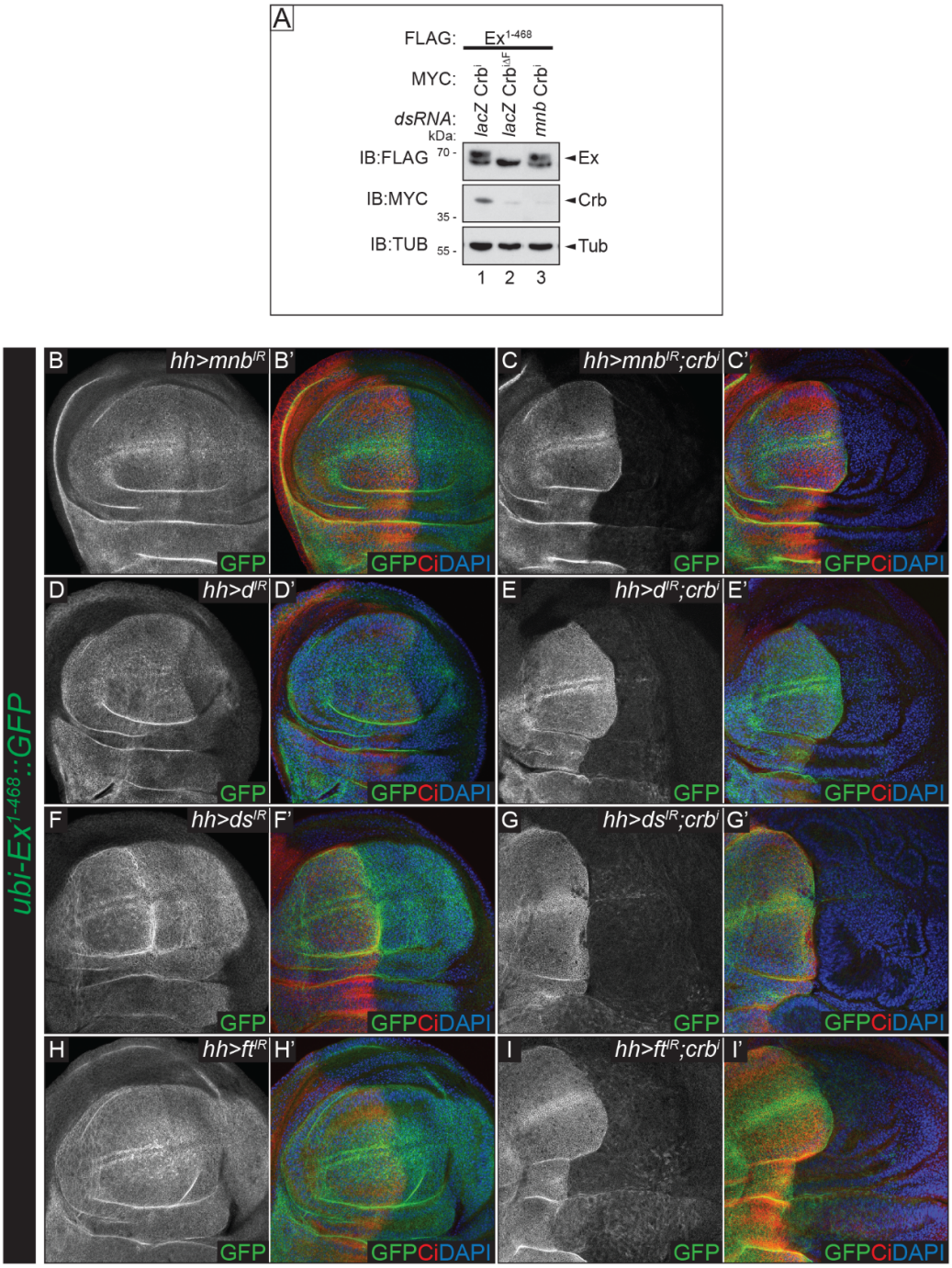

Figure 3-6 Depletion of Fat pathway components has modest effects on Ex stability

(Continued on next page)

(Continued from previous page) Immunoblot of S2 cell lysates expressing FLAG-tagged Ex^{1-468} (A) treated with dsRNA against *lacZ* as a control (A – lanes 1-2) or a pool of two independent dsRNA against *mnb* (A – lane 3). Expression of Myc-tagged Crb^{i} but not $Crb^{i\Delta F}$ caused an electrophoretic shift in Ex^{1-468} (A – lanes 1-2), which is not affected by *mnb* dsRNA treatment (A – lane 3). Lysates were probed with the indicated antibodies and Tub used as a loading control (A). Confocal micrographs of third instar larvae wing imaginal discs expressing *ubi-ex$^{1-468}$::GFP* (B-I'). Single channel images show GFP staining in maximum intensity projection of the apical domain. Nuclei are marked by DAPI staining (blue) and the posterior compartment where *hh-Gal4* is expressed is marked by the absence of Ci staining (red). Expression of *mnb^{IR}* (B), *ds^{IR}* (F), *or ft^{IR}* (H) under the control of *hh-Gal4* had no effect on *ubi-ex$^{1-468}$::GFP levels*. Expression of *d^{IR}* caused a reduction in *ubi-ex$^{1-468}$::GFP* levels (D). Co-expression of *crb^{i}* with *mnb^{IR}* (C), *d^{IR}* (E), *ds^{IR}* (G), *or ft^{IR}* (I) had no effect on *ubi-ex$^{1-468}$::GFP levels* compared to expression of *crb^{i}* alone (see Figure 3-1B).

Chapter 4 - Results 2 – Candidate Kinase Screen to Identify Regulators of Expanded Stability

4.1. Candidate Kinases Identified as Expanded Interacting Partners through Mass Spectrometry

As discussed in '1.3.12 - The Crumbs Complex', Crb acts as a dual regulator of Hpo signalling through the regulation of Ex protein localisation and stability (Chen et al., 2010; Grzeschik et al., 2010; Ling et al., 2010; Ribeiro et al., 2014; Robinson et al., 2010). Overexpression of *crb*^{i} drives tissue overgrowth via Yki, and also induces Ex phosphorylation and depletion through ubiquitin conjugation, and proteasomal degradation (Chen et al., 2010; Grzeschik et al., 2010; Ling et al., 2010; Ribeiro et al., 2014; Robinson et al., 2010). While the E3 ligase responsible for Ex degradation has been recently described (Ribeiro et al., 2014), the identity of the kinase(s) responsible for phosphorylating Ex is still unknown. This section will describe the work performed to identify a kinase(s) that is directly involved in the Crb-mediated phosphorylation and degradation of Ex.

To identify potential regulators of Ex protein stability, mass spectrometry (MS) was performed to identify proteins that specifically interact with Ex upon Crb^{i} overexpression. For these experiments, a FLAG-tagged Ex truncation spanning amino acids 1-468 was used, as Ex$^{1\text{-}468}$ had previously been identified as the minimal region of Ex that is sensitive to Crb-mediated degradation (Ribeiro et al., 2014). Ex$^{1\text{-}468}$ was isolated from *Drosophila* S2 cells by performing immunoprecipitation (IP) with FLAG beads, and purified Ex and associated complexes were analysed via MS. These data led to the identification of the SCF$^{Slmb/\beta\text{-}TrCP}$ E3 ligase complex as a crucial regulator of Ex stability, Ex requiring phosphorylation-dependent priming to be recognised by Slmb (Ribeiro et al., 2014).

Ex-interacting kinases were also detected within the same MS data set used to identify Slmb as a regulator of Ex stability. These were used as the starting point for investigations into potential kinases involved in Ex degradation (Table 4-1 – performed by (Ribeiro et al., 2014)). Despite the fact that several kinases were identified in this MS experiment, due to the transient nature of kinase-substrate interactions, they are often difficult to capture by MS. Therefore, these experiments can only provide a snapshot of the total protein interaction network within a cell, and thus unfortunately, this list is unlikely to be exhaustive (Amano et al., 2010).

Table 4-1 Summary of MS Ex binding partners

Summary of MS results including protein name, protein name abbreviation and CG number (CG#). Unique and total denote the number of unique and total peptides detected in the MS analysis for each specific protein, respectively. S2 cell lysates were processed for MS analysis after co-immunoprecipitation of FLAG-tagged GFP as a negative binding control or FLAG-tagged Ex^{1-468} in the presence of Myc-tagged Crb^{i} or $Crb^{i\Delta F}$. Experiment was performed by Paulo Ribeiro and this MS data has previously been used in the identification of Slmb as a regulator of Ex stability (Ribeiro et al., 2014).

Protein Name	Protein Abbreviation	CG#	GFP		Ex^{1-468} + Crb^{i}		Ex^{1-468} + $Crb^{i\Delta F}$	
			Unique	Total	Unique	Total	Unique	Total
Expanded	Ex	CG4114	0	0	27	601	26	423
Hippo	Hpo	CG11228	0	0	10	12	10	12
Germinal Centre Kinase III	GckIII	CG5169	0	0	4	4	0	0
Gilgamesh	Gish	CG6963	0	0	3	3	0	0
Doughnut on 2	Dnt	CG17559	0	0	2	3	0	0
Eph Receptor Tyrosine Kinase	Eph	CG1511	0	0	2	2	0	0
PDGF- and VEFG-Receptor Related	Pvr	CG8222	0	0	12	18	0	0
G Protein-Coupled Receptor Kinase 2	Gprk2	CG17998	0	0	9	9	0	0
Saxophone	Sax	CG1891	0	0	2	2	0	0
Thickveins	Tkv	CG14026	0	0	11	12	0	0
Punt	Put	CG7904	0	0	3	6	0	0

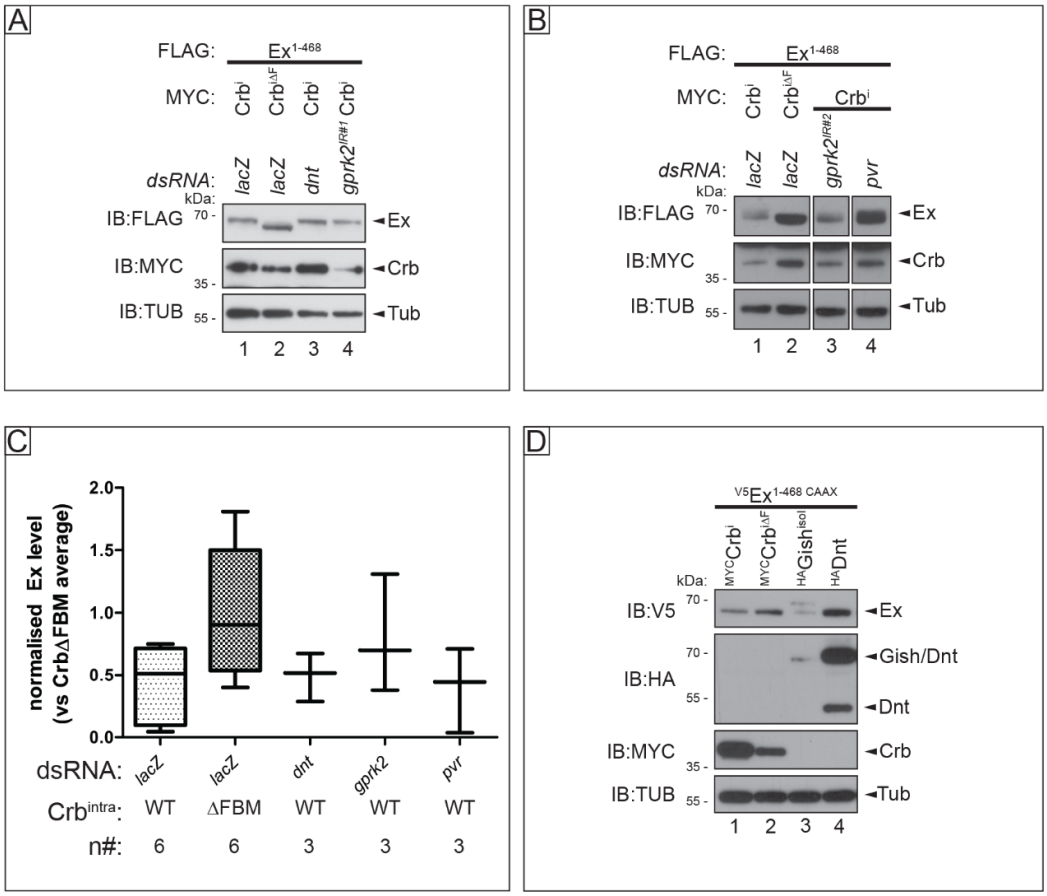

Figure 4-1 Functional screen of MS candidate kinases and their effect on Ex stability in S2 cells

Immunoblot of S2 cell lysates expressing FLAG-tagged Ex^{1-468} (A-B) and treated with dsRNA targeting *lacZ* (control dsRNA treatment; A, B – lanes 1-2), *dnt* (A – lane 3), $gprk2^{IR\#1}$ (A – lane 4), $gprk2^{IR\#2}$ (B – lane 3) and *pvr* (B – lane 4). Expression of Myc-tagged Crb^{i} (A, B - lanes 1, 3-4) but not of $Crb^{i\Delta F}$ (A, B – lanes 2) caused an electrophoretic shift and depletion in Ex^{1-468}, which was not abrogated by any dsRNA treatment. A box and whiskers, min to max plot showing immunoblot quantification of Ex levels relative to the $Crb^{\Delta FBM}$ negative control (C) (protocol outlined in '2.1.15'). Groups were compared to the $Crb^{\Delta FBM}$ negative control group by a one-way ANOVA with a Dunnet's multiple comparison post hoc test. Expression of Myc-tagged Crb^{i} (C – lane 1) or HA-tagged $Gish^{isol}$ (C – lane 3) but not of Myc-tagged $Crb^{i\Delta F}$ (C – lane 2) or HA-tagged Dnt (C – lane 4) caused degradation and electrophoretic shift of V5-tagged $Ex^{1-468\ CAAX}$. Lysates were analysed using the indicated antibodies and Tub was used as a loading control (A-B, D).

Several of these initial candidate kinases were then screened in *Drosophila* S2 cells by RNAi-mediated depletion, in combination with Crb^{i} overexpression to assess levels of Ex protein. Immunoblots were quantified using ImageJ as described in section '2.1.15' and levels of Ex were normalised to the loading control tubulin, and the levels of Crb expression, itself normalised to tubulin. Quantified levels of Ex were then normalised to the negative control condition of Ex levels in the presence of the $Crb^{\Delta FBM}$ (set to 1). Candidate kinase(s) that could recover Crb-mediated Ex electrophoretic mobility shift (corresponding to phosphorylation) or degradation were taken forward for further analysis. RNAi-mediated depletion of the kinases *doughnut on 2 (dnt)* and *G protein-coupled receptor kinase 2* (*gprk2*) showed no stabilisation of Ex relative to the Crb^{i} positive control, although the variability of results and number of repeats was too low to obtain statistical significance, even in the positive control (Figure 4-1A lanes 3-4 and C). Indeed, Ex protein was still electrophoretically shifted due to Crb-mediated Ex phosphorylation suggesting that neither Dnt nor Gprk2 influenced phosphorylation and therefore Ex stability. An additional *gprk2* dsRNA was also assessed, which also failed to modulate Crb-mediated Ex degradation (Figure 4-1B lane 3). Moreover, when Ex levels were analysed *in vivo* using the *ubi-ex$^{1-468}$::GFP* reporter, *gprk2* RNAi-mediated depletion showed no effect on GFP levels, suggesting this protein is not involved in the regulation of Ex stability (Figure 4-2A). A Dnt overexpression construct was generated, and its ability to phosphorylate and promote degradation of Ex in S2 cells was assessed. This was performed using an Ex construct containing a C-terminal CAAX palmitoylation site ($Ex^{1-468\ CAAX}$), thereby promoting its localisation to the cellular membranes where Crb-mediated regulation of Ex occurs, therefore promoting maximal interactions between Ex and the putative kinases tested (Genevet and Tapon, 2011; Hancock et al., 1990; Sun et al., 2015). Neither a mobility shift nor depletion of Ex was observed upon overexpression of Dnt in S2 cells compared to Crb^{i} or Gilgamesh (Gish) controls, both of which cause either a mobility shift or

depletion in the Ex construct (the role of Gish will be discussed later in 'Chapter 5 - Results 3') (Figure 4-1D – lane 4).

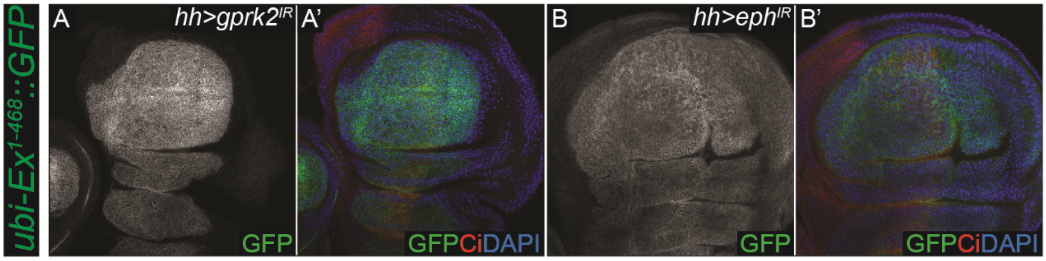

Figure 4-2 *In vivo* functional screen of MS candidate kinases and their effect on Ex stability

Confocal micrographs of third instar larvae wing imaginal discs expressing *ubi-ex$^{1-468}$::GFP* (A-B'). Single channel images show GFP staining in maximum intensity projection of the apical domain. Nuclei are marked by DAPI staining (blue) and the posterior compartment where *hh-Gal4* is expressed domain is marked by the absence of Ci staining (red). Depletion of *gprk2* or *eph* using respectively *hh>gprk2^{IR}* (A) or *hh>eph^{IR}* (B) had no effect on the levels of *ubi-ex$^{1-468}$::GFP*.

In addition, the receptor tyrosine kinase PDGF and VEGF-Receptor Related Receptor Tyrosine Kinase (Pvr), was assessed in S2 cells. Despite the appearance that depletion of this kinase is able to increase levels of Ex (Figure 4-1B – lane 4), quantification of levels of Ex in combination with *pvr* knockdown suggest this kinase does not influence the ability of Crb to stimulate Ex degradation (Figure 4-1C). However, it is important to note that in this context, the number of experiments assessed, and the variablilty of results did not result in a statistical significance between Ex levels in the Crb^{i} positive control and the Crb$^{\Delta FBM}$ negative control, or the kinases tested (Figure 4-1C). Rather, the conclusion were based on a trend towards a decrease in Ex levels upon Crb^{i} overexpression, which was not abrogated by knockdown of the kinases tested. *In vivo* analysis of another kinase identified in the MS data *Eph*

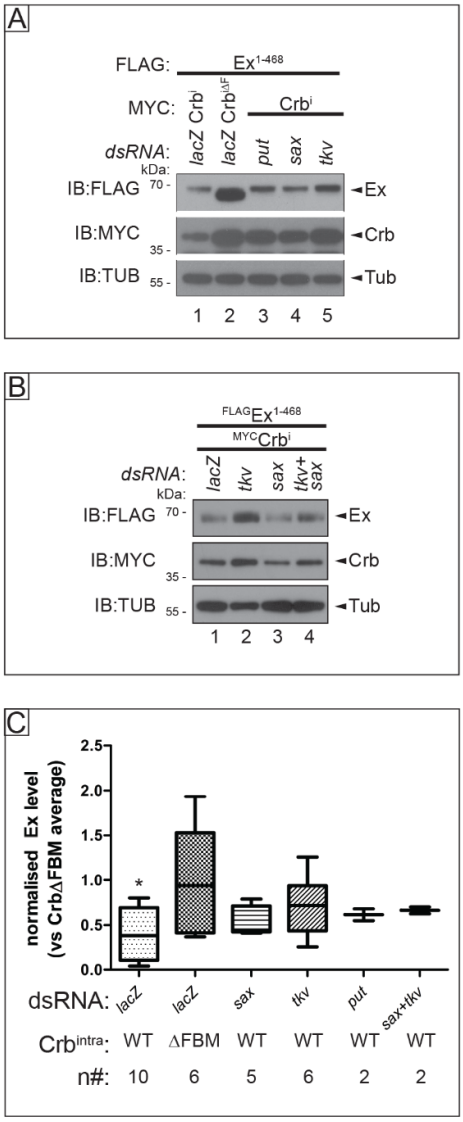

Figure 4-3 Effect of depletion of BMP pathway kinases on Ex protein stability in S2 cells

Immunoblot of S2 cell lysates expressing FLAG-tagged Ex^{1-468} (A, B) and treated with dsRNA against *lacZ* as a control (A – lanes 1-2, B – lanes 1), *put* (A – lane 3), *sax* (A – lane 4, B – lane 3) and *tkv* (A – lane 5, B – lane 2) or *tkv* + *sax* (B – lane 4). Expression of Myc-tagged Crb^{i} (A – lanes 1, 3-5 and B - lanes 1-4), but not $Crb^{i\Delta F}$ (A – lane 2) caused depletion and electrophoretic shift in Ex^{1-468}, which was mildy abrogated by BMP kinase dsRNA treatment. Lysates were probed with the indicated antibodies and Tub was used as a loading control (A-B). A box and whiskers, min to max plot showing immunoblot quantification of Ex levels relative to the $Crb^{\Delta FBM}$ negative control (C) (protocol outlined in '2.1.15'). Groups were compared to the $Crb^{\Delta FBM}$ negative control group by a one-way ANOVA with a Dunnet's multiple comparison post hoc test (* = $P < 0.05$).

Receptor Tyrosine Kinase (eph) by combining *hh>Gal4*, *UAS*-RNAi-mediated depletion with the *ubi-ex$^{1-468}$::GFP* reporter showed no change in Ex levels in the posterior compartment (Figure 4-2B).These data suggest none of these kinases tested are able to modulate the ability of Crb to stimulate Ex degradation.

Within the MS data set were three receptor tyrosine kinases of the Bone Morphogenetic Protein (BMP) pathway, a Tissue Growth Factor (TGF) β-like pathway stimulated by ligands such as Dpp, which controls a whole host of biological functions throughout development including growth and patterning (Hamaratoglu et al., 2014). This signalling cascade is initiated by ligand dimers binding to receptor heterodimers comprised of a type I receptor Thickveins (Tkv) or Saxophone (Sax), and the type II receptor Put. Activated Put phosphorylates the type I receptor, which in turn phosphorylates Mad, activating the Dpp transcriptional response (Hamaratoglu et al., 2014). Given the fact that several proteins from this pathway were recovered in the MS experiments, their role in the regulation of Ex was tested. As with the previous kinases tested, the ability of Crb^{i} to phosphorylate and degrade Ex$^{1-468}$ was assessed in cells treated with dsRNA targeting *tkv*, *sax* or *put*. Depletion of any of each of these kinases had no effect on the abilty of Crb^{i} to stimulate phosphorylation of Ex$^{1-468}$ as measured by electrophoretic mobility shift (Figure 4-3A). Interestingly, knockdown of these BMP kinases may cause a mild stabilisation of Ex$^{1-468}$, despite the persistence of the phosphorylation induced by Crb (Figure 4-3A-C). In this instance, quantification of Ex$^{1-468}$ levels led to a significant difference between Ex in combination with Crb^{i} compared to Crb$^{\Delta FBM}$ however, variability in results, or too few repeats did not result in a statistically significant difference between Ex$^{1-468}$ upon treatment with depleted BMP kinases compared to the Crb$^{\Delta FBM}$ control, althought there is a trend suggesting mild Ex^{-468} stabilisation (Figure 4-3C).

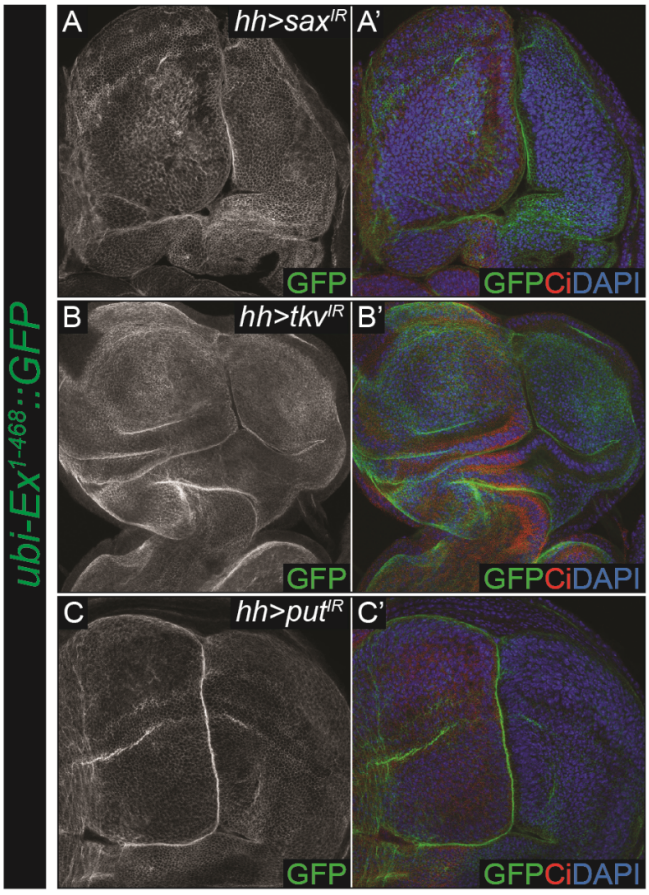

Figure 4-4 Effect of depletion of BMP pathway kinases on Ex stability *in vivo*

Confocal micrographs of third instar larvae wing imaginal discs expressing *ubi-ex$^{1-468}$::GFP* (A-C'). Single channel images show GFP staining in maximum intensity projection of the apical domain. Nuclei are marked by DAPI staining (blue) and the posterior compartment where *hh-Gal4* is expressed is marked by the absence of Ci staining (red). Depletion of *sax* (A), *tkv* (B) or *put* (C) in the hh-Gal4-expressing compartment using *sax^{IR}*, *tkv^{IR}* or *put^{IR}* had no effect on *ubi-ex$^{1-468}$::GFP levels*.

In addition, these receptors work as dimers, potentially masking the effect of depleting individual kinases in the pathway, as alternative receptor dimers may form, allowing signalling to persist. Therefore, co-depletion of *sax* and *tkv*, both type I receptors was performed, however the stability of Ex^{-468} was not enhanced compared to single dsRNA treatments (Figure 4-3B-C).

Unfortunately, when the *ubi-ex$^{1-468}$::GFP* reporter was analysed *in vivo*, knockdown of either *sax*, *tkv* or *put* had no effect on GFP levels when *UAS*-RNAi was driven in the posterior compartment by *hh>Gal4* (Figure 4-4).

Overexpression constructs of the type I receptors Sax and Tkv were generated and transfected into S2 cells in an attempt to see Ex phosphorylation and depletion. When tested with Ex$^{1-468}$, neither of these constructs caused a depletion of Ex unlike the positive controls Crb^{i} or Gish (Figure 4-5A-B), althought the number of repeats was too low to statistically confirm this. Interestingly, when Tkv was overexpressed with the Ex$^{1-468\ CAAX}$, which should be localised to cell membranes, an electrophoretic mobility shift but not a depletion of Ex was observed, similar to that caused by overexpression of the positive controls Crb^{i} and Gish (Figure 4-5C lane 5 and D) suggestive of a potential phosphorylation of Ex not involved in regulating Ex stability.

4.2. **Core Hippo Kinases as Potential Regulators of Expanded**

Ex is one of the most important upstream inputs of the Hippo pathway in *Drosophila* and can associate with Hpo and Wts in an apically localised activated kinase complex (Genevet and Tapon, 2011; Sun et al., 2015). Indeed, Hpo kinase was detected as an Ex interacting partner through the MS analysis from whichpotential Ex kinases were selected (Table 4-1), although there was no difference in binding preference depending on whether Crb^{i} or Crb$^{i\Delta F}$ was expressed consistent with previous reports (Reddy and Irvine, 2011; Yu et al., 2010). It is therefore attractive to speculate that within this complex there is phosphorylation of Ex allowing tight regulation of pathway activity. Indeed, it has been reported that Wts can phosphorylate the C-terminus of Ex inhibiting degradation through Slmb, reinforcing the activity of the Hpo pathway by preventing excessive activity of Yki (Zhang et al., 2015a). It is therefore possible

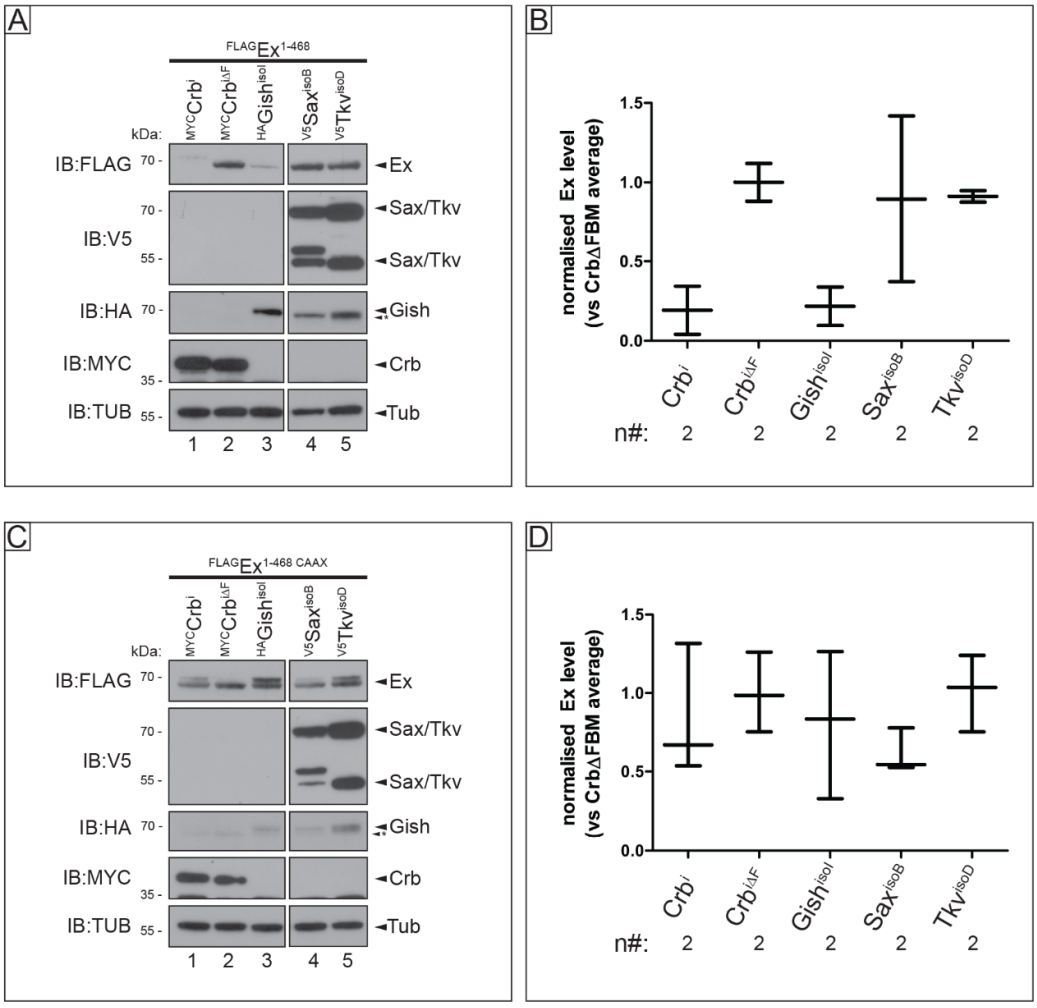

Figure 4-5 Effect of overexpression of BMP pathway kinases on Ex protein stability in S2 cells

Immunoblot of S2 cell lysates expressing FLAG-tagged Ex^{1-468} (A) or $Ex^{1-468\ CAAX}$ (C), and concurrent box and whiskers, min to max plot showing immunoblot quantification of Ex levels relative to the $Crb^{\Delta FBM}$ negative control (B and D) (protocol outlined in '2.1.15'). Groups were compared to the $Crb^{\Delta FBM}$ negative control group by a one-way ANOVA with a Dunnet's multiple comparison post hoc test. Expression of Myc-tagged Crb^{i} and HA-tagged $Gish^{isoI}$ but not Myc-tagged $Crb^{i\Delta F}$ caused degradation (A lanes 1-3, B) or an electrophoretic shift but no degradation (C lanes 1-3, D) of Ex. Expression of V5-tagged Sax^{isoB} caused neither degradation or an electrophoretic mobility shift in Ex (A-D), whereas V5-tagged Tkv^{isoD} had no effect on Ex^{1-468} (A – lane 5, B), but caused an electrophoretic shift in $Ex^{1-468\ CAAX}$ (B – lane 5). Lysates were analysed using the indicated antibodies and Tub was used as a loading control (A-B).

that the converse mechanism of Hpo regulation could exist, whereby under certain conditions Ex is phosphorylated within the Hpo kinase complex, and degraded to deactivate Hpo signalling switching on a Yki transcriptional programme.

To test this hypothesis, the core Hpo kinases were depleted through dsRNA treatment in S2 cells, and Crb-dependent Ex stability was assessed. The Crb-sensitive N-terminal fragment $Ex^{1\text{-}468}$ was used, which does not contain the C-terminal Wts phosphorylation site, therefore ruling out the stabilising effect of Wts on Ex (Zhang et al., 2015a). Depletion of the core kinases *hpo* or *wts* did not impact the stability of the $Ex^{1\text{-}468}$, confirmed upon quantification (Figure 4-6A lanes 3-4 and E). RNAi-mediated depletion *in vivo* suggests the *ubi-ex$^{1\text{-}468}$::GFP* reporter was mildly stabilised by *hpo^{IR}*, however when co-expressed with *crb^{i}*, *ubi-ex$^{1\text{-}468}$::GFP* was totally lost from the apical membrane (Figure 4-7A-B). The apparent upregulation of *ubi-ex$^{1\text{-}468}$::GFP* in *hpo^{IR}* may be the result of a Yki-dependent upregulation of apical proteins (Genevet et al., 2009). Depletion of *wts* had no effect on the *ubi-ex$^{1\text{-}468}$::GFP* reporter (Figure 4-7C). According to published reports, if the reporter was full length Ex, we would expect that depletion of *wts* would result in loss of Ex protein due to decreased levels of C-terminal Ex phosphorylation, and concomitant degradation (Zhang et al., 2015a). The effect of overexpression of Hpo and Wts, along with the Wts adaptor protein Mats on $Ex^{1\text{-}468\ CAAX}$ was also assessed, which resulted in a mobility shift but no degradation of Ex compared to the Crb^{i} control (Figure 4-6B). The significance of this phosphorylation is still unclear. The mobility shift could be a technical artefact due to the use of $Ex^{1\text{-}468\ CAAX}$, which is forced to cellular membranes, or there could be an unknown regulatory mechanism of these kinases on Ex alluded to in the introduction to this section.

To confirm that the ability of Wts to stabilise Ex had no effect on Crb-mediated Ex degradation, stability of Ex^{FL} was analysed with overexpression of Wts and Crb (full length and intra). Consistent with published work, Wts overexpression resulted in enhanced stability of Ex compared to an empty vector control

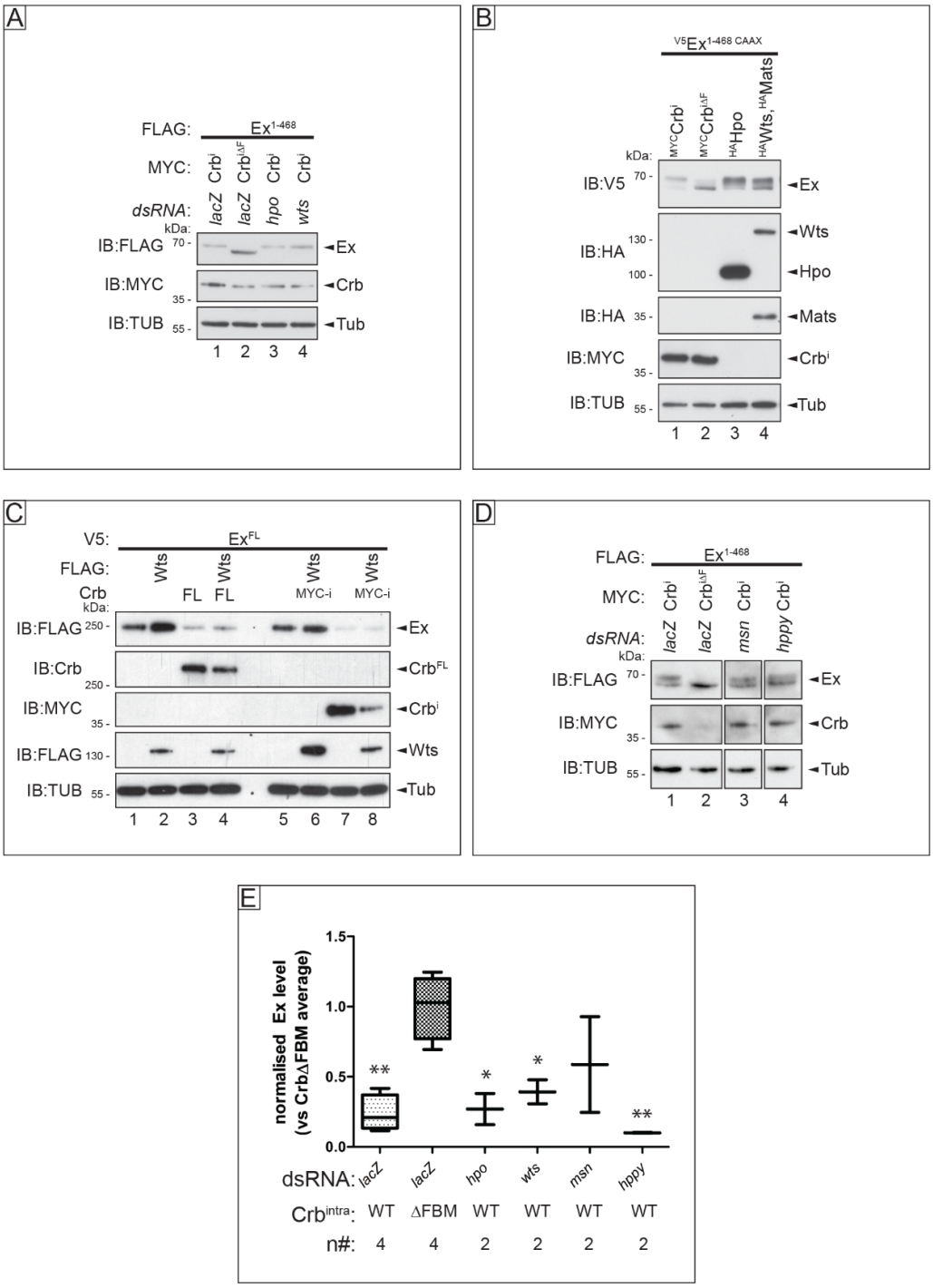

Figure 4-6 Effect of Hippo pathway kinases on Ex protein stability in S2 cells

(Continued on next page)

(Continued from previous page) Immunoblot of S2 cell lysates expressing FLAG-tagged Ex^{1-468} (A, D) and treated with dsRNA against *lacZ* as a control (A, D – lanes 1-2), *hpo* (A – lane 3), *wts* (A – lane 4) a pool of two independent dsRNA against *msn* (D – lane 3) or *hppy* (D – lane 4). Expression of Myc-tagged Crb^{i} (A – lanes 1, 3-4, D – lanes 1, 3-4), but not $Crb^{i\Delta F}$ (A, D – lanes 2) caused depletion and/or electrophoretic shift in Ex^{1-468}, which was not affected by any dsRNA treatment. Box and whiskers, min to max plot showing immunoblot quantification of Ex levels relative to the $Crb^{\Delta FBM}$ negative control (E) (protocol outlined in '2.1.15'). Groups were compared to the $Crb^{\Delta FBM}$ negative control group by a one-way ANOVA with a Dunnet's multiple comparison post hoc test (** = P < 0.01, * = P < 0.05). Expression of Myc-tagged Crb^{i} (B – lane 1), HA-tagged Hpo (B – lane 3) or HA-tagged Wts and Mats (B – lane 4), but not of Myc-tagged $Crb^{i\Delta F}$ (B – lane 2) caused degradation and/or electrophoretic shift of V5-tagged $Ex^{1-468\ CAAX}$ (B). Compared to empty control (C – lanes 1, 5), expression of FLAG-tagged Wts stabilised Ex^{FL} (C – lanes 2, 6). Expression of Crb^{FL} (C – lane 3-4) or Myc-tagged Crb^{i} (C – lane 7-8) caused degradation of Ex^{FL}, irrespective of the presence or absence of FLAG-tagged Wts coexpression (C – lanes 4, 8). Lysates were probed with the indicated antibodies and Tub was used as a loading control (A-D).

(Figure 4-6C lanes 1-2, 5-6). However, when Wts was co-expressed with Crb^{FL} or Crb^{i}, Ex was completely degraded suggesting Crb is the dominant factor in the regulation of Ex stability (Figure 4-6C lanes 3-4, 7-8).

Additional proteins acting on the core kinase cascade have recently been identified including Msn and Hppy (Li et al., 2014a; Meng et al., 2015), which were analysed as potential regulators of Ex stability. In S2 cells, depletion of these kinases appeared to have little effect on the abiliy for Crb to stimulate Ex degradation, despite the lack of statistical significance for *msn* upon immunoblot quantification (Figure 4-6D and E). Depletion of *msn in vivo* appeared to have no effect on stabilising the *ubi-ex$^{1-468}$::GFP* reporter, whilst co-expression with *crb^{i}* resulted in no change from Crb-phenotype of Ex degradation, corroborating the data obtained in S2 cells suggesting *msn* has no effect on regulating Ex stability (Figure 4-7G-H). As well as Hppy and Msn, another Germinal Center Kinase, Germinal Center Kinase III (GckIII) exists which has been speculated to be involved in Hpo signalling (Ribeiro et al., 2010; Zheng et al., 2015). Depletion of this kinase was tested *in vivo*, with two independent RNAi lines showing mild increase in *ubi-ex$^{1-468}$::GFP* intensity suggesting this kinase is perhaps involved in regulating Ex stability (Figure 4-7D-E). When combined with co-expression of

crb^{i} however, depletion of the kinase did not recover *ubi-ex*$^{1-468}$*::GFP* as would be expected if this kinase initiated Crb-dependent Ex phosphorylation and degradation (Figure 4-7F). Indeed, in *Drosophila* there have been no reports of *gckIII* regulating growth, and there is limited evidence for any functional significance of the effect of GckIII on Ex.

Despite preliminary data suggesting Hpo and Wts can phosphorylate the N-terminus of Ex (Figure 4-6B), the impact of this phosphorylation remains unclear, and, collectively, these data suggest none of the core Hpo kinases are involved in priming Ex for degradation upon Crb-mediated stimulus.

4.3. **Additional Candidate Kinases and their Role in Regulating Expanded Stability**

In addition to the kinases identified by MS, or kinases that are obviously closely localised with Ex, there were two other kinases that were prioritised for analysis: the apical kinase aPKC, and Shaggy (Sgg), the *Drosophila* orthologue of Glycogen Synthase Kinase-3β (Gsk3β).

aPKC has a critical role in determining apical polarity in epithelial cells and is regulated by the adaptor proteins Par6 and Baz, the *Drosophila* orthologue of Par3, which control the positioning and activity of aPKC, forming the apical Par complex (Tepass, 2012). The Par complex is involved in excluding basal polarity complexes from the apical domain thus helping to determine and maintain the apical domain, and the kinase activity of aPKC plays a crucial role in these processes (Tepass, 2012). In addition, aPKC has been reported to directly phosphorylate the intra-cellular region of Crb (Sotillos et al., 2004). This phosphorylation is necessary to maintain apical localisation of Crb, and is thought to be involved in regulating FERM-dependent Crb interactions (Sotillos et al., 2004; Tepass, 2012). As the interaction between Ex and Crb is dependent on the FERM domain of Ex, and due to the apical localisation of both Ex and aPKC, this

kinase has been speculated to be an Ex kinase (Genevet and Tapon, 2011; Ribeiro et al., 2014).

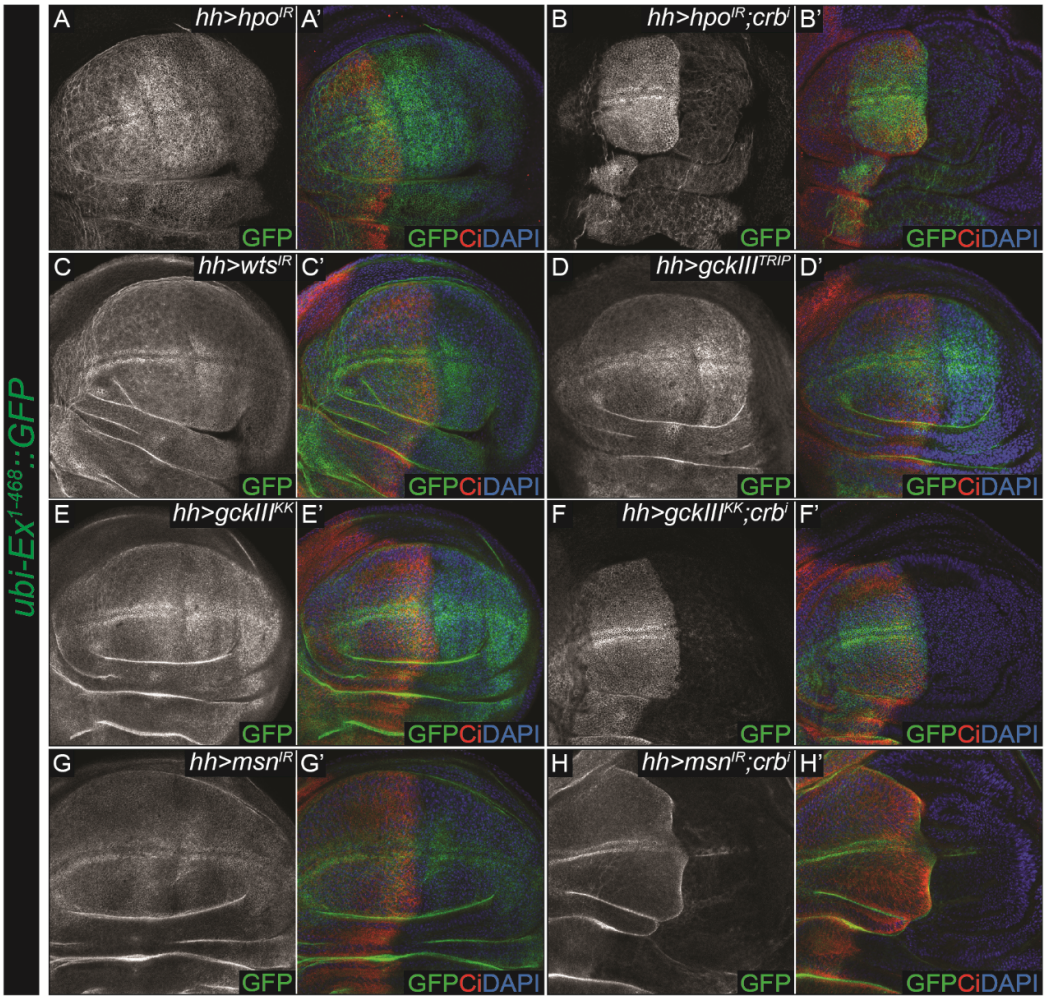

Figure 4-7 Effect of Hippo pathway kinases on Ex protein stability *in vivo*

Confocal micrographs of third instar larvae wing imaginal discs expressing *ubi-ex$^{1-468}$::GFP* (A-H'). Single channel images show GFP staining in maximum intensity projection of the apical domain. Nuclei are marked by DAPI staining (blue) and the posterior compartment where *hh-Gal4* is expressed is marked by the absence of Ci staining (red). Expression of *hpo^{IR}* (A), *wts^{IR}* (C) or *msn^{IR}* (G) under the control of *hh-Gal4* had no effect on *ubi-ex$^{1-468}$::GFP* levels. Expression of RNAi transgenes targeting *gckIII* (respectively *gckIII^{TRIP}* and *gckIII^{KK}* in D and E) caused a mild increase in the levels of the *ubi-ex$^{1-468}$::GFP* reporter. Coexpression of *crb^{i}* with *hpo^{IR}* (B), *gckIII^{KK}* (F) or *msn^{IR}* (H) did not abrogate the depletion in *ubi-ex$^{1-468}$::GFP levels* caused by expression of *crb^{i}* alone (see Figure 3-1B).

However, when aPKC was tested in cells, there was no evidence to suggest it has a role in the regulation of Ex stability. When S2 cells were treated with dsRNA against aPKC, along with an inhibitor of aPKC CRT^{0668} (a kind gift from Dr Philippe Riou and Dr Peter Parker - The Francis Crick Institute), Ex stability remained unchanged when compared to the Crb^{i} control (Figure 4-8A). Moreover, when different versions of aPKC were expressed in cells, there was no depletion or electrophoretic mobility shift in Ex, unlike in Crb^{i} expressing cells. Wildtype and kinase dead (KD) aPKC, either with or without a CAAX palmitoylation sequence to promote its membrane localisation (Hancock et al., 1990) (where canonical aPKC activity occurs) were used in these experiments (Figure 4-8B). *In vivo* expression of a constitutively active truncated form of aPKC (aPKCΔN) that lacks the C-terminal pseudosubstrate region of full-length aPKC, and that cannot bind to Par6 so is no longer apically restricted (Betschinger et al., 2003; Drier et al., 2002), causes lethality before the L3 larval stage when under the control of *hh-Gal4*, and therefore was not possible to assess its effect on Ex stability.

Sgg has an important role in priming substrates for Slmb/β-TrCP-mediated degradation through phosphorylation of substrate phosphodegron sequences (Skaar et al., 2013), which is discussed more thoroughly in '1.2.3 - F-box E3 Ligases'. Sgg is involved in regulating the stability of the Hh effector Ci (Price and Kalderon, 2002), the circadian clock regulators Timeless (Tim) and Per (Martinek et al., 2001; Top et al., 2016) and the Wingless effector Arm (Peifer et al., 1994) among others. As Sgg often primes Slmb substrates for degradation, the potential effect of Sgg in the regulation of Ex stability was tested. In S2 cells, overexpression of wildtype, constitutively active, or kinase dead versions of Sgg had no effect on the mobility or stability of Ex$^{1\text{-}468}$ or Ex$^{1\text{-}468\ CAAX}$ (Figure 4-9A). Overexpression the B isoform of Sgg *in vivo* had no effect on the *ubi-ex$^{1\text{-}468}$::GFP* reporter (Figure 4-9B). However, overexpression of Sgg^{A81T}, a kinase dead form of Sgg (Bourouis, 2002) resulted in very disrupted morphology of the posterior compartment compared to the anterior internal control, this folding of the tissue could explain the apparent increased intensity of *ubi-ex$^{1\text{-}468}$::GFP* (Figure 4-9C). The disrupted morphology could be the result of a dominant negative function of

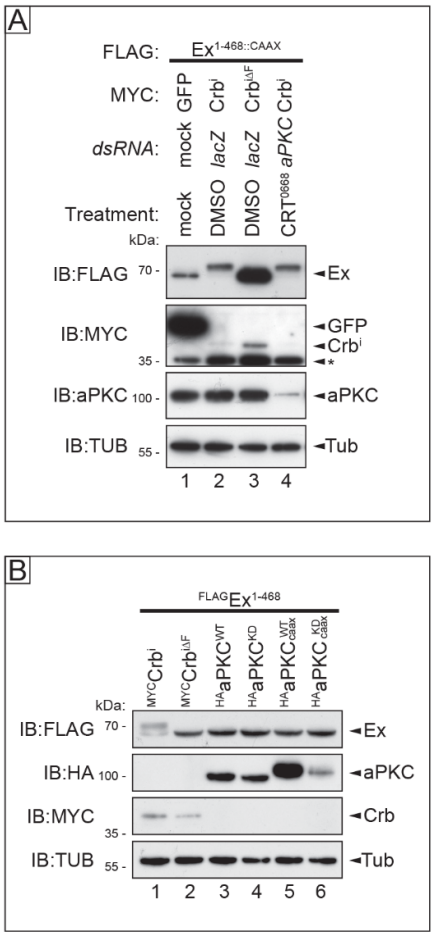

Figure 4-8 aPKC has no effect on Ex protein stability in S2 cells

Immunoblot of S2 cell lysates expressing FLAG-tagged $Ex^{1\text{-}468\ CAAX}$ (A) treated with mock drug (H_2O) (A – lane 1) , DMSO (A – lanes 2,3) or CRT^{0668} (A – lane 4) and with dsRNA targeting *lacZ* as a control (A – lanes 2,3) or *aPKC* (A – lane 4). Expression of Myc-tagged Crb^{i} (A – lane 2,4) caused depletion and/or electrophoretic shift in FLAG-tagged $Ex^{1\text{-}468\ CAAX}$ when compared to GFP (A – lane 1) or Myc-tagged $Crb^{i\Delta F}$ (A – lane 3) controls, which was not influenced by treatment with the aPKC inhibitor CRT^{0668} and *aPKC* dsRNA treatment (A – lane 4). Expression of Myc-tagged Crb^{i} (B – lane 1) but not $Crb^{i\Delta F}$ (B – lane 2), HA-tagged $aPKC^{WT}$ (B – lane 3), $aPKC^{KD}$ (B – lane 4), $aPKC^{WT\ CAAX}$ (B – lane 5) or $aPKC^{KD\ CAAX}$ (B – lane 6) caused depletion and electrophoretic mobility shift of $Ex^{1\text{-}468}$. S2 cell lysates were probed with the indicated antibodies and Tub was used as loading control (A-B).

the Sgg^{A81T} construct sequestering endogenous Sgg substrates through physically interaction. However, this was in stark contrast to *sgg* knockdown in S2 cells (Figure 4-9A) and RNAi-mediated depletion of *sgg in vivo*, which showed no change in *ubi-ex$^{1-468}$::GFP* levels (Figure 4-9D). When *sgg^{IR}* was combined with *crb^{i}* overexpression, *ubi-ex$^{1-468}$::GFP* was totally lost from the posterior compartment, similar to the *crb^{i}* alone phenotype (Figure 4-9E). These data suggest that, at least in the conditions tested, Sgg is not involved in the regulation of Ex stability *in vitro* or *in vivo*.

4.4. **Concluding Remarks**

This chapter has attempted to identify a potential Ex degradative kinase using a candidate based approach with MS data, and current literature as the basis for candidate selection. Of the kinases tested, the BMP pathway seems to be the most promising as a potential regulator of Ex and Hippo signalling, because, at least in S2 cells, kinase depletion appears to result in mild stabilisation of Ex, and overexpression of Tkv causes an electrophoretic mobility shift in $Ex^{1-468\ CAAX}$.

However, the discrepancy between analysis performed in S2 cells and *in vivo* needs to be rectified. Interestingly, the Hippo and BMP pathways interact in *Drosophila* (Oh and Irvine, 2011) and mammals, CRB3 regulating the localisation of both YAP and SMAD (Varelas et al., 2010). Therefore it would be interesting to discover whether in *Drosophila* these pathways regulate, and are regulated by Ex.

In addition, the ability of the core Hippo kianses Hpo and Wts to stimulate Ex N-terminal phosphorylation warrants further investigation, althought this signalling event is unlikely to act downstream of Crb, or influence Ex stability. Interestingly, Wts has been reported to phosphorylate Ex at S1116 within the C-terminus to promote Ex function by inhibiting degradation by Slmb (Zhang et al., 2015a).

Analysis of the Ex protein sequence revealed only one Wts HXRXXS consensus sequence at the Ex^{S1116} site, suggesting that the mobility shift seen in $Ex^{1\text{-}468}$ upon Wts overexpression (Figure 4-6C) may not be a result of direct phosphorylation. As no clear Hpo or MST1/2 consensus has been established, it is difficult to assess whether Hpo directly phosphorylates Ex, or whether this effect is indirect (Figure 4-6C). Interestingly, LATS reportedly phosphorylates AMOT in mammal (Adler et al., 2013; Chan et al., 2013; Dai et al., 2013; Hirate et al., 2013), which alters its ability to regulate YAP (Moleirinho et al., 2014; Ragni et al., 2017). Perhaps the phosphorylation of Ex induced by Hpo and Wts influences Ex activity in a similary manner to LATS-mediated phosphorylation of AMOT.

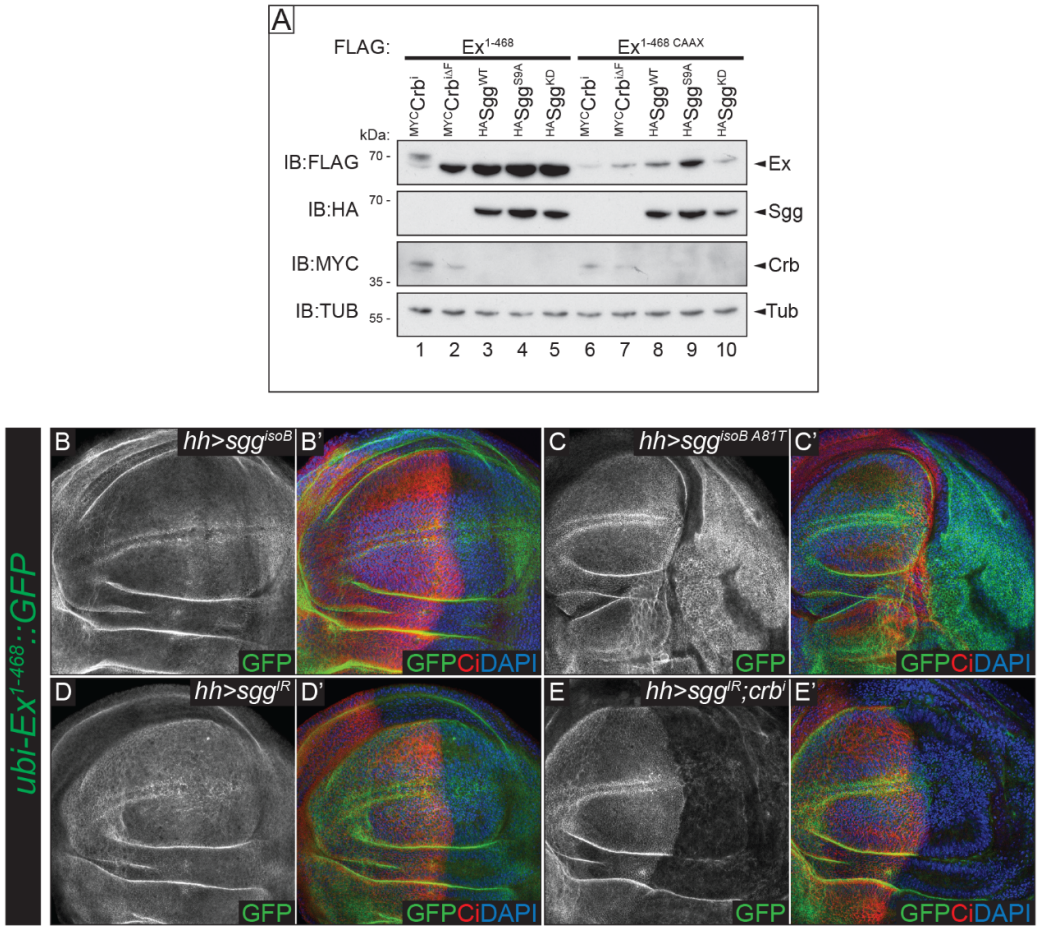

Figure 4-9 Sgg has no effect on Ex in S2 cells or *in vivo*

Immunoblot of S2 cell lysates expressing FLAG-tagged $Ex^{1\text{-}468}$ (A – lanes 1-5) or $Ex^{1\text{-}468\ CAAX}$ (A – lane 6-10). Expression of Myc-tagged Crb^{i} (A – lanes 1, 6) but not $Crb^{i\Delta F}$ (A – lanes 2, 7), HA-tagged Sgg^{WT} (A - lanes 3, 8), constitutively active Sgg^{S9A} (A – lanes 4, 9) or kinase-deficient Sgg^{KD} (A – lanes 5, 10) caused electrophoretic shift/depletion of $Ex^{1\text{-}468}$ (A - lanes 1-5) and $^{FLAG}Ex^{1\text{-}468\ CAAX}$ (A – lanes 6-10). Lysates were analysed with the indicated antibodies and Tub was used a loading control (A-B). Confocal micrographs of third instar larvae wing imaginal discs expressing *ubi-ex$^{1\text{-}468}$::GFP* (B-E'). Single channel images show GFP staining in maximum intensity projection of the apical domain. Nuclei are marked by DAPI staining (blue) and the posterior compartment expressing *hh-Gal4* is marked by the absence of Ci staining (red). *hh-Gal4*-mediated expression of *sgg^{isoB}* (B) or of a *sgg* RNAi transgene (D, *sgg^{IR}*) had no effect on *ubi-ex$^{1\text{-}468}$::GFP levels*. Expression of a kinase dead version of *sgg* (C, *sgg$^{isoB\ A81T}$*) disrupted the morphology of the posterior compartment and increased *ubi-ex$^{1\text{-}468}$::GFP levels*. Coexpression of *crb^{i}* with *sgg^{IR}* (E) had no effect on *ubi-ex$^{1\text{-}468}$::GFP levels* compared to expression of *crb^{i}* alone under the control of *hh-Gal4* (see Figure 3-1B).

Chapter 5 - Results 3 – The Role of Casein Kinase 1 Family Kinases in the Regulation of Expanded

5.1. **An Introduction to the CK1 Family Kinases**

The MS experiments described in the previous chapter also revealed Gilgamesh (Gish) as a potential Ex binding partner (Table 4-1). Gish is a member of the Casein Kinase 1 (CK1) family of kinases and the *Drosophila* orthologue of CK1γ, Therefore, the ability of Gish, and related kinases to regulate Ex stability was assessed.

CK1s are highly conserved, serine/threonine (S/T) kinases (Figure 5-1A) that are ubiquitously expressed among eukaryotes and involved in a wide array of biological processes (Knippschild et al., 2005; Schittek and Sinnberg, 2014). Of particular interest is the fact that CK1 kinases are commonly involved in the phospho-dependent targeting of their substrates for degradation, often through interactions with F-box proteins such as Slmb (Skaar et al., 2013). Prominent substrates of the CK1s include Arm (Liu et al., 2002; Yanagawa et al., 2002), Ci (Jia et al., 2005), and Per (Price et al., 1998), CK1 phosphorylation stimulating ubiquitylation. Interestingly, the CK1s also regulate Hippo signalling by phosphorylating and activating Ft in *Drosophila* (Feng and Irvine, 2009; Sopko et al., 2009), and YAP in mammals (Zhao et al., 2010). There are seven family members, *ck1*α *(Drosophila ck1*α), *ck1*β (which is only found in bovine species) (Cheong and Virshup, 2011), *ck1*δ and *ck1*ε (orthologues of *Drosophila discs overgrown* (*dco*)) and *ck1*γ1-3 (*Drosophila gish*), along with numerous splice variants (Figure 5-1A).

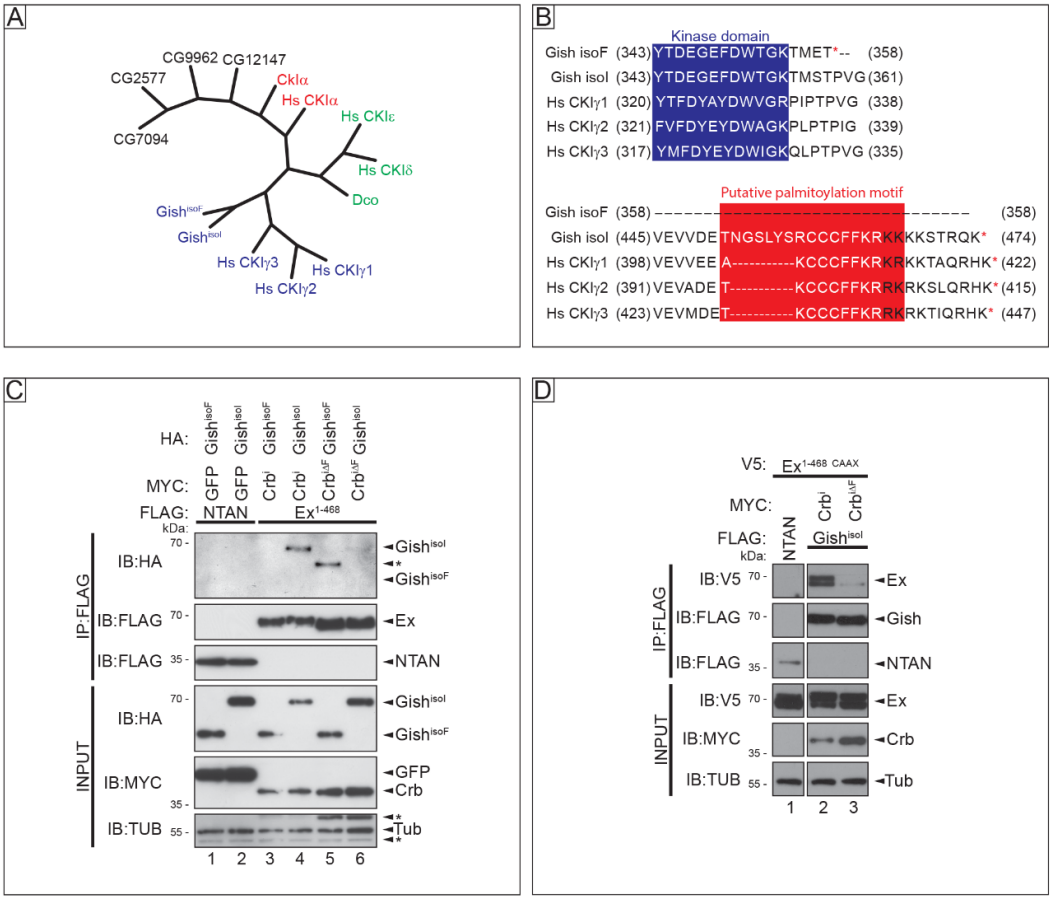

Figure 5-1 CK1 family and Gish interaction with Ex

Phylogenetic analysis of the CK1 family kinases complied using PhyML and DrawTree tools in the Phylogeny online tool (http://www.phylogeny.fr/simple_phylogeny.cgi) (Dereeper et al., 2008). CK1α and orthologues in red, CK1δ/ε and orthologues in green, CK1γ and orthologues in blue, and uncharacterised *Drosophila* CK1s in black (A). CK1 kinase sequence alignment using MUSCLE (Edgar, 2004) showing only the kinase domain, and putative palmitoylation motif (Davidson et al., 2005) of Gish^{isoI}, Gish^{isoF} and human (Hs) CK1γ1-3 (B). Immunoblot of S2 cell lysates after co-immunoprecipitation of FLAG-tagged NTAN as a negative binding control (C – lanes 1, 2, D – lane 1), FLAG-tagged Ex$^{1-468}$ (A – lanes 3-6) or FLAG-tagged Gish^{isoI} (B – lanes 2, 3). Myc-tagged Crb^{i} expression but not Crb$^{i\Delta F}$ stimulated the association between Ex$^{1-468}$ and HA-tagged Gish^{isoI} (C – lanes 3, 5). Neither Crb^{i} nor Crb$^{i\Delta F}$ induced the interaction between Ex$^{1-468}$ and HA-tagged Gish^{isoF} (C – lanes 4, 6). Crb^{i} expression but not Crb$^{i\Delta F}$ stimulated the association between Gish^{isoI} and V5-tagged Ex$^{1-468\ CAAX}$ (D – lanes 2, 3). Lysates and FLAG immunoprecipitates were analysed with the indicated antibodies and Tub was used as a loading control (C, D).

5.2. **Gilgamesh Interacts with Expanded**

To confirm the initial interaction between Ex and Gish defined in the MS data set (Table 4-1), immunoprecipitation of FLAG-tagged Ex was performed in S2 cells. Two different isoforms of Gish were co-expressed with Ex, isoform (iso) I ($Gish^{isoI}$) and F ($Gish^{isoF}$). These are two different products of *gish*, with the iso^{I} variant containing a C-terminal palmitoylation site that presumably allow it to localise at the membrane. In contrast, the iso^{F} of Gish lacks the putative palmitoylation site (Figure 5-1B). Crb and Ex both localise at the apical membrane, which is presumably where Crb stimulates Ex degradation. Therefore, as $Gish^{isoI}$ localises to the membranes through its palmitoylation sequence, it was one of the predominant isoforms analysed. Upon Crb^{i} stimulation, purified Ex and associated interacting complexes were also found to contain $Gish^{isoI}$ (Figure 5-1C lane 4). However, no Gish was identified when Ex was purified in the presence of $Crb^{i\Delta F}$, suggesting the kinase-substrate is dependent on the FERM domain of Crb and the ability of Crb to stimulate Ex degradation (Figure 5-1C lanes 5-6). Unlike $Gish^{isoI}$, $Gish^{isoF}$ was not identified in Ex-purified immunoprecipitates, suggesting that this kinase isoform does not interact with Ex, and that perhaps the difference in localisation of these kinases is important for their interaction and substrate specificity. The interaction between Ex and Gish was also confirmed by reciprocal immunoprecipitation, purifying FLAG-$Gish^{isoI}$. Similarly to previous results, Ex was identified as a Gish-interacting protein only when co-expressed with Crb^{i} and not $Crb^{i\Delta F}$ (Figure 5-1D).

5.3. **Stimulation of Expanded Phosphorylation and Degradation by Overexpression of CK1 Family Kinases**

As Ex and CK1 family members appear to interact in a Crb-dependent manner, and phosphorylation stimulated by Crb induces Ex degradation, the role of CK1s in regulating Ex phosphorylation and degradation was assessed. CK1 family members CK1α, Dco and Gish were overexpressed in S2 cells and caused an

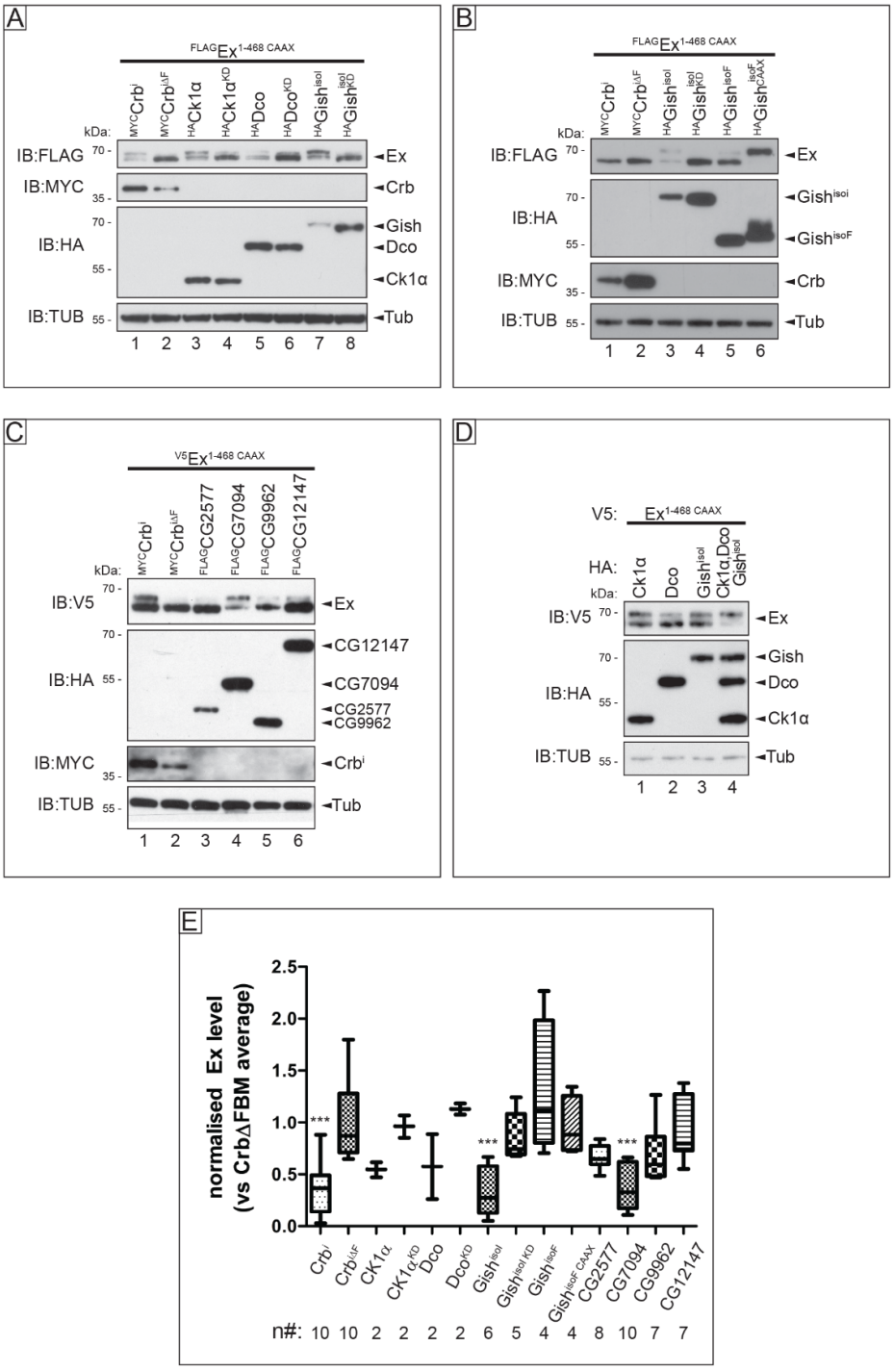

Figure 5-2 Overexpression of CK1 family kinases in S2 cells regulates Ex protein levels

(Continued on next page)

(Continued from previous page) Immunoblot of S2 cell lysates expressing FLAG-tagged $Ex^{1-468\ CAAX}$ (A-B) or V5-tagged $Ex^{1-468\ CAAX}$ (C, D). Expression of Myc-tagged Crb^{i} (A, B, C - lanes 1) but not $Crb^{i\Delta F}$ (A, B, C – lanes 2) as controls caused electrophoretic mobility shift and Ex protein depletion. Expression of HA-tagged CK1α (A – lane 3), HA-tagged Dco (A – lane 5) and HA-tagged $Gish^{isoI}$ (A – lane 7) but not the respective kinase dead constructs (A – lanes 4, 6, 8) caused electrophoretic mobility shift and depletion of FLAG-tagged $Ex^{1-468\ CAAX}$. Expression of HA-tagged $Gish^{isoI}$ (B – lane 3) and HA-tagged $Gish^{isoF\ CAAX}$ (B – lane 6), but not of HA-tagged $Gish^{isoI\ KD}$ (B – lane 4) or HA-tagged $Gish^{isoF}$ (B – lane 5), caused electrophoretic mobility shift and depletion of FLAG-tagged Ex^{1-468}. Expression of HA-tagged CG7094 (C – lane 4), but not of HA-tagged CG2577, CG9962 or CG12147 (C – lanes 3, 5, 6), caused electrophoretic mobility shift and depletion of V5-tagged $Ex^{1-468\ CAAX}$. Co-expression of HA-tagged CK1α, Dco and $Gish^{isoI}$ (D – lane 4) increased the electrophoretic mobility shift of V5-tagged $Ex^{1-468\ CAAX}$ compared to expression of individual kinases (D – lanes 1-3). Lysates were probed with the indicated antibodies and Tub served as loading control (A-D). Box and whiskers, min to max plot showing immunoblot quantification of Ex levels relative to the $Crb^{\Delta FBM}$ negative control (E) (protocol outlined in '2.1.15'). Groups were compared to the $Crb^{\Delta FBM}$ negative control group by a one-way ANOVA with a Dunnet's multiple comparison post hoc test (*** = $P < 0.001$).

electrophoretic shift, corresponding to Ex phosphorylation and depletion in $Ex^{1-468\ CAAX}$, although the mobility shift induced by Dco expression is far weaker than either CK1α or Gish(Figure 5-2A and E). Point mutations within the conserved kinase were introduced to render the kinases inactive ($CK1\alpha^{K49R}$, Dco^{K38R} and $Gish^{isoI\ K91R}$). The kinase dead CK1s were also overexpressed in S2 cells and induced no mobility shift in $Ex^{1-468\ CAAX}$ suggesting the mobility shift and depletion of Ex stimulated by the CK1 family kinases is dependent on their enzymatic activity (Figure 5-2A). Immunoblot quantification revealed that of these three kinases, only Gish overexpression resulted in a statistically significant reduction in Ex levels when comared to the $Crb^{\Delta FBM}$ negative control, although CK1α and Dco both show a trend to induce a reduction in Ex levels, and it is likely that with an increased number of repeats, these data would become statistically significant (Figure 5-2E). Interestingly immunoblot quantification also reveals that the kinase dead CK1s are also statistically indistinct from the $Crb^{\Delta FBM}$ negative control providing further evidence that the kinase activity of the CK1s is important in the regulation of $Ex^{1-468\ CAAX}$ stability in S2 cells (Figure 5-2E). $Ex^{1-468\ CAAX}$ was used

in these experiments because S2 cells do not express Crb^{i}, which means Ex may not localise correctly to the site of initial phosphorylation or degradation. Therefore, Ex was forced to the membrane in order to simulate its localisation when Crb is expressed.

Protein subcellular localisation is critical in regulating cellular processes. Gish is known to associate with cellular membranes *in vivo* through analysis of a GFP-fused Gish protein trap within the endogenous locus (known as Spider-GFP) (Martin et al., 2009; Morin et al., 2001). Indeed, $Gish^{isoF}$ which is the only Gish isoform not to contain a putative palmitoylation sequence (Figure 5-1B), does not interact with Ex upon Crb^{i} overexpression (Figure 5-1C). Therefore, the ability of these Gish isoforms to regulate Ex phosphorylation and degradation was assessed. As described, $Gish^{isoI}$ was able to stimulate an electrophoretic mobility in Ex, unlike the kinase dead version of the protein (Figure 5-2A). When $Gish^{isoF}$ was overexpressed, there was a much less dramatic shift in Ex, and Ex levels were not reduced when compared to the $Crb^{\Delta FBM}$ negative control (Figure 5-2B lane 5 and E) suggesting that this isoform was much less potent at phosphorylating Ex. A palmitoylation CAAX sequence was then cloned onto $Gish^{isoF}$ in order to localise this kinase to the cellular membranes. $Gish^{isoF\ CAAX}$ could readily induce a dramatic mobility shift in Ex, implying that this kinase can phosphorylate Ex (Figure 5-2B – lane 6). However, unlike Crb or $Gish^{isoI}$ overexpression, Ex was not degraded upon $Gish^{isoF\ CAAX}$ overexpression (Figure 5-2B and E). This result was somewhat unexpected and perhaps the CAAX-tag limits the ability of $Gish^{isoF}$ to stimulate Ex degradation, or it is possible that forcing the localisation of $Gish^{isoF\ CAAX}$ to the membrane can induce Ex phosphorylation without stimulating its degradation.

The ability of several uncharacterised CK1-like kinases, CG2577, CG7094, CG9962 and CG12147 to regulate Ex was also tested by overexpression in S2 cells. CG7094, CG9962 and CG12147 all appeared to induce a mobility shift in Ex (Figure 5-2C lane 4-6). Of these kinases CG7094 appeared to induce the most

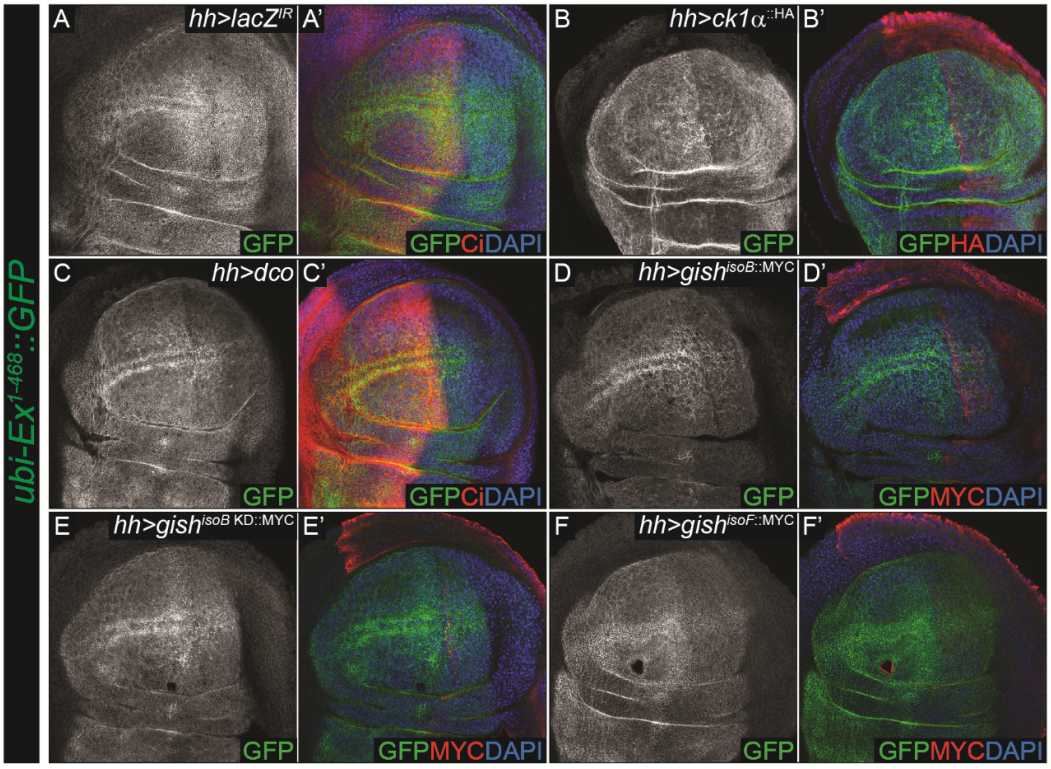

Figure 5-3 Overexpression of CK1 family kinases regulates Ex *in vivo*

Confocal micrographs of third instar larvae wing imaginal discs expressing *ubi-ex$^{1-468}$::GFP* (A-H'). Single channel images show GFP staining in maximum intensity projection of the apical domain. Nuclei are marked by DAPI staining (blue) and the posterior compartment where *hh-Gal4* is expressed is marked by the absence of Ci staining (red in A' and C'), the presence of HA staining (red in B') or MYC staining (red in D'-F'). Image depicting expression of the control *lacZ^{IR}* in the *hh-Gal4* domain (A) is the same as in 'Figure 3-1A', and does not affect *ubi-ex$^{1-468}$::GFP* levels. Unlike *gish$^{isoB\ KD}$* (E), expression of *ck1α* (B), *dco* (C), *gish^{isoB}* (D), or *gish^{isoF}* (F) under the control of *hh-Gal4* caused depletion of *ubi-ex$^{1-468}$::GFP* levels.

dramatic mobility shift in Ex, which also results in statistically significant depletion of Ex when compared to the Crb$^{\Delta FBM}$ negative control (Figure 5-2C lane 4 and E). The fact that so many members of the CK1 family appear to be able to induce Ex phosphorylation suggests there may be overlapping substrate specificity between these kinases. To test whether this was indeed the case, multiple CK1s, CK1α,

Dco and Gish^{isoI} were expressed alone, or in combination. CK1s expressed alone resulted in electrophoretic shift as previously discussed. Interestingly, when all three kinases were overexpressed, a higher proportion of Ex$^{1\text{-}468\ CAAX}$ was shifted, with the lower, un-phosphorylated band almost undetectable (Figure 5-2D). This data is in agreement with a potential synergistic action of CK1 kinases in the regulation of Ex function, although it cannot be ruled out that simply expressing three times as much of any single kinase would yield the same result.

The role of the CK1s was also tested *in vivo* by *hh-Gal4* controlled overexpression of UAS-CK1s, in combination with the *ubi-ex$^{1\text{-}468}$::GFP* reporter. Overexpression of kinase active CK1α, Dco and Gish^{isoB}, an isoform closely related to Gish^{isoI} that contains the C-terminal palmitoylation site, and Gish^{isoF} all induced depletion of the *ubi-ex$^{1\text{-}468}$::GFP* reporter (Figure 5-3B-D, F). A kinase dead form of Gish^{isoB} was also overexpressed and did not result in depletion of *ubi-ex$^{1\text{-}468}$::GFP* in the *hh*-positive posterior compartment (Figure 5-3E). These data support the results obtained in S2 cells suggesting that the CK1 family of kinases can regulate Ex stability through phosphorylation. Interestingly, *in vivo*, even Gish^{isoF} was able to induce a depletion in the *ubi-ex$^{1\text{-}468}$::GFP* reporter in contrast to cell experiments. This could be due to differential localisation of Gish^{isoF} *in vivo* compared to in S2 cells, although this remains unclear. Moreover, the CK1 family kinase are able to phosphorylate apically localised substrates such as Ft, Arrow (Arr) and Smoothened (Smo) (Chen et al., 2011; Davidson et al., 2005; Feng and Irvine, 2009; Sopko et al., 2009; Zhang et al., 2006), suggesting that despite not possessing a palmitoylation sequence, these kinases are able to stimulate depletion of Ex, at least upon overexpression.

Ex$^{1\text{-}468}$ was identified as the minimal region of Ex that is required for Crb-induced degradation, whereas Ex$^{1\text{-}450}$, only eighteen amino acids shorter is no longer phosphorylated and degraded upon expression of Crb (Ribeiro et al., 2014). In order to determine whether the CK1s also induced Ex phosphorylation in a similar manner, either Crb^{i}, Crb$^{i\Delta F}$, which does not induce Ex phosphorylation, or Gish^{isoI} were overexpressed with either Ex$^{1\text{-}450\ CAAX}$ or Ex$^{1\text{-}468\ CAAX}$. As previously reported,

Crb^{i} could only induce a mobility shift in $Ex^{1\text{-}468}$, whereas $Crb^{i\Delta F}$ failed to induce a shift in either Ex construct (Figure 5-4A lanes 1-2, 4-5) (Ribeiro et al., 2014). $Gish^{isol}$ behaved similarly to Crb^{i}, and was only able to induce a mobility shift in $Ex^{1\text{-}468\ CAAX}$, but not in $Ex^{1\text{-}450\ CAAX}$ (Figure 5-4A lanes 3, 6). This suggests that Gish, and perhaps the other CK1s, stimulate phosphorylation of Ex within the same region that is phosphorylated upon expression of Crb. However, it cannot be ruled out that the region between Ex^{450} and Ex^{468} is only responsible for the interaction between the kinase and Ex, and not the site of phosphorylation per se. Within this region, there are several serine and threonine residues, which are potential candidates for the CK1 phosphorylation site (Figure 5-4B), in addition to several other S/T residues present directly N-terminal to this region of Ex. The most obvious candidate for CK1 phosphorylation is S453, which has been shown previously, and in this report, to be essential for regulating Ex stability (Ribeiro et al., 2014).

As phosphorylation of Ex results in Slmb-mediated binding and degradation, the ability of the CK1 kinases to stimulate Ex:Slmb interaction was assessed. Overexpression of Ck1α, Dco or Gish, followed by Slmb-immunopurification, stimulated the interaction between Slmb and $Ex^{1\text{-}468\ CAAX}$ (Figure 5-4C). Therefore, in S2 cells, kinase overexpression is sufficient to induce Ex:Slmb interactions independently of Crb^{i}, providing further evidence that these kinases are important in the regulation of Ex phosphorylation and stability. Interestingly, in addition to the isolation of Ex, immunopurification of Slmb also pulled-down CK1α and not Dco or Gish, so perhaps CK1α constitutively associates closely with Slmb due to the number of substrates it targets for degradation (Figure 5-4C lane 2).

5.4. **Loss of Function Analysis of CK1 Family Kinases and Expanded Stability**

In addition to gain of function experiments, loss of function assays were also carried out, initially in S2 cells. RNAi-mediated knockdown of *gish* resulted in

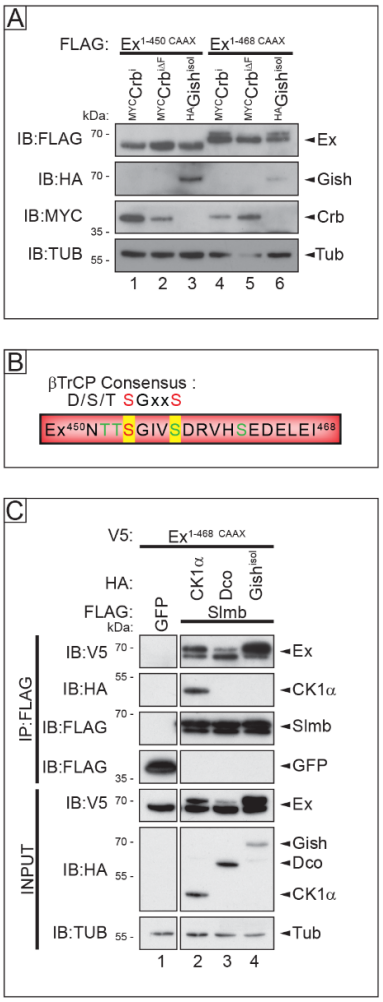

Figure 5-4 CK1 kinases regulate the Ex Slmb phosphodegron region and binding to Slmb

Immunoblot of S2 cell lysates expressing FLAG-tagged $Ex^{1\text{-}450\ CAAX}$ (A – lanes 1-3) and FLAG-tagged $Ex^{1\text{-}468\ CAAX}$ (A – lanes 4-6). Expression of Myc-tagged Crb^{i} (A - lanes 1, 4) and HA-tagged $Gish^{isoi}$ (A – 3, 6) caused an electrophoretic shift in FLAG-tagged $Ex^{1\text{-}468\ CAAX}$ but not on $Ex^{1\text{-}450\ CAAX}$, whereas expression of Myc-tagged $Crb^{i\Delta F}$ did not cause an electrophoretic shift in either (A – lanes 2, 5). A cartoon depiction of the $Ex^{450\text{-}468}$ region highlighting the canonical β-TrCP consensus sequence, the S453 residue (red), which is important for regulating Ex stability, and the S/T residues (green) included in this part of Ex (B). S2 cell lysates expressing V5-tagged $Ex^{1\text{-}468\ CAAX}$ after co-immunoprecipitation of FLAG-tagged GFP as a negative binding control (C – lane 1) or FLAG-tagged Slmb (C – lanes 2-4). Expression of HA-tagged CK1α, Dco or $Gish^{isoi}$ induced the interaction between V5-tagged $Ex^{1\text{-}468\ CAAX}$ and Slmb (C – lanes 2-4). Note that HA-tagged CK1α also associated with Slmb (C – lane 2). Lysates and FLAG immunoprecipitates were probed with the indicated antibodies and Tub was used as loading control (A, C).

dramatic stabilisation of Ex^{1-468} despite overexpression of Crb^{i} (Figure 5-5A). Also, it is important to note that unlike in the cases of Crb or kinase overexpression where a doublet of Ex is visible, with one band corresponding to phosphorylated and one band corresponding to un-phosphorylated Ex, when *gish* is depleted the Ex upper band is nearly undetectable and the un-phosphorylated lower band completely dominates (Figure 5-5A). This suggests that knocking down *gish* creates a situation whereby Crb can no longer stimulate Ex phosphorylation, thus the electrophoretic mobility of Ex is impeded. In addition to *gish* depletion stabilising Ex^{1-468} even in the presence of Crb, *gish* depletion could also block Crb-mediated degradation of Ex^{FL}, which suggests that the mechanisms identified in relation to the N-terminal truncation used throughout this thesis are also applicable to full-length Ex (Figure 5-5B). Unfortunately, dsRNA efficiently targeting *dco* or *ck1α* in cells could not be generated, therefore limiting the analysis of these kinases. In addition, the alternative, uncharacterised CK1 family kinases are not sufficiently expressed in S2 cells to warrant analysis of their loss of function phenotypes in this system. In order to confirm that the dsRNA use to target *gish* efficiently knocked down the desired kinase, $Gish^{isoI}$ was overexpressed in S2 cells treated with dsRNA targeting lacZ as a negative control, and dsRNA targeting *gish*. Overexpressed $Gish^{isoI}$ was undetectable in cells treated with *gish* dsRNA confirming the effectiveness of this reagent (Figure 5-5C). Loss of function phenotypes were also analysed *in vivo*. RNAi-mediated knockdown of *gish* resulted in an increase in the *ubi-ex$^{1-468}$::GFP* reporter in the *hh*-positive posterior compartment (Figure 5-5D). In combination with *crb^{i}* overexpression, *gish* depletion caused severe morphological disruption with enhanced cell death, judged by the presence of pyknotic nuclei in DAPI nuclear staining (Figure 5-5E'). Despite this phenotype, there was a recovery of *ubi-ex$^{1-468}$::GFP* in the *crb^{i}* overexpression domain (Figure 5-5E). These data suggest that *gish* may regulate the stability of Ex *in vivo*, thereby corroborating the data obtained in S2 cells. Regrettably, expression of *UAS-ck1α^{IR}* under the control of *hh-Gal4* resulted in the complete absence of any imaginal disc tissue due to the strength of the RNAi line, so the effect on Ex stability could not be analysed in this context.

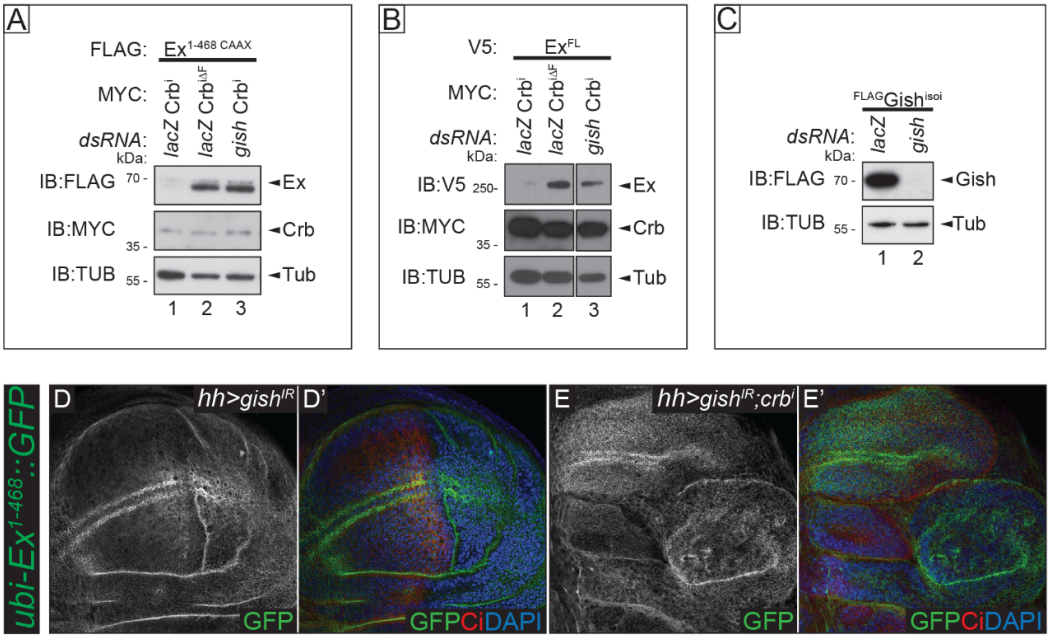

Figure 5-5 Depletion of *gish* stabilises Ex in S2 cells and *in vivo*

Immunoblot of S2 cell lysates expressing FLAG-tagged $Ex^{1\text{-}468\ CAAX}$ (A), V5-tagged Ex^{FL} (B) or FLAG-tagged $Gish^{isoI}$ (C) treated with dsRNA against *lacZ* as a control (A, B– lanes 1, 2, C – lane 1) or *gish* (A, B – lanes 3, C – lane 2). Expression of Myc-tagged Crb^{i}, but not $Crb^{i\Delta F}$, caused an electrophoretic shift and depletion in FLAG-tagged $Ex^{1\text{-}468\ CAAX}$ (A lanes 1, 2) and V5-tagged Ex^{FL} (B – lanes 1, 2), which was abrogated by depletion of *gish* (A, B – lanes 3). Expression of FLAG-tagged $Gish^{isoI}$ was abrogated by depletion of *gish* (C – lane 2). Lysates were analysed using the indicated antibodies and Tub was used as a loading control (A, B). Confocal micrographs of third instar larvae wing imaginal discs expressing *ubi-ex$^{1\text{-}468}$::GFP* (D-E'). Single channel images show GFP staining in maximum intensity projection of the apical domain. Nuclei are marked by DAPI staining (blue) and the posterior compartment where *hh-Gal4* is expressed is marked by the absence of Ci staining (red). Expression of *gish^{IR}* under the control of *hh-Gal4* increased the levels of the *ubi-ex$^{1\text{-}468}$::GFP* reporter (D). Co-expression of *crb^{i}* and *gish^{IR}* (E) prevented *crb^{i}* from depleting *ubi-ex$^{1\text{-}468}$::GFP* when compared to *crb^{i}* alone (see Figure 3-1B), albeit leading to a disruption in tissue morphology (E).

In collaboration with Maxine Holder, Francis Crick Institute, RNAi-mediated depletion of the uncharacterised CK1-like kinases was carried out in wing imaginal discs. RNAi targeting *CG2577*, *CG7094, CG9962* or *CG12147* alone had no effect on the levels of the *ubi-ex$^{1\text{-}468}$::GFP* reporter (collaborator data not

shown). However, in combination with *crb^{i}* overexpression, depletion of *CG2577*, *CG9962* and, in particular, *CG7094* resulted in mild stabilisation of the *ubi-ex$^{1-468}$::GFP* reporter specifically along the dorsal-ventral compartment boundary (collaborator data not shown). Depletion of *CG12147* did not result in stabilisation of *ubi-ex$^{1-468}$::GFP* in the presence of *crb^{i}* (collaborator data not shown). These data are in agreement with the overexpression data in S2 cells, which suggested that CG7094 may be able to phosphorylate and deplete Ex protein. Interestingly, the RNAi line used for depletion of CG2577 had one predicted off-target hit against CG7094, which may explain why depletion of *CG2577* in combination with *crb^{i}* resulted in mild stabilisation of the *ubi-ex$^{1-468}$::GFP* reporter, as this may be the influence of the off-target effect of the RNAi-line. Why the *ubi-ex$^{1-468}$::GFP* reporter is only stabilised along the dorsal-ventral compartment boundary remains unknown.

Following on from RNAi experiments, the *ubi-ex$^{1-468}$::GFP* reporter was analysed in homozygous mutant clones for CK1 family kinases, which were generated in wing imaginal discs. Note that this *in vivo* analysis was performed in collaboration with Maxine Holder (Francis Crick Institute). See '2.3.6 - The FLP/FRT System' (Figure 2-1B) for details. Homozygous mutant clones for *dco^{3}*, a hypomorphic *dco* allele that causes dramatic overgrowth phenotypes through the inhibition of Fat signalling (Feng and Irvine, 2009; Sopko et al., 2009; Zilian et al., 1999), or *gish^{KG03891}*, a P-element insertion in the third exon of *gish*, which causes penetrant recessive lethality (Bellen et al., 2004; Tan et al., 2010) had no effect on the levels of the *ubi-ex$^{1-468}$::GFP* reporter (collaborator data not shown). To assess whether the *gish* allele initially used was null, an additional *gish* mutant allele was generated my Maxine Holder (Francis Crick Insitute) using CRISPR-Cas9 mediated double strand DNA breaks (Port et al., 2014), which created a frameshift, followed by a stop codon at amino acid 96 targeting all *gish* isoforms. This new allele, *gish^{17}* is recessive lethal and deemed to be null. Clones for this new, null *gish* allele also did not result in any overt changes in the levels of *ubi-ex$^{1-468}$::GFP* compared to surrounding wildtype tissue (collaborator data not shown) corroborating the result from the published *gish* allele. However, *ck1α*

mutant clones did induce an increase in the *ubi-ex$^{1-468}$::GFP* reporter but only in the wing pouch and not in the notum (collaborator data not shown), consistent with previous results describing *slmb* regulation Ex degradation only in the pouch (Ribeiro et al., 2014). No *ck1α* null mutants currently exist and the *ck1α^{8B12}* allele used in these experiments contains a G43D point mutation, which is unable to stimulate Arm degradation (Legent et al., 2012). These data seem to suggest that *in vivo*, *ck1α* is the most important kinase in the regulation of Ex stability, and not *gish*.

To confirm that *ck1α* mutant clones specifically up-regulate Ex protein, rather than simply increasing the apical domain, *ck1α* clones were analysed for the apical markers Crb and Spider-GFP. In *ck1α* clones within the pouch, the levels of both Crb and Spider-GFP (Gish) were increased, which was not the case with Crb staining in *gish* mutant clones (collaborator data not shown). This suggests there is a broad increase in apical abundance in *ck1α* clones, potentially limiting the significance of the increase in *ubi-ex$^{1-468}$::GFP* reporter (collaborator data not shown). However, it is interesting to note that Gish increases in *ck1α* mutant clones. As potential redundancy appears to be an issue with the CK1s, perhaps loss of *ck1α* results in the compensatory up-regulation of other CK1 members, in this case *gish*, thereby limiting the potential damage to tissue homeostasis caused by loss of *ck1α* (collaborator data not shown).

In cells, overexpression of the CK1 family kinases is sufficient to induce interaction with Slmb (Figure 5-4C). Therefore, whether loss of function of *gish* could block the interaction of Ex with Slmb was analysed. Immunoprecipitated FLAG-Slmb interacts with Ex upon Crb^{i} overexpression, and this interaction is dependent on an intact FBM within Crb (Figure 5-6A lanes 2-3). However, when cells were also treated with dsRNA against *gish*, the Crb^{i} induced Ex:Slmb interaction was abolished (Figure 5-6A lane 4). This suggests that the phosphorylation of Ex by Gish is vital to its recognition by Slmb, and its subsequent degradation in S2 cells. To further assess this, the ubiquitylation status of Ex was analysed through ubiquitylation assays, where overexpressed

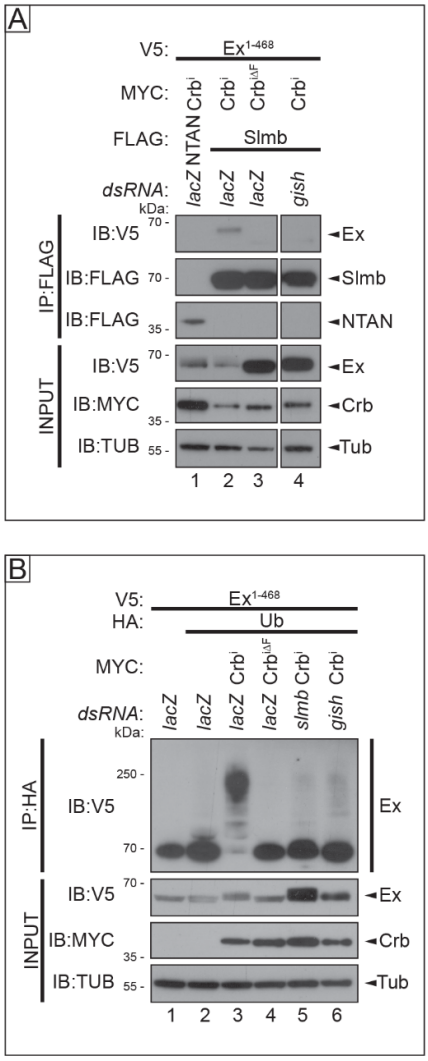

Figure 5-6 Depletion of *gish* inhibits Ex:Slmb binding and Ex ubiquitylation

Immunoblots of S2 cell lysates expressing V5-tagged Ex^{1-468} after treatment with dsRNA against *lacZ* as a control (A - lanes 1-3) or *gish* (A – lane 4) and co-immunoprecipitation of FLAG-tagged NTAN as a negative binding control (C – lanes 1) or FLAG-tagged Slmb (A – lanes 2-4). Myc-tagged Crb^{i} expression but not expression of $Crb^{i\Delta F}$ stimulated association between Slmb and Ex^{1-468} (A – lanes 2, 3), which was abrogated by treatment with *gish* dsRNA (A – lane 4). S2 cell lysates expressing V5-tagged $Ex^{1-468\ CAAX}$ after treatment with dsRNA against *lacZ* as a control (B - lanes 1-4), *slmb* (B – lane 5) or *gish* (B – lane 6) and co-immunoprecipitation of HA-tagged Ub. Myc-tagged Crb^{i} expression (B – lane 3), but not expression of Ub alone (B – lane 2) or of Myc-tagged $Crb^{i\Delta F}$ (B – lane 4), induced V5-tagged Ex^{1-468} ubiquitylation, which is abrogated by *slmb* (B – lane 5) or *gish* (B – lane 6) dsRNA-mediated depletion. Lysates and purified immunoprecipitates were probed with the indicated antibodies and Tub was used as a loading control (A, B).

HA-tagged ubiquitin was isolated from S2 cells by HA-specific immunoprecipitation. Proteins that have been tagged by ubiquitin will produce a smear when immunoblotted after SDS-PAGE. Using this method, Crb^{i} overexpression, but not $Crb^{i\Delta F}$ induced ubiquitylation of Ex (Figure 5-6B lanes 3-4), consistent with the role of these constructs in the regulation of Ex stability. As previously described, when cells overexpressing Crb^{i} were also treated with dsRNA against *slmb*, Ex was no longer ubiquitylated as the E3-ligase responsible for tagging Ex with Ubi had been depleted (Figure 5-6B lane 5) (Ribeiro et al., 2014). Furthermore, when cells were treated with dsRNA against *gish,* Ex ubiquitylation was also lost (Figure 5-6B lane 6), suggesting that this kinase is essential in priming Ex for ubiquitylation and subsequent degradation.

5.5. **The Role of CK1 Family Kinases in Regulating the Hippo Pathway**

Ex is a very potent regulator of Yki activity acting both in a Hpo core kinase-dependent and independent manner (Badouel et al., 2009; Hamaratoglu et al., 2006). Therefore, proteins that impinge on Ex function would be expected to influence the activity of Yki. This is indeed the case with Crb, where overexpression of Crb^{i} results in Ex degradation and increased Yki activity (Chen et al., 2010; Grzeschik et al., 2010; Ling et al., 2010; Robinson et al., 2010). To test the ability of the CK1 kinases to regulate Yki activity, the Hippo pathway enhancer trap *ex-lacZ* was used as readout for Yki activity (Boedigheimer and Laughon, 1993). *UAS*-transgenes were expressed in wing imaginal discs under the control of *hh-Gal4*. GFP control discs showed no difference between β-Gal staining in the posterior and anterior compartments. As expected, wing discs with RNAi-mediated depletion of *hpo*, or Crb^{i} overexpression both caused an increase in β-Gal staining as a result of Yki activation, althought the increase in β-Gal staining in the Crb^{i} expressing control was very mild (Figure 5-7A-C). Of all the

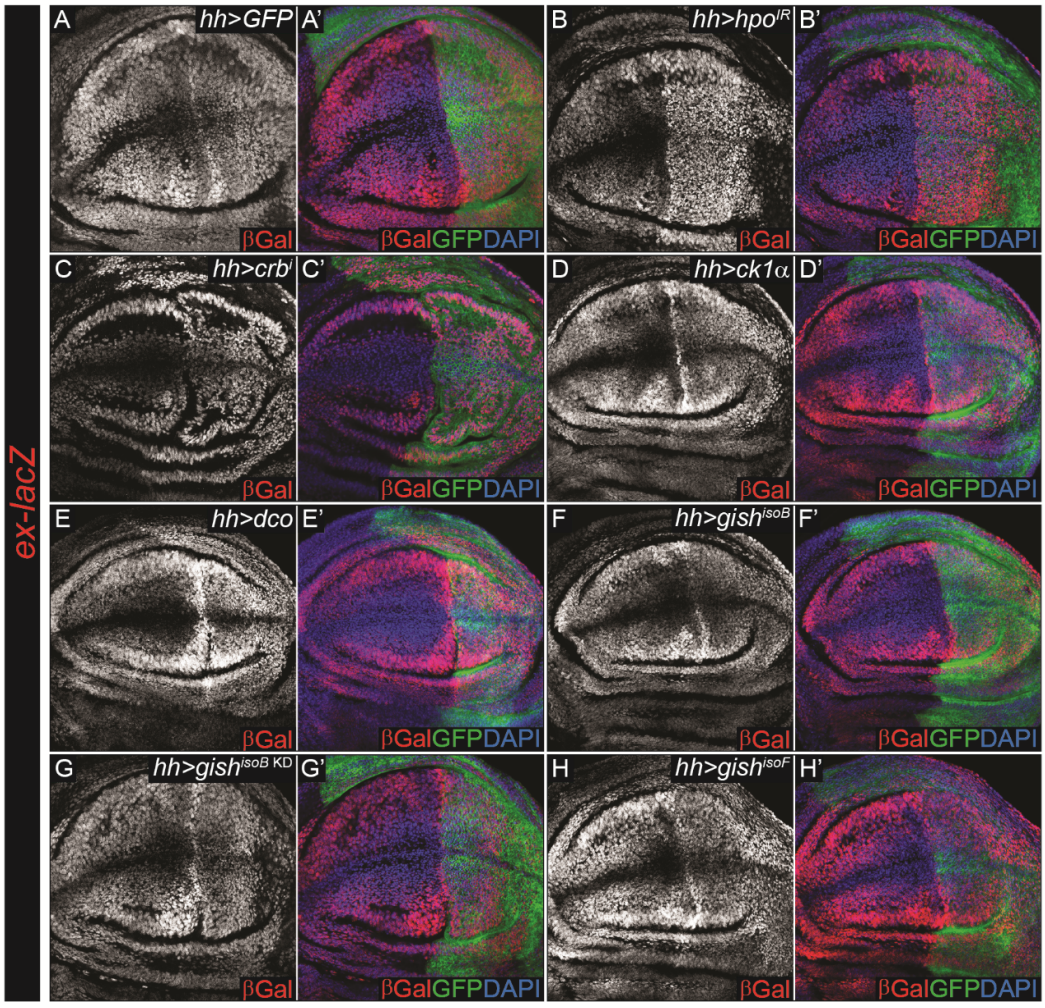

Figure 5-7 Overexpression of CK1 family kinases regulates *ex-lacZ in vivo*

Confocal micrographs of third instar larvae wing imaginal discs expressing an *ex-lacZ* enhancer-trap (A-H') Single channel images show β-Gal staining in a planar section in line with the nuclei of the wing pouch. Nuclei are marked by DAPI staining (blue) and the posterior compartment expressing *hh-Gal4* is marked by expression of GFP. Expression of *GFP* under the control of *hh*-Gal4 (negative control) did not alter levels of β-Gal (A). Expression of the positive controls hpo^{IR} (B) and crb^{i} (C) using *hh-Gal4* led to an increase in β-Gal levels in the posterior compartment. Expression of *ck1α* (D) and *dco* (E) increased levels of β-Gal, whereas expression of $gish^{isoB}$ (F), $gish^{isoB\ KD}$ (G) or $gish^{isoF}$ (H) did not alter β-Gal levels.

CK1 transgenes tested, only *ck1α* overexpression resulted in mild autonomous increase in β-Gal staining, suggesting this gene activates Yki (Figure 5-7D). Overexpression of *dco*, *gish*^{isoB}, *gish*$^{isoB\ KD}$ and *gish*^{isoF} had no effect on β-Gal staining when compared to the anterior compartment internal control (Figure 5-7E-H). It would be expected that if these kinases promote degradation of Ex, there would be an increase in Yki activity through inactivation of Hippo signalling, Yki thus being free to enter the nucleus and initiate its transcriptional programme. Here only *ck1α* can regulate the Hippo pathway, consistent with its putative role in degrading Ex, and activating Yki.

In addition, in collaboration with Maxine Holder of the Francis Crick Institute, to gain of function analysis of Hippo reporters, *ck1α* and *gish* mutant clones were analysed for Yki activity using the *diap1-lacZ* and *ex-lacZ* reporters respectively. In *ck1α* mutant tissue, levels of *diap1-lacZ* were dramatically decreased, whereas *ex-lacZ* remained unchanged in *gish* mutant tissue (collaborator data not show). This is consistent with *ck1α* appearing to be the prominent CK1 isoform in regulating Ex *in vivo*. Furthermore, a decrease in Yki reporter activity in *ck1α* clones is also consistent with an increase in Ex levels seen in *ck1α* clones (collaborator data not show), which should inhibit Yki. Interestingly *ck1α* clones also increase the apical proteins Crb and Gish , and produce large rounded clones (collaborator data not show), which are phenotypes common to core Hippo pathway mutants which all up-regulate Yki activity (Edgar, 2006; Genevet et al., 2009; Xu et al., 1995). However, this is in direct contrast to the obvious down-regulation of *diap1-lacZ* seen in *ck1α* mutant clones (collaborator data not show). Perhaps this suggests that despite an increase in the apical membrane, Ex levels are stabilised which results in Yki inhibition. More work needs to be carried out to confirm this hypothesis, and the phenotypes observed may be the result of the wide ranging functions of *ck1α* (Knippschild et al., 2014; Schittek and Sinnberg, 2014).

5.6. **Concluding Remarks**

This chapter establishes the CK1 family of kinases as important regulators of Ex stability and the Hippo pathway. In S2 cells the CK1 kinase Gish appears to be crucial in mediating the Crb-dependent degradation signal for Ex, whereas *in vivo* the kinase seems more likely to be CK1α. Precise delineation of the CK1-Ex regulatory axis is complex due to potential synergistic action of the CK1 family members, and and discrepancies between the analyses in cells and *in vivo* is still required. However, despite these shortcomings, the results from this chapter suggest the CK1s are novel regulators of the *Drosophila* tumour suppressor Ex, and will be discussed in more detail in '8.1 - The Regulation of Ex Stabilty by Phosphorylation and Deubiquitylation'.

Chapter 6 - Results 4 – The Reversibility of Expanded Degradation

Crb regulates Ex by stimulating its phosphorylation, ubiquitylation and degradation through the proteasome. However, phosphorylation and ubiquitylation are both reversible post-translational protein modifications. The subsequent chapter will deal with the identification of a potential DUB, that can stabilise Ex protein thus reversing the action of the Ex kinase, and E3-ligase stimulating Ex degradation upon Crb-mediated stimulus.

6.1. **Usp2 – A Novel Regulator of Expanded Stability**

The *Drosophila* DUB CG14619 or Ubiquitin Specific Protease 2 (Usp2) has a high level of homology with the mammalian Usp2. However, Usp2 also has a low level of homology with the mammalian Ubiquitin Specific Protease 37 (Usp37), which in mammals can interact with the SCF components β-TrCP1 and 2, SKP1 and CUL1, and is itself targeted for SCF-mediated ubiquitylation and degradation (Burrows et al., 2012). As Ex stability is regulated by the $Slmb^{SCF}$ complex, the ability of *Drosophila* Usp2 as a potential regulator of Ex stability was assessed. Initial experiments were performed by my PhD supervisor, Paulo Ribeiro, these data being included in the appendix to this thesis.

To this end, Usp2 isoform A overexpression was analysed in S2 cells in combination with Crb^{FL}, which stimulates Ex phosphorylation and degradation. Interestingly, Usp2 overexpression robustly stabilises Ex^{1-468} protein, despite Crb^{FL} expression (Figure 9-1A). Moreover, Usp2 overexpression does not inhibit the ability of Crb^{FL} to induce Ex^{1-468} phosphorylation, seen clearly as the Crb-induced Ex doublet still forms (Figure 9-1A lane 3). This suggests Usp2 may act downstream of the Crb-dependent Ex kinase, but upstream of Slmb and can therefore stabilise Ex protein even when it has been phosphorylated and targeted for degradation. DUB protease domains are highly conserved and contain amino

acid residues vital to their catalytic function, the USP family containing two conserved cysteine and histidine boxes, which contain the catalytic triad and active site residues (Amerik and Hochstrasser, 2004). Point mutations of these key residues can render DUBs catalytically inactive (Amerik and Hochstrasser, 2004). In order to test whether the ability of Usp2 to stabilise Ex in cells is dependent on the DUB enzyme activity, Usp2 isoform A and C were rendered catalytically inactive by generating point mutations at C540A and C622A respectively, these cysteine residues being key to enzyme activity (Engel et al., 2014). Wild-type Usp2 isoforms A and C are able to stabilise Ex upon Crb^{FL} induced overexpression, with the Ex doublet remaining intact (corresponding to phosphorylated and un-phosphorylated) as described above (Figure 9-1B lanes 3, 6). Compared to Crb^{FL} expression, which completely degraded Ex^{1-468}, catalytic mutants of Usp2 appeared to still be able to stabilise Ex protein (Figure 9-1B lanes 4, 7). This could be explained through Usp2 mutants retaining some DUB activity, Usp2 catalytic mutants promoting the interaction of the endogenous Usp2 with Ex or that Usp2 catalytic mutants interact with Ubi-Ex sterically inhibiting degradation. However, the Usp2 wild-type isoforms appeared much more efficient at stabilising Ex upon Crb^{FL} overexpression than the catalytic mutants suggesting the catalytic DUB domain of Usp2 is important for regulating Ex protein stability (Figure 9-1B lanes 3-4, 6-7).

As a putative regulator of Ex stability, *usp2* should have a role in regulating tissue size. Therefore, adult wing size was assessed with weak *UAS-usp2*$^{(III)}$ overexpression (construct located on the third chromosome) and RNAi-mediated *UAS-usp2* knockdown. This was also carried out in combination with weak *ex* overexpression to analyse genetic interactions with this gene. In this instance, *nub-Gal4* was used to promote *UAS*-transgene expression in the whole wing pouch (Cifuentes and García-Bellido, 1997). Compared to control wings overexpressing GFP, wings overexpressing *ex* were smaller but maintained correct morphology and patterning as expected (Figure 9-2A-B, K-L). When *usp2* was overexpressed, wings were also significantly smaller than *nub>GFP* control with complete loss of the anterior cross vein (Figure 9-2C, K-L). Moreover, there

was a genetic interaction when *usp2* overexpression was combined with *ex* overexpression, as adult wings were smaller than the *UAS-GFP* control, and the *UAS-usp2$^{(III)}$* or *UAS-ex* alone (Figure 9-2D, K-L). This suggests *usp2* and *ex* can work together in the regulation of adult tissue size. One possible explanation for this is that Usp2 can directly stabilise Ex through its DUB activity, blocking Ex proteasomal degradation and enhancing the ability of Ex to inhibit Yki, similarly to that of Ex^{S453A} (Figure 3-3F, Figure 9-2D, K-L). An alternative possibility is that *usp2* and *ex* regulate growth in parallel, or that *usp2* affects growth through a Hippo-independent mechanism. However, these *in vivo* results combined with the data generated in S2 cells suggest that Usp2 employs a possible Hippo pathway and Ex-specific mechanism of growth regulation. In contrast to *usp2* overexpression data, data obtained by RNAi-mediated depletion of *usp2* does not fit with this proposed model. Three different RNAi lines targeting *usp2* result in mild but significant undergrowth wings compared to the *nub>GFP* control (Figure 9-2E, G, I, K-L). These RNAi lines also appear to interact with *UAS-ex* as the combination of *ex* overexpression and *usp2* depletion results in mildly smaller wings than *UAS-ex* alone (Figure 9-2F, H, J, K-L). These sets of data are difficult to reconcile with one another as they provide the same phenotype with opposite predicted levels of Usp2. As Usp2 likely has many potential substrates, this result does not rule out the possibility that Usp2 regulates Ex. Indeed, the efficiency of the Usp2 RNAi lines needs to be established by Quantitative Real Time-PCR (qRT-PCR), or through combining Usp2 overexpression and knockdown in the same tissue to test whether the overexpression phenotypes can be rescued.

In addition to analysing adult wing phenotypes, analysis of Ex levels using the *ubi-ex$^{1-468}$::GFP* reporter in wing imaginal discs was also carried out using two *UAS-usp2* overexpression lines obtained from Marie-Odile Fauvarque (Institut de Biosciences et Biotechnologies de Grenoble) (Engel et al., 2014). These two UAS lines present dramatically different phenotypes, which is presumably the result of varying degrees of *usp2* overexpression, perhaps due to their different genomic insertion sites, resulting in a dramatic affect on expression levels (Figure 6-1). Overexpression of the stronger *usp2* transgene *(usp2$^{(II)}$)* under the control of *hh-*

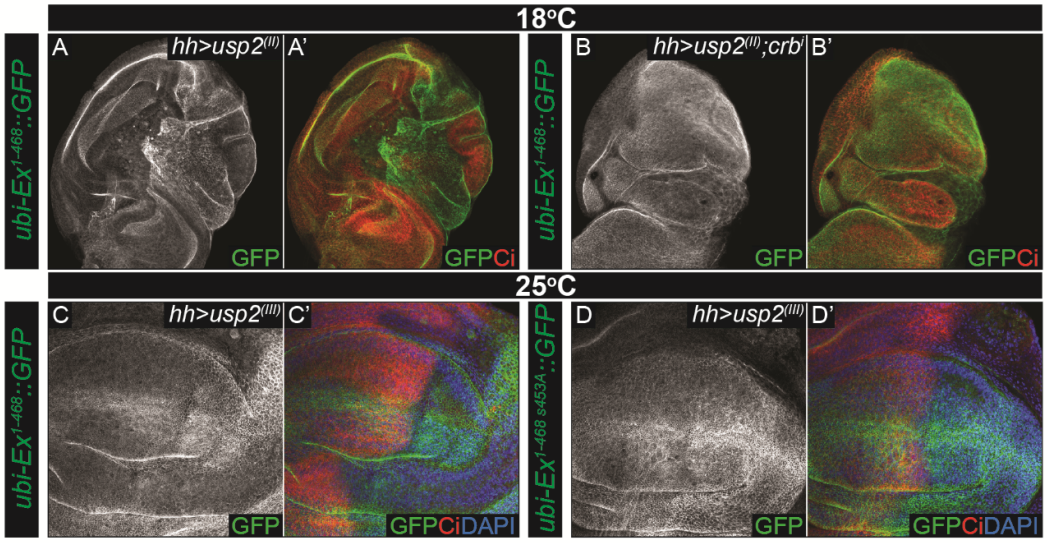

Figure 6-1 Effect of Usp2 on Ex stability *in vivo*

Confocal micrographs of third instar larvae wing imaginal discs expressing *ubi-ex$^{1-468}$::GFP* (A-C') or *ubi-ex$^{1-468\ S453A}$::GFP* (D-D'). Single channel images show GFP staining in maximum intensity projection of the apical domain. Nuclei are marked by DAPI staining (blue in C-D) and the posterior compartment expressing *hh-Gal4* is marked by the absence of Ci staining (red in A-D'). Experiments whereby expression of *usp2$^{(II)}$* (A) or *usp2$^{(II)}$; crb^{i} (B)* was induced by *hh-Gal4* at 18°C resulted in a severe disruption of tissue organisation and morphology (A-B), or the complete absence of the posterior compartment in the case of *usp2* and *crb^{i}* co-expression (B). Expression of *usp2$^{(III)}$* under the control of *hh-Gal4* at 25°C led to an increase in the levels of *ubi-ex$^{1-468}$::GFP* (C) and *ubi-ex$^{1-468\ S453A}$::GFP* (D).

Gal4 results in highly disrupted posterior and anterior compartments even when developing larvae were raised at 18°C making the analysis of the *ubi-ex$^{1-468}$::GFP* reporter difficult, although there is a suggestion that GFP levels are increased when Usp2 is expressed (Figure 6-1A). When this strong transgenic Usp2 line was used in combination with *crb^{i}* overexpression, there was complete exclusion of the posterior compartment (Figure 6-1B).

In wing imaginal discs overexpressing a weaker *usp2* transgene *(usp2$^{(III)}$)*, which survive when developing at 25°C, the *ubi-ex$^{1-468}$::GFP* reporter increases in the

hh-positive posterior compartment, which suggests *usp2* may regulate *ex* post-translationally (Figure 6-1C). Moreover, *usp2* overexpression also resulted in the mutant *ubi-ex*$^{1\text{-}468\ S453A}$*::GFP* reporter levels increasing (Figure 6-1D) which indicates that despite the Ex^{S453A} mutation being highly effective at stabilising Ex, this mutant version of Ex can still be degraded, alluding to additional regulatory sites in Ex, beyond that of S453. Alternatively, this result could imply that Usp2 regulates basal levels of Crb-mediated Ex degradation if Crb regulates Ex beyond the S453 residue alone. One limitation of the experiments carried out using the weak *usp2*$^{(III)}$ overexpression construct is that due to experimental genetic limitations, this line cannot easily be tested with *UAS-crb*^{i} overexpression, and so the ability of Usp2 to regulate Crb-mediated regulation of Ex specifically has not been assessed yet.

As *usp2* overexpression potentially regulates growth (Figure 9-2) by stabilising Ex (Figure 9-1, Figure 6-1), it would be expected that *usp2* would also control the activity of Yki. Therefore, the *ex-lacZ* enhancer trap was used as a readout of Yki activity in combination with *usp2* overexpression (Boedigheimer and Laughon, 1993). As Yki regulates *ex* expression, activity of Yki can be inferred from analysing the activity of this promoter through β-Gal staining. Driving strong *usp2*$^{(II)}$ expression using *ap-Gal4*, which drives *UAS-transgene* expression in the dorsal compartment of the wing disc (Cohen et al., 1992; Rincon-Limas et al., 1999), or weak *usp2*$^{(III)}$ expression by *hh-Ga4* resulted in severely disrupted wing disc morphology associated with cell death as judged by pyknotic nuclei, and it was difficult to assess β-Gal staining (Figure 6-2A-D'). As an alternative *ptc-Gal4* was used, which drives expression along the anterior-posterior compartment boundary (Brand and Perrimon, 1993; Phillips et al., 1990). Staining of β-Gal, the translated product of the *lacZ* gene was first analysed in control wings overexpressing either *GFP* or *hpo*^{IR} under the control of *ptc*. As expected, RNA-mediated depletion of *hpo* resulted in an increase in β-Gal staining, as *hpo* depletion results in de-repressed Yki, as well as an expansion of the GFP-positive area, corresponding to an increase in proliferation and apoptosis-resistance (Figure 6-2E-F). In discs overexpressing the weak *usp2*$^{(III)}$ transgene, there

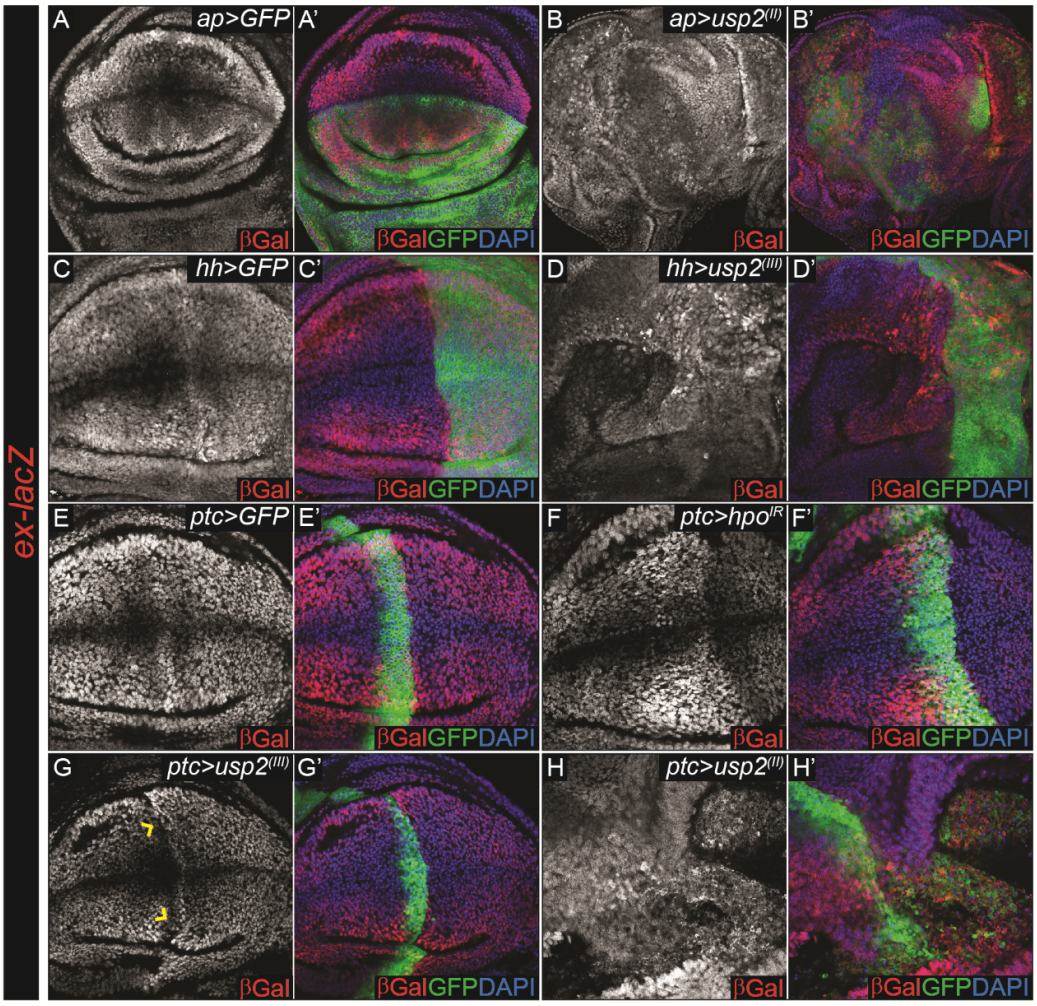

Figure 6-2 Usp2 overexpression regulates *ex-lacZ in vivo*

Confocal micrographs of third instar larvae wing imaginal discs expressing an *ex-lacZ* enhancer trap (A-H'). Single channel images show β-Gal staining in a planar section in line with the nuclei of the wing pouch. Nuclei are marked by DAPI staining (blue). The dorsal compartment expressing *ap-Gal4* is marked by expression of GFP (A', B'), and the posterior compartment expressing *hh-Gal4* is marked by expression of GFP (C', D'). The anterior-posterior compartment boundary where *ptc-Gal4* is expressed is marked by the presence of GFP (E'-H'). *ap-Gal4* (A), *hh-Gal4* (C) or *ptc-Gal4* (E)-mediated expression of *GFP* as a negative control had no overt effect on the levels of β-Gal. Expression of *ptc>hpo^{IR}* was used as a positive control and resulted in an increase in the levels of β-Gal (F). Expression of *ptc>usp2$^{(III)}$* decreased levels of β-Gal (G). Expression of the weak Usp2 overexpression construct *usp2$^{(III)}$* by *hh-Gal4* (D) or the stronger Usp2 overexpression construct *usp2$^{(II)}$* by *ap-Gal4* (B) or *ptc-Gal4* (H) severely disrupted tissue morphology and induced apoptosis, thereby making it difficult to assess its effect on β-Gal levels representative of *ex* expression.

appeared to be a slight decrease in β-Gal staining within the GFP-positive expression domain, suggesting Yki-activity was repressed (Figure 6-2G – see yellow arrows). Moreover, the size of the GFP-positive domain was reduced, suggesting limited proliferative potential or enhanced apoptosis (Figure 6-2G), consistent with the adult wing analysis (Figure 9-2). These data support the role of *usp2* as a positive regulator of Ex, as Usp2 overexpression would result in increased Ex levels, and subsequent increased Hpo pathway activity and decreased Yki activity and, therefore, growth inhibition. However, overexpression of the strong *usp2$^{(II)}$* transgene resulted in severely disrupted morphology making β-Gal staining difficult to interpret, as in the case of *ap-Gal4* and *hh-Gal4* driven *usp2* expression (Figure 6-2H). There also appeared to be large areas where there was extensive cell death in discs overexpressing this strong *usp2$^{(II)}$* transgene, judged by the DAPI nuclear staining and the appearance of pyknotic nuclei, which would conform to the model of increased Ex levels, and the promotion of apoptosis (Figure 6-2H'). Mammalian USP2 has been shown to regulate apoptosis through several mechanisms (Mahul-Mellier et al., 2012a; Mahul-Mellier et al., 2012b; Oh et al., 2011), so whether the cell death observed is the result of excessive Ex or due to other factors remains to be seen, and more needs to be done to confirm these observations, such as analysing additional Yki-target genes, or through epistatic analysis with other Hippo pathway members.

6.2. **Concluding Remarks**

Although the data obtained in this section are somewhat preliminary, there is evidence to suggest *usp2* could regulate growth through the modulation of Ex stability, which will be discussed more thoroughly in '8.1 - The Regulation of Ex Stabilty by Phosphorylation and Deubiquitylation'. However, discrepancies between depletion and overexpression of *usp2* need to be reconciled before a definite role of *usp2* in the Hpo pathway is confirmed, analysis of mutant *usp2*, rather than RNAi lines could help this process.

Chapter 7 - Results 5 – A Screen to Identify Ubiquitylating Enzymes Involved in Regulating Tissue Growth

There are approximately forty five putative DUBs that have been identified in *Drosophila* (Zhang et al., 2012), many of these proteins remaining uncharacterised. In order to assess which of these DUBs are important in regulating tissue growth, a library of DUB-RNAi lines, including deSUMOylases and deNEDDylases was expressed in the adult wing using the *nub-Gal4* driver, and the total area of the wing in the different samples was used as the phenotypic readout. All DUB families are represented except the newly identified MINDY family, which has no known orthologues in *Drosophila*. Being interested in the mechanisms that regulate Hippo signalling, and in particular *ex*, these same RNAi lines were used to carry out a modifier screen, with the aim of discovering genetic interactions between DUB depletion and weak overexpression of full-length *ex*, which reduces overall wing size by 40% (Figure 7-1, Figure 7-2, Figure 7-3, Figure 7-4, Table 7-1).

Crosses were carried out in batches, each with a *nub>GFP* and/or a *nub>ex* control. To be able to compare the results obtained from different crosses, rather than using the raw area measured in pixels, results were standardised to the *nub>GFP* control group, for which the average wing size area was set to 100%. Each sample, or group was then calculated as a fraction of this control group, giving the size as a percentage of the mean *nub>GFP* control. These normalised results were then plotted and, for simplicity, the results were organised by DUB family (Figure 7-1, Figure 7-2, Figure 7-3, Figure 7-4). Note that the results for the USP family of DUBs were split into three individual plots as this is the largest DUB family (Figure 7-1). Where possible, the data for an individual *nub>DUB^{IR}* genotype was plotted adjacent to its concordant *nub>ex, DUB^{IR}* genotype to aid analysis, however not all DUBs are represented in both arms of the screen (Figure 7-1, Figure 7-2, Figure 7-3, Figure 7-4, Table 7-1).

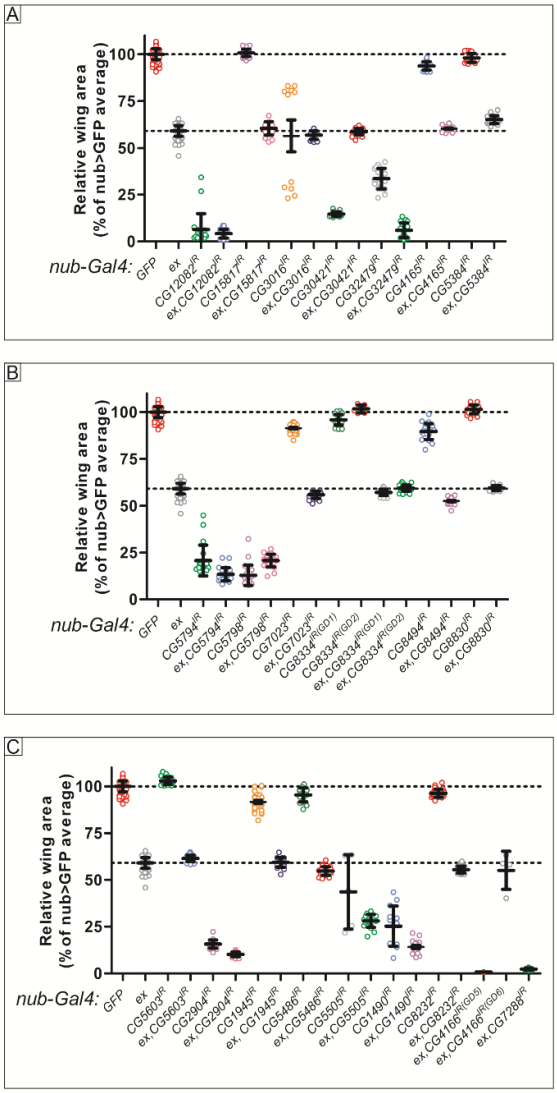

Figure 7-1 Summary of the role of USP family DUBs in tissue growth

Graphs summarising the results of the *in vivo* screen for the role of USP family members in the regulation of tissue growth. Shown are the results obtained with RNAi-mediated depletion of DUBs using *nub-Gal4* or *nub-Gal4, UAS-ex* as drivers. Results of the USP screen are shown in three graphs due to the large number of members of this DUB family. Quantification of wing area was performed using ImageJ according to the protocol detailed in the Materials and Methods and wing area was normalised to control wings expressing GFP under the control of *nub-Gal4* (A-C). Individual data points are shown as well as the average ± SD of each of the genotypes analysed. Dashed line at 100% represents the mean of *nub-Gal4, UAS-GFP* controls and the dashed line at 60% represents the average relative size of *nub-Gal4, UAS-ex* controls. Groups were compared by a one-way ANOVA with a Turkey's range post hoc test. See Table 7-1 for details and statistical analysis.

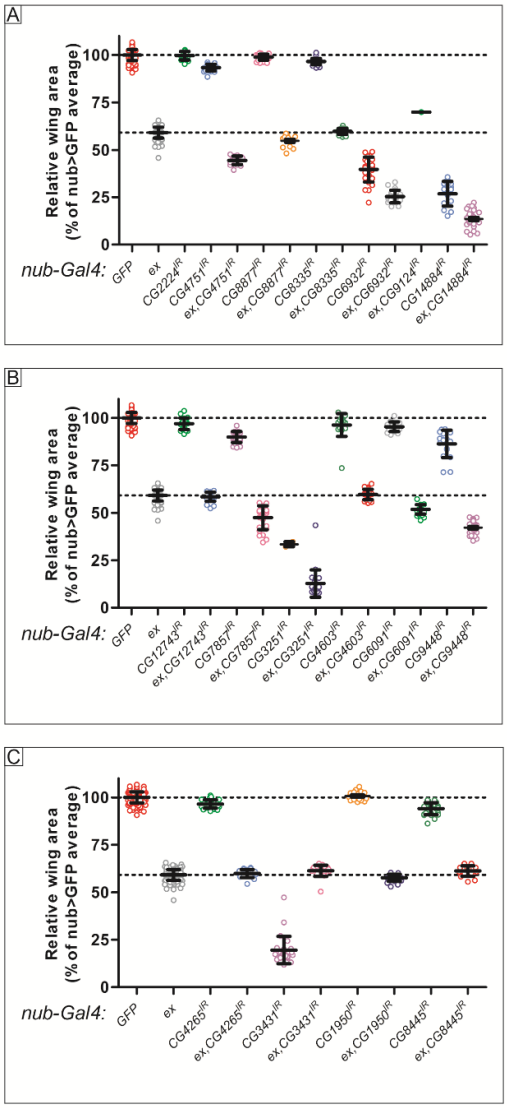

Figure 7-2 Summary of the role of JAMM, OTU and UCH family DUBs in tissue growth

Graphs summarising the results of the *in vivo* screen for the role of JAMM (A), OTU (B) or UCH (C) DUB family members in the regulation of tissue growth. Shown are the results obtained with RNAi-mediated depletion of DUBs using *nub-Gal4* or *nub-Gal4, UAS-ex* as drivers. Quantification of wing area was performed using ImageJ according to the protocol detailed in the Materials and Methods and wing area was normalised to control wings expressing GFP under the control of *nub-Gal4* (A-C). Individual data points are shown as well as the average ± SD of each of the genotypes analysed. Dashed line at 100% represents the mean of *nub-Gal4, UAS-GFP* controls and the dashed line at 60% represents the average relative size of *nub-Gal4, UAS-ex* controls. Groups were compared by a one-way ANOVA with a Turkey's range post hoc test. See Table 7-1 for details and statistical analysis.

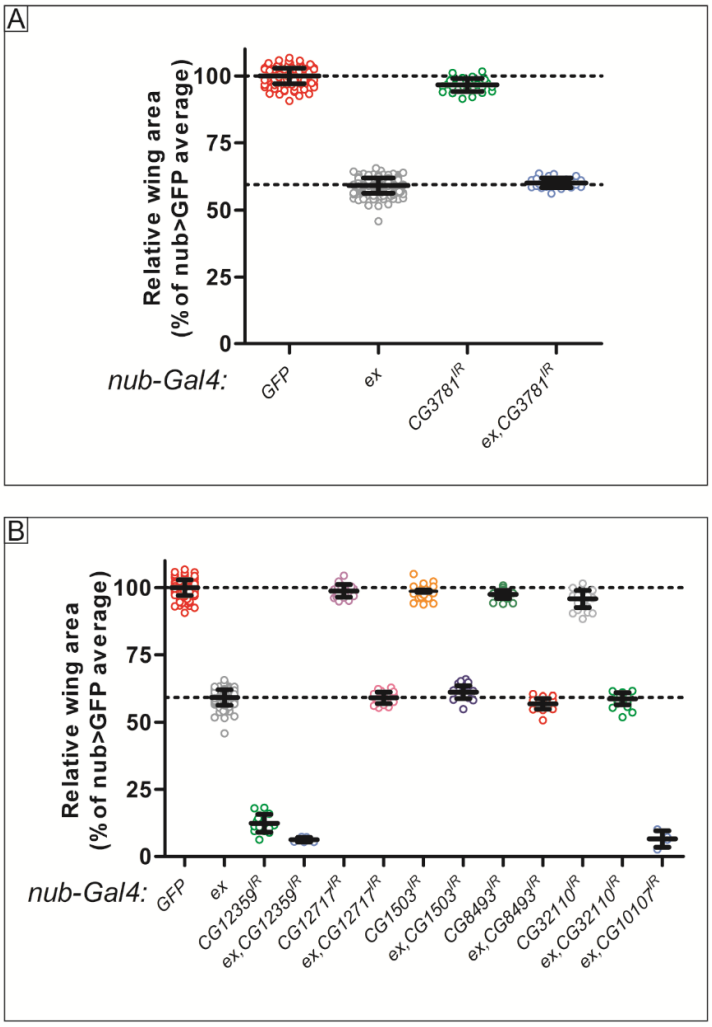

Figure 7-3 Summary of the role of the Josephine DUB family and ULPs in tissue growth

Graphs summarising the results of the *in vivo* screen for the role of the Josephine DUB family (A) or the role of different ULPs (B) in the regulation of tissue growth. Shown are the results obtained with RNAi-mediated depletion of DUBs using *nub-Gal4* or *nub-Gal4, UAS-ex* as drivers. Quantification of wing area was performed using ImageJ according to the protocol detailed in the Materials and Methods and wing area was normalised to control wings expressing GFP under the control of *nub-Gal4* (A-C). Individual data points are shown as well as the average ± SD of each of the genotypes analysed. Dashed line at 100% represents the mean of *nub-Gal4, UAS-GFP* controls and the dashed line at 60% represents the average relative size of *nub-Gal4, UAS-ex* controls. Groups were compared by a one-way ANOVA with a Turkey's range post hoc test. See Table 7-1 for details and statistical analysis.

	Gene	RNAi Line	nub>GFP, RNAi			nub>ex, RNAi				
			n =	% nub>GFP average	Significance vs nub>GFP ctrl	n =	% nub>GFP average	Significance vs nub>GFP ctrl	% nub>ex average	Significance vs nub>ex ctrl
Controls	GFP	n/a	144	100	n/a	n/a	n/a	n/a	n/a	n/a
	ex	n/a	n/a	n/a	n/a	185	59.2	***	100	n/a
USP Family	CG12082	NIG 12082-R2	20	6.3	***	29	4.2	***	7.0	***
	CG1490	VDRC 110324 KK	13	25.3	***	19	14.2	***	23.9	***
	CG14619	VDRC 104382 KK	34	96.7	***	19	55.7	***	94.1	***
	CG14619	NIG-FLY 14619R-1	n/a	n/a	n/a	20	47.8	***	80.8	***
	CG14619	NIG-FLY 14619R-3	n/a	n/a	n/a	13	46.1	***	77.9	***
	CG15817	VDRC 100992 KK	34	100.7	ns	18	60.5	***	102.2	ns
	CG1945	VDRC 107716 KK	31	91.8	***	20	59.5	***	100.6	ns
	CG2904	VDRC 106671 KK	24	15.7	***	20	10.2	***	17.2	***
	CG3016	VDRC 7090 GD	11	56.5	***	26	56.9	***	96.2	ns
	CG30421	VDRC 103553 KK	22	14.7	***	25	58.8	***	99.3	ns
	CG32479	VDRC 37859 GD	20	33.5	***	21	5.9	***	10.0	***
	CG4165	VDRC 110286 KK	24	93.8	***	21	60.4	***	102.0	ns
	CG4166	VDRC 45775 GD (GD5)	n/a	n/a	n/a	1	0.8	n/a	1.3	n/a
	CG4166	VDRC 45776 GD (GD6)	n/a	n/a	n/a	4	55.2	***	93.2	ns
	CG5384	VDRC 110227 KK	20	98.0	ns	22	65.2	***	110.1	***
	CG5486	VDRC 103743 KK	20	95.5	ns	26	54.8	***	92.6	***
	CG5505	VDRC 105989 KK	5	43.6	***	19	28.0	***	47.4	***
	CG5603	VDRC 101414 KK	26	102.9	ns	25	61.6	***	104.2	ns
	CG5794	VDRC 106192 KK	20	20.8	***	26	13.5	***	22.7	***
	CG5798	VDRC 107623 KK	23	12.9	***	23	20.8	***	35.1	***
	CG7023	VDRC 100586 KK	34	91.4	***	23	55.9	***	94.4	***
	CG7288	n/a	n/a	n/a	n/a	11	2.3	***	3.9	***
	CG8232	NIG 8232R-1	26	96.4	ns	26	55.5	***	93.8	***
	CG8334	VDRC 18981 GD (GD1)	24	95.9	ns	25	57.2	***	96.6	ns
	CG8334	VDRC 18982 GD (GD2)	6	101.7	ns	26	59.4	***	100.4	ns
	CG8494	VDRC 42609 GD	21	89.7	***	22	52.6	***	88.9	***
	CG8830	VDRC 28960 GD	21	101.4	ns	20	59.5	***	100.6	ns
UCH Family	CG1950	NIG 1950R-1	16	100.7	ns	24	57.6	***	97.4	ns
	CG3431	VDRC 103481 KK	26	19.6	***	22	61.4	***	103.7	ns
	CG4265	VDRC 103614 KK	27	96.5	ns	21	59.9	***	101.3	ns
	CG8445	VDRC 107757 KK	28	94.1	***	19	61.2	***	103.5	ns
JAMM Family	CG14884	NIG 14884-R1	16	26.8	***	27	13.5	***	22.8	***
	CG18174	n/a	n/a	n/a	n/a	n/a	n/a	n/a	n/a	n/a
	CG2224	VRDC 108622 KK	16	99.7	ns	n/a	n/a	n/a	n/a	n/a
	CG3416	n/a	n/a	n/a	n/a	n/a	n/a	n/a	n/a	n/a
	CG4673	n/a	n/a	n/a	n/a	n/a	n/a	n/a	n/a	n/a
	CG4751	VDRC 45530 GD	26	93.4	***	22	44.5	***	75.2	***
	CG6932	105385 KK	29	39.6	***	21	25.3	***	42.8	***
	CG8335	VDRC 108169 KK	32	96.5	ns	24	59.8	***	101.1	ns
	CG8877	DRC 18565 GD	26	98.9	ns	14	54.9	***	92.7	***
	CG9124	VDRC 36087 GD	n/a	n/a	n/a	1	70.0	n/a	118.3	n/a
	CG9769	n/a	n/a	n/a	n/a	n/a	n/a	n/a	n/a	n/a
OTU Family	CG12743	VDRC 108845 KK	24	97.0	ns	24	58.5		98.9	ns
	CG3251	VDRC 100532 KK	2	33.5	***	24	12.8	***	21.5	***
	CG4603	VDRC 21893 GD	19	96.3	ns	29	59.7	***	100.9	ns
	CG4968	n/a	n/a	n/a	n/a	n/a	n/a	n/a	n/a	n/a
	CG6091	VDRC 109912 KK	19	95.4	ns	24	51.8	***	87.6	***
	CG7857	VDRC 105469 KK	25	90.0	***	25	47.5	***	80.2	***
	CG9448	VDRC 24030 GD	17	86.3	***	31	42.2	***	71.3	***
Jos Family	CG3781	108379 KK	30	96.6	ns	28	60.2	***	101.7	ns
ULP proteases	CG10107	VDRC 103524 KK	n/a	n/a	n/a	4	6.5	***	11.0	***
	CG11023	n/a	n/a	n/a	n/a	n/a	n/a	n/a	n/a	n/a
	CG12359	VDRC 106625 KK	16	12.4	***	7	6.3	***	10.6	***
	CG12717	VDRC 106239 KK	23	98.8	ns	23	59.0	***	99.8	ns
	CG1503	110486 KK	33	98.6	ns	27	61.2	***	103.3	ns
	CG32110	VDRC 107634 KK	31	95.8	*	33	58.7	***	99.2	ns
	CG41423	n/a	n/a	n/a	n/a	n/a	n/a	n/a	n/a	n/a
	CG8493	VDRC 100591 KK	30	97.5	ns	25	56.8	***	96.0	ns
MCPIP Family	CG10889	NIG 10889R-2	15	78.0	***	23	3.0	***	5.1	***

DUBS Tested alone: 44/55
% DUBS Tested alone: 80
# DUBS Tested with ex: 47/55
% DUBS Tested with ex: 85.5

N.B. Significance Determined by a One Way ANOVA With A Turkey's Range Post Hoc Test in GraphPad Prism
n/a - not/applicable
ns - not significant
* P value <0.05
*** P value <0.0001

Table 7-1 Summary of *in vivo* wing area DUB RNAi
(Continued from previous page) A table to summarise the entire dataset obtained during the *in vivo* DUB RNAi screen to identify DUB genes that regulate tissue growth. Stock number (column 3) corresponds to the code number attributed to RNAi lines by the RNAi stock repositories. KK and GD lines were obtained from the Vienna *Drosophila* RNAi Centre (VDRC, Austria) and NIG RNAi lines were sourced from the National Institute of Genetics (NIG-Fly, Japan). Gene names and CG numbers are according to Flybase. Wing area of individual genotypes was normalised to the average wing area of *nub-Gal4, UAS-GFP* controls (columns 5, 8) and to the average wing area of *nub-Gal4, UAS-ex* controls (column 10). Analysis of the statistical significance of the screen results was performed using one-way ANOVA with a Turkey's range post hoc test (columns 6, 9, 11).

When compared to *nub>GFP* control wings, RNAi-mediated depletion of many DUBs caused a reduction in tissue size, whereas no genotype resulted in an increase in wing size (Figure 7-1, Figure 7-2, Figure 7-3, Figure 7-4, Table 7-1). Within the population of DUBs that significantly perturb tissue growth, there seems to be no trend within a particular DUB family. The DUB showing the most drastic disruption of wing growth is CG12082. RNAi-mediated depletion of *CG12082* resulted in wings that were 6.3% the size of control *nub>GFP* wings (Figure 7-1 A). Overexpression of a weak *ex* construct causes a 40% reduction in wing size, with the wings appearing narrower that the *nub>GFP* controls (Figure 7-1, Figure 7-2, Figure 7-3, Figure 7-4, Table 7-1). When DUB-RNAi lines were expressed in combination with *ex* overexpression, the majority of lines tested phenocopied overexpression of *ex* alone and therefore did not genetically interact with *ex* (Figure 7-1, Figure 7-2, Figure 7-3, Figure 7-4, Table 7-1).

As *nub>ex* alone causes a reduction in wing area, in addition to comparing the results to the *nub>GFP* control group, *nub>ex, DUB^{IR}* were also compared to a standardised *nub>ex* control group, in order to present results as a percentage of the *nub>ex* control group, which for this analysis was set to 100%. Depletion of DUBs with a value statistically indistinct from 100 had no effect on the reduction of size caused by *ex*-overexpression alone. However, many genotypes were significantly smaller than the *nub>ex* control (Table 7-1), and therefore genetically interact with this tumour suppressor gene. To investigate the functional relevance

of the putative genetic interaction between the DUBs and *ex,* only the DUBs for which *nub>DUB^{IR}* and *nub>ex, DUB^{IR}* data was collected were taken forward for further analysis. To visualise how these results relate to each other more readily, the normalised *nub>GFP* control values for each *nub>DUB^{IR}/ nub>ex, DUB^{IR}* pair were sorted in descending order, in relation to the *nub>DUB^{IR}* result, and plotted on the same axis (Figure 7-5A). These genotypes broadly followed the same trend, whereby DUBs that did not dramatically influence tissue size, did not influence the ability of *ex* overexpression nor reduced tissue size. Hence, most *nub>DUB^{IR}* genotypes cluster close to the 100% value, i.e. the do not dramatically influence growth, with their concomitant *nub>ex, DUB^{IR}* value clustering around 60% wing size, comparable to the *nub>ex* alone control (Figure 7-5A). In cases where the depletion of DUBs resulted in a decrease in tissue size (i.e. relative wing values significantly less than 100%), concurrent overexpression of *ex* generally resulted in enhanced reduction in tissue size, with the reduction in size remaining at around 40%, mirroring the effect of the *DUB^{IR}* alone and suggesting no genetic interaction (Figure 7-5A). In order to dissect the genetic interaction between each DUB and *ex*, the *nub>DUB^{IR} /nub>ex, DUB^{IR}* pairs were directly compared by calculating the percentage difference in wing size between them, and comparing this value to the percentage difference in size between the *nub>GFP* and *nub>ex* controls, which is 40% (Figure 7-5B). To obtain these values, the standardised *nub>ex, DUB^{IR}* value was subtracted from the *nub>DUB^{IR}* alone standardised value. These results were then sorted into descending order and plotted, with the difference between the controls being marked by a gridline at 40% (Figure 7-5B). Most of the values represented were in close proximity to the 40% mark, corroborating what was discussed earlier and that in general, *DUB^{IR}* depletion did not enhance the tissue undergrowth caused by *ex*-overexpression. In cases where the value for an individual DUB is between 40% and 0%, the difference between the *nub>DUB^{IR}* and the *nub>ex, DUB^{IR}* is less than between the controls, suggesting the *UAS-ex* phenotype has been suppressed. Values of approximately 0% are observed when there is no different between the *nub>DUB^{IR}* and the *nub>ex, DUB^{IR}*, *UAS-ex* having no influence over the *UAS- DUB^{IR}* phenotype (Figure 7-5B).

Strikingly, upon analysis of these figures (Figure 7-5), three DUBs stand out as genetically interacting with *ex*. Depletion of either *CG3431* or *CG30421* caused a dramatic and significant decrease in tissue size compared to the *nub>GFP* control, an 80% and 85% size reduction respectively (Table 7-1). However, in combination with overexpression of *ex*, wing size is reduced by only 39% for CG3431, or 41% for CG30421 (Table 7-1), with the wings being much larger

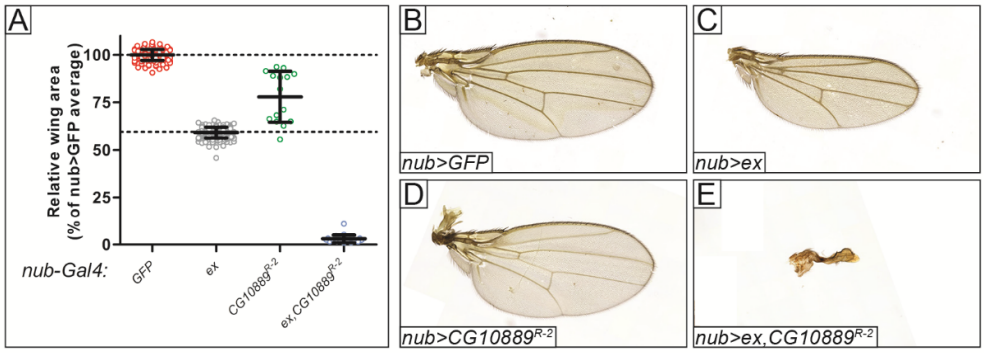

Figure 7-4 DUB screen identifies the MCPIP family member CG10889 as a regulator of tissue growth *in vivo*

Graph summarising the results of the *in vivo* screen for the role of the MCPIP family (A) in the regulation of tissue growth. Shown are the results obtained with RNAi-mediated depletion of *CG10889* using *nub-Gal4* or *nub-Gal4, UAS-ex* as drivers. Quantification of wing area was performed using ImageJ according to the protocol detailed in the Materials and Methods and wing area was normalised to control wings expressing GFP under the control of *nub-Gal4* (A). Individual data points are shown as well as the average ± SD of each of the genotypes analysed. Dashed line at 100% represents the mean of *nub-Gal4, UAS-GFP* controls and the dashed line at 60% represents the average relative size of *nub-Gal4, UAS-ex* controls. All groups showed statistical difference as determined by a one-way ANOVA analysis with a Dunnett's multiple comparison post hoc test (*** = P < 0.0001). See Table 7-1 for details and statistical analysis (A). Adult wings expressing different transgenes under the control of *nub-Gal4*. Shown are the adult wings of flies expressing a GFP transgene as control (B), *ex* (C) $CG10889^{R-2}$ (D) and $ex,CG10889^{R-2}$ (E).

than with expression of DUB RNAi alone. This manifested itself as a highly negative value when comparing the percentage difference between the *nub>*DUB^{IR} and the *nub>ex,* DUB^{IR}, purple circles highlighting these data points (Figure 7-5 - highlighted by purple circles). Raw data for these DUBs (i.e. adult wing areas) can be seen in (Figure 7-1A, Figure 7-2C). As *ex* overexpression

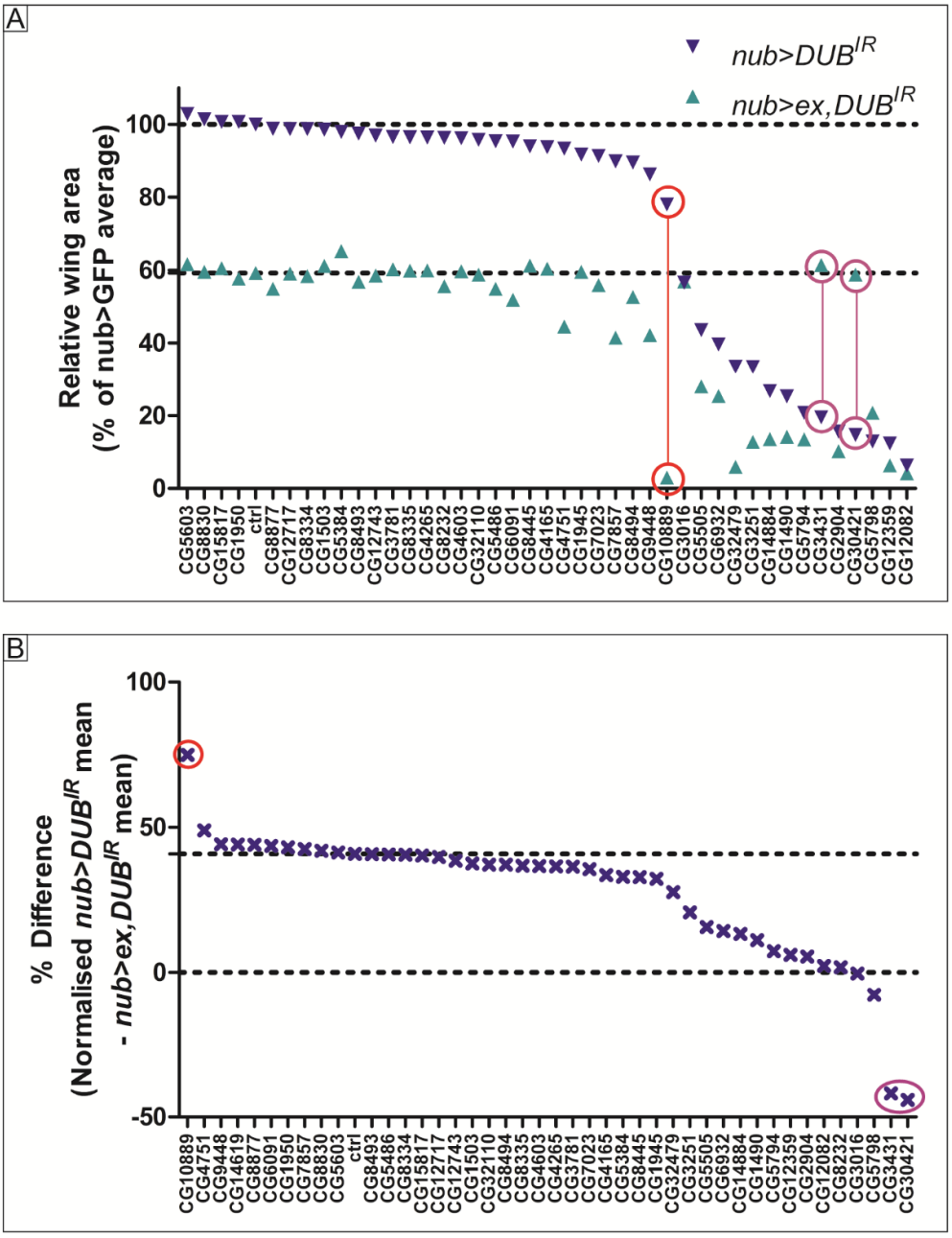

Figure 7-5 Compilation of DUB screen results

Pairwise comparison of the relative wing areas quantified in the *in vivo* RNAi screen. Blue inverted triangles represent data obtained with DUB depletion using *nub-Gal4* as a driver, while the green triangles depict the data obtained when DUBs were depleted in the presence of *UAS-ex* co-expression (*nub-Gal4, UAS-ex*) (A) **(Continued on next page)**.

(Continued from previous page) Wing area was normalised to the average size of control wings expressing *nub-Gal4, UAS-GFP*. Data are organised by descending wing area relative to the *nub-Gal4, UAS-GFP* mean value. Dashed line at 100% represents the average wing size of *nub-Gal4, UAS-GFP* controls, while the dashed line at 60% represents the average relative wing size of wings expressing *UAS-ex* under the control of the *nub-Gal4* driver. Pairwise percentage difference between the mean relative wing size of *nub-Gal4, UAS-DUB^{IR}* samples and the mean relative wing size of *nub-Gal4, UAS-ex, UAS-DUB^{IR}* (B). Dashed line at 40% represents the difference between the *nub-Gal4 and nub-Gal4, UAS-ex* values obtained in control genotypes (*UAS-GFP*). Dashed line at 0% represents no difference between the *nub-Gal4 and nub-Gal4, UAS-ex* values (B). Red and purple circles/lines highlight the genes that are further discussed in the main body of the thesis (*CG10889*, *CG3431* and *CG30421*) (A-B). See Table 7-1 for details and statistical analysis.

alone causes a large reduction in tissue size, it is difficult to explain how depletion of a DUB that causes tissue undergrowth could be rescued by overexpression of *ex*. One possible explanation for this comes with the observation that for both CG3431 and CG30421, the *nub>ex, DUB^{IR}* value is statistically indistinct from the *nub>ex* control (Figure 7-5**,** Table 7-1). This could suggest that there has been an error during phenotypic analysis, and that the *Drosophila* whose wings were analysed did not possess the *DUB^{IR}*, but only the *UAS-ex* construct. This would be a very simple explanation for wings of animals of these genotypes being exactly the same size as *nub>ex* control animals. However, this analysis needs to be repeated in order to confirm this conclusion, as it cannot yet be ruled out that overexpression of *ex* results in modification of key DUB substrates such that expression of *UAS-DUB^{IR}* no longer regulates growth.

The other positive candidate for further analysis based on these parameters is CG10889, which will be discussed further in the subsequent section.

7.1. **CG10889 – A Regulator of Growth and a Novel Yorkie Interacting Protein**

One of the positive candidates form the DUB screen was CG10889, the *Drosophila* orthologue of mammalian ZCH12A/MCPIP1, which is a putative DUB that regulates JNK and NF-κB signalling, but is more commonly thought to be an RNA-interacting protein (Fraile et al., 2012; Liang et al., 2010). Results from the screen showed depletion of *CG10889* caused a modest, but significant 12% reduction in wing size compared to *nub>GFP* (Figure 7-4, Table 7-1). Interestingly, *nub>ex, CG10889^{IR}* dramatically enhanced the effect of either *ex* or *CG10889^{IR}* alone (Figure 7-4, Table 7-1). Of all of the DUBs analysed, CG10889 showed by far the largest enhancement of the *nub>ex* undergrowth phenotype (Figure 7-5), highlighted by a percentage-difference score of 75%, compared to the 40% between the controls (Figure 7-5 - highlighted by red circles). These data suggest that CG10889 and *ex* genetically interact with regards to wing size, which is particularly interesting as a global mass spectrometry study in *Drosophila* identified CG10889 as a putative interaction partner of the Hippo pathway effector Yki (Guruharsha et al., 2011). In order to confirm preliminary data demonstrating RNAi-mediated knockdown of CG10889 reduced wing size without disrupting patterning, depletion of *CG10889* was repeated using *nub>Gal4*, and *MS1096>Gal4*, a whole wing driver (Capdevila and Guerrero, 1994). Consistently, depletion of *CG10889* resulted in a decrease in total wing area (Figure 7-6B, F, G-H). As a potential genetic interaction between *ex* and CG10889 was identified genetic interaction with the key Hippo pathway kinase Wts was also assessed. *CG10889* depletion was able to suppress the overgrowth induced by RNAi-mediated depletion of *wts* (Figure 7-6C-D), suggesting that *CG10889* may positively interact with Yki, alluding to a potential involvement in Hippo signalling.

Biochemically, the interaction between Yki and CG10889 was confirmed through co-immunoprecipitation experiments where FLAG-tagged Yki was purified from *Drosophila* S2 cells (Figure 7-7A). Interestingly, this interaction was enhanced by

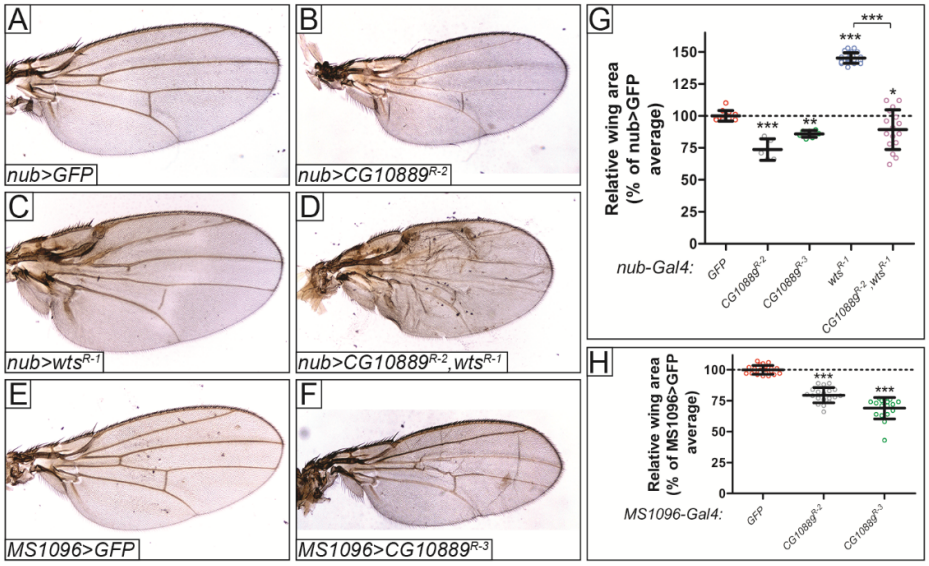

Figure 7-6 CG10889 regulates tissue growth *in vivo*

Adult wings expressing GFP under the control of *nub-Gal4* (A) were used as controls for the expression of *CG10889*$^{R-2}$ (B), *wts*$^{R-1}$ (C), or *CG10889*$^{R-2}$*,wts*$^{R-1}$ (D). Adult wings expressing GFP under the control of *MS1096-Gal4* (E) were used as controls for the expression of *CG10889*$^{R-3}$ (F). Note that the results obtained with knockdown of *CG10889* using *nub-Gal4* as a driver were obtained independently of the main DUB *in vivo* screen. Quantification of wing area was carried out in ImageJ and wing area was normalised to the average wing size of controls expressing GFP under the control of *nub-Gal4*. Individual data points are shown as well as the average ± SD of each of the genotypes analysed. The statistical significance of the differences in the relative wing area size between the indicated genotypes was assessed by a one-way ANOVA with a Dunnett's multiple comparison post hoc test (* = P < 0.05, ** = P < 0.001 and *** = P < 0.0001) (G). Comparison between *nub-Gal4, UAS-wts*$^{R-1}$ and *nub-Gal4, UAS-CG10889*$^{R-}$*, UAS-wts*$^{R-1}$ was obtained by performing a Student's T-test analysis (G). Quantification of results obtained using *MS1096-Gal4* as driver. Wing area was normalised to the average wing size of controls expressing GFP under the control of *MS1096-Gal4*. The statistical significance of the differences in the relative wing area size between the indicated genotypes was determined by a one-way ANOVA with a Dunnett's multiple comparison post hoc test (*** = P < 0.0001) (H).

mutations in conserved amino acid residues of the putative DUB enzymatic domain of CG10889 (D138N or C154A) (Liang et al., 2010) (Figure 7-7A lanes 3-5). This suggests that enzymatically inactive CG10889 interacts more robustly with Yki, potentially through a more stable interaction with the Yki Ubi chain,

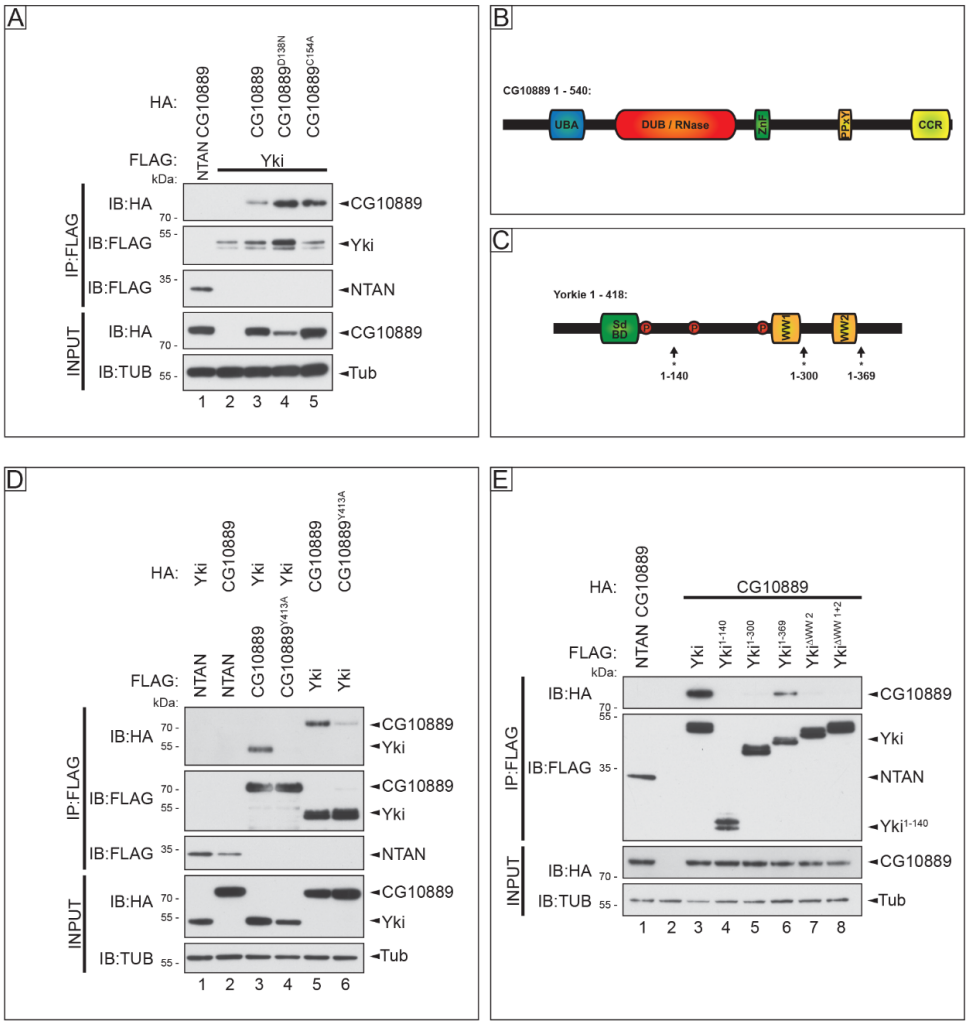

Figure 7-7 CG10889 interacts with Yki in S2 cells

Immunoblot of S2 cell lysates after co-immunoprecipitation of FLAG-tagged NTAN as a negative binding control (A - lane 1) or FLAG-tagged Yki (A – lanes 2-5). HA-tagged CG10889, $CG10889^{D138N}$ and $CG10889^{C154A}$ associated with Yki (A – lanes 3-5). Schematic representation of CG10889 (B) and Yki (C) highlighting their respective domain architecture. The different domains of CG10889 are UBA (Ubiquitin Associated Domain), ZnF (Zinc Finger), CCR (C-Terminal Conserved Region) and their nomenclature is based on *Liang et al.* (Liang et al., 2010) (B). For Yki, the different protein domains are Sd BD (Sd Binding Domain) and WW domains. Circled Ps represent Wts phosphorylation sites S111, S168 and S250 (Oh and Irvine, 2009), while the asterisks depict the termini of Yki truncations used in (E). Yki domain architecture nomenclature was based on *Wu et al. (Wu et al., 2008)* (C). S2 cell lysates after co-immunoprecipitation of FLAG-tagged NTAN as a negative binding control (D – lanes 1 and 2), FLAG-tagged CG10889 (D – lane 3), PPxY point mutant $CG10889^{Y413A}$ (D – lane 4) or FLAG-tagged Yki (D – lanes 5 and 6). **(Continued on next page)**.

(Continued from previous page) HA-tagged Yki associated with FLAG-tagged CG10889 but not CG10889^{Y413A} (compare D – lanes 3 and 4). HA-tagged CG10889 but not CG10889^{Y413A} interacted with FLAG-tagged Yki (D – compare lanes 5 and 6). S2 cell lysates expressing HA-tagged CG10889 after co-immunoprecipitation of FLAG-tagged NTAN as a negative binding control (E – lane 1), FLAG-tagged Yki (E – lane 3), Yki$^{1-140}$ (E – lane 4), Yki$^{1-300}$ (E – lane 5), Yki$^{1-369}$ (E – lane 6), Yki$^{\Delta WW2}$ containing a point mutation in the WW2 domain (E – lane 7), or Yki$^{\Delta WW1+2}$ containing point mutations in WW1 and WW2 (E – lane 8). HA-tagged CG10889 only bound FLAG-tagged Yki constructs with an intact WW2 domain (E – lanes 3, 6). S2 cell lysates and purified immunoprecipitates were analysed with the indicated antibodies and Tub was used as a loading control (A, D and E).

which CG10889 can no longer cleave. Many of the Hippo pathway interactions are governed by WW-PPxY domain interactions, and Yki contains two WWdomains (Figure 7-7C) (Genevet and Tapon, 2011). Analysis of the protein sequence of CG10889 revealed a C-terminal PPxY motif, in addition to ubiquitin binding domains, an RNase domain, a zinc finger and a C-terminal conserved region (Figure 7-7B) (Liang et al., 2010). A cDNA construct containing a point mutation in the CG10889 PPxY motif, Y413A, was unable to interact with Yki through reciprocal co-IP experiments in S2 cells (Figure 7-7D), suggesting that the PPxY motif in CG10889 is essential for this interaction. To further characterise this binding, co-IP experiments were carried out using Yki truncations or mutations that remove one or both of its WW domains. Deletion of both WW domains, or mutation of the C-terminal WW domain (WW2) completely abrogated binding between CG10889 and Yki (Figure 7-7E). Together, these data suggest that the interaction between Yki and CG10889 is dependent on the PPxY motif of CG10889, and the WW2 domain of Yki.

Due to the interaction with Yki, and the fact that depletion of CG10889 caused a decrease in wing area, the ability of CG10889 to modulate the expression of the Yki-target *ex* was assessed, using the *ex-lacZ* enhancer trap as an *in vivo* readout. Using the *hh-Gal4* driver, RNAi-mediated depletion of *CG10889* showed no obvious reduction in the expression of β-Gal, as would be expected if the undergrowth observed were the result of Yki inhibition (Figure 7-8A-B). In contrast, there even appeared to be a slight elevation in β-Gal staining upon *CG10889* depletion (Figure 7-8C-D). Other Yki-transcriptional targets must be

assessed to assess the potential for CG10889 to regulate Hippo signalling, particularly as some reports suggest some Hippo pathway genes can regulate particular subsets of Yki-targets such as *mop* (Gilbert et al., 2011) or through perturbation of BMP signalling (Oh and Irvine, 2011).

These preliminary results point to a role of CG10889 in the regulation of tissue growth, however, more work needs to be done to assess by what mechanism growth is regulated, and whether the interaction with Yki has any functional relevance in this regard.

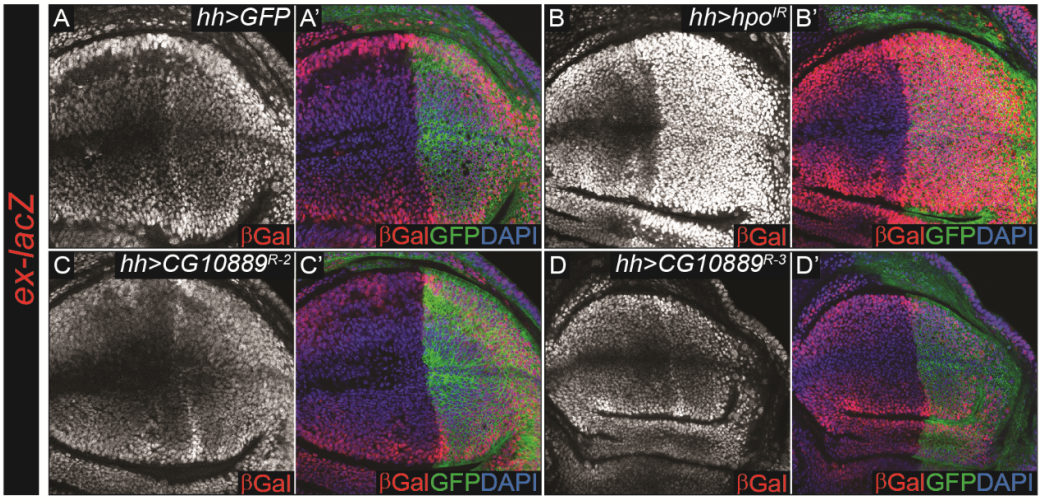

Figure 7-8 CG10889-mediated regulation of *ex-lacZ in vivo*

Confocal micrographs of third instar larvae wing imaginal discs expressing the *ex-lacZ* enhancer-trap (A-D'). Single channel images show β-Gal staining in a planar section in line with the nuclei of the wing pouch. Nuclei are marked by DAPI staining (blue) and the posterior compartment where *hh-Gal4* is expressed is marked by the presence of GFP. Expression of GFP under the control of *hh-Gal4* had no effect on the levels of β-Gal (A). Expression of hpo^{IR} was used as positive control and resulted in a marked increase in the levels of β-Gal (B). *hh-Gal4*-mediated expression of $CG10889^{R-2}$ mildly increased β-Gal levels (C), unlike the expression of $CG10889^{R-3}$, which had no effect (D).

7.2. **Concluding Remarks**

Screening for DUBs that regulate tissue growth, and genetically interact with the Hippo pathway has yielded several candidate genes which, when knocked down reduce overall tissue size (Figure 7-5, Table 7-1). Moreover, several of these candidates also interact with *ex*. Of particular note was *CG10889* which genetically interacts with *ex* and *wts*, and physically interacts with Yki, thus is a potential candidate as a novel regulator of Hippo signalling.

Chapter 8 - Discussion

8.1. The Regulation of Ex Stabilty by Phosphorylation and Deubiquitylation

Crb promotes the phosphorylation and interaction of Ex with the E3 ligase component Slmb, ultimately targeting Ex for proteasomal degradation (Chen et al., 2010; Grzeschik et al., 2010; Ribeiro et al., 2014; Robinson et al., 2010). The coordinated regulation of Ex stability requires the involvement of many proteins, including kinases that trigger the initial binding between Slmb and Ex, and potential negative regulators of this mechanism such as a DUB that could reverse the Ex degradative signal. During the course of this thesis, evidence has been presented to suggest the CK1 family of kinases, and the DUB Usp2 may play antagonistic roles in the regulation of Ex stability and therefore the Hippo pathway.

Indeed, at least in S2 cells, the CK1γ orthologue Gish interacts with Ex (Figure 5-1C-D), stimulates interaction of Ex with Slmb (Figure 5-4C), and can stimulate Ex phosphorylation and degradation (Figure 5-2). Moreover, RNAi-mediated depletion of *gish* stabilises Ex, even in the presence of Crb overexpression (Figure 5-5), as well as inhibiting Crb-induced Ex interaction with Slmb (Figure 5-6A), and ubiquitylation (Figure 5-6B). On the contrary, expression of the DUB Usp2 stabilises Ex protein in S2 cells, and *in vivo* (Figure 6-1 and Figure 9-1), which regulates wing growth (Figure 9-2) and influences Yki activity (Figure 6-2**)**. These data allude to a model whereby Crb stimulates the CK1 family kinases triggering Ex phosphorylation and ubiquitylation by Slmb, which is antagonised by the DUB Usp2 (Figure 8-1). Interestingly, the CK1s play a prominent role in regulating the stability of many key signalling proteins in *Drosophila* and mammals, including Per/PER2 (Chiu et al., 2008; Eide et al., 2005; Price et al., 1998)**)**, which is a substrate shared with USP2 (Yang et al., 2012; Yang et al., 2014). Per/PER2 protein levels are rhythmically regulated by coordinated

degradation by *Slmb/β-TrCP* (Eide et al., 2005; Grima et al., 2002), which requires phosphorylation by Dco/CK1δ/ε (Chiu et al., 2008; Eide et al., 2005) analogous to the regulation of Ex (see 'Chapter 5 - Results 3 – The Role of Casein Kinase 1 Family Kinases in the Regulation of Expanded') (Ribeiro et al., 2014; Zhang et al., 2015a). In the case of PER, USP2 regulates its subcellular localisation rather than stability, although this still depends on the DUB catalytic activity, relocating PER from the nucleus to the cytosol (Yang et al., 2012; Yang et al., 2014). Therefore there is a possibility that the CK1/Slmb/Usp2 axis is conserved in the regulation of Ex and Hippo signalling, as well as Per and the circadian rhythm.

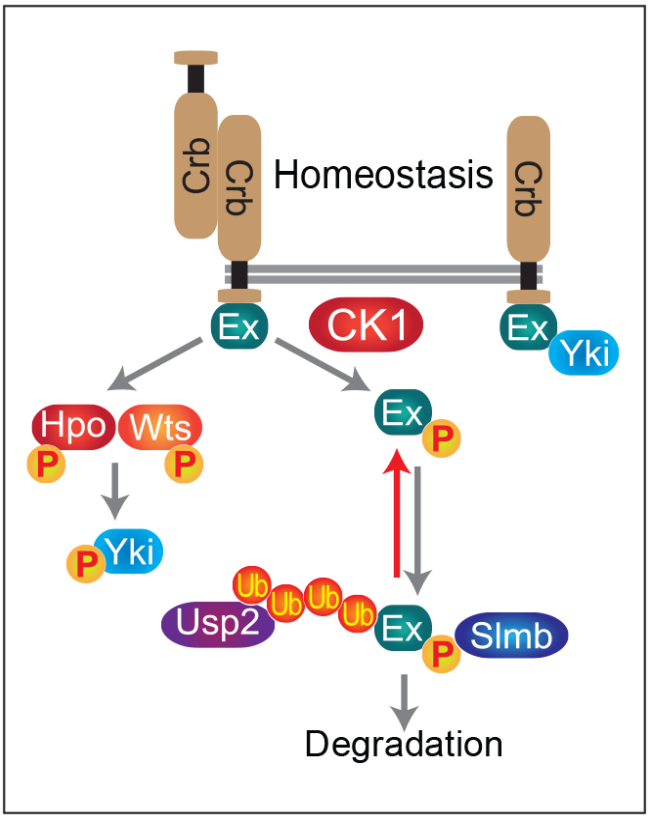

Figure 8-1 A revised model of Crb-mediated regulation of Ex

Crb-mediated regulation of Ex phosphorylation and degradation requires the action of the CK1 family kinases, and can be reversed by the DUB Usp2.

In addition to the CK1s and Usp2, the BMP kinases Sax, Tkv and Put could potentially be involved in the regulation of Ex stability (see 4.1), because at least in S2 cells, dsRNA-mediated depletion of these kinases results in mild stabilisation of Ex levels (Figure 4-3), and overexpression of Tkv causes phosphorylation of Ex, despite not stimulating Ex degradation (Figure 4-5). In mammals, CRB3 inhibits the BMP and Hippo pathways by limiting the translocation of a SMAD:YAP complex into the nucleus, which is dependent on the functional orthologue of Ex AMOT (Varelas et al., 2010). The interaction between YAP and SMAD is conserved in *Drosophila*, Yki and Mad forming dimers (Oh and Irvine, 2011), and it may therefore be possible that the Crb-mediated regulation of Mad may also be conserved, which would be particularly interesting if Ex played a similar role to AMOT in *Drosophila*, physically tethering both Yki and Mad away from the nucleus in a Crb-dependent manner, as Ex is known to do with Yki alone (Badouel et al., 2009; Oh et al., 2009). If the receptor kinases of the BMP pathway regulate Ex, stimulating either its degradation, or by degradative-independent phosphorylation, it would be interesting to see whether this process could disrupt a Yki:Mad complex, this relieving Crb-dependent inhibition, contributing to the activation of Mad. However, it is not yet known whether the interaction between Yki and Mad is regulated by Crb in *Drosophila*, or if this is the case, whether the BMP kinases would have any influence over this regulation of Yki:Mad, let alone whether Ex and Ex phosphorylation would be involved. In mammals at least, the TGFβ ligand and the TGFβ Receptor I are able to promote the interaction between SMAD and YAP and their nuclear translocation by stimulating the E3 ligase ITCH to ubiquitylate and degrade RASSF1A, which otherwise inhibits SMAD:YAP interaction (Pefani et al., 2016). Therefore, the BMP receptors in *Drosophila* could possibly regulate the Hippo pathway, and this could be dependent on Ex.

One caveat for much of the work presented is the discrepancy between results generated in S2 cells, and *in vivo* data, and many of positive findings of this thesis were identified using S2 cells. Whilst using S2 cells and cell lines in general can be of great benefit to dissecting the molecular detail of signalling pathways, and

individual relationships between proteins, care must be taken when extrapolating hypothesis to the whole organism. S2 cells only represent one population of cells, and thus cannot be entirely representative of the complex interplay between many genes in many cell types throughout a whole tissue or animal. Therefore perhaps some of the biochemical data obtained in this thesis may not truly reflect what occurs in *Drosophila*, or alternatively the *in vivo* techniques used are not sensitive enough to detect the observations made in S2 cells. To this end, robust methods to quantify levels of the *ubi-ex$^{1-468}$::GFP* and the *ex-lacZ* reporters would be extremely beneficial for *in vivo* analysis and could provide more conclusive evidence as to whether the CK1s or the BMP kinases, or Usp2 do regulate levels of Ex protein, and whether these genes influence Yki activity.

One of the prominent discrepancies between S2 cell and *in vivo* data is the difference between the CK1 family kinases. In S2 cells, much of the work has been focussed on Gish, which at least in this context, is a very promising candidate for a regulator of Ex stability downstream of Crb (see Chapter 5 -. However, *in vivo* mutations in *gish* do not influence levels of the *ubi-ex$^{1-468}$::GFP* reporter, or Yki activity as measured by *ex-lacZ*, whereas *ck1*α mutation both increases levels of the *ubi-ex$^{1-468}$::GFP* and decreases levels of *ex-lacZ* (collaborator data not shown). Moreover, overexpression of CK1α also stimulates a decrease in the *ubi-ex$^{1-468}$::GFP* reporter (Figure 5-3) and an increase in *ex-lacZ* (Figure 5-7 **)**, in keeping with the model whereby Ex stability is negatively regulated by the CK1 kinases . Therefore, undue focus may have been put onto Gish, and instead CK1α is likely to be the primary kinase *in vivo* in the regulation of Ex stability. It would be interesting to perform the same biochemical analysis of CK1α in S2 cells as has been carried out with Gish, analysing binding of CK1α to Ex, and whether dsRNA-mediated knockdown of *ck1*α causes stabilisation of the Ex protein, inhibition of Ex:Slmb interaction and inhibition of Ex ubiquitylation.

Another important issue that remains unresolved is whether the CK1 family kinases act synergistically or redundantly to regulate Ex stability. These kinases

are all highly conserved within the kinase domain, despite containing variable C-termini (Knippschild et al., 2005; Knippschild et al., 2014), (Figure 5-1A). The high homology between CK1 kinases possibly explains why many family members induce Ex electrophoretic mobility shift and/or depletion in a kinase-dependent manner (Figure 5-2, Figure 5-3). This includes uncharacterised CK1s (Figure 5-2C), such as CG7094, which is able to partially recover *ubi-ex$^{1-468}$::GFP* levels *in vivo* (collaborator data not shown). Interestingly, combined expression of CK1α, Dco and Gish^{isoI} results in a more robust electrophoretic mobility shift when compared to individual kinase expression (Figure 5-2D). The ability of several members of the CK1 family to induce phosphorylation of Ex, raises a serious limitation in the identification of the Ex degradative kinase, as throughout this thesis, potential redundancy between these kinases is never explicitly tested, and so there can be no conclusion as to whether these kinases act synergistically or redundantly. Therefore it would be very interesting to perform double or even triple mutant knockouts of members of this kinase family assessing levels of Ex. Previous studies analysing the role of CK1 kinases have reported some degree of synergy between family members. In S2 cells and *in vivo,* the Ft kinase Dco, which promotes Ft-dependent growth inhibition (Sopko et al., 2009), is also influenced by CK1α (Feng and Irvine, 2009). Furthermore, several CK1s can act on Hh signalling, regulating Ci and Smo phosphorylation, and in Wnt signalling in the regulation of LRP5/6 (Jia et al., 2005; Li et al., 2016; Swarup et al., 2015; Swarup and Verheyen, 2012; Zeng et al., 2005).

It may also be important to analyse the effect of CK1 family mutants in combination with Crb overexpression by generating Mosaic Analysis with a Repressible Marker (MARCM) clones (Lee and Luo, 1999). In cells, loss of function of *gish* was always carried out in the presence of Crb overexpression. Therefore, the reason for the discrepancy between the results in cells and *in vivo* may be the fact that the system needs to be primed by Crb overexpression. In the developing wing, the homeostatic regulation of Ex stability by Crb is likely to be subtle, and thus priming the system with Crb may be necessary in order to detect the changes in Ex (Figure 8-1).

In addition, to fully elucidate the mechanisms of Ex degradation, the specific residue(s) that are phosphorylated must be identified through *in vitro* kinase assays or phosphoproteomics. If the CK1 kinases are found to directly phosphorylate Ex, the residues they regulate will go some way to help dissect whether these kinases act synergistically or redundantly. Previously, the Ex^{S453} residue has been shown to be vital for Crb-mediated regulation of Ex stability, as its mutation to alanine abrogated Ex:Slmb binding, ubiquitylation and degradation (Ribeiro et al., 2014). Ex^{S453} is part of the canonical Slmb phosphodegron ^{452}TSGIVS^{457}, where it is assumed that S453 phosphorylation is required for Slmb recognition (Figure 5-4B) (Ribeiro et al., 2014). Within the phosphodegron, S457 appears to be an attractive potential site for Ex phosphorylation. However, previous reports failed to uncover any effect of this residue on regulating Ex stability or interaction with Slmb (Ribeiro et al., 2014). S462 was also analysed, and its mutation limited but did not abolish the ability of Slmb to bind and degrade Ex (Ribeiro et al., 2014). Interestingly, Crb-induced electrophoretic mobility shift occurred in single or double point mutations of these residues suggesting that despite regulating Ex stability, further residues of Ex are phosphorylated upon Crb stimulation (Ribeiro et al., 2014). The functional significance of the S453 residue had not previously been established *in vivo.* The inability of Crb^{i} to degrade *ubi-ex$^{1-468\ S453A}$::GFP* (Figure 3-1C-D), and the fact a *UAS-ex^{S453A}* transgene regulated growth in a manner insensitive to Crb^{i} overexpression (Figure 3-3), suggest that S453 is important for Ex function. However, this does not prove that S453 residue is the target for CK1 phosphorylation.

Interestingly, the Ex^{S453} site does not conform to the canonical CK1 consensus site of pS/T-X_{1-2}-S. However, analysing the sequence of Ex^{1-468} using online ELM (http://elm.eu.org/) and NetPhos (http://www.cbs.dtu.dk/services/NetPhos/) tools, a combined total of fourteen potential S/T residues within Ex^{1-468} conform to the CK1 consensus sequence (Table 8-1). As Crb^{i} or Gish overexpression does not affect Ex^{1-450} (Figure 5-4A), this suggests that CK1s phosphorylate Ex within $Ex^{450-468}$. Of the potential CK1 sites identified, only two lie within this region, Ex^{T451} and Ex^{T452}. Therefore, follow-up work should address whether these residues are

important. Interestingly, Ex^{T452} is highly conserved among most insect species (Ribeiro et al., 2014). Moreover, conserved S/T residues exist immediately upstream to Slmb/βTrCP phospho-recognition sites in mammalian PER1, PER2 (Ribeiro et al., 2014), and Ci (Smelkinson et al., 2007) suggestive of potential functional significance of this sequence.

Table 8-1 A Summary of Potential CK1 Sites Within Ex1-468

A table highlighting sites within Ex^{1-468} conforming to CK1 the consensus sequences identified using ELM (http://elm.eu.org/) and NetPhos (http://www.cbs.dtu.dk/services/NetPhos/).

Residue	Sequence Context	Identification Software
Ex^{S25}	SPGSRFL	ELM
Ex^{S93}	SKLSKYG	ELM
Ex^{S102}	SWRSSHT	ELM
Ex^{T105}	SSHTHGL	ELM
Ex^{S185}	TSNSKDD	NetPhos
Ex^{T208}	SATTTLP	ELM
Ex^{S338}	STNSSSN	ELM
Ex^{S396}	SGESRIT	ELM
Ex^{T372}	SRITLYA	ELM
Ex^{S445}	SVISSTS	ELM
Ex^{S448}	SSTSSNT	ELM
Ex^{S449}	STSSNTT	ELM / NetPhos
Ex^{T451}	SSNTTSG	ELM
Ex^{T452}	SNTTSGI	ELM / NetPhos

Ft, which is phosphorylated by Dco, and to a lesser extent CK1α, contains up to forty six potential CK1 phosphorylation sites within the intracellular domain, the electrophoretic shift induced by Dco corresponding to multiple phosphorylation events (Feng and Irvine, 2009; Sopko et al., 2009). This has made the identification of a specific phosphorylation site in Ft difficult, and no single reported residue exists. In a similar fashion, Crb-mediated phosphorylation of Ex appears to involve several phosphorylation events, and the S453A point mutation is still shifted upon Crb expression, despite Ex increased stability (Ribeiro et al., 2014). Perhaps one or more CK1 kinases phosphorylate Ex, which is the case with Ft (Feng and Irvine, 2009) Ci (Jia et al., 2005; Smelkinson et al., 2007) and Per (Chiu et al., 2011; Chiu et al., 2008). Alternatively, multiple kinases phosphorylate Ex upon Crb stimulation, of which the CK1s are only one family. It

is likely that an initial phosphorylation, probably within the $Ex^{450-468}$ region, primes Ex for further phosphorylation to ultimately stimulate Ex degradation. If the hypothetical CK1 Ex^{T451} and Ex^{T452} sites are important for regulating Ex stability, as is the Ex^{S453}, these phosphorylation sites could cooperate in regulating Ex stability.

Whilst the importance of the apical localisation of Crb and Ex has been discussed (Chapter 3 - and Chapter 5 -, in addition to localisation at the apical membrane, Crb can be internalised into endosomes. Inhibiting the function of genes such as *cdc42, Rab11* or *aPKC* promotes Crb internalisation (Fletcher et al., 2012; Harris and Tepass, 2008; Kim et al., 2009; Roeth et al., 2009), whereas genes such as *adaptor protein-2 (AP-2)* or *neuralised (neu)* promote uptake of Crb into the endosomes (Lin et al., 2015; Perez-Mockus et al., 2017). Overexpressed Crb localises at the membrane and is also found in endosomes (Fletcher et al., 2012). Moreover, Crb can be recycled back to the membrane after endocytosis through the action of the retromer complex, interacting with Vacuolar Protein Sorting 35 (Vps35) and Vacuolar Protein Sorting 26B (Vps26B) (Pocha et al., 2011; Zhou et al., 2011). Interestingly, Ex is also important for Crb stabilisation at the plasma membrane (Fletcher et al., 2012), and it has been proposed that Ex promotes endocytosis of apical proteins, with mutation in *ex* and *mer* resulting in accumulated apical receptors (Maitra et al., 2006). It may therefore be important to investigate the site of Crb-mediated Ex degradation and the role of the CK1 family and Usp2 play here, particularly since Gish is able to regulate Rab11 localisation in the developing wing (Gault et al., 2012), and in mammals, USP2 regulates the subcellular localisation PER2 (Yang et al., 2012; Yang et al., 2014). This could potentially be tested through Dynamin inhibition using the Dynamin inhibitor dynasore in cells (Macia et al., 2006), or the Dynamin mutant $shibire^{ts-1}$ *in vivo* to modulate endocytosis in a temperature sensitive manner (Koenig et al., 1998).

8.2. **Physiological Relevance of Crumbs-Mediated Expanded Degradation**

Crb is able to regulate Ex stability via interaction between the FBM of Crb, and the Ex FERM domain (Figure 3-1) (Chen et al., 2010; Grzeschik et al., 2010; Ling et al., 2010; Ribeiro et al., 2014; Robinson et al., 2010). However, besides the artificial overexpression of Crb^{FL} or Crb^{i}, which have both been used to stimulate Ex degradation, the physiological context that represents Crb overexpression remains an open question. One of the main upstream activators of Hippo signalling is the ability to sense changes in tissue architecture. To this end, Crb-Crb trans-homodimers, which may be important for cell-cell communication, adhesion and stabilisation of Crb at the apical membrane (Chen et al., 2010; Fletcher et al., 2012; Hafezi et al., 2012; Letizia et al., 2013; Pellikka et al., 2002; Thompson et al., 2013; Zou et al., 2012), are ideally placed to allow tissues to respond to changes in morphology or integrity. The response of Crb to epithelial status can be observed in wing imaginal discs, where Crb staining is lost in wildtype cells in direct contact with crb mutant tissue (Chen et al., 2010; Hafezi et al., 2012). Moreover, Crb wildtype cells in contact with cells expressing a Crb extracellular domain construct (CrbECD) concentrate along the expression boundary (Hafezi et al., 2012). Indeed, as well as losing Crb, the membrane of a wildtype cell directly in contact with crb mutant tissue also loses Ex and Patj (Chen et al., 2010). These data imply Crb is able to sense epithelial integrity through its homophilic trans-interactions and can transit extracellular signals, into the intracellular domain. Therefore, if Crb levels are disrupted, for example by loss of polarity or apoptosis, this may trigger signalling downstream of Crb (Ribeiro et al., 2014). Interestingly, genetically wounding wing imaginal discs by disrupting polarity or inducing apoptosis causes non-autonomous activation of Yki, which facilitates tissue regeneration and wound healing (Grusche et al., 2011; Sun and Irvine, 2011). This observation potentially provides context for physiological regulation of Ex by Crb, as Crb is regulated non-autonomously by loss of polarity in neighbouring tissue (Chen et al., 2010; Hafezi et al., 2012) and the ability of these genes to regulate regeneration should be investigated. In a

recent paper, which generates wounds through the 'pinch and puncture' technique in the larval epidermis, suggests *ex* is vital in regulating regeneration as *ex* overexpression completely blocks the regenerative capacity of the tissue. Interestingly, the capacity for *ex* to regulate regeneration is much greater than that of *wts*, suggesting the activity of Ex independent of the kinase cascade is crucial in its regulation of regeneration (Badouel et al., 2009; Tsai et al., 2017).

If Crb is lost from the wound/wildtype interface, as it is at the *crb* mutant/wildtype interface (Chen et al., 2010; Hafezi et al., 2012), a non-autonomous increase in Yki activity could be the result of a loss in apical Ex. In this model, Crb may be asymmetrically redistributed away from the mutant or wound cell interface. If Crb is asymmetrically distributed, it would be expected that this increased membrane concentration of Crb would result in more trans- and cis-homodimers, as is the case inside the salivary gland placode during development (Roper, 2012). Moreover, this increased Crb would also increase membrane concentrations of Ex (Hafezi et al., 2012), negating the potential for these cells to stimulate Yki activity. Perhaps the increased number of Crb-homophilic interactions stimulates Ex degradation, promoting full activity of Yki, thus allowing the cell to recover. However, in contrast to this hypothesis, Ex expression and interaction with Crb is also important for stabilising Crb at the apical membrane (Fletcher et al., 2012).

The role of YAP/TAZ in regulating tissue regeneration is conserved in tissues such as the intestine or liver (Cai et al., 2010; Su et al., 2015; Wu et al., 2013; Yimlamai et al., 2014). However, the role of CRB orthologues, or indeed Ex orthologues FRMD6 and AMOT in regeneration has not been determined. Recently, the Hippo pathway was shown to be important in regulating optimal myelin elongation in mouse neurones, which is dependent on YAP phosphorylation and activity (Fernando et al., 2016). Interestingly, this process relies on CRB3 and the mammalian Ex N-terminal orthologue FRMD6, which limit the myelin elongation to the appropriate length. In this system, growth is directionally regulated, and therefore could be analogous to regeneration, where proliferation occurs towards the wound. While the authors did not demonstrate

the molecular mechanisms employed in this system, it is possible that in this context CRB3 regulates FRMD6 directly in a similar manner to regulation of Ex by Crb in *Drosophila*. Analysing the protein sequence of FRMD6, there appears to be a conserved putative β–TrCP consensus site: ^{435}TSGVES^{440} (Ribeiro et al., 2014). Therefore, it will be interesting to see whether CRB3 can regulate FRMD6 directly, and whether this potential regulation is in part via β–TrCP-mediated regulation of FRMD6 stability. Can CRB3 also regulate AMOT in a regenerative context? AMOT inhibits cell migration (Aase et al., 2007; Dai et al., 2013), and this function is modulated by direct LATS phosphorylation (Dai et al., 2013), and therefore could be involved in regenerative growth. AMOT protein stability is also regulated by ubiquitylation, mediated by the Nedd4-like E3 ligase family (Wang et al., 2012), and this process is counteracted by DUB3 and USP9x (Nguyen et al., 2016; Nguyen et al., 2017). AMOT localisation is controlled by CRB3 (Varelas et al., 2010), but whether the regulation of AMOT turnover is dependent on CRB3 remains to be established.

In addition to sensing major epithelial disruption such as wounds, the Hippo pathway and YAP are important mediators of contact inhibition (Zhao et al., 2007). Mouse kidney epithelial cells lacking *CRB3* are refractory to contact inhibition (Karp et al., 2008). This is consistent with the finding that Crb mediates density sensing, as CRB3 is able control the activity of YAP/TAZ through interaction with AMOT, stimulating their phosphorylation and cytoplasmic retention at high density (Varelas et al., 2010). If this system is conserved, Crb may sense epithelial density in *Drosophila* tissues, and control Yki activity in an Ex dependent manner. The Hippo pathway is also responsive to tension through regulation by the cytoskeleton, and in particular F-actin (Dupont et al., 2011; Yu and Guan, 2013). The spectrin cytoskeleton has also recently been shown to regulate Hippo signalling, interacting with both Crb and Ex (Deng et al., 2015; Fletcher et al., 2015; Wong et al., 2015). In the wing and eye epithelium, β_H-Spectrins may aid the formation of an active Hippo pathway complex containing Crb and Ex (Fletcher et al., 2015). Individual Spectrins and the Spectrin network can respond to tension (Fletcher et al., 2015; Johnson et al., 2007; Meng and

Sachs, 2012). In certain situations, changes in cellular tension may change the activity of Crb, stimulating the degradation of Ex to promote tissue growth. Moreover, one study suggested the spectrin network can interact with cortical actomyosin through non-muscle myosin II to regulate Hippo signalling, further compounding the links between tension and Hippo signalling (Deng et al., 2015). Crb is able to regulate the activity of the Rok in an aPKC-dependent manner (Roper, 2012), and perhaps there is a dynamic relationship between tension and growth through Spectrin, Actin and Crb complex interactions.

8.3. **CG10889 – A Regulator of Growth**

Through screening for DUBs that regulate tissue size, and interact with the Hippo pathway gene *ex*, CG10889 was identified as a potential regulator of growth (Figure 7-4). This uncharacterised protein was also identified as a putative Yki-interacting protein in *Drosophila* (Guruharsha et al., 2011). In S2 tissue culture cells, the Yki:CG10889 interaction was confirmed through co-immunoprecipitation experiments, and mapped to the PPxY motif of CG10889 and the WW domains of Yki, particularly the C-terminal WW domain (Figure 7-7). PPxY-WW domain interactions are particularly prominent in the Hpo pathway, with Sav, Kib and Yki containing WW domains and Ex, Wts and Hpo all containing PPxY domains. The Yki:CG10889 interaction could therefore prove important for growth control. It remains to be determined whether the PPxY motif of CG10889 facilitates its interaction with other members of the Hpo pathway, for example the WW domain protein Sav. It is conceivable that CG10889 regulates growth in a Sav-dependent manner and this would partially explain the lack of effect on Yki target genes, as *sav* mutants have the weakest effect on Yki target gene expression of the Hpo cassette, despite displaying overgrowth phenotypes (Wu et al., 2003). It is also possible that the CG10889 interaction with Yki modulates the interaction between Yki and other binding partners in a similar mechanism to that used by Rassf or Jub to regulate Hpo and Wts, respectively (Das Thakur et al., 2010; Khokhlatchev et al., 2002; Polesello et al., 2006).

Growth control via the Hpo pathway involves regulation of the transcriptional co-activator Yki. As *CG10889* genetically interacts with *ex*, and physically interacts with Yki, its effect on growth was analysed. Indeed, RNAi-mediated knockdown of *CG10889* results in tissue undergrowth, which is enhanced by co-expression of *ex* in adult wings (Figure 7-4, Figure 7-6). Furthermore, combining *CG10889* and *wts* depletion resulted in a partial suppression of the *wts-RNAi* overgrowth phenotype in adult wings (Figure 7-6). When analysed with the knowledge of Yki:CG10889 binding in cells, these data suggest that CG10889 may be required for growth control through the Hippo signalling, and that CG10889 could regulate the ubiquitylation status of Yki, cleaving Ubi to stabilise Yki and promote Yki function, although a genetic interaction with *yki* itself is yet to be confirmed.

Interestingly, preliminary data presented here suggests mutations in the putative DUB domains of CG10889 result in increased association of Yki:CG10889 (Figure 7-7) suggesting inability of CG10889 to deubiquitylate Yki could result in a prolonged interaction. As of yet, no Yki E3 ligase has been identified in *Drosophila*, whereas in mammals β-TrCP has been proposed to regulate YAP stability. However, the β-TrCP recognition sequence is not conserved in Yki (Zhao et al., 2010).

When assessing the activity of Yki through the *ex-lacZ* reporter, there was no change, or even a mild enhancement of Yki activity upon *CG10889* knockdown. Despite this, adult wings were decreased in size, which is inconsistent with the effect on Yki target gene expression (Figure 7-8), and analysis of different Yki target genes may yield positive results. It also remains a possibility that despite detecting a Yki:CG10889 interaction in cells, and the genetic interactions of *CG10889* with *ex* and *wts,* CG10889 may regulate growth via a different signalling pathway in parallel to Hippo signalling, or that the growth phenotype observed is a result of off target effects of the RNAi line.

The mammalian orthologue of CG10889 is Monocyte Chemotactic Protein-Induced Protein (MCPIP) 1. MCPIP was initially identified as a protein

upregulated in human peripheral blood monocytes treated with Monocyte Chemotactic Protein 1 (MCP1) (Zhou et al., 2006), which is also transcriptionally induced by pro-inflammatory molecules such as TNF, IL-1β (Interleukin 1β) and LPS (Lipopolysaccharide), and as such is important during inflammatory responses (Jura et al., 2012; Kasza et al., 2010; Liang et al., 2010; Matsushita et al., 2009; Skalniak et al., 2009). MCPIP contains a CCCH-type zing finger domain commonly associated with RNA binding proteins. Indeed, MCPIP contains an RNase domain highly homologous to PilT N-terminus (PIN) domain, as well as a Ubiquitin Associated (UBA) domain (Figure 7-7) (Liang et al., 2010; Xu et al., 2012). In addition to its RNase activity, MCPIP has been identified as a putative DUB, although the direct enzymatic DUB activity remains controversial (Liang et al., 2010; Niu et al., 2013). MCPIP promotes the deubiquitylation of TNF Receptor Associated Factor (TRAF) 2, 3 and 6, TRAF Family Member-Associated NF-κB Activator (TANK) and NEMO to inhibit the cellular response to NF-κB in response to genotoxicity and inflammation as part of a NF-κB negative feedback loop (Liang et al., 2010; Niu et al., 2013; Wang et al., 2015a). Intriguingly, two of these studies suggest the DUB activity of MCPIP is conferred through interaction with the bona fide DUB USP10, MCPIP acting as a scaffold to promote interaction of USP10 with its substrates (Niu et al., 2013; Wang et al., 2015a). It remains to be confirmed whether CG10889 possesses DUB activity, or whether CG10889 provides a scaffold for an additional Yki regulating protein, for example the *Drosophila* USP10 orthologue CG32479. Interestingly, depletion of CG32479 in the adult wing caused a large reduction in adult wing size, previously associated with disruption of Notch signalling (Zhang et al., 2012) (Figure 7-1A). This size reduction is enhanced in combination with *ex* overexpression, but to a lesser extent than CG10889 (Figure 7-4), suggesting that CG32479 could also interact with *ex* and the Hippo pathway. Consistent with a potential role for CG10889 in regulating Yki and growth, MCPIP knockout mice display undergrowth (Liang et al., 2010). It will be important to analyse whether the *CG10889* genetically interacts with *yki*, and whether this is dependent on *CG32479*, if the RNase activity of MCPIP is conserved in *Drosophila*, and whether this could influence Yki activity.

8.4. **Concluding Remarks**

This study has identified the CK1 family as novel regulators of Ex stability and therefore Hippo signalling. Overexpression of the CK1 kinases results in depletion of Ex in S2 cells and *in vivo* and promote Yki function accordingly. Furthermore, knockdown of specific CK1 family members can increase Ex levels, consistent with a role of CK1 family members in regulating Ex stability. More work needs to be done in order to clarify whether this phosphorylation is direct, and to determine the importance of each family member, resolving the potential redundancy observed between these highly homologous family members (Figure 8-1).

Usp2 has also been identified as a putative regulator of Ex stability, and is able to stabilise Ex levels in a catalytic-dependent manner, reversing degradative stimulus induced by Crb expression. It will be interesting to identify the specific physiological context of Crb-mediated regulation of Ex stability, and therefore the context in which the CK1s and Usp2 may specifically regulate Ex levels (Figure 8-1).

In addition, the DUB CG10889 was identified as a novel DUBs which regulates growth, interacting with key Hippo pathway members *ex, wts* and *yki.* The mechanisms by which CG10889 regulates growth remain to be determined, and it will be informative to see whether this is dependent on the ability of CG10889 to interact with Yki.

Chapter 9 - Appendix

Initial experiments obtained for ‘Results 4 – The Reversibility of Expanded Degradation’ was performed by Paulo Ribeiro, Barts Cancer Institute, and is included here in the ‘Appendix’ with his permission, because its inculsion is vital as explanation to the experimental rational:

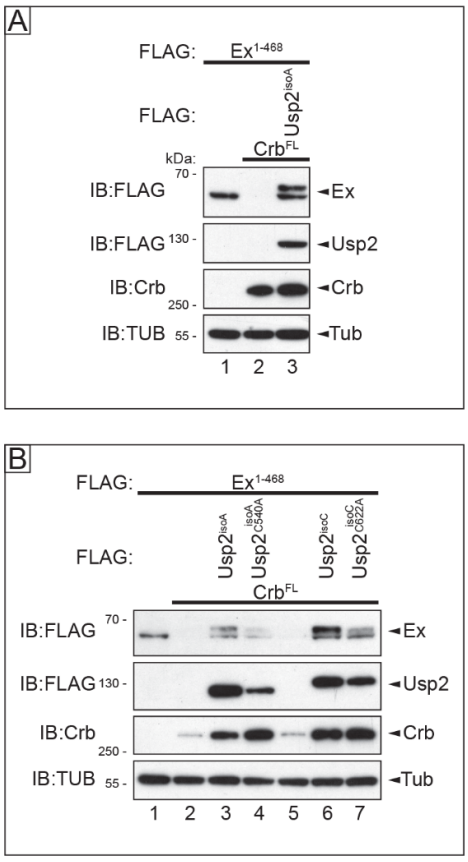

Figure 9-1 Usp2 regulates Ex protein levels in S2 cells

Immunoblot of S2 cell lysates expressing FLAG-tagged Ex^{1-468} (A, B). Compared to Ex^{1-468} alone (A, B – lanes 1), expression of Crb^{FL} caused depletion of Ex^{1-468} (A – lane 2, B - lanes 2, 5). Expression of FLAG-tagged $Usp2^{isoA}$ (A, B – lanes 3) or $Usp2^{isoC}$ (B – lane 6) caused stabilisation of Ex^{1-468} despite co-expression of Crb^{FL}. Expression of FLAG-tagged $Usp2^{isoA\ C504A}$ (B – lane 4) or $Usp2^{isoC\ C622A}$ (B – lane 7) was not as efficient in the stabilisation of Ex^{1-468} in the presence of Crb^{FL}. Lysates were analysed with the indicated antibodies and Tub was used as a loading control (A-D). Data courtesy of Paulo Ribeiro (Barts Cancer Institute).

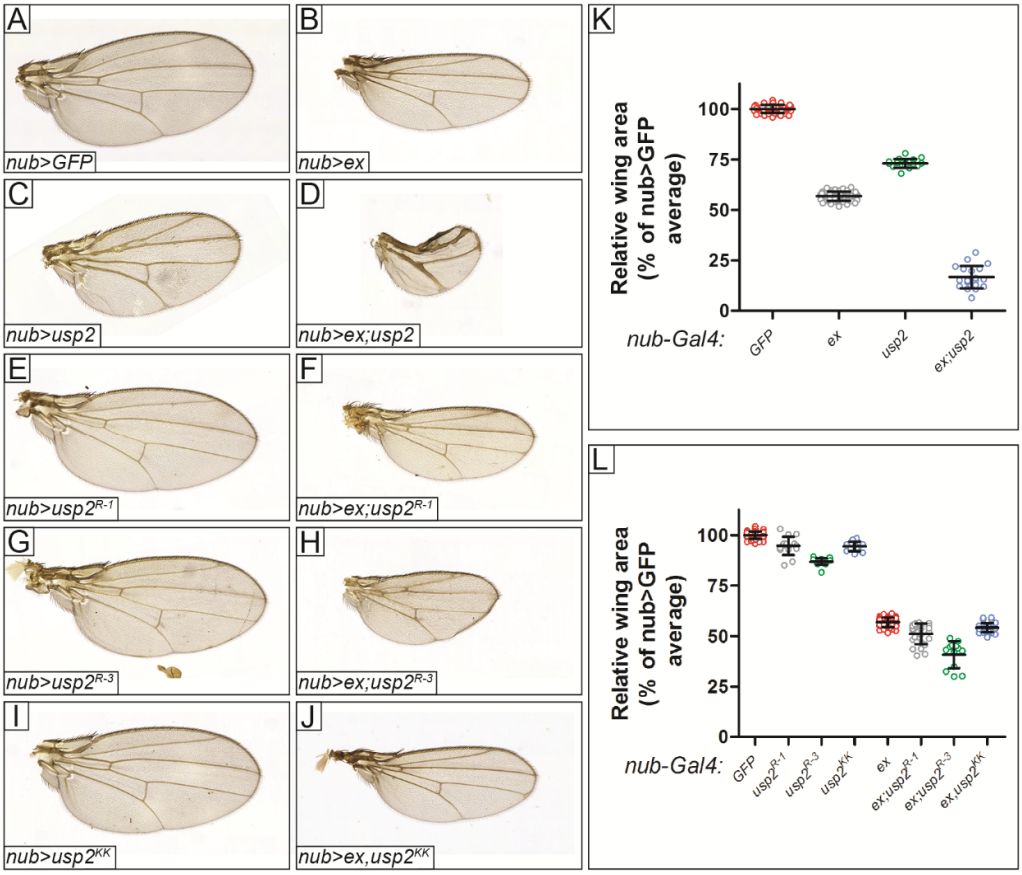

Figure 9-2 Usp2 as a regulator of wing growth

Adult wings expressing different transgenes under the control of *nub-Gal4*. Shown are the adult wings of flies expressing a GFP transgene as control (A), *ex* (B) *usp2$^{(III)}$* (C), *ex; usp2$^{(III)}$* (D), *usp2^{R-1}* (E), *ex; usp2^{R-1}* (F), *usp2^{R-3}* (G), *ex; usp2^{R-3}* (H), *usp2^{KK}* (I) or *ex, usp2^{KK}* (J). Quantified using ImageJ and wing area was normalised to *nub>GFP* expressing control wings (K, L). Results obtained with *usp2* overexpression (K), or with different *Usp2-RNAi* lines (L). Individual data points are shown as well as the average ± SD for each of the genotypes analysed (K, L). All genotypes obtained with *usp2* overexpression (K) were statistically different (*** = P < 0.0001) determined through a one-way ANOVA analysis with a Turkey's range post hoc test. All genotypes obtained with different *Usp2-RNAi* lines (L) were statistical different (*** = P < 0.0001) with the exception of the comparison between *nub>ex* and *nub>ex, usp2^{KK}* where the statistical difference was * = P < 0.05, determined through a one-way ANOVA analysis with a Turkey's range post hoc test. Data courtesy of Paulo Ribeiro (Barts Cancer Institute).

Reference List

Aase, K., Ernkvist, M., Ebarasi, L., Jakobsson, L., Majumdar, A., Yi, C., Birot, O., Ming, Y., Kvanta, A., Edholm, D.*, et al.* (2007). Angiomotin regulates endothelial cell migration during embryonic angiogenesis. Genes & development *21*, 2055-2068.

Abdul Rehman, S.A., Kristariyanto, Y.A., Choi, S.Y., Nkosi, P.J., Weidlich, S., Labib, K., Hofmann, K., and Kulathu, Y. (2016). MINDY-1 Is a Member of an Evolutionarily Conserved and Structurally Distinct New Family of Deubiquitinating Enzymes. Molecular cell *63*, 146-155.

Aberle, H., Bauer, A., Stappert, J., Kispert, A., and Kemler, R. (1997). beta-catenin is a target for the ubiquitin-proteasome pathway. The EMBO journal *16*, 3797-3804.

Adams, J. (2003). The proteasome: structure, function, and role in the cell. Cancer Treatment Reviews *29*, 3-9.

Adams, M.D., Celniker, S.E., Holt, R.A., Evans, C.A., Gocayne, J.D., Amanatides, P.G., Scherer, S.E., Li, P.W., Hoskins, R.A., Galle, R.F.*, et al.* (2000). The genome sequence of Drosophila melanogaster. Science *287*, 2185-2195.

Adler, J.J., Heller, B.L., Bringman, L.R., Ranahan, W.P., Cocklin, R.R., Goebl, M.G., Oh, M., Lim, H.S., Ingham, R.J., and Wells, C.D. (2013). Amot130 adapts atrophin-1 interacting protein 4 to inhibit yes-associated protein signaling and cell growth. The Journal of biological chemistry *288*, 15181-15193.

Adler, P.N., Charlton, J., and Liu, J. (1998). Mutations in the cadherin superfamily member gene dachsous cause a tissue polarity phenotype by altering frizzled signaling. Development *125*, 959-968.

Aerne, B.L., Gailite, I., Sims, D., and Tapon, N. (2015). Hippo Stabilises Its Adaptor Salvador by Antagonising the HECT Ubiquitin Ligase Herc4. PloS one *10*, e0131113.

Alarcon, C., Zaromytidou, A.I., Xi, Q., Gao, S., Yu, J., Fujisawa, S., Barlas, A., Miller, A.N., Manova-Todorova, K., Macias, M.J.*, et al.* (2009). Nuclear CDKs drive Smad transcriptional activation and turnover in BMP and TGF-beta pathways. Cell *139*, 757-769.

Amano, M., Tsumura, Y., Taki, K., Harada, H., Mori, K., Nishioka, T., Kato, K., Suzuki, T., Nishioka, Y., Iwamatsu, A.*, et al.* (2010). A proteomic approach for comprehensively screening substrates of protein kinases such as Rho-kinase. PloS one *5*, e8704.

Ambegaonkar, A.A., Pan, G., Mani, M., Feng, Y., and Irvine, K.D. (2012). Propagation of Dachsous-Fat planar cell polarity. Current biology : CB *22*, 1302-1308.

Amerik, A.Y., and Hochstrasser, M. (2004). Mechanism and function of deubiquitinating enzymes. Biochimica et biophysica acta *1695*, 189-207.

Angus, L., Moleirinho, S., Herron, L., Sinha, A., Zhang, X., Niestrata, M., Dholakia, K., Prystowsky, M.B., Harvey, K.F., Reynolds, P.A.*, et al.* (2012). Willin/FRMD6 expression activates the Hippo signaling pathway kinases in mammals and antagonizes oncogenic YAP. Oncogene *31*, 238-250.

Aragona, M., Panciera, T., Manfrin, A., Giulitti, S., Michielin, F., Elvassore, N., Dupont, S., and Piccolo, S. (2013). A mechanical checkpoint controls multicellular growth through YAP/TAZ regulation by actin-processing factors. Cell *154*, 1047-1059.

Azpiazu, N., and Morata, G. (2000). Function and regulation of homothorax in the wing imaginal disc of Drosophila. Development *127*, 2685-2693.

Bachmann, A., Grawe, F., Johnson, K., and Knust, E. (2008a). Drosophila Lin-7 is a component of the Crumbs complex in epithelia and photoreceptor cells and prevents light-induced retinal degeneration. Eur J Cell Biol *87*, 123-136.

Bachmann, A., Grawe, F., Johnson, K., and Knust, E. (2008b). DrosophilaLin-7 is a component of the Crumbs complex in epithelia and photoreceptor cells and prevents light-induced retinal degeneration. Eur J Cell Biol *87*.

Bachmann, A., Schneider, M., Theilenberg, E., Grawe, F., and Knust, E. (2001). Drosophila Stardust is a partner of Crumbs in the control of epithelial cell polarity. Nature *414*, 638-643.

Bachmann, A., Timmer, M., Sierralta, J., Pietrini, G., Gundelfinger, E.D., Knust, E., and Thomas, U. (2004). Cell type-specific recruitment of Drosophila Lin-7 to distinct MAGUK-based protein complexes defines novel roles for Sdt and Dlg-S97. Journal of cell science *117*, 1899-1909.

Badouel, C., Gardano, L., Amin, N., Garg, A., Rosenfeld, R., Le Bihan, T., and McNeill, H. (2009). The FERM-domain protein Expanded regulates Hippo pathway activity via direct interactions with the transcriptional activator Yorkie. Developmental cell *16*, 411-420.

Baena-Lopez, L.A., Rodriguez, I., and Baonza, A. (2008). The tumor suppressor genes dachsous and fat modulate different signalling pathways by regulating dally and dally-like. Proceedings of the National Academy of Sciences of the United States of America *105*, 9645-9650.

Barlow, J., Mathias, A., and Williamson, R. (1963). A simple method for the quantitive isolation of undegraded high molecular weight ribonucleic acid. Biochemical Biophysical Research Communications *13*, 61-66.

Basu, S., Totty, N., Irwin, M., Sudol, M., and Downward, J. (2003). Akt Phosphorylates the Yes-Associated Protein, Yap, to Induce Interaction with 14-3-3 and Attenuation of p73-Mediated Apoptosis. Molecular cell *11*, 11-23.

Bate, M., and Arias, A.M. (1991). The embryonic origin of imaginal discs in Drosophila. Development *112*, 755-761.

Baumgartner, R., Poernbacher, I., Buser, N., Hafen, E., and Stocker, H. (2010). The WW domain protein Kibra acts upstream of Hippo in Drosophila. Developmental cell *18*, 309-316.

Beira, J.V., and Paro, R. (2016). The legacy of Drosophila imaginal discs. Chromosoma *125*, 573-592.

Bellen, H.J., Levis, R.W., Liao, G., He, Y., Carlson, J.W., Tsang, G., Evans-Holm, M., Hiesinger, P.R., Schulze, K.L., Rubin, G.M.*, et al.* (2004). The BDGP gene disruption project: single transposon insertions associated with 40% of Drosophila genes. Genetics *167*, 761-781.

Bennett, F.C., and Harvey, K.F. (2006). Fat cadherin modulates organ size in Drosophila via the Salvador/Warts/Hippo signaling pathway. Current biology : CB *16*, 2101-2110.

Betschinger, J., Mechtler, K., and Knoblich, J.A. (2003). The Par complex directs asymmetric cell division by phosphorylating the cytoskeletal protein Lgl. Nature *422*, 326-330.

Bhat, M.A., Izaddoost, S., Lu, Y., Cho, K.O., Choi, K.W., and Bellen, H.J. (1999). Discs Lost, a novel multi-PDZ domain protein, establishes and maintains epithelial polarity. Cell *96*, 833-845.

Bier, E., Vaessin, H., Shepherd, S., Lee, K., McCall, K., Barbel, s., Ackerman, L., Carretto, R., Uemura, T., Grell, E.*, et al.* (1989). Searching for pattern and mutation in the *Drosopihla* genome with P-lacZ vector. Genes & development *3*, 1273-1287.

Bilder, D. (2004). Epithelial polarity and proliferation control: links from the *Drosophila* neoplastic tumor suppressors. Genes & development *18*, 1909-1925.

Bilder, D., Li, M., and Perrimon, N. (2000). Cooperative regulation of cell polarity and growth by Drosophila tumor suppressors. Science *289*, 113-116.

Blaumueller, C., and Mlodzik, M. (2000). The *Drosophila* tumor suppressor *expanded* regulates growth, apoptosis, and patterning during development. 92.

Boedigheimer, M., and Laughon, A. (1993). expanded: a gene involved in the control of cell proliferation in imaginal discs. Development *118*, 1291-1301.

Boedigheimer, M.J., Nguyen, K.P., and Bryant, P.J. (1997). Expanded functions in the apical cell domain to regulate the growth rate of imaginal discs. Developmental Genetics *20*, 103-110.

Boggiano, J.C., Vanderzalm, P.J., and Fehon, R.G. (2011). Tao-1 phosphorylates Hippo/MST kinases to regulate the Hippo-Salvador-Warts tumor suppressor pathway. Developmental cell *21*, 888-895.

Bosch, J.A., Sumabat, T.M., Hafezi, Y., Pellock, B.J., Gandhi, K.D., and Hariharan, I.K. (2014). The Drosophila F-box protein Fbxl7 binds to the protocadherin fat and regulates Dachs localization and Hippo signaling. Elife *3*, e03383.

Bossuyt, W., Chen, C.L., Chen, Q., Sudol, M., McNeill, H., Pan, D., Kopp, A., and Halder, G. (2014). An evolutionary shift in the regulation of the Hippo pathway between mice and flies. Oncogene *33*, 1218-1228.

Bosveld, F., Bonnet, I., Guirao, B., Tlili, S., Wang, Z., Petitalot, A., Marchand, R., Bardet, P.L., Marcq, P., Graner, F*., et al.* (2012). Mechanical control of morphogenesis by Fat/Dachsous/Four-jointed planar cell polarity pathway. Science *336*, 724-727.

Bourouis, M. (2002). Targeted increase in Shaggy activity levels blocks wingless signaling. genesis *34*, 99-102.

Brand, A.H., and Perrimon, N. (1993). Targeted gene expression as a means of altering cell fates and generating dominant phenotypes. Development *118*.

Brennecke, J., Hipfner, D.R., Stark, A., Russell, R.B., and Cohen, S.M. (2003). bantam encodes a developmentally regulated microRNA that controls cell proliferation and regulates the proapoptotic gene hid in Drosophila. Cell *113*, 25-36.

Bretscher, A., Edwards, K., and Fehon, R.G. (2002). ERM proteins and merlin: integrators at the cell cortex. Nature reviews Molecular cell biology *3*, 586-599.

Bridges, C.B. (1916). Non-Disjunction as Proof of the Chromosome Theory of Heredity (Concluded). Genetics *1*, 107-163.

Bridges, C.B., and Brehme, K.S. (1944). The mutants of Drosophila melanogaster, Vol 552.

Brittle, A., Thomas, C., and Strutt, D. (2012). Planar polarity specification through asymmetric subcellular localization of Fat and Dachsous. Current biology : CB *22*, 907-914.

Brittle, A.L., Repiso, A., Casal, J., Lawrence, P.A., and Strutt, D. (2010). Four-jointed modulates growth and planar polarity by reducing the affinity of dachsous for fat. Current biology : CB *20*, 803-810.

Brumby, A.M., and Richardson, H.E. (2003). scribble mutants cooperate with oncogenic Ras or Notch to cause neoplastic overgrowth in Drosophila. The EMBO journal *22*, 5769-5779.

Bryant, P., Huettner, B., Held Jr, L., Ryerse, J., and Szidonya, J. (1988). Mutations at the *fat* locus interfere with cell proliferation control and epithelial morphogenesis in*Drosophila*. Development Biology *129*, 541-554.

Bryant, P.J., and Levinson, P. (1985). Intrinsic growth control in the imaginal primordia of Drosophila, and the autonomous action of a lethal mutation causing overgrowth. Developmental biology *107*, 355-363.

Bryant, P.J., and Simpson, P. (1984). Intrinsic and extrinsic control of growth in developing organs. The Quarterly review of biology *59*, 387-415.

Bulgakova, N.A., and Knust, E. (2009). The Crumbs complex: from epithelial-cell polarity to retinal degeneration. Journal of cell science *122*, 2587-2596.

Burrows, A.C., Prokop, J., and Summers, M.K. (2012). Skp1-Cul1-F-box ubiquitin ligase (SCF(betaTrCP))-mediated destruction of the ubiquitin-specific protease USP37 during G2-phase promotes mitotic entry. The Journal of biological chemistry *287*, 39021-39029.

Cagan, R.L., and Ready, D.F. (1989). Notch is required for successive cell decisions in the developing Drosophila retina. Genes & development *3*, 1099-1112.

Cai, J., Zhang, N., Zheng, Y., de Wilde, R.F., Maitra, A., and Pan, D. (2010). The Hippo signaling pathway restricts the oncogenic potential of an intestinal regeneration program. Genes & development *24*, 2383-2388.

Callus, B.A., Verhagen, A.M., and Vaux, D.L. (2006). Association of mammalian sterile twenty kinases, Mst1 and Mst2, with hSalvador via C-terminal coiled-coil domains, leads to its stabilization and phosphorylation. The FEBS journal *273*, 4264-4276.

Camargo, F.D., Gokhale, S., Johnnidis, J.B., Fu, D., Bell, G.W., Jaenisch, R., and Brummelkamp, T.R. (2007). YAP1 increases organ size and expands undifferentiated progenitor cells. Current biology : CB *17*, 2054-2060.

Campbell, K., Knust, E., and Skaer, H. (2009). Crumbs stabilises epithelial polarity during tissue remodelling. Journal of cell science *122*, 2604-2612.

Cao, X., Pfaff, S.L., and Gage, F.H. (2008). YAP regulates neural progenitor cell number via the TEA domain transcription factor. Genes & development *22*, 3320-3334.

Capdevila, J., and Guerrero, I. (1994). Targeted expression of the signaling molecule decapentaplegic induces pattern duplications and growth alterations in Drosophila wings. The EMBO journal *13*, 4459-4468.

Casal, J., Struhl, G., and Lawrence, P.A. (2002). Developmental compartments and planar polarity in Drosophila. Current Biology *12*, 1189-1198.

Chan, E.H.Y., Nousiainen, M., Chalamalasetty, R.B., Schäfer, A., Nigg, E.A., and Silljé, H.H.W. (2005). The Ste20-like kinase Mst2 activates the human large tumor suppressor kinase Lats1. Oncogene *24*, 2076-2086.

Chan, S.W., Lim, C.J., Chong, Y.F., Pobbati, A.V., Huang, C., and Hong, W. (2011). Hippo pathway-independent restriction of TAZ and YAP by angiomotin. The Journal of biological chemistry *286*, 7018-7026.

Chan, S.W., Lim, C.J., Guo, F., Tan, I., Leung, T., and Hong, W. (2013). Actin-binding and cell proliferation activities of angiomotin family members are regulated by Hippo pathway-mediated phosphorylation. The Journal of biological chemistry *288*, 37296-37307.

Chen, C., Gajewski, K., Hamaratoglu, F., Bossuyt, W., Sansores-Garcia, L., Tao, C., and Halder, G. (2010). The apical-basal cell polarity determinant Crumbs regulates Hippo signaling in Drosophila. Proceedings of the National Academy of Sciences of the United States of America *107*, 15810–15815.

Chen, C.L., Schroeder, M.C., Kango-Singh, M., Tao, C., and Halder, G. (2012). Tumor suppression by cell competition through regulation of the Hippo pathway. Proceedings of the National Academy of Sciences of the United States of America *109*, 484-489.

Chen, Q., Zhang, N., Xie, R., Wang, W., Cai, J., Choi, K.S., David, K.K., Huang, B., Yabuta, N., Nojima, H.*, et al.* (2015). Homeostatic control of Hippo signaling activity revealed by an endogenous activating mutation in YAP. Genes & development *29*, 1285-1297.

Chen, Y., Sasai, N., Ma, G., Yue, T., Jia, J., Briscoe, J., and Jiang, J. (2011). Sonic Hedgehog dependent phosphorylation by CK1alpha and GRK2 is required for ciliary accumulation and activation of smoothened. PLoS biology *9*, e1001083.

Chen, Z.J., and Sun, L.J. (2009). Nonproteolytic functions of ubiquitin in cell signaling. Molecular cell *33*, 275-286.

Cheong, J.K., and Virshup, D.M. (2011). Casein kinase 1: Complexity in the family. The international journal of biochemistry & cell biology *43*, 465-469.

Chiu, J.C., Ko, H.W., and Edery, I. (2011). NEMO/NLK phosphorylates PERIOD to initiate a time-delay phosphorylation circuit that sets circadian clock speed. Cell *145*, 357-370.

Chiu, J.C., Vanselow, J.T., Kramer, A., and Edery, I. (2008). The phospho-occupancy of an atypical SLIMB-binding site on PERIOD that is phosphorylated by DOUBLETIME controls the pace of the clock. Genes & development *22*, 1758-1772.

Cho, E., Feng, Y., Rauskolb, C., Maitra, S., Fehon, R.G., and Irvine, K.D. (2006). Delineation of a Fat tumor suppressor pathway. Nature Genetics *38*, 1142-1150.

Cho, E., and Irvine, K.D. (2004). Action of fat, four-jointed, dachsous and dachs in distal-to-proximal wing signaling. Development *131*, 4489-4500.

Choi, S., Kim, W., and Chung, J. (2011). Drosophila salt-inducible kinase (SIK) regulates starvation resistance through cAMP-response element-binding protein (CREB)-regulated transcription coactivator (CRTC). The Journal of biological chemistry *286*, 2658-2664.

Chung, H.L., Augustine, G.J., and Choi, K.W. (2016). Drosophila Schip1 Links Expanded and Tao-1 to Regulate Hippo Signaling. Developmental cell *36*, 511-524.

Ciechanover, A. (2012). Intracellular protein degradation: from a vague idea thru the lysosome and the ubiquitin-proteasome system and onto human diseases and drug targeting. Biochimica et biophysica acta *1824*, 3-13.

Ciechanover, A., Hod, Y., and Hershko, A. (1978). A heat-stable polypeptide component of an ATP-dependent proteolytic system from reticulocytes. Biochemical and biophysical research communications *81*, 1100-1105.

Cifuentes, F.J., and García-Bellido, A. (1997). Proximo–distal specification in the wing disc of Drosophila by the nubbin gene. Proceedings of the National Academy of Sciences *94*, 11405-11410.

Clark, H., Brentrup, D., Schneitz, K., Bieber, A., Goodman, C., and Noll, M. (1995). Dachsous encodes a member of the cadherin superfamily that controls imaginal disc morphogenesis in Drosophila Genes & development *9*, 1530-1542.

Codelia, V.A., Sun, G., and Irvine, K.D. (2014). Regulation of YAP by Mechanical Strain through Jnk and Hippo Signaling. Current biology : CB.

Cohen, B., McGuffin, M.E., Pfeifle, C., Segal, D., and Cohen, S.M. (1992). apterous, a gene required for imaginal disc development in Drosophila encodes a member of the LIM family of developmental regulatory proteins. Genes & development *6*, 715-729.

Colombani, J., Polesello, C., Josue, F., and Tapon, N. (2006). Dmp53 activates the Hippo pathway to promote cell death in response to DNA damage. Current biology : CB *16*, 1453-1458.

Dai, X., She, P., Chi, F., Feng, Y., Liu, H., Jin, D., Zhao, Y., Guo, X., Jiang, D., Guan, K.L.*, et al.* (2013). Phosphorylation of angiomotin by Lats1/2 kinases inhibits F-actin binding, cell migration, and angiogenesis. The Journal of biological chemistry *288*, 34041-34051.

Das, T., Safferling, K., Rausch, S., Grabe, N., Boehm, H., and Spatz, J.P. (2015). A molecular mechanotransduction pathway regulates collective migration of epithelial cells. Nature cell biology *17*, 276-287.

Das Thakur, M., Feng, Y., Jagannathan, R., Seppa, M.J., Skeath, J.B., and Longmore, G.D. (2010). Ajuba LIM proteins are negative regulators of the Hippo signaling pathway. Current biology : CB *20*, 657-662.

Davidson, G., Wu, W., Shen, J., Bilic, J., Fenger, U., Stannek, P., Glinka, A., and Niehrs, C. (2005). Casein kinase 1 gamma couples Wnt receptor activation to cytoplasmic signal transduction. Nature *438*, 867-872.

De Duve, C., Gianetto, R., Appelmans, F., and Wattiaux, R. (1953). Enzymic content of the mitochondria fraction. Nature *172*, 1143-1144.

Degoutin, J.L., Milton, C.C., Yu, E., Tipping, M., Bosveld, F., Yang, L., Bellaiche, Y., Veraksa, A., and Harvey, K.F. (2013). Riquiqui and minibrain are regulators of the hippo pathway downstream of Dachsous. Nature cell biology *15*, 1176-1185.

Deng, H., Wang, W., Yu, J., Zheng, Y., Qing, Y., and Pan, D. (2015). Spectrin regulates Hippo signaling by modulating cortical actomyosin activity. Elife *4*, e06567.

DeRan, M., Yang, J., Shen, C.H., Peters, E.C., Fitamant, J., Chan, P., Hsieh, M., Zhu, S., Asara, J.M., Zheng, B.*, et al.* (2014). Energy Stress Regulates Hippo-YAP Signaling Involving AMPK-Mediated Regulation of Angiomotin-like 1 Protein. Cell reports *9*, 495-503.

Dereeper, A., Guignon, V., Blanc, G., Audic, S., Buffet, S., Chevenet, F., Dufayard, J.F., Guindon, S., Lefort, V., Lescot, M.*, et al.* (2008). Phylogeny.fr: robust phylogenetic analysis for the non-specialist. Nucleic acids research *36*, W465-469.

Dietzl, G., Chen, D., Schnorrer, F., Su, K.C., Barinova, Y., Fellner, M., Gasser, B., Kinsey, K., Oppel, S., Scheiblauer, S.*, et al.* (2007). A genome-wide transgenic RNAi library for conditional gene inactivation in Drosophila. Nature *448*, 151-156.

Doggett, K., Grusche, F.A., Richardson, H.E., and Brumby, A.M. (2011). Loss of the Drosophila cell polarity regulator Scribbled promotes epithelial tissue overgrowth and cooperation with oncogenic Ras-Raf through impaired Hippo pathway signaling. BMC developmental biology *11*, 57.

Dong, J., Feldmann, G., Huang, J., Wu, S., Zhang, N., Comerford, S.A., Gayyed, M.F., Anders, R.A., Maitra, A., and Pan, D. (2007). Elucidation of a universal size-control mechanism in Drosophila and mammals. Cell *130*, 1120-1133.

Drier, E.A., Tello, M.K., Cowan, M., Wu, P., Blace, N., Sacktor, T.C., and Yin, J.C.P. (2002). Memory enhancement and formation by atypical PKM activity in Drosophila melanogaster. Nat Neurosci *5*, 316-324.

Dupont, S., Morsut, L., Aragona, M., Enzo, E., Giulitti, S., Cordenonsi, M., Zanconato, F., Le Digabel, J., Forcato, M., Bicciato, S.*, et al.* (2011). Role of YAP/TAZ in mechanotransduction. Nature *474*, 179-183.

Eaton, S., and Kornberg, T.B. (1990). Repression of ci-D in posterior compartments of Drosophila by engrailed. Genes & development *4*, 1068-1077.

Edgar, B.A. (2006). From cell structure to transcription: Hippo forges a new path. Cell *124*, 267-273.

Edgar, R.C. (2004). MUSCLE: multiple sequence alignment with high accuracy and high throughput. Nucleic acids research *32*, 1792-1797.

Eide, E.J., Woolf, M.F., Kang, H., Woolf, P., Hurst, W., Camacho, F., Vielhaber, E.L., Giovanni, A., and Virshup, D.M. (2005). Control of mammalian circadian rhythm by CKIepsilon-regulated proteasome-mediated PER2 degradation. Molecular and cellular biology *25*, 2795-2807.

Engel, E., Viargues, P., Mortier, M., Taillebourg, E., Couté, Y., Thevenon, D., and Fauvarque, M.-O. (2014). Identifying USPs regulating immune signals in Drosophila: USP2 deubiquitinates Imd and promotes its degradation by interacting with the proteasome. Cell Communication and Signaling *12*, 41.

Enomoto, M., Kizawa, D., Ohsawa, S., and Igaki, T. (2015). JNK signaling is converted from anti- to pro-tumor pathway by Ras-mediated switch of Warts activity. Developmental biology *403*, 162-171.

Feng, Y., and Irvine, K.D. (2007). Fat and expanded act in parallel to regulate growth through warts. Proceedings of the National Academy of Sciences of the United States of America *104*, 20362-20367.

Feng, Y., and Irvine, K.D. (2009). Processing and phosphorylation of the Fat receptor. Proceedings of the National Academy of Sciences of the United States of America *106*, 11989-11994.

Fernandez, B.G., Gaspar, P., Bras-Pereira, C., Jezowska, B., Rebelo, S.R., and Janody, F. (2011). Actin-Capping Protein and the Hippo pathway regulate F-actin and tissue growth in Drosophila. Development *138*, 2337-2346.

Fernando, R.N., Cotter, L., Perrin-Tricaud, C., Berthelot, J., Bartolami, S., Pereira, J.A., Gonzalez, S., Suter, U., and Tricaud, N. (2016). Optimal myelin elongation relies on YAP activation by axonal growth and inhibition by Crb3/Hippo pathway. Nature communications *7*, 12186.

Fletcher, G.C., Elbediwy, A., Khanal, I., Ribeiro, P.S., Tapon, N., and Thompson, B.J. (2015). The Spectrin cytoskeleton regulates the Hippo signalling pathway. The EMBO journal *34*, 940-954.

Fletcher, G.C., Lucas, E.P., Brain, R., Tournier, A., and Thompson, B.J. (2012). Positive feedback and mutual antagonism combine to polarize Crumbs in the Drosophila follicle cell epithelium. Current biology : CB *22*, 1116-1122.

Flores-Benitez, D., and Knust, E. (2016). Dynamics of epithelial cell polarity in Drosophila: how to regulate the regulators? Current opinion in cell biology *42*, 13-21.

Fraile, J.M., Quesada, V., Rodriguez, D., Freije, J.M., and Lopez-Otin, C. (2012). Deubiquitinases in cancer: new functions and therapeutic options. Oncogene *31*, 2373-2388.

Frescas, D., and Pagano, M. (2008). Deregulated proteolysis by the F-box proteins SKP2 and beta-TrCP: tipping the scales of cancer. Nature reviews Cancer *8*, 438-449.

Fuchs, S.Y., Spiegelman, V.S., and Kumar, K.G. (2004). The many faces of beta-TrCP E3 ubiquitin ligases: reflections in the magic mirror of cancer. Oncogene *23*, 2028-2036.

Gailite, I., Aerne, B.L., and Tapon, N. (2015). Differential control of Yorkie activity by LKB1/AMPK and the Hippo/Warts cascade in the central nervous system. Proceedings of the National Academy of Sciences *112*, E5169-E5178.

Ganem, N.J., Cornils, H., Chiu, S.Y., O'Rourke, K.P., Arnaud, J., Yimlamai, D., Thery, M., Camargo, F.D., and Pellman, D. (2014). Cytokinesis failure triggers hippo tumor suppressor pathway activation. Cell *158*, 833-848.

Garcia-Bellido, A. (1975). Genetic control of wing disc development in Drosophila. Ciba Foundation symposium *0*, 161-182.

Gaspar, P., Holder, M.V., Aerne, B.L., Janody, F., and Tapon, N. (2015). Zyxin antagonizes the FERM protein expanded to couple F-actin and Yorkie-dependent organ growth. Current biology : CB *25*, 679-689.

Gateff, E., and Schneiderman, H.A. (1974). Developmental capacities of benign and malignant neoplasms of Drosophila. Roux's Archives of Developmental Biology *176*, 23-65.

Gault, W.J., Olguin, P., Weber, U., and Mlodzik, M. (2012). Drosophila CK1-gamma, gilgamesh, controls PCP-mediated morphogenesis through regulation of vesicle trafficking. The Journal of cell biology *196*, 605-621.

Genevet, A., Polesello, C., Blight, K., Robertson, F., Collinson, L., Pichaud, F., and Tapon, N. (2009). The Hippo pathway regulates apical-domain size independently of its growth-control function. Journal of cell science *122*, 2360-2370.

Genevet, A., and Tapon, N. (2011). The Hippo pathway and apico-basal cell polarity. The Biochemical journal *436*, 213-224.

Genevet, A., Wehr, M.C., Brain, R., Thompson, B.J., and Tapon, N. (2010). Kibra is a regulator of the Salvador/Warts/Hippo signaling network. Developmental cell *18*, 300-308.

Gilbert, M.M., Tipping, M., Veraksa, A., and Moberg, K.H. (2011). A screen for conditional growth suppressor genes identifies the Drosophila homolog of HD-PTP as a regulator of the oncoprotein Yorkie. Developmental cell *20*, 700-712.

Glantschnig, H., Rodan, G.A., and Reszka, A.A. (2002). Mapping of MST1 kinase sites of phosphorylation. Activation and autophosphorylation. The Journal of biological chemistry *277*, 42987-42996.

Golic, K.G., and Lindquist, S. (1989). The FLP recombinase of yeast catalyzes site-specific recombination in the Drosophila genome. Cell *59*, 499-509.

Gong, R., Hong, A.W., Plouffe, S.W., Zhao, B., Liu, G., Yu, F.-X., Xu, Y., and Guan, K.-L. (2015). Opposing roles of conventional and novel PKC isoforms in Hippo-YAP pathway regulation. Cell research *25*, 985-988.

Goulev, Y., Fauny, J.D., Gonzalez-Marti, B., Flagiello, D., Silber, J., and Zider, A. (2008). SCALLOPED interacts with YORKIE, the nuclear effector of the hippo tumor-suppressor pathway in Drosophila. Current biology : CB *18*, 435-441.

Graves, J.D., Draves, K.E., Gotoh, Y., Krebs, E.G., and Clark, E.A. (2001). Both Phosphorylation and Caspase-mediated Cleavage Contribute to Regulation of the Ste20-like Protein Kinase Mst1 during CD95/Fas-induced Apoptosis. Journal of Biological Chemistry *276*, 14909-14915.

Gregorieff, A., Liu, Y., Inanlou, M.R., Khomchuk, Y., and Wrana, J.L. (2015). Yap-dependent reprogramming of Lgr5(+) stem cells drives intestinal regeneration and cancer. Nature *526*, 715-718.

Grima, B., Lamouroux, A., Chelot, E., Papin, C., Limbourg-Bouchon, B., and Rouyer, F. (2002). The F-box protein Slimb controls the levels of clock protiens Period and Timeless. Nature *420*, 178-182.

Grusche, F.A., Degoutin, J.L., Richardson, H.E., and Harvey, K.F. (2011). The Salvador/Warts/Hippo pathway controls regenerative tissue growth in Drosophila melanogaster. Developmental biology *350*, 255-266.

Grzeschik, N.A., Parsons, L.M., Allott, M.L., Harvey, K.F., and Richardson, H.E. (2010). Lgl, aPKC, and Crumbs regulate the Salvador/Warts/Hippo pathway through two distinct mechanisms. Current biology : CB *20*, 573-581.

Guruharsha, K.G., Rual, J.F., Zhai, B., Mintseris, J., Vaidya, P., Vaidya, N., Beekman, C., Wong, C., Rhee, D.Y., Cenaj, O.*, et al.* (2011). A protein complex network of Drosophila melanogaster. Cell *147*, 690-703.

Hafezi, Y., Bosch, J.A., and Hariharan, I.K. (2012). Differences in levels of the transmembrane protein Crumbs can influence cell survival at clonal boundaries. Developmental biology *368*, 358-369.

Halder, G., and Carroll, S.B. (2001). Binding of the Vestigial co-factor switches the DNA-target selectivity of the Scalloped selector protein. Development *128*, 3295-3305.

Halder, G., Polaczyk, P., Kraus, M.E., Hudson, A., Kim, J., Laughon, A., and Carroll, S. (1998). The Vestigial and Scalloped proteins act together to directly regulate wing-specific gene expression in Drosophila. Genes & development *12*, 3900-3909.

Hamaratoglu, F., Affolter, M., and Pyrowolakis, G. (2014). Dpp/BMP signaling in flies: from molecules to biology. Seminars in cell & developmental biology *32*, 128-136.

Hamaratoglu, F., Gajewski, K., Sansores-Garcia, L., Morrison, C., Tao, C., and Halder, G. (2009). The Hippo tumor-suppressor pathway regulates apical-domain size in parallel to tissue growth. Journal of cell science *122*, 2351-2359.

Hamaratoglu, F., Willecke, M., Kango-Singh, M., Nolo, R., Hyun, E., Tao, C., Jafar-Nejad, H., and Halder, G. (2006). The tumour-suppressor genes NF2/Merlin and Expanded act through Hippo signalling to regulate cell proliferation and apoptosis. Nature cell biology *8*, 27-36.

Hancock, J., Paterson, H., and Marshall, C. (1990). A Polybasic Domain or Palmitoylation Is Required in Addition to the CAAX Motif to Localize p21ras to the Plasma Membrane. Cell *63*, 133-139.

Hansen, C.G., Moroishi, T., and Guan, K.L. (2015). YAP and TAZ: a nexus for Hippo signaling and beyond. Trends in cell biology *25*, 499-513.

Hao, Y., Chun, A., Cheung, K., Rashidi, B., and Yang, X. (2008). Tumor suppressor LATS1 is a negative regulator of oncogene YAP. The Journal of biological chemistry *283*, 5496-5509.

Hariharan, I.K. (2015). Organ Size Control: Lessons from Drosophila. Developmental cell *34*, 255-265.

Hariharan, I.K., and Bilder, D. (2006). Regulation of imaginal disc growth by tumor-suppressor genes in Drosophila. Annual review of genetics *40*, 335-361.

Hariharan , I.K., and Haber , D.A. (2003). Yeast, Flies, Worms, and Fish in the Study of Human Disease. New England Journal of Medicine *348*, 2457-2463.

Harris, K.P., and Tepass, U. (2008). Cdc42 and Par proteins stabilize dynamic adherens junctions in the Drosophila neuroectoderm through regulation of apical endocytosis. The Journal of cell biology *183*, 1129-1143.

Harris, T.J., and Peifer, M. (2004). Adherens junction-dependent and -independent steps in the establishment of epithelial cell polarity in Drosophila. The Journal of cell biology *167*, 135-147.

Harris, T.J.C., and Peifer, M. (2007). aPKC Controls Microtubule Organization to Balance Adherens Junction Symmetry and Planar Polarity during Development. Developmental cell *12*, 727-738.

Harvey, K.F., Pfleger, C.M., and Hariharan, I.K. (2003). The Drosophila Mst Ortholog, hippo, Restricts Growth and Cell Proliferation and Promotes Apoptosis. Cell *114*, 457-467.

Harvey, K.F., Zhang, X., and Thomas, D.M. (2013). The Hippo pathway and human cancer. Nature reviews Cancer *13*, 246-257.

Hashimoto, H., Kikuchi, Y., Nogi, Y., and Fukasawa, T. (1983). Regulation of Expression of the Galactose Gene Cluster in *Saccharomyces cerevisiae*: Isolation and Characterization of the Regulatory Gene Gal4. Molecular and General Genetics *191*, 31-38.

Hergovich, A., Schmitz, D., and Hemmings, B.A. (2006). The human tumour suppressor LATS1 is activated by human MOB1 at the membrane. Biochemical and biophysical research communications *345*, 50-58.

Herranz, H., Stamataki, E., Feiguin, F., and Milan, M. (2006). Self-refinement of Notch activity through the transmembrane protein Crumbs: modulation of gamma-secretase activity. EMBO reports *7*, 297-302.

Hirabayashi, S., Baranski, T.J., and Cagan, R.L. (2013). Transformed Drosophila Cells Evade Diet-Mediated Insulin Resistance Through Wingless Signaling. Cell *154*, 664-675.

Hirabayashi, S., and Cagan, R.L. (2015). Salt-inducible kinases mediate nutrient-sensing to link dietary sugar and tumorigenesis in Drosophila. eLife *4*, e08501.

Hirabayashi, S., Nakagawa, K., Sumita, K., Hidaka, S., Kawai, T., Ikeda, M., Kawata, A., Ohno, K., and Hata, Y. (2008). Threonine 74 of MOB1 is a putative key phosphorylation site by MST2 to form the scaffold to activate nuclear Dbf2-related kinase 1. Oncogene *27*, 4281-4292.

Hirate, Y., Hirahara, S., Inoue, K., Suzuki, A., Alarcon, V.B., Akimoto, K., Hirai, T., Hara, T., Adachi, M., Chida, K.*, et al.* (2013). Polarity-dependent distribution of angiomotin localizes Hippo signaling in preimplantation embryos. Current biology : CB *23*, 1181-1194.

Ho, L.L., Wei, X., Shimizu, T., and Lai, Z.C. (2010). Mob as tumor suppressor is activated at the cell membrane to control tissue growth and organ size in Drosophila. Developmental biology *337*, 274-283.

Hong, A.W., Meng, Z., Yuan, H.X., Plouffe, S.W., Moon, S., Kim, W., Jho, E.H., and Guan, K.L. (2017). Osmotic stress-induced phosphorylation by NLK at Ser128 activates YAP. EMBO reports *18*, 72-86.

Hong, J.H., Hwang, E.S., McManus, M.T., Amsterdam, A., Tian, Y., Kalmukova, R., Mueller, E., Benjamin, T., Spiegelman, B.M., Sharp, P.A.*, et al.* (2005). TAZ, a transcriptional modulator of mesenchymal stem cell differentiation. Science *309*, 1074-1078.

Hong, Y., Stronach, B., Perrimon, N., Jan, L.Y., and Jan, Y.N. (2001). Drosophila Stardust interacts with Crumbs to control polarity of epithelia but not neuroblasts. Nature *414*, 634-638.

Hu, L., Xu, J., Yin, M.X., Zhang, L., Lu, Y., Wu, W., Xue, Z., Ho, M.S., Gao, G., Zhao, Y.*, et al.* (2016). Ack promotes tissue growth via phosphorylation and suppression of the Hippo pathway component Expanded. Cell discovery *2*, 15047.

Huang, J., Wu, S., Barrera, J., Matthews, K., and Pan, D. (2005). The Hippo signaling pathway coordinately regulates cell proliferation and apoptosis by inactivating Yorkie, the Drosophila Homolog of YAP. Cell *122*, 421-434.

Hufnagel, L., Teleman, A.A., Rouault, H., Cohen, S.M., and Shraiman, B.I. (2007). On the mechanism of wing size determination in fly development. Proceedings of the National Academy of Sciences of the United States of America *104*, 3835-3840.

Humbert, P.O., Grzeschik, N.A., Brumby, A.M., Galea, R., Elsum, I., and Richardson, H.E. (2008). Control of tumourigenesis by the Scribble/Dlg/Lgl polarity module. Oncogene *27*, 6888-6907.

Hunter, P. (2008). The paradox of model organisms. The use of model organisms in research will continue despite their shortcomings. EMBO reports *9*, 717-720.

Imajo, M., Ebisuya, M., and Nishida, E. (2015). Dual role of YAP and TAZ in renewal of the intestinal epithelium. Nature cell biology *17*, 7-19.

Ishikawa, H., Takeuchi, H., Haltiwanger, R., and Irvine, K.D. (2008). Four-jointed Is a Golgi Kinase That Phosphorylates a Subset of Cadherin Domains. Science *321*, 401-404.

Isono, E., and Nagel, M.K. (2014). Deubiquitylating enzymes and their emerging role in plant biology. Frontiers in plant science *5*, 56.

Jennings, B.H. (2011). Drosophila – a versatile model in biology & medicine. Materials Today *14*, 190-195.

Jia, J., Zhang, L., Zhang, Q., Tong, C., Wang, B., Hou, F., Amanai, K., and Jiang, J. (2005). Phosphorylation by double-time/CKIepsilon and CKIalpha targets cubitus interruptus for Slimb/beta-TRCP-mediated proteolytic processing. Developmental cell *9*, 819-830.

Jia, J., Zhang, W., Wang, B., Trinko, R., and Jiang, J. (2003). The *Drosophila* Ste20 family kinase dMST functions as a tumor suppressor by restricting cell proliferation and promoting apoptosis. Genes & development *17*, 2514-2519.

Jiang, J., and Struhl, G. (1998). Regulation of the Hedgehog and Wingless signalling pathways by the F-box/WD40-repeat protein Slimb. Nature *391*, 493-496.

Johnson, C.P., Tang, H.-Y., Carag, C., Speicher, D.W., and Discher, D.E. (2007). Forced Unfolding of Proteins Within Cells. Science (New York, NY) *317*, 663-666.

Jura, J., Skalniak, L., and Koj, A. (2012). Monocyte chemotactic protein-1-induced protein-1 (MCPIP1) is a novel multifunctional modulator of inflammatory reactions. Biochimica et biophysica acta *1823*, 1905-1913.

Jurgens, G., Wieschaus, E., Nusslein-Volhard, C., and Kluding, H. (1984). Mutations affecting the pattern of the larval cuticle inDrosophila melanogaster : II. Zygotic loci on the third chromosome. Wilhelm Roux's archives of developmental biology *193*, 283-295.

Justice, R., Zilian, O., Woods, D., Noll, M., and Bryant, P. (1995). The Drosophila tumor suppressor gene warts encodes a homolog o-f human myotonic dystrophy kinase and is required for the control of cell shape and proliferation. Genes & development *9*, 534-546.

Kanai, F., Marignani, P.A., Sarbassova, D., Yagi, R., Hall, R.A., Donowitz, M., Hisaminato, A., Fujiwara, T., Ito, Y., Cantley, L.C.*, et al.* (2000). TAZ: a novel

transcriptional co-activator regulated by interactions with 14-3-3 and PDZ domain proteins. The EMBO journal *19*, 6778-6791.

Kango-Singh, M., Nolo, R., Tao, C., Verstreken, P., Hiesinger, P.R., Bellen, H.J., and Halder, G. (2002). Shar-pei mediates cell proliferation arrest during imaginal disc growth in Drosophila. Development *129*, 5719-5730.

Karp, C.M., Tan, T.T., Mathew, R., Nelson, D., Mukherjee, C., Degenhardt, K., Karantza-Wadsworth, V., and White, E. (2008). Role of the polarity determinant crumbs in suppressing mammalian epithelial tumor progression. Cancer research *68*, 4105-4115.

Karpowicz, P., Perez, J., and Perrimon, N. (2010). The Hippo tumor suppressor pathway regulates intestinal stem cell regeneration. Development *137*, 4135-4145.

Kasza, A., Wyrzykowska, P., Horwacik, I., Tymoszuk, P., Mizgalska, D., Palmer, K., Rokita, H., Sharrocks, A.D., and Jura, J. (2010). Transcription factors Elk-1 and SRF are engaged in IL1-dependent regulation of ZC3H12A expression. BMC Molecular Biology *11*, 14.

Kempkens, Ö., Médina, E., Fernandez-Ballester, G., Özüyaman, S., Le Bivic, A., Serrano, L., and Knust, E. (2006). Computer modelling in combination with in vitro studies reveals similar binding affinities of Drosophila Crumbs for the PDZ domains of Stardust and DmPar-6. European Journal of Cell Biology *85*, 753-767.

Khokhlatchev, A., Rabizadeh, S., Xavier, R., Nedwidek, M., Chen, T., Zhang, X.-F., Seed, B., and Avruch, J. (2002). Identification of a Novel Ras-Regulated Proapoptotic Pathway. Current biology : CB *12*, 253-265.

Kim, S., Gailite, I., Moussian, B., Luschnig, S., Goette, M., Fricke, K., Honemann-Capito, M., Grubmüller, H., and Wodarz, A. (2009). Kinase-activity-independent functions of atypical protein kinase C in Drosophila. Journal of cell science *122*, 3759-3771.

Klebba, J.E., Buster, D.W., Nguyen, A.L., Swatkoski, S., Gucek, M., Rusan, N.M., and Rogers, G.C. (2013). Polo-like kinase 4 autodestructs by generating its Slimb-binding phosphodegron. Current biology : CB *23*, 2255-2261.

Klebes, A., and Knust, E. (2000). A conserved motif in Crumbs is required for E-cadherin localisation and zonula adherens formation in Drosophila. Current biology : CB *10*.

Knippschild, U., Gocht, A., Wolff, S., Huber, N., Lohler, J., and Stoter, M. (2005). The casein kinase 1 family: participation in multiple cellular processes in eukaryotes. Cellular signalling *17*, 675-689.

Knippschild, U., Kruger, M., Richter, J., Xu, P., Garcia-Reyes, B., Peifer, C., Halekotte, J., Bakulev, V., and Bischof, J. (2014). The CK1 Family: Contribution to Cellular Stress Response and Its Role in Carcinogenesis. Frontiers in oncology *4*, 96.

Knoblich, J.A., Sauer, K., Jones, L., Richardson, H., Saint, R., and Lehner, C.F. (1994). Cyclin E controls S phase progression and its down-regulation during Drosophila embryogenesis is required for the arrest of cell proliferation. Cell *77*, 107-120.

Ko, H.W., Jiang, J., and Edery, I. (2002). Role for Slimb in the degradation of Drosophila Period protein phosphorylated by Doubletime. Nature *420*, 673-678.

Koenig, J.H., Yamaoka, K., and Ikeda, K. (1998). Omega images at the active zone may be endocytotic rather than exocytotic: Implications for the vesicle hypothesis of transmitter release. Proceedings of the National Academy of Sciences of the United States of America *95*, 12677-12682.

Komander, D., Clague, M.J., and Urbe, S. (2009). Breaking the chains: structure and function of the deubiquitinases. Nature reviews Molecular cell biology *10*, 550-563.

Komander, D., and Rape, M. (2012). The ubiquitin code. Annual review of biochemistry *81*, 203-229.

Komuro, A., Nagai, M., Navin, N.E., and Sudol, M. (2003). WW domain-containing protein YAP associates with ErbB-4 and acts as a co-transcriptional activator for the carboxyl-terminal fragment of ErbB-4 that translocates to the nucleus. The Journal of biological chemistry *278*, 33334-33341.

Koontz, L.M., Liu-Chittenden, Y., Yin, F., Zheng, Y., Yu, J., Huang, B., Chen, Q., Wu, S., and Pan, D. (2013). The Hippo effector Yorkie controls normal tissue growth by antagonizing scalloped-mediated default repression. Developmental cell *25*, 388-401.

Kremerskothen, J., Plaas, C., Büther, K., Finger, I., Veltel, S., Matanis, T., Liedtke, T., and Barnekow, A. (2003). Characterization of KIBRA, a novel WW domain-containing protein. Biochemical and biophysical research communications *300*, 862-867.

Kristariyanto, Y.A., Abdul Rehman, S.A., Weidlich, S., Knebel, A., and Kulathu, Y. (2017). A single MIU motif of MINDY-1 recognizes K48-linked polyubiquitin chains. EMBO reports *18*, 392-402.

Kwon, Y., Vinayagam, A., Sun, X., Dephoure, N., Gygi, S.P., Hong, P., and Perrimon, N. (2013). The Hippo signaling pathway interactome. Science *342*, 737-740.

Lai, Z.C., Wei, X., Shimizu, T., Ramos, E., Rohrbaugh, M., Nikolaidis, N., Ho, L.L., and Li, Y. (2005). Control of cell proliferation and apoptosis by mob as tumor suppressor, mats. Cell *120*, 675-685.

LaJeunesse, D., McCartney, B., and Fehon, R.G. (1998). Structural Analysis of Drosophila Merlin Reveals Functional Domains Important for Growth Control and Subcellular Localization. The Journal of cell biology *141*, 1589-1599.

Lawrence, P.A., and Casal, J. (2013). The mechanisms of planar cell polarity, growth and the Hippo pathway: some known unknowns. Developmental biology *377*, 1-8.

Lawrence, P.A., and Struhl, G. (1996). Morphogens, Compartments, and Pattern: Lessons from Drosophila? Cell *85*, 951-961.

Lee, J.H., Kim, T.S., Yang, T.H., Koo, B.K., Oh, S.P., Lee, K.P., Oh, H.J., Lee, S.H., Kong, Y.Y., Kim, J.M.*, et al.* (2008). A crucial role of WW45 in developing epithelial tissues in the mouse. The EMBO journal *27*, 1231-1242.

Lee, K.-K., Ohyama, T., Yajima, N., Tsubuki, S., and Yonehara, S. (2001). MST, a Physiological Caspase Substrate, Highly Sensitizes Apoptosis Both Upstream and Downstream of Caspase Activation. Journal of Biological Chemistry *276*, 19276-19285.

Lee, K.K., and Yonehara, S. (2002). Phosphorylation and dimerization regulate nucleocytoplasmic shuttling of mammalian STE20-like kinase (MST). The Journal of biological chemistry *277*, 12351-12358.

Lee, M.J., Ran Byun, M., Furutani-Seiki, M., Hong, J.H., and Jung, H.S. (2014). YAP and TAZ regulate skin wound healing. The Journal of investigative dermatology *134*, 518-525.

Lee, T., and Luo, L. (1999). Mosaic analysis with a repressible cell marker for studies of gene function in neuronal morphogenesis. Neuron *22*, 451-461.

Legent, K., Steinhauer, J., Richard, M., and Treisman, J.E. (2012). A screen for X-linked mutations affecting Drosophila photoreceptor differentiation identifies Casein kinase 1alpha as an essential negative regulator of wingless signaling. Genetics *190*, 601-616.

Lehtinen, M.K., Yuan, Z., Boag, P.R., Yang, Y., Villen, J., Becker, E.B., DiBacco, S., de la Iglesia, N., Gygi, S., Blackwell, T.K.*, et al.* (2006). A conserved MST-FOXO signaling pathway mediates oxidative-stress responses and extends life span. Cell *125*, 987-1001.

Lei, Q.Y., Zhang, H., Zhao, B., Zha, Z.Y., Bai, F., Pei, X.H., Zhao, S., Xiong, Y., and Guan, K.L. (2008). TAZ promotes cell proliferation and epithelial-mesenchymal transition and is inhibited by the hippo pathway. Molecular and cellular biology *28*, 2426-2436.

Letizia, A., Ricardo, S., Moussian, B., Martin, N., and Llimargas, M. (2013). A functional role of the extracellular domain of Crumbs in cell architecture and apicobasal polarity. Journal of cell science *126*, 2157-2163.

Li, Q., Li, S., Mana-Capelli, S., Roth Flach, R.J., Danai, L.V., Amcheslavsky, A., Nie, Y., Kaneko, S., Yao, X., Chen, X.*, et al.* (2014a). The conserved misshapen-warts-Yorkie pathway acts in enteroblasts to regulate intestinal stem cells in Drosophila. Developmental cell *31*, 291-304.

Li, S., Cho, Y.S., Yue, T., Ip, Y.T., and Jiang, J. (2015). Overlapping functions of the MAP4K family kinases Hppy and Msn in Hippo signaling. Cell discovery *1*, 15038.

Li, S., Li, S., Han, Y., Tong, C., Wang, B., Chen, Y., and Jiang, J. (2016). Regulation of Smoothened Phosphorylation and High-Level Hedgehog Signaling Activity by a Plasma Membrane Associated Kinase. PLoS biology *14*, e1002481.

Li, W., Cooper, J., Zhou, L., Yang, C., Erdjument-Bromage, H., Zagzag, D., Snuderl, M., Ladanyi, M., Hanemann, C.O., Zhou, P.*, et al.* (2014b). Merlin/NF2 Loss-Driven Tumorigenesis Linked to CRL4(DCAF1)-Mediated Inhibition of the Hippo Pathway Kinases Lats1 and 2 in the Nucleus. Cancer cell *26*, 48-60.

Liang, J., Saad, Y., Lei, T., Wang, J., Qi, D., Yang, Q., Kolattukudy, P.E., and Fu, M. (2010). MCP-induced protein 1 deubiquitinates TRAF proteins and negatively regulates JNK and NF-kappaB signaling. The Journal of experimental medicine *207*, 2959-2973.

Lin, Y.H., Currinn, H., Pocha, S.M., Rothnie, A., Wassmer, T., and Knust, E. (2015). AP-2-complex-mediated endocytosis of Drosophila Crumbs regulates polarity by antagonizing Stardust. Journal of cell science *128*, 4538-4549.

Ling, C., Zheng, Y., Yin, F., Yu, J., Huang, J., Wu, S., and Pan, D. (2010). The apical transmembrane protein Crumbs functions as a tumor suppressor that regulates Hippo signaling by binding to Expanded. Proceedings of the National Academy of Sciences of the United States of America *107*, 10532–10537.

Liu, B., Zheng, Y., Yin, F., Yu, J., Silverman, N., and Pan, D. (2016). Toll Receptor-Mediated Hippo Signaling Controls Innate Immunity in Drosophila. Cell *164*, 406-419.

Liu, C., Li, Y., Semenov, M., Han, C., Baeg, G.H., Tan, Y., Zhang, Z., Lin, X., and He, X. (2002). Control of beta-catenin phosphorylation/degradation by a dual-kinase mechanism. Cell *108*, 837-847.

Lv, M., Lv, M., Chen, L., Qin, T., Zhang, X., Liu, P., and Yang, J. (2015). Angiomotin promotes breast cancer cell proliferation and invasion. Oncology reports *33*, 1938-1946.

Ma, B., Chen, Y., Chen, L., Cheng, H., Mu, C., Li, J., Gao, R., Zhou, C., Cao, L., Liu, J., *et al.* (2015). Hypoxia regulates Hippo signalling through the SIAH2 ubiquitin E3 ligase. Nature cell biology *17*, 95-103.

Ma, B., Cheng, H., Gao, R., Mu, C., Chen, L., Wu, S., Chen, Q., and Zhu, Y. (2016). Zyxin-Siah2-Lats2 axis mediates cooperation between Hippo and TGF-beta signalling pathways. Nature communications *7*, 11123.

Ma, D., Yang, C.-h., McNeill, H., Simon, M.A., and Axelrod, J.D. (2003). Fidelity in planar cell polarity signalling. Nature *421*, 543-547.

Macia, E., Ehrlich, M., Massol, R., Boucrot, E., Brunner, C., and Kirchhausen, T. (2006). Dynasore, a cell-permeable inhibitor of dynamin. Developmental cell *10*, 839-850.

Mahoney, P., Weber, U., Onofrechuk, P., Biessmann, H., Bryant, P., and Goodman, C. (1991). The *fat* tumor suppressor gene in *Drosophila* encodes a novel member of the cadherin gene superfamily. Cell *67*, 853-868.

Mahul-Mellier, A.L., Datler, C., Pazarentzos, E., Lin, B., Chaisaklert, W., Abuali, G., and Grimm, S. (2012a). De-ubiquitinating proteases USP2a and USP2c cause apoptosis by stabilising RIP1. Biochimica et biophysica acta *1823*, 1353-1365.

Mahul-Mellier, A.L., Pazarentzos, E., Datler, C., Iwasawa, R., AbuAli, G., Lin, B., and Grimm, S. (2012b). De-ubiquitinating protease USP2a targets RIP1 and TRAF2 to mediate cell death by TNF. Cell death and differentiation *19*, 891-899.

Mailand, N., Gibbs-Seymour, I., and Bekker-Jensen, S. (2013). Regulation of PCNA-protein interactions for genome stability. Nature reviews Molecular cell biology *14*, 269-282.

Maitra, S., Kulikauskas, R.M., Gavilan, H., and Fehon, R.G. (2006). The tumor suppressors Merlin and Expanded function cooperatively to modulate receptor endocytosis and signaling. Current biology : CB *16*, 702-709.

Manning, S.A., and Harvey, K.F. (2015). Warts Opens Up for Activation. Developmental cell *35*, 666-668.

Mao, Y., Kucuk, B., and Irvine, K.D. (2009). Drosophila lowfat, a novel modulator of Fat signaling. Development *136*, 3223-3233.

Mao, Y., Rauskolb, C., Cho, E., Hu, W.L., Hayter, H., Minihan, G., Katz, F.N., and Irvine, K.D. (2006). Dachs: an unconventional myosin that functions downstream of Fat to regulate growth, affinity and gene expression in Drosophila. Development *133*, 2539-2551.

Martin, A.C., Kaschube, M., and Wieschaus, E.F. (2009). Pulsed contractions of an actin-myosin network drive apical constriction. Nature *457*, 495-499.

Martinek, S., Inonog, S., Manoukian, A.S., and Young, M.W. (2001). A role for the segment polarity gene shaggy/GSK-3 in the Drosophila circadian clock. Cell *105*, 769-779.

Matakatsu, H., and Blair, S.S. (2004). Interactions between Fat and Dachsous and the regulation of planar cell polarity in the Drosophila wing. Development *131*, 3785-3794.

Matakatsu, H., and Blair, S.S. (2006). Separating the adhesive and signaling functions of the Fat and Dachsous protocadherins. Development *133*, 2315-2324.

Matakatsu, H., and Blair, S.S. (2008). The DHHC palmitoyltransferase approximated regulates Fat signaling and Dachs localization and activity. Current biology : CB *18*, 1390-1395.

Matakatsu, H., Blair, S.S., and Fehon, R.G. (2017). The palmitoyltransferase Approximated promotes growth via the Hippo pathway by palmitoylation of Fat. The Journal of cell biology *216*, 265-277.

Matis, M., and Axelrod, J.D. (2013). Regulation of PCP by the Fat signaling pathway. Genes & development *27*, 2207-2220.

Matsushita, K., Takeuchi, O., Standley, D.M., Kumagai, Y., Kawagoe, T., Miyake, T., Satoh, T., Kato, H., Tsujimura, T., Nakamura, H.*, et al.* (2009). ZC3H12A is an RNase essential for controlling immune responses by regulating mRNA decay. Nature *458*.

McCartney, B., Kulikauskas, R., LaJeunesse, D., and Fehon, R.G. (2000). The neurofibromatosis-2 homologue, Merlin, and the tumor suppressor expanded function together in Drosophila to regulate cell proliferation and differentiation. Development *127*, 1315-1324.

McNeill, H., and Woodgett, J.R. (2010). When pathways collide: collaboration and connivance among signalling proteins in development. Nature reviews Molecular cell biology *11*, 404-413.

Meng, F., and Sachs, F. (2012). Orientation-based FRET sensor for real-time imaging of cellular forces. Journal of cell science *125*, 743-750.

Meng, Z., Moroishi, T., and Guan, K.-L. (2016). Mechanisms of Hippo pathway regulation. Genes & development *30*, 1-17.

Meng, Z., Moroishi, T., Mottier-Pavie, V., Plouffe, S.W., Hansen, C.G., Hong, A.W., Park, H.W., Mo, J.S., Lu, W., Lu, S.*, et al.* (2015). MAP4K family kinases act in parallel to MST1/2 to activate LATS1/2 in the Hippo pathway. Nature communications *6*, 8357.

Metzger, M.B., Hristova, V.A., and Weissman, A.M. (2012). HECT and RING finger families of E3 ubiquitin ligases at a glance. Journal of cell science *125*, 531-537.

Miller, D.T., and Cagan, R.L. (1998). Local induction of patterning and programmed cell death in the developing Drosophila retina. Development *125*, 2327-2335.

Miller, E., Yang, J., DeRan, M., Wu, C., Su, Andrew I., Bonamy, Ghislain M.C., Liu, J., Peters, Eric C., and Wu, X. (2012). Identification of Serum-Derived Sphingosine-1-Phosphate as a Small Molecule Regulator of YAP. Chemistry & Biology *19*, 955-962.

Misra, J.R., and Irvine, K.D. (2016). Vamana Couples Fat Signaling to the Hippo Pathway. Developmental cell *39*, 254-266.

Mo, J.S., Meng, Z., Kim, Y.C., Park, H.W., Hansen, C.G., Kim, S., Lim, D.S., and Guan, K.L. (2015). Cellular energy stress induces AMPK-mediated regulation of YAP and the Hippo pathway. Nature cell biology *17*, 500-510.

Mo, J.S., Yu, F.X., Gong, R., Brown, J.H., and Guan, K.L. (2012). Regulation of the Hippo-YAP pathway by protease-activated receptors (PARs). Genes & development *26*, 2138-2143.

Mohr, O.L. (1923). Modifications of the sex-ratio through a sex-linked semi-lethal in Drosophila melanogaster. (Besides notes on an autosomal section deficiency). Studia Mendeliana, ad centesimum diem natalem Gregorii Mendelii a grata patria celebrandum, adiuvante ministerio Pragensi edita, 266-287.

Moleirinho, S., Guerrant, W., and Kissil, J.L. (2014). The Angiomotins - From discovery to function. FEBS letters.

Moleirinho, S., Hoxha, S., Mandati, V., Curtale, G., Troutman, S., Ehmer, U., and Kissil, J.L. (2017). Regulation of localization and function of the transcriptional co-activator YAP by angiomotin. Elife *6*.

Moleirinho, S., Tilston-Lunel, A., Angus, L., Gunn-Moore, F., and Reynolds, P.A. (2013). The expanding family of FERM proteins. The Biochemical journal *452*, 183-193.

Moon, S., Kim, W., Kim, S., Kim, Y., Song, Y., Bilousov, O., Kim, J., Lee, T., Cha, B., Kim, M.*, et al.* (2017). Phosphorylation by NLK inhibits YAP-14-3-3-interactions and induces its nuclear localization. EMBO reports *18*, 61-71.

Morais-de-Sa, E., Mirouse, V., and St Johnston, D. (2010). aPKC phosphorylation of Bazooka defines the apical/lateral border in Drosophila epithelial cells. Cell *141*, 509-523.

Morais-de-Sa, E., Vega-Rioja, A., Trovisco, V., and St Johnston, D. (2013). Oskar is targeted for degradation by the sequential action of Par-1, GSK-3, and the SCF(-)Slimb ubiquitin ligase. Developmental cell *26*, 303-314.

Morata, G., and Lawrence, P.A. (1975). Control of compartment development by the engrailed gene in Drosophila. Nature *255*, 614-617.

Morgan, T.H. (1910). Sex limited inheritance in Drosophila. Science *32*, 120-122.

Morin, X., Daneman, R., Zavortink, M., and Chia, W. (2001). A protein trap strategy to detect GFP-tagged proteins expressed from their endogenous loci in Drosophila. Proceedings of the National Academy of Sciences of the United States of America *98*, 15050-15055.

Moroishi, T., Hayashi, T., Pan, W.W., Fujita, Y., Holt, M.V., Qin, J., Carson, D.A., and Guan, K.L. (2016). The Hippo Pathway Kinases LATS1/2 Suppress Cancer Immunity. Cell *167*, 1525-1539 e1517.

Morrison, H., Sherman, L.S., Legg, J., Banine, F., Isacke, C., Haipek, C.A., Gutmann, D.H., Ponta, H., and Herrlich, P. (2001). The NF2 tumor suppressor gene product, merlin, mediates contact inhibition of growth through interactions with CD44. Genes & development *15*, 968-980.

Mukhopadhyay, D., and Riezman, H. (2007). Proteasome-independent functions of ubiquitin in endocytosis and signaling. Science *315*, 201-205.

Muller, H.A., and Wieschaus, E. (1996). armadillo, bazooka, and stardust are critical for early stages in formation of the zonula adherens and maintenance of the polarized blastoderm epithelium in Drosophila. The Journal of cell biology *134*, 149-163.

Muller, H.J. (1928). The measurement of gene mutation rate in Drosophila, its high variability, and its dependence upon temperature. Genetics *13*, 279-357.

Murakami, M., Nakagawa, M., Olson, E.N., and Nakagawa, O. (2005). A WW domain protein TAZ is a critical coactivator for TBX5, a transcription factor implicated in Holt-Oram syndrome. Proceedings of the National Academy of Sciences of the United States of America *102*, 18034-18039.

Murakami, M., Tominaga, J., Makita, R., Uchijima, Y., Kurihara, Y., Nakagawa, O., Asano, T., and Kurihara, H. (2006). Transcriptional activity of Pax3 is co-activated by TAZ. Biochemical and biophysical research communications *339*, 533-539.

Narimatsu, M., Samavarchi-Tehrani, P., Varelas, X., and Wrana, J.L. (2015). Distinct polarity cues direct Taz/Yap and TGFbeta receptor localization to differentially control TGFbeta-induced Smad signaling. Developmental cell *32*, 652-656.

Nemetschke, L., and Knust, E. (2016). Drosophila Crumbs prevents ectopic Notch activation in developing wings by inhibiting ligand-independent endocytosis. Development *143*, 4543-4553.

Neto-Silva, R.M., de Beco, S., and Johnston, L.A. (2010). Evidence for a growth-stabilizing regulatory feedback mechanism between Myc and Yorkie, the Drosophila homolog of Yap. Developmental cell *19*, 507-520.

Neufeld, T.P., de la Cruz, A.F., Johnston, L.A., and Edgar, B.A. (1998). Coordination of growth and cell division in the Drosophila wing. Cell *93*, 1183-1193.

Nguyen, H.T., Andrejeva, D., Gupta, R., Choudhary, C., Hong, X., Eichhorn, P.J., Loya, A.C., and Cohen, S.M. (2016). Deubiquitylating enzyme USP9x regulates hippo pathway activity by controlling angiomotin protein turnover. Cell discovery *2*, 16001.

Nguyen, H.T., Kugler, J.M., and Cohen, S.M. (2017). DUB3 Deubiquitylating Enzymes Regulate Hippo Pathway Activity by Regulating the Stability of ITCH, LATS and AMOT Proteins. PloS one *12*, e0169587.

Ni, L., Zheng, Y., Hara, M., Pan, D., and Luo, X. (2015). Structural basis for Mob1-dependent activation of the core Mst-Lats kinase cascade in Hippo signaling. Genes & development *29*, 1416-1431.

Niu, J., Shi, Y., Xue, J., Miao, R., Huang, S., Wang, T., Wu, J., Fu, M., and Wu, Z.H. (2013). USP10 inhibits genotoxic NF-kappaB activation by MCPIP1-facilitated deubiquitination of NEMO. The EMBO journal *32*, 3206-3219.

Nolo, R., Morrison, C.M., Tao, C., Zhang, X., and Halder, G. (2006). The bantam microRNA is a target of the hippo tumor-suppressor pathway. Current biology : CB *16*, 1895-1904.

Oh, H., and Irvine, K.D. (2008). In vivo regulation of Yorkie phosphorylation and localization. Development *135*, 1081-1088.

Oh, H., and Irvine, K.D. (2009). In vivo analysis of Yorkie phosphorylation sites. Oncogene *28*, 1916-1927.

Oh, H., and Irvine, K.D. (2011). Cooperative regulation of growth by Yorkie and Mad through bantam. Developmental cell *20*, 109-122.

Oh, H., Reddy, B.V., and Irvine, K.D. (2009). Phosphorylation-independent repression of Yorkie in Fat-Hippo signaling. Developmental biology *335*, 188-197.

Oh, K.H., Yang, S.W., Park, J.M., Seol, J.H., Iemura, S., Natsume, T., Murata, S., Tanaka, K., Jeon, Y.J., and Chung, C.H. (2011). Control of AIF-mediated cell death by antagonistic functions of CHIP ubiquitin E3 ligase and USP2 deubiquitinating enzyme. Cell death and differentiation *18*.

Ohnishi, S., Guntert, P., Koshiba, S., Tomizawa, T., Akasaka, R., Tochio, N., Sato, M., Inoue, M., Harada, T., Watanabe, S.*, et al.* (2007). Solution structure of an atypical WW domain in a novel beta-clam-like dimeric form. FEBS letters *581*, 462-468.

Oka, T., Schmitt, A.P., and Sudol, M. (2012). Opposing roles of angiomotin-like-1 and zona occludens-2 on pro-apoptotic function of YAP. Oncogene *31*, 128-134.

Orenic, T.V., Slusarski, D.C., Kroll, K.L., and Holmgren, R.A. (1990). Cloning and characterization of the segment polarity gene cubitus interruptus Dominant of Drosophila. Genes & development *4*, 1053-1067.

Pagliarini, R.A., and Xu, T. (2003). A genetic screen in Drosophila for metastatic behavior. Science *302*, 1227-1231.

Pan, G., Feng, Y., Ambegaonkar, A.A., Sun, G., Huff, M., Rauskolb, C., and Irvine, K.D. (2013). Signal transduction by the Fat cytoplasmic domain. Development *140*, 831-842.

Pantalacci, S., Tapon, N., and Leopold, P. (2003). The Salvador partner Hippo promotes apoptosis and cell-cycle exit in Drosophila. Nature cell biology *5*, 921-927.

Paramasivam, M., Sarkeshik, A., Yates, J.R., 3rd, Fernandes, M.J., and McCollum, D. (2011). Angiomotin family proteins are novel activators of the LATS2 kinase tumor suppressor. Molecular biology of the cell *22*, 3725-3733.

Park, K.S., Whitsett, J.A., Di Palma, T., Hong, J.H., Yaffe, M.B., and Zannini, M. (2004). TAZ interacts with TTF-1 and regulates expression of surfactant protein-C. The Journal of biological chemistry *279*, 17384-17390.

Parsons, L.M., Grzeschik, N.A., and Richardson, H.E. (2014). lgl Regulates the Hippo Pathway Independently of Fat/Dachs, Kibra/Expanded/Merlin and dRASSF/dSTRIPAK. Cancers *6*, 879-896.

Pefani, D.E., Pankova, D., Abraham, A.G., Grawenda, A.M., Vlahov, N., Scrace, S., and E, O.N. (2016). TGF-beta Targets the Hippo Pathway Scaffold RASSF1A to Facilitate YAP/SMAD2 Nuclear Translocation. Molecular cell *63*, 156-166.

Peifer, M., Sweeton, D., Casey, M., and Wieschaus, E. (1994). wingless signal and zeste-white 3 kinase trigger opposing changes in the intracellular distribution of armadillo. Development *120*, 369-380.

Pellikka, M., Tanentzapf, G., Pinto, M., Smith, C., McGlade, C.J., Ready, D.F., and Tepass, U. (2002). Crumbs, the Drosophila homologue of human CRB1/RP12, is essential for photoreceptor morphogenesis. Nature *416*, 143-149.

Pellock, B.J., Buff, E., White, K., and Hariharan, I.K. (2007). The Drosophila tumor suppressors Expanded and Merlin differentially regulate cell cycle exit, apoptosis, and Wingless signaling. Developmental biology *304*, 102-115.

Penalva, C., and Mirouse, V. (2012). Tissue-specific function of Patj in regulating the Crumbs complex and epithelial polarity. Development *139*, 4549-4554.

Peng, H.W., Slattery, M., and Mann, R.S. (2009). Transcription factor choice in the Hippo signaling pathway: homothorax and yorkie regulation of the microRNA bantam in the progenitor domain of the Drosophila eye imaginal disc. Genes & development *23*, 2307-2319.

Perez-Mockus, G., Roca, V., Mazouni, K., and Schweisguth, F. (2017). Neuralized regulates Crumbs endocytosis and epithelium morphogenesis via specific Stardust isoforms. The Journal of cell biology *216*, 1405-1420.

Perrimon, N., Ni, J.Q., and Perkins, L. (2010). In vivo RNAi: today and tomorrow. Cold Spring Harbor perspectives in biology *2*, a003640.

Petroski, M.D., and Deshaies, R.J. (2005). Function and regulation of cullin-RING ubiquitin ligases. Nature reviews Molecular cell biology *6*, 9-20.

Phillips, R.G., Roberts, I.J., Ingham, P.W., and Whittle, J.R. (1990). The Drosophila segment polarity gene patched is involved in a position-signalling mechanism in imaginal discs. Development *110*, 105-114.

Pickart, C.M., and Eddins, M.J. (2004). Ubiquitin: structures, functions, mechanisms. Biochimica et biophysica acta *1695*, 55-72.

Pocha, S.M., Wassmer, T., Niehage, C., Hoflack, B., and Knust, E. (2011). Retromer controls epithelial cell polarity by trafficking the apical determinant Crumbs. Current biology : CB *21*, 1111-1117.

Polesello, C., Huelsmann, S., Brown, N.H., and Tapon, N. (2006). The Drosophila RASSF homolog antagonizes the hippo pathway. Current biology : CB *16*, 2459-2465.

Poon, C.L., Lin, J.I., Zhang, X., and Harvey, K.F. (2011). The sterile 20-like kinase Tao-1 controls tissue growth by regulating the Salvador-Warts-Hippo pathway. Developmental cell *21*, 896-906.

Popovic, D., Vucic, D., and Dikic, I. (2014). Ubiquitination in disease pathogenesis and treatment. Nature medicine *20*, 1242-1253.

Port, F., Chen, H.M., Lee, T., and Bullock, S.L. (2014). Optimized CRISPR/Cas tools for efficient germline and somatic genome engineering in Drosophila. Proceedings of the National Academy of Sciences of the United States of America *111*, E2967-2976.

Praskova, M., Xia, F., and Avruch, J. (2008). MOBKL1A/MOBKL1B phosphorylation by MST1 and MST2 inhibits cell proliferation. Current biology : CB *18*, 311-321.

Price, J.L., Blau, J., Rothenfluh, A., Abodeely, M., Kloss, B., and Young, M.W. (1998). double-time Is a Novel Drosophila Clock Gene that Regulates PERIOD Protein Accumulation. Cell *94*, 83-95.

Price, M.A. (2006). CKI, there's more than one: casein kinase I family members in Wnt and Hedgehog signaling. Genes & development *20*, 399-410.

Price, M.A., and Kalderon, D. (2002). Proteolysis of the Hedgehog signaling effector Cubitus interruptus requires phosphorylation by Glycogen Synthase Kinase 3 and Casein Kinase 1. Cell *108*, 823-835.

Ragni, C.V., Diguet, N., Le Garrec, J.F., Novotova, M., Resende, T.P., Pop, S., Charon, N., Guillemot, L., Kitasato, L., Badouel, C*., et al.* (2017). Amotl1 mediates sequestration of the Hippo effector Yap1 downstream of Fat4 to restrict heart growth. Nature communications *8*, 14582.

Rauskolb, C., Sun, S., Sun, G., Pan, Y., and Irvine, K.D. (2014). Cytoskeletal Tension Inhibits Hippo Signaling through an Ajuba-Warts Complex. Cell *158*, 143-156.

Rawls, A.S., Guinto, J.B., and Wolff, T. (2002). The cadherins fat and dachsous regulate dorsal/ventral signaling in the Drosophila eye. Current biology : CB *12*, 1021-1026.

Reddy, B.V., and Irvine, K.D. (2008). The Fat and Warts signaling pathways: new insights into their regulation, mechanism and conservation. Development *135*, 2827-2838.

Reddy, B.V., and Irvine, K.D. (2011). Regulation of Drosophila glial cell proliferation by Merlin-Hippo signaling. Development *138*, 5201-5212.

Reiter, L.T., Potocki, L., Chien, S., Gribskov, M., and Bier, E. (2001). A systematic analysis of human disease-associated gene sequences in Drosophila melanogaster. Genome research *11*, 1114-1125.

Ren, F., Wang, B., Yue, T., Yun, E.-Y., Ip, T., and Jiang, J. (2010a). Hippo signaling regulates *Drosophila* intestine stem cell proliferation through multiple pathways. PNAS *107*, 21064-21069.

Ren, F., Zhang, L., and Jiang, J. (2010b). Hippo signaling regulates Yorkie nuclear localization and activity through 14-3-3 dependent and independent mechanisms. Developmental biology *337*, 303-312.

Reyes-Turcu, F.E., Ventii, K.H., and Wilkinson, K.D. (2009). Regulation and cellular roles of ubiquitin-specific deubiquitinating enzymes. Annual review of biochemistry *78*, 363-397.

Ribeiro, P., Holder, M., Frith, D., Snijders, A.P., and Tapon, N. (2014). Crumbs promotes expanded recognition and degradation by the SCFSlimb/beta-TrCP ubiquitin ligase. Proceedings of the National Academy of Sciences of the United States of America.

Ribeiro, P.S., Josué, F., Wepf, A., Wehr, M.C., Rinner, O., Kelly, G., Tapon, N., and Gstaiger, M. (2010). Combined Functional Genomic and Proteomic Approaches Identify a PP2A Complex as a Negative Regulator of Hippo Signaling. Molecular cell *39*, 521-534.

Richardson, E.C., and Pichaud, F. (2010). Crumbs is required to achieve proper organ size control during Drosophila head development. Development *137*, 641-650.

Richardson, H.E., and Portela, M. (2017). Tissue growth and tumorigenesis in Drosophila: cell polarity and the Hippo pathway. Current opinion in cell biology *48*, 1-9.

Rincon-Limas, D.E., Lu, C.H., Canal, I., Calleja, M., Rodriguez-Esteban, C., Izpisua-Belmonte, J.C., and Botas, J. (1999). Conservation of the expression and function of apterous orthologs in Drosophila and mammals. Proceedings of the National Academy of Sciences of the United States of America *96*, 2165-2170.

Robinson, B.S., Huang, J., Hong, Y., and Moberg, K.H. (2010). Crumbs regulates Salvador/Warts/Hippo signaling in Drosophila via the FERM-domain protein Expanded. Current biology : CB *20*, 582-590.

Rodrigues-Campos, M., and Thompson, B.J. (2014). The ubiquitin ligase FbxL7 regulates the Dachsous-Fat-Dachs system in Drosophila. Development.

Rodriguez, I. (2004). The dachsous gene, a member of the cadherin family, is required for Wg-dependent pattern formation in the Drosophila wing disc. Development *131*, 3195-3206.

Roeth, J.F., Sawyer, J.K., Wilner, D.A., and Peifer, M. (2009). Rab11 helps maintain apical crumbs and adherens junctions in the Drosophila embryonic ectoderm. PloS one *4*, e7634.

Rogulja, D., Rauskolb, C., and Irvine, K.D. (2008). Morphogen control of wing growth through the Fat signaling pathway. Developmental cell *15*, 309-321.

Roper, K. (2012). Anisotropy of Crumbs and aPKC drives myosin cable assembly during tube formation. Developmental cell *23*, 939-953.

Rubin, G.M., and Lewis, E.B. (2000). A brief history of Drosophila's contributions to genome research. Science *287*, 2216-2218.

Rubin, G.M., and Spradling, A.C. (1982). Genetic transformation of Drosophila with transposable element vectors. Science *218*, 348-353.

Salah, Z., and Aqeilan, R.I. (2011). WW domain interactions regulate the Hippo tumor suppressor pathway. Cell death & disease *2*, e172.

Sansores-Garcia, L., Bossuyt, W., Wada, K., Yonemura, S., Tao, C., Sasaki, H., and Halder, G. (2011). Modulating F-actin organization induces organ growth by affecting the Hippo pathway. The EMBO journal *30*, 2325-2335.

Santinon, G., Pocaterra, A., and Dupont, S. (2016). Control of YAP/TAZ Activity by Metabolic and Nutrient-Sensing Pathways. Trends in cell biology *26*, 289-299.

Scheel, H., and Hofmann, K. (2003). A novel interaction motif, SARAH, connects three classes of tumor suppressor. Current biology : CB *13*, R899-900.

Schittek, B., and Sinnberg, T. (2014). Biological functions of casein kinase 1 isoforms and putative roles in tumorigenesis. Molecular cancer *13*, 231.

Schlegelmilch, K., Mohseni, M., Kirak, O., Pruszak, J., Rodriguez, J.R., Zhou, D., Kreger, B.T., Vasioukhin, V., Avruch, J., Brummelkamp, T.R.*, et al.* (2011). Yap1 acts downstream of alpha-catenin to control epidermal proliferation. Cell *144*, 782-795.

Schneider, I. (1972). Cell lines derived from late embryonic stages of Drosophila melanogaster. Journal of Embryology and Experimental Morphology *27*, 353-365.

Schwank, G., Tauriello, G., Yagi, R., Kranz, E., Koumoutsakos, P., and Basler, K. (2011). Antagonistic growth regulation by Dpp and Fat drives uniform cell proliferation. Developmental cell *20*, 123-130.

Sebe-Pedros, A., Zheng, Y., Ruiz-Trillo, I., and Pan, D. (2012). Premetazoan origin of the hippo signaling pathway. Cell reports *1*, 13-20.

Senecoff, J.F., Bruckner, R.C., and Cox, M.M. (1985). The FLP recombinase of the yeast 2-micron plasmid: characterization of its recombination site. Proceedings of the National Academy of Sciences of the United States of America *82*, 7270-7274.

Shaw, R.L., Kohlmaier, A., Polesello, C., Veelken, C., Edgar, B.A., and Tapon, N. (2010). The Hippo pathway regulates intestinal stem cell proliferation during Drosophila adult midgut regeneration. Development *137*, 4147-4158.

Silva, E., Tsatskis, Y., Gardano, L., Tapon, N., and McNeill, H. (2006). The tumor-suppressor gene fat controls tissue growth upstream of expanded in the hippo signaling pathway. Current biology : CB *16*, 2081-2089.

Simmonds, A.J., Liu, X., Soanes, K.H., Krause, H.M., Irvine, K.D., and Bell, J.B. (1998). Molecular interactions between Vestigial and Scalloped promote wing formation in Drosophila. Genes & development *12*, 3815-3820.

Simon, M.A., Xu, A., Ishikawa, H.O., and Irvine, K.D. (2010). Modulation of fat:dachsous binding by the cadherin domain kinase four-jointed. Current biology : CB *20*, 811-817.

Sisco, M., Kryger, Z.B., O'Shaughnessy, K.D., Kim, P.S., Schultz, G.S., Ding, X.Z., Roy, N.K., Dean, N.M., and Mustoe, T.A. (2008). Antisense inhibition of connective tissue growth factor (CTGF/CCN2) mRNA limits hypertrophic scarring without affecting wound healing in vivo. Wound repair and regeneration : official publication of the Wound Healing Society [and] the European Tissue Repair Society *16*, 661-673.

Skaar, J.R., Pagan, J.K., and Pagano, M. (2013). Mechanisms and function of substrate recruitment by F-box proteins. Nature reviews Molecular cell biology *14*, 369-381.

Skalniak, L., Mizgalska, D., Zarebski, A., Wyrzykowska, P., Koj, A., and Jura, J. (2009). Regulatory feedback loop between NF-kappaB and MCP-1-induced protein 1 RNase. The FEBS journal *276*, 5892-5905.

Smelkinson, M.G., Zhou, Q., and Kalderon, D. (2007). Regulation of Ci-SCFSlimb binding, Ci proteolysis, and hedgehog pathway activity by Ci phosphorylation. Developmental cell *13*, 481-495.

Sopko, R., Silva, E., Clayton, L., Gardano, L., Barrios-Rodiles, M., Wrana, J., Varelas, X., Arbouzova, N.I., Shaw, S., Saburi, S.*, et al.* (2009). Phosphorylation of the tumor suppressor fat is regulated by its ligand Dachsous and the kinase discs overgrown. Current biology : CB *19*, 1112-1117.

Sorrentino, G., Ruggeri, N., Specchia, V., Cordenonsi, M., Mano, M., Dupont, S., Manfrin, A., Ingallina, E., Sommaggio, R., Piazza, S.*, et al.* (2014). Metabolic control of YAP and TAZ by the mevalonate pathway. Nature cell biology *16*, 357-366.

Sotillos, S., Diaz-Meco, M.T., Caminero, E., Moscat, J., and Campuzano, S. (2004). DaPKC-dependent phosphorylation of Crumbs is required for epithelial cell polarity in Drosophila. The Journal of cell biology *166*, 549-557.

Spradling, A.C., and Rubin, G.M. (1982). Transposition of cloned P elements into Drosophila germ line chromosomes. Science *218*, 341-347.

Spradling, A.C., Stern, D., Beaton, A., Rhem, E.J., Laverty, T., Mozden, N., Misra, S., and Rubin, G.M. (1999). The Berkeley Drosophila Genome Project gene disruption project: Single P-element insertions mutating 25% of vital Drosophila genes. Genetics *153*, 135-177.

Spradling, A.C., Stern, D.M., Kiss, I., Roote, J., Laverty, T., and Rubin, G.M. (1995). Gene disruptions using P transposable elements: an integral component of the Drosophila genome project. Proceedings of the National Academy of Sciences of the United States of America *92*, 10824-10830.

Staley, B.K., and Irvine, K.D. (2010). Warts and Yorkie mediate intestinal regeneration by influencing stem cell proliferation. Current biology : CB *20*, 1580-1587.

Staley, B.K., and Irvine, K.D. (2012). Hippo signaling in Drosophila: recent advances and insights. Developmental dynamics : an official publication of the American Association of Anatomists *241*, 3-15.

Stewart, M., Murphy, C., and Fristrom, J.W. (1972). The recovery and preliminary characterization of X chromosome mutants affecting imaginal discs of Drosophila melanogaster. Developmental biology *27*, 71-83.

Strano, S., Munarriz, E., Rossi, M., Castagnoli, L., Shaul, Y., Sacchi, A., Oren, M., Sudol, M., Cesareni, G., and Blandino, G. (2001). Physical interaction with Yes-associated protein enhances p73 transcriptional activity. The Journal of biological chemistry *276*, 15164-15173.

Strassburger, K., Tiebe, M., Pinna, F., Breuhahn, K., and Teleman, A.A. (2012). Insulin/IGF signaling drives cell proliferation in part via Yorkie/YAP. Developmental biology *367*, 187-196.

Strutt, H., and Strutt, D. (2002). Nonautonomous planar polarity patterning in Drosophila: dishevelled-independent functions of frizzled. Developmental cell *3*, 851-863.

Sturtevant, A.H. (1913). A third group of linked genes in Drosophila ampelophila. Science *37*, 990-992.

Su, T., Bondar, T., Zhou, X., Zhang, C., He, H., and Medzhitov, R. (2015). Two-signal requirement for growth-promoting function of Yap in hepatocytes. Elife *4*.

Su, T., Ludwig, M.Z., Xu, J., and Fehon, R.G. (2017). Kibra and Merlin Activate the Hippo Pathway Spatially Distinct from and Independent of Expanded. Developmental cell *40*, 478-490 e473.

Sun, G., and Irvine, K.D. (2011). Regulation of Hippo signaling by Jun kinase signaling during compensatory cell proliferation and regeneration, and in neoplastic tumors. Developmental biology *350*, 139-151.

Sun, G., and Irvine, K.D. (2013). Ajuba family proteins link JNK to Hippo signaling. Science signaling *6*, ra81.

Sun, S., Reddy, B.V., and Irvine, K.D. (2015). Localization of Hippo signalling complexes and Warts activation in vivo. Nature communications *6*, 8402.

Swarup, S., Pradhan-Sundd, T., and Verheyen, E.M. (2015). Genome-wide identification of phospho-regulators of Wnt signaling in Drosophila. Development *142*, 1502-1515.

Swarup, S., and Verheyen, E.M. (2012). Wnt/Wingless signaling in Drosophila. Cold Spring Harbor perspectives in biology *4*.

Szymaniak, A.D., Mahoney, J.E., Cardoso, W.V., and Varelas, X. (2015). Crumbs3-Mediated Polarity Directs Airway Epithelial Cell Fate through the Hippo Pathway Effector Yap. Developmental cell *34*, 283-296.

Tan, Y., Yu, D., Pletting, J., and Davis, R.L. (2010). Gilgamesh Is Required for rutabaga-Independent Olfactory Learning in Drosophila. Neuron *67*, 810-820.

Tanaka, K. (2009). The proteasome: overview of structure and functions. Proceedings of the Japan Academy Series B, Physical and biological sciences *85*, 12-36.

Tanentzapf, G., and Tepass, U. (2003). Interactions between the crumbs, lethal giant larvae and bazooka pathways in epithelial polarization. Nature cell biology *5*, 46-52.

Tang, F., Gill, J., Ficht, X., Barthlott, T., Cornils, H., Schmitz-Rohmer, D., Hynx, D., Zhou, D., Zhang, L., Xue, G.*, et al.* (2015). The kinases NDR1/2 act downstream of the Hippo homolog MST1 to mediate both egress of thymocytes from the thymus and lymphocyte motility. Science signaling *8*, ra100.

Taniguchi, K., Wu, L.W., Grivennikov, S.I., de Jong, P.R., Lian, I., Yu, F.X., Wang, K., Ho, S.B., Boland, B.S., Chang, J.T.*, et al.* (2015). A gp130-Src-YAP module links inflammation to epithelial regeneration. Nature *519*, 57-62.

Tanimoto, H., Itoh, S., Dijke, P., and Tabata, T. (2000). Hedgehog Creates a Gradient of DPP Activity in *Drosophila* Wing Imaginal Discs. Molecular cell *5*, 59-71.

Tapon, N., Harvey, K., Bell, D., Wahrer, D., Schiripo, T., Haber, D., and Hariharan, I.K. (2002). salvador Promotes Both Cell Cycle Exit and Apoptosis in Drosophila andi s Mutated in Human Cancer Cell Lines. Cell *110*, 467-478.

Taylor, L.K., Wang, H.C., and Erikson, R.L. (1996). Newly identified stress-responsive protein kinases, Krs-1 and Krs-2. Proceedings of the National Academy of Sciences of the United States of America *93*, 10099-10104.

Tepass, U. (1996). Crumbs, a component of the apical membrane, is required for zonula adherens formation in primary epithelia of Drosophila. Developmental biology *177*, 217-225.

Tepass, U. (2012). The apical polarity protein network in Drosophila epithelial cells: regulation of polarity, junctions, morphogenesis, cell growth, and survival. Annual review of cell and developmental biology *28*, 655-685.

Tepass, U., Gruszynski-DeFeo, E., Haag, T.A., Omatyar, L., Torok, T., and Hartenstein, V. (1996). shotgun encodes Drosophila E-cadherin and is preferentially required during cell rearrangement in the neurectoderm and other morphogenetically active epithelia. Genes & development *10*, 672-685.

Tepass, U., and Hartenstein, V. (1994). The development of cellular junctions in the Drosophila embryo. Developmental biology *161*, 563-596.

Tepass, U., and Knust, E. (1990). Phenotypic and developmental analysis of mutations at the crumbs locus, a gene required for the development of epithelia in Drosophila melanogaster. Roux's Archives of Developmental Biology *199*, 189-206.

Tepass, U., and Knust, E. (1993). Crumbs and stardust act in a genetic pathway that controls the organization of epithelia in Drosophila melanogaster. Developmental biology *159*, 311-326.

Tepass, U., Tanentzapf, G., Ward, R., and Fehon, R. (2001). Epithelial cell polarity and cell junctions in Drosophila. Annual review of genetics *35*, 747-784.

Tepass, U., Theres, C., and Knust, E. (1990). crumbs encodes an EGF-like protein expressed on apical membranes of Drosophila epithelial cells and required for organization of epithelia. Cell *61*, 787-799.

Thompson, B.J., and Cohen, S.M. (2006). The Hippo pathway regulates the bantam microRNA to control cell proliferation and apoptosis in Drosophila. Cell *126*, 767-774.

Thompson, B.J., Pichaud, F., and Roper, K. (2013). Sticking together the Crumbs - an unexpected function for an old friend. Nature reviews Molecular cell biology *14*, 307-314.

Top, D., Harms, E., Syed, S., Adams, E.L., and Saez, L. (2016). GSK-3 and CK2 Kinases Converge on Timeless to Regulate the Master Clock. Cell reports *16*, 357-367.

Tsai, C.R., Anderson, A.E., Burra, S., Jo, J., and Galko, M.J. (2017). Yorkie regulates epidermal wound healing in Drosophila larvae independently of cell proliferation and apoptosis. Developmental biology *427*, 61-71.

Tseng, A.S., and Hariharan, I.K. (2002). An overexpression screen in Drosophila for genes that restrict growth or cell-cycle progression in the developing eye. Genetics *162*, 229-243.

Udan, R.S., Kango-Singh, M., Nolo, R., Tao, C., and Halder, G. (2003). Hippo promotes proliferation arrest and apoptosis in the Salvador/Warts pathway. Nature cell biology *5*, 914-920.

van der Veen, A.G., and Ploegh, H.L. (2012). Ubiquitin-like proteins. Annual review of biochemistry *81*, 323-357.

Varelas, X., Sakuma, R., Samavarchi-Tehrani, P., Peerani, R., Rao, B.M., Dembowy, J., Yaffe, M.B., Zandstra, P.W., and Wrana, J.L. (2008). TAZ controls Smad nucleocytoplasmic shuttling and regulates human embryonic stem-cell self-renewal. Nature cell biology *10*, 837-848.

Varelas, X., Samavarchi-Tehrani, P., Narimatsu, M., Weiss, A., Cockburn, K., Larsen, B.G., Rossant, J., and Wrana, J.L. (2010). The Crumbs complex couples cell density sensing to Hippo-dependent control of the TGF-beta-SMAD pathway. Developmental cell *19*, 831-844.

Villano, J.L., and Katz, F.N. (1995). four-jointed is required for intermediate growth in the proximal-distal axis in Drosophila. Development *121*, 2767-2777.

Visser-Grieve, S., Hao, Y., and Yang, X. (2012). Human homolog of Drosophila expanded, hEx, functions as a putative tumor suppressor in human cancer cell lines independently of the Hippo pathway. Oncogene *31*, 1189-1195.

Vrabioiu, A.M., and Struhl, G. (2015). Fat/Dachsous Signaling Promotes Drosophila Wing Growth by Regulating the Conformational State of the NDR Kinase Warts. Developmental cell *35*, 737-749.

Wada, K., Itoga, K., Okano, T., Yonemura, S., and Sasaki, H. (2011). Hippo pathway regulation by cell morphology and stress fibers. Development *138*, 3907-3914.

Walther, R.F., Nunes de Almeida, F., Vlassaks, E., Burden, J.J., and Pichaud, F. (2016). Pak4 Is Required during Epithelial Polarity Remodeling through Regulating AJ Stability and Bazooka Retention at the ZA. Cell reports *15*, 45-53.

Walther, R.F., and Pichaud, F. (2010). Crumbs/DaPKC-dependent apical exclusion of Bazooka promotes photoreceptor polarity remodeling. Current biology : CB *20*, 1065-1074.

Wang, B., Goode, J., Best, J., Meltzer, J., Schilman, P.E., Chen, J., Garza, D., Thomas, J.B., and Montminy, M. (2008). The insulin-regulated CREB coactivator TORC promotes stress resistance in Drosophila. Cell Metab *7*, 434-444.

Wang, C., An, J., Zhang, P., Xu, C., Gao, K., Wu, D., Wang, D., Yu, H., Liu, J.O., and Yu, L. (2012). The Nedd4-like ubiquitin E3 ligases target angiomotin/p130 to ubiquitin-dependent degradation. The Biochemical journal *444*, 279-289.

Wang, S.L., Hawkins, C.J., Yoo, S.J., Müller, H.A.J., and Hay, B.A. (1999). The Drosophila Caspase Inhibitor DIAP1 Is Essential for Cell Survival and Is Negatively Regulated by HID. Cell *98*, 453-463.

Wang, W., Huang, J., and Chen, J. (2011). Angiomotin-like proteins associate with and negatively regulate YAP1. The Journal of biological chemistry *286*, 4364-4370.

Wang, W., Huang, X., Xin, H.B., Fu, M., Xue, A., and Wu, Z.H. (2015a). TRAF Family Member-associated NF-kappaB Activator (TANK) Inhibits Genotoxic Nuclear Factor kappaB Activation by Facilitating Deubiquitinase USP10-dependent Deubiquitination of TRAF6 Ligase. The Journal of biological chemistry *290*, 13372-13385.

Wang, W., Xiao, Z.D., Li, X., Aziz, K.E., Gan, B., Johnson, R.L., and Chen, J. (2015b). AMPK modulates Hippo pathway activity to regulate energy homeostasis. Nature cell biology *17*, 490-499.

Wang, Z., Wu, Y., Wang, H., Zhang, Y., Mei, L., Fang, X., Zhang, X., Zhang, F., Chen, H., Liu, Y.*, et al.* (2014). Interplay of mevalonate and Hippo pathways regulates RHAMM transcription via YAP to modulate breast cancer cell motility. Proceedings of the National Academy of Sciences of the United States of America *111*, E89-98.

Wehr, M.C., Holder, M.V., Gailite, I., Saunders, R.E., Maile, T.M., Ciirdaeva, E., Instrell, R., Jiang, M., Howell, M., Rossner, M.J.*, et al.* (2013). Salt-inducible kinases regulate growth through the Hippo signalling pathway in Drosophila. Nature cell biology *15*, 61-71.

Wei, X., Shimizu, T., and Lai, Z.-C. (2007). Mob as tumor suppressor is activated by Hippo kinase for growth inhibition in Drosophila. The EMBO journal *26*, 1772–1781.

Willecke, M., Hamaratoglu, F., Kango-Singh, M., Udan, R., Chen, C.L., Tao, C., Zhang, X., and Halder, G. (2006). The fat cadherin acts through the hippo tumor-suppressor pathway to regulate tissue size. Current biology : CB *16*, 2090-2100.

Willecke, M., Hamaratoglu, F., Sansores-Garcia, L., Tao, C., and Halder, G. (2008). Boundaries of Dachsous Cadherin activity modulate the Hippo signaling pathway to induce cell proliferation. Proceedings of the National Academy of Sciences of the United States of America *105*, 14897-14902.

Wilson, R.C., and Doudna, J.A. (2013). Molecular mechanisms of RNA interference. Annual review of biophysics *42*, 217-239.

Wodarz, A., Grawe, F., and Knust, E. (1993). CRUMBS is involved in the control of apical protein targeting during *Drosophila* epithelial development. Mechanisms of Development *44*, 175-187.

Wodarz, A., Hinz, U., Engelbert, M., and Knust, E. (1995). Expression of Crumbs Confers Apical Character on Plasma Membrane Domains of Ectodermal Epithelia of Drosophila. Cell *82*, 67-76.

Wodarz, A., Ramrath, A., Grimm, A., and Knust, E. (2000). Drosophila Atypical Protein Kinase C Associates with Bazooka and Controls Polarity of Epithelia and Neuroblasts. The Journal of cell biology *150*, 1361-1374.

Wong, K.K., Li, W., An, Y., Duan, Y., Li, Z., Kang, Y., and Yan, Y. (2015). beta-Spectrin regulates the hippo signaling pathway and modulates the basal actin network. The Journal of biological chemistry *290*, 6397-6407.

Wu, H., Xiao, Y., Zhang, S., Ji, S., Wei, L., Fan, F., Geng, J., Tian, J., Sun, X., Qin, F.*, et al.* (2013). The Ets transcription factor GABP is a component of the hippo pathway essential for growth and antioxidant defense. Cell reports *3*, 1663-1677.

Wu, S., Huang, J., Dong, J., and Pan, D. (2003). hippo Encodes a Ste-20 Family Protein Kinase that Restricts Cell Proliferation and Promotes Apoptosis in Conjunction with salvador and warts. Cell *114*, 445-456.

Wu, S., Liu, Y., Zheng, Y., Dong, J., and Pan, D. (2008). The TEAD/TEF family protein Scalloped mediates transcriptional output of the Hippo growth-regulatory pathway. Developmental cell *14*, 388-398.

Xu, J., Peng, W., Sun, Y., Wang, X., Xu, Y., Li, X., Gao, G., and Rao, Z. (2012). Structural study of MCPIP1 N-terminal conserved domain reveals a PIN-like RNase. Nucleic acids research *40*, 6957-6965.

Xu, T., and Rubin, M. (1993). Analysis of genetic mosaics in developing adult *Drosophila* tissues. Development *117*, 1223-1237.

Xu, T., Wang, W., Zhang, S., Stewart, R., and Yu, W. (1995). Identifying tumor suppressors in genetic mosaics: the *Drosophila lats* gene encodes a putative protein kinase. Development *121*, 1053-1063.

Xu, Y., Wang, K., and Yu, Q. (2016). FRMD6 inhibits human glioblastoma growth and progression by negatively regulating activity of receptor tyrosine kinases. Oncotarget *7*, 70080-70091.

Yagi, R., Chen, L.F., Shigesada, K., Murakami, Y., and Ito, Y. (1999). A WW domain-containing yes-associated protein (YAP) is a novel transcriptional co-activator. The EMBO journal *18*, 2551-2562.

Yamamoto, M., Ohsawa, S., Kunimasa, K., and Igaki, T. (2017). The ligand Sas and its receptor PTP10D drive tumour-suppressive cell competition. Nature *542*, 246-250.

Yanagawa, S.i., Matsuda, Y., Lee, J.S., Matsubayashi, H., Sese, S., Kadowaki, T., and Ishimoto, A. (2002). Casein kinase I phosphorylates the Armadillo protein and induces its degradation in Drosophila. The EMBO journal *21*, 1733-1742.

Yang, C.H., Axelrod, J.D., and Simon, M.A. (2002). Regulation of Frizzled by fat-like cadherins during planar polarity signaling in the Drosophila compound eye. Cell *108*, 675-688.

Yang, Y., Duguay, D., Bédard, N., Rachalski, A., Baquiran, G., Na, C.H., Fahrenkrug, J., Storch, K.-F., Peng, J., Wing, S.S.*, et al.* (2012). Regulation of behavioral circadian rhythms and clock protein PER1 by the deubiquitinating enzyme USP2. Biology open *1*, 789-801.

Yang, Y., Duguay, D., Fahrenkrug, J., Cermakian, N., and Wing, S.S. (2014). USP2 regulates the intracellular localization of PER1 and circadian gene expression. Journal of biological rhythms *29*, 243-256.

Ye, Y., and Rape, M. (2009). Building ubiquitin chains: E2 enzymes at work. Nature reviews Molecular cell biology *10*, 755-764.

Yen, H.C., Xu, Q., Chou, D., Zhao, Z., and Elledge, S.J. (2008). Global Protein Stability Profiling in Mammalian Cells. Science *322*, 918-923.

Yi, C., Shen, Z., Stemmer-Rachamimov, A., Dawany, N., Troutman, S., Showe, L.C., Liu, Q., Shimono, A., Sudol, M., Holmgren, L.*, et al.* (2013). The p130 isoform of angiomotin is required for Yap-mediated hepatic epithelial cell proliferation and tumorigenesis. Science signaling *6*, ra77.

Yi, C., Troutman, S., Fera, D., Stemmer-Rachamimov, A., Avila, J.L., Christian, N., Persson, N.L., Shimono, A., Speicher, D.W., Marmorstein, R.*, et al.* (2011). A tight junction-associated Merlin-angiomotin complex mediates Merlin's regulation of mitogenic signaling and tumor suppressive functions. Cancer cell *19*, 527-540.

Yimlamai, D., Christodoulou, C., Galli, G.G., Yanger, K., Pepe-Mooney, B., Gurung, B., Shrestha, K., Cahan, P., Stanger, B.Z., and Camargo, F.D. (2014). Hippo Pathway Activity Influences Liver Cell Fate. Cell *157*, 1324-1338.

Yin, F., Yu, J., Zheng, Y., Chen, Q., Zhang, N., and Pan, D. (2013). Spatial organization of Hippo signaling at the plasma membrane mediated by the tumor suppressor Merlin/NF2. Cell *154*, 1342-1355.

Yu, F.X., and Guan, K.L. (2013). The Hippo pathway: regulators and regulations. Genes & development *27*, 355-371.

Yu, F.X., Meng, Z., Plouffe, S.W., and Guan, K.L. (2015a). Hippo pathway regulation of gastrointestinal tissues. Annual review of physiology *77*, 201-227.

Yu, F.X., Zhang, Y., Park, H.W., Jewell, J.L., Chen, Q., Deng, Y., Pan, D., Taylor, S.S., Lai, Z.C., and Guan, K.L. (2013). Protein kinase A activates the Hippo pathway to modulate cell proliferation and differentiation. Genes & development *27*, 1223-1232.

Yu, F.X., Zhao, B., and Guan, K.L. (2015b). Hippo Pathway in Organ Size Control, Tissue Homeostasis, and Cancer. Cell *163*, 811-828.

Yu, F.X., Zhao, B., Panupinthu, N., Jewell, J.L., Lian, I., Wang, L.H., Zhao, J., Yuan, H., Tumaneng, K., Li, H.*, et al.* (2012). Regulation of the Hippo-YAP pathway by G-protein-coupled receptor signaling. Cell *150*, 780-791.

Yu, J., Zheng, Y., Dong, J., Klusza, S., Deng, W.M., and Pan, D. (2010). Kibra functions as a tumor suppressor protein that regulates Hippo signaling in conjunction with Merlin and Expanded. Developmental cell *18*, 288-299.

Yue, T., Tian, A., and Jiang, J. (2012). The cell adhesion molecule echinoid functions as a tumor suppressor and upstream regulator of the Hippo signaling pathway. Developmental cell *22*, 255-267.

Zanconato, F., Cordenonsi, M., and Piccolo, S. (2016). YAP/TAZ at the Roots of Cancer. Cancer cell *29*, 783-803.

Zecca, M., and Struhl, G. (2010). A feed-forward circuit linking wingless, fat-dachsous signaling, and the warts-hippo pathway to Drosophila wing growth. PLoS biology *8*, e1000386.

Zeidler, M.P., Perrimon, N., and Strutt, D.I. (1999). The four-jointed gene is required in the Drosophila eye for ommatidial polarity specification. Current Biology *9*, 1363-1372.

Zeidler, M.P., Perrimon, N., and Strutt, D.I. (2000). Multiple Roles for four-jointed in Planar Polarity and Limb Patterning. Developmental biology *228*, 181-196.

Zeng, X., Tamai, K., Doble, B., Li, S., Huang, H., Habas, R., Okamura, H., Woodgett, J., and He, X. (2005). A dual-kinase mechanism for Wnt co-receptor phosphorylation and activation. Nature *438*, 873-877.

Zhang, H., Li, C., Chen, H., Wei, C., Dai, F., Wu, H., Dui, W., Deng, W.M., and Jiao, R. (2015a). SCF(Slmb) E3 ligase-mediated degradation of Expanded is inhibited by the Hippo pathway in Drosophila. Cell research *25*, 93-109.

Zhang, J., Liu, M., Su, Y., Du, J., and Zhu, A.J. (2012). A targeted in vivo RNAi screen reveals deubiquitinases as new regulators of Notch signaling. G3 *2*.

Zhang, L., Jia, J., Wang, B., Amanai, K., Wharton, K.A., Jr., and Jiang, J. (2006). Regulation of wingless signaling by the CKI family in Drosophila limb development. Developmental biology *299*, 221-237.

Zhang, L., Ren, F., Zhang, Q., Chen, Y., Wang, B., and Jiang, J. (2008). The TEAD/TEF family of transcription factor Scalloped mediates Hippo signaling in organ size control. Developmental cell *14*, 377-387.

Zhang, L., Tang, F., Terracciano, L., Hynx, D., Kohler, R., Bichet, S., Hess, D., Cron, P., Hemmings, B.A., Hergovich, A.*, et al.* (2015b). NDR functions as a physiological YAP1 kinase in the intestinal epithelium. Current biology : CB *25*, 296-305.

Zhang, Y., Wang, X., Matakatsu, H., Fehon, R., and Blair, S.S. (2016). The novel SH3 domain protein Dlish/CG10933 mediates fat signaling in Drosophila by binding and regulating Dachs. Elife *5*.

Zhao, B., Li, L., Lu, Q., Wang, L.H., Liu, C.Y., Lei, Q., and Guan, K.L. (2011). Angiomotin is a novel Hippo pathway component that inhibits YAP oncoprotein. Genes & development *25*, 51-63.

Zhao, B., Li, L., Tumaneng, K., Wang, C.Y., and Guan, K.L. (2010). A coordinated phosphorylation by Lats and CK1 regulates YAP stability through SCF(beta-TRCP). Genes & development *24*, 72-85.

Zhao, B., Li, L., Wang, L., Wang, C.Y., Yu, J., and Guan, K.L. (2012). Cell detachment activates the Hippo pathway via cytoskeleton reorganization to induce anoikis. Genes & development *26*, 54-68.

Zhao, B., Wei, X., Li, W., Udan, R.S., Yang, Q., Kim, J., Xie, J., Ikenoue, T., Yu, J., Li, L.*, et al.* (2007). Inactivation of YAP oncoprotein by the Hippo pathway is involved in cell contact inhibition and tissue growth control. Genes & development *21*, 2747-2761.

Zhao, B., Ye, X., Yu, J., Li, L., Li, W., Li, S., Yu, J., Lin, J.D., Wang, C.Y., Chinnaiyan, A.M.*, et al.* (2008). TEAD mediates YAP-dependent gene induction and growth control. Genes & development *22*, 1962-1971.

Zheng, Y., Wang, W., Liu, B., Deng, H., Uster, E., and Pan, D. (2015). Identification of Happyhour/MAP4K as Alternative Hpo/Mst-like Kinases in the Hippo Kinase Cascade. Developmental cell *34*, 642-655.

Zhou, B., Wu, Y., and Lin, X. (2011). Retromer regulates apical-basal polarity through recycling Crumbs. Developmental biology *360*, 87-95.

Zhou, D., Conrad, C., Xia, F., Park, J.S., Payer, B., Yin, Y., Lauwers, G.Y., Thasler, W., Lee, J.T., Avruch, J.*, et al.* (2009). Mst1 and Mst2 maintain hepatocyte quiescence and suppress hepatocellular carcinoma development through inactivation of the Yap1 oncogene. Cancer cell *16*, 425-438.

Zhou, L., Azfer, A., Niu, J., Graham, S., Choudhury, M., Adamski, F.M., Younce, C., Binkley, P.F., and Kolattukudy, P.E. (2006). Monocyte chemoattractant protein-1 induces a novel transcription factor that causes cardiac myocyte apoptosis and ventricular dysfunction. Circulation research *98*, 1177-1185.

Zhou, W., and Hong, Y. (2012). Drosophila Patj plays a supporting role in apical-basal polarity but is essential for viability. Development *139*, 2891-2896.

Zhou, X., Wang, S., Wang, Z., Feng, X., Liu, P., Lv, X.B., Li, F., Yu, F.X., Sun, Y., Yuan, H.*, et al.* (2015). Estrogen regulates Hippo signaling via GPER in breast cancer. The Journal of clinical investigation *125*, 2123-2135.

Zilian, O., Frei, E., Burke, R., Brentrup, D., Gutjahr, T., Bryant, P.J., and Noll, M. (1999). double-time is identical to discs overgrown, which is required for cell survival, proliferation and growth arrest in Drosophila imaginal discs. Development *126*, 5409-5420.

Ziosi, M., Baena-Lopez, L.A., Grifoni, D., Froldi, F., Pession, A., Garoia, F., Trotta, V., Bellosta, P., Cavicchi, S., and Pession, A. (2010). dMyc functions downstream of Yorkie to promote the supercompetitive behavior of hippo pathway mutant cells. PLoS genetics *6*, e1001140.

Zou, J., Wang, X., and Wei, X. (2012). Crb apical polarity proteins maintain zebrafish retinal cone mosaics via intercellular binding of their extracellular domains. Developmental cell *22*, 1261-1274.